

U.S. Department of Energy • Office of Fossil Energy  
National Energy Technology Laboratory

# The Energetics of Carbon Dioxide Capture in Power Plants

**Gerold Göttlicher**



U.S. Department of Energy • Office of Fossil Energy  
National Energy Technology Laboratory

# The Energetics of Carbon Dioxide Capture in Power Plants

**Gerold Göttlicher**

February 2004



Updated license edition of the publication “Energetik der Kohlendioxidrückhaltung in Kraftwerken.”  
Fortschritt-Berichte VDI Reihe 6 Nr. 421 (VDI Progress Reports Series 6 No. 421).

© VDI-Verlag, Dusseldorf 1999

Translated by APEX Translations, Inc.

The National Energy Technology Laboratory (NETL) of the U.S. Department of Energy (DOE) is pleased to provide this English translation of Dr. Göttlicher's book. While the views in this book may not necessarily be those of DOE, the work stands as a benchmark in the field of CO<sub>2</sub> capture from power plants for the purposes of carbon sequestration.

I would like to acknowledge those at NETL who made contributions to the translation and publication project. The project was initiated by Dr. Larry Headley, Associate Director of the Office of Science and Technology, and supported by Dr. Curt White, Focus Area Leader for Carbon Sequestration Science and Dr. Gilbert McGurl, Deputy Associate Director of the Office of System and Policy Support. A special thanks goes to Patrick Le who coordinated the review of the translation. He was assisted by Edward Parsons, Hsue-Peng Loh, and Dale Keairns. Thomas Russial, Lisa Jarr, Henry Pennline, Ron Cutright, Gary Martin, Lynn Billanti, Debbie Sugg, and Tami Kapaldo also made important contributions.

Finally, I would like to acknowledge the work of Apex Translations, Inc., and especially Dr. Florian Deltgen, for doing the translation in a very professional, timely, and accommodating manner.

Robert P. Warzinski  
Research Chemist, NETL

## PREFACE TO TRANSLATION

Since the first version of this book in 1999, the concerns over rising CO<sub>2</sub> emissions present an even greater challenge to the development of the future energy supply system. Accordingly, new proposals and demonstration projects have been developed to address this issue.

Reducing CO<sub>2</sub> emissions associated with power production by measures such as efficiency improvements or switching to low carbon fuels are limited by the residual carbon content of the fuel and the availability of the primary energy sources, respectively. Also, the utilization of renewable energy sources is restricted by capacities, as well as by the high cost of the present state of this technology. On the other hand, we will have to depend on reliable, abundant energy sources. Coal reserves, for example, are sufficient to provide a sustainable energy supply for centuries. If fossil fuels continue to be the primary energy supply for the next several decades, CO<sub>2</sub> capture and storage, also called carbon management [1], is the only transition solution to both secure energy supplies and reduced CO<sub>2</sub> emissions as we move to new energy supply systems.

Apart from nuclear energy, CO<sub>2</sub> capture and storage by far offers the largest potential for reducing CO<sub>2</sub> emissions at lower costs than utilization of renewable energy sources [2]. Although CO<sub>2</sub> avoidance by efficiency improvement at a certain point will start to get very expensive compared to CO<sub>2</sub> capture (Figure 1), the development of a low emission, i.e., highly efficient, power plant is advantageous for the application of CO<sub>2</sub> capture. The capture requirements would be reduced in proportion to the lower CO<sub>2</sub> emissions. Regarding CO<sub>2</sub> storage, there are potential options; however, there are possible ecological problems in CO<sub>2</sub> storage in the ocean, safety problems in underground storage, and impact problems of possible increases in primary energy consumption that must be considered and understood before this technology is feasible on a large scale. Regardless of the challenges, the vision of clean future energy at acceptable costs has to be pursued.

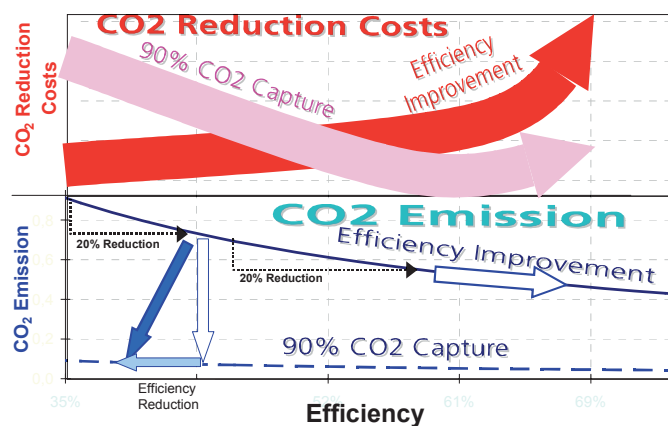


Figure 1: Trends of emission reduction and CO<sub>2</sub> reduction costs by efficiency improvement and CO<sub>2</sub> capture

CO<sub>2</sub> emission reduction in power plants cannot be the only approach to reducing total CO<sub>2</sub> emissions. The effect of CO<sub>2</sub> capture can be increased if it is also applied to centralized hydrogen production from fossil fuels. Such a system of carbon management would include centralized power production, as well as fuel supply, from centralized hydrogen plants to the transportation sector and to domestic heating or to decentralized production of combined heat and power (Figure 2). For such a hydrogen production system, the gasification of coal or the reforming of natural gas is required with subsequent separation of

the CO<sub>2</sub> and H<sub>2</sub> produced, such as in Process Family I in the book, to provide the hydrogen for export and the CO<sub>2</sub> for storage.

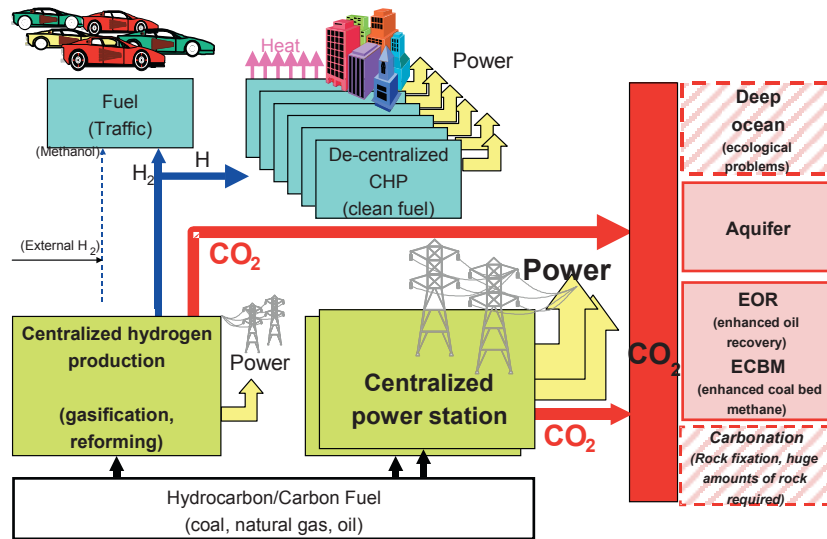
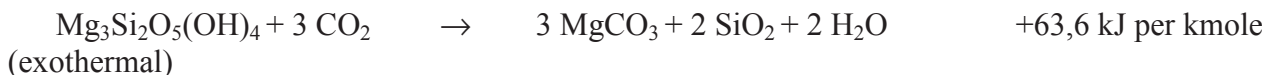


Figure 2: Carbon management system supplying CO<sub>2</sub> emission free power and fuel.

Regarding the development of a CO<sub>2</sub> emission free fossil fuel-fired power plant, the following statements should be considered:

- The development of a low emission, i.e., highly efficient, power plant is also advantageous for the application of CO<sub>2</sub> capture.
- Additional energy demand due to efficiency reduction or power reduction caused by CO<sub>2</sub> capture is unwanted and would partly negate the effect of emission reduction by increased climate effective emissions during mining, transport, and further utilization.
- One principle to be followed for minimization of the energy required for CO<sub>2</sub> capture is to avoid the dilution of the combustion products, e.g. by nitrogen, thus permitting CO<sub>2</sub> separation at the highest concentration possible. Theoretically, exergy could even be gained by avoiding exergy losses of gas mixing during combustion.
- As already mentioned in Chapter 2.2.1 (Overview), CO<sub>2</sub> is not the end product of chemical carbon conversion, but in the global chemical carbon cycle the lowest energy level is finally reached in the carbonates of the ocean sediments:



In nature this exothermal integration of carbon into the sediments runs extremely slowly [3], preventing the technical utilization of the released energy. At present, there are no methods to utilize the energy of this reaction.

An optimized system considering all the above statements does not yet exist.

The direct fixation of fuel carbon in carbonates (see reaction above) without the intermediate production of CO<sub>2</sub> and with the utilization of the additional energy potential of the carbonation reaction should be considered as a conceivable process for CO<sub>2</sub> capture. Such a process is depicted in Figure 3 where the

only by-products are steam and a mixture of ash and carbonates. However, a practicable technical solution has not yet been found.

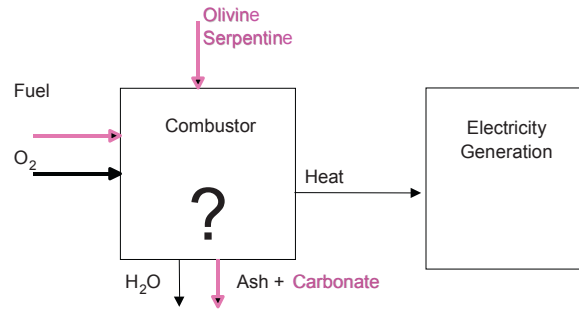


Figure 3: Open technical feasibility of direct fixation of fuel carbon in carbonates

From the comparison of the ideal processes described in Chapter 3.10, it is obvious that the combustion in oxygen and recirculated  $\text{CO}_2$  in the long term offers by far the best option. Indeed, the development of oxygen production with membranes is already outlined which will cause clearly lower energy consumption and costs. Furthermore, proposals already exist for which no additional energy demand for oxygen supply would be required. Instead of supplying oxygen via the energy intensive intermediate step of producing highly pure oxygen, the oxygen is directly transferred via intermediate reactions with metal oxides as described in the book in Figure 2.18 or membrane reactors at high temperatures (Perovskit membranes, e.g. Figure 4) [4, 5, 6]. With the introduction of condensing  $\text{CO}_2$  cycles, even the energy demand for  $\text{CO}_2$  liquefaction could be eliminated. Such high-temperature membranes are also used in high-temperature fuel cells. The gas separation effect of the fuel cells could be used very effectively if this kind of membrane reactor would also be applied to oxidize the residual fuel without mixing with nitrogen from air.

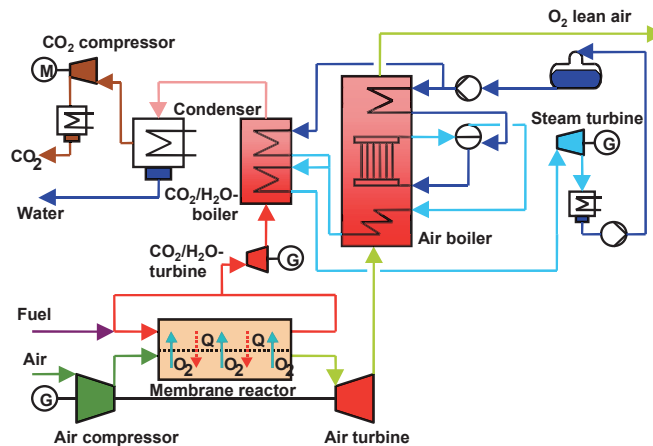


Figure 4: Gas turbine process with oxygen supplied by membrane reactor (Advanced Zero Emission Plant – AZEP [4]). The efficiency reduction would be less than 5 percentage points.

In the ZECA (Zero Coal Alliance) process [7], with the combination of a hydro-gasification process with a calcium/calcium oxide cycle acting as a combined CO shift – gas separation system and a SOFC with chemical heat recuperation in the calcium/calcium oxide cycle, an efficiency of 70% has been claimed when all components including the pressurized fuel cell become available (Figure 5). While  $\text{CO}_2$  capture is inherent in this kind of hydro-gasification, the high efficiency of 70% is only attainable in combination with the almost complete utilization of the high temperature exhaust gas of the high tem-





## ORIGINAL PREFACE

This dissertation was written during the period I spent as a Research Associate at the Chair of Energy Supply and Energy Management Technologies, at GH Essen University, in the course of research projects sponsored by the European Commission.

My cordial thanks to Professor Dr. Ing. R. Pruschek for helping me to accomplish my project work in an intensive and application-oriented manner and supporting me in carrying out international research. The in-depth discussions we held contributed to the success of this dissertation. I would also like to thank Professor Dr. Ing. K. Görner as co-referent. I am equally indebted to Professor Dr. Ing. I.F.W. Romey who, upon assuming office in the 1996/1997 winter semester, provided me with the opportunity to continue my work in the field of power plant technology and complete this dissertation.

I am thankful for the close collaborative relationship with my colleagues. I would especially like to thank Dr. Ing. Reinhard Kloster for contributing towards the excellent, highly productive atmosphere in the office we shared for many years, as well as Dr. Ing. Gerd Oeljeklaus and Dr. Ing. Uwe Rauh for their continuous readiness to help. I thank Markus Koerdts, Martin Adorni and Bianka Rohloff for their commitment in writing their theses, which provided me with valuable support.

Finally, I would like to express my loving thanks to my parents for enabling me to follow this education path and, in particular, to my dear wife Sigrid for her boundless support and endless patience.

Gerold Göttlicher

*O glücklich, wer noch hoffen kann,  
aus diesem Meer des Irrtums aufzutauchen!  
Was man nicht weiß, das eben brauchte man  
und was man weiß, kann man nicht brauchen.*

Johann Wolfgang von Goethe, *Faust I*

*Willst du, Freund, die erhabensten Höhn der Weisheit erfliegen,  
wag es, auf die Gefahr, daß dich die Klugheit verlacht.  
Die kurzsichtige sieht nur das Ufer, das dir zurückflieht,  
Jenes nicht, wo dereinst landet dein mutiger Flug.*

Friedrich von Schiller, *Epigram*

*Dedicated to my children and all other children*

## CONTENTS

<b>1</b>	<b>INTRODUCTION .....</b>	<b>1</b>
1.1	The Problem .....	1
1.2	Task Definition .....	2
1.3	CO <sub>2</sub> Capture: Definitions .....	4
<b>2</b>	<b>STATE OF THE SCIENCE AND TECHNOLOGY.....</b>	<b>6</b>
2.1	Baseline Efficiencies .....	6
2.2	Power Plants with CO <sub>2</sub> Capture .....	8
2.2.1	Overview .....	8
2.2.2	Gas Separation Methods .....	12
2.2.3	Process Family I: CO <sub>2</sub> Separation from Synthesis Gas Subsequent to CO Conversion.....	20
2.2.4	Process Family II: Carbon Dioxide Concentration in the Exhaust Gas .....	35
2.2.5	Process Family III: CO <sub>2</sub> Separation from Flue Gases .....	45
2.2.6	Process Family IV: Carbon Separation.....	48
2.2.7	Process Family V: CO <sub>2</sub> Capture with Fuel Cells .....	51
2.2.8	Review of the Literature with Conversion to a Common Basis .....	56
<b>3</b>	<b>ENERGY AND EXERGY ANALYSIS .....</b>	<b>64</b>
3.1	Calculation Methods in the Energy and Exergy Analysis of Power Plant Systems .....	65
3.1.1	Calculations for Gas Turbines .....	66
3.1.2	Calculations for the Heat Recovery Steam Cycle .....	66
3.1.3	Calculations for Coal Gasification.....	71
3.1.4	Calculations for an IGCC Power Plant .....	75
3.1.5	Baseline Case for Performing Calculations for an IGCC Power Plant .....	76
3.2	Boundary Conditions and Process Data .....	78
3.3	CO <sub>2</sub> Compression and Liquefaction .....	80
3.4	Gas Separation.....	82
3.4.1	Estimated Energy Requirements of Gas Separation Processes.....	82
3.4.2	Reversible Separation Work and Exergetic Efficiency of Technical Gas Separation Processes.....	95
3.5	Process Family I: CO <sub>2</sub> Separation From Synthesis Gas After CO Shift.....	99
3.5.1	CO Conversion, Steam Reforming.....	99
3.5.2	Processes with Coal Gasification .....	103
3.5.3	Chemically Recuperated Gas Turbines (CRGT).....	118
3.6	Process Family II: CO <sub>2</sub> -Rich Exhaust Gas .....	121

3.6.1	Oxygen Requirement and Oxygen Purity .....	121
3.6.2	Analysis of the Oxygen Supply .....	123
3.6.3	Operation at Increased Pressure.....	125
3.6.4	Joule Cycle (Standard Gas Turbine) and Joule/Rankine Cycle (Gas/ Steam Turbine Combined Cycle) .....	126
3.6.5	Other Cycles with CO <sub>2</sub> as Working Fluid .....	127
3.6.6	Parameter Studies for IGCC Power Plants with CO <sub>2</sub> Recycling.....	130
3.6.7	Processes with Coal Gasification and H <sub>2</sub> /CO Separation .....	134
3.7	Process Family III: CO <sub>2</sub> Separation from Flue Gases.....	138
3.8	Process Family IV: Carbon Separation .....	139
3.9	Process Family V: CO <sub>2</sub> Capture with Fuel Cells.....	139
3.10	Minimum Energy Requirements of CO <sub>2</sub> Capture.....	140
<b>4</b>	<b>ECONOMIC COMPARISON OF POWER PLANT CYCLES WITH CO<sub>2</sub> CAPTURE.....</b>	<b>141</b>
4.1	Procedure .....	141
4.2	Review of Literature .....	143
4.3	Development Potential.....	150
4.4	Comparison with Alternative Measures .....	152
<b>5</b>	<b>SUMMARY .....</b>	<b>154</b>
<b>6</b>	<b>APPENDIX .....</b>	<b>159</b>
6.1	Supplementary Information on the Climate Issue.....	159
6.2	Possible Approaches Towards Reducing CO <sub>2</sub> Emissions in the Energy Supply Sector .....	161
6.3	The Natural, Geochemical Carbon Cycle and Global Carbon Reservoirs .....	165
6.4	CO <sub>2</sub> Pipeline Transport .....	166
6.5	Data Tables .....	168
6.6	Electrical Equivalence Factor of Heat Utilization (Extraction Steam).....	178
6.7	Calculation of Electricity Generating Costs .....	181
<b>7</b>	<b>Literature .....</b>	<b>182</b>

**ABBREVIATIONS**

ABB	Asea Brown Boveri AG
AFBC	Atmospheric Fluidized Bed Combustion
AFC	Alkaline Fuel Cell
ASU	Air Separation Unit
BASF	Badische Anilin & Soda Fabrik AG
BFW	Boiler Feed Water
BGL	British Gas Lurgi
BP	British Petroleum Company plc
BRC	Binary Rankine Cycle (: 2fold-Clausius Rankine Cycle)
CASH	Compressed Air Storage with Humidification (+ Humid Air Turbine) (:HAT Cycle with Storage of Compressed Air)
CC	Combined Cycle
CE	Coal Equivalent, 1 t CE = 29305 kJ
CFBC	Circulating Fluidized Bed Combustion
CFC	Circulating Fluidized Combustion (equivalent to CFBC)
CFZ	Controlled Freezing Zone
CPERI	Chemical Process Engineering Institute (Aristotle University of Thessaloniki, Greece)
CRE	Coal Research Establishment (British Coal)
CRGT	Chemically Recuperated Gas Turbine
DENOX	Secondary measures for the reduction of NO <sub>x</sub> emissions
DESOX	Secondary measures for the reduction of SO <sub>x</sub> emissions
ECN	Energieonderzoek Centrum Nederland / The Netherlands Energy Research Foundation
ENDESA	Empresa Nacional de Electricidad S.A.
EOR	Enhanced Oil Recovery
EPDC	Electric Power Development Company
EPRI	Electric Power Research Institute
FBD	Fluidized Bed Drier
FC	Fuel Cell
FG	Flue Gas
FGD	Flue Gas Desulfurization
FW	Feed Water
GE	General Electric Company
GKSS	GKSS Research Center
GSP	Gaskombinat Schwarze Pumpe ( <i>East German company prior to reunification</i> )
GT	Gas Turbine
GTCC	Gas/Steam Turbine Combined Cycle
GUD	<i>Gas und Dampf</i> (gas and steam power plant), registered trademark of the Siemens corporation for the Gas/Steam Turbine Combined Cycle
HAT	Humid Air Turbine (:gas turbine with humidified air)
HE	Heat Exchanger
HP	High Pressure
HT	High Temperature
HPC	Hot Potassium Carbonate
HRSG	Heat Recovery Steam Generator
HTW	High Temperature Winkler (gasification process)
IEA	International Energy Agency

IEA-GHG	International Energy Agency - Greenhouse Gas R&D
IEN	Instytut Energetyki, Warsaw, Poland
IG/CASH	CASH with integrated coal gasification
IGCC	Integrated Coal Gasification Combined Cycle
IGCC hybrid	IGCC with partial gasification and combustion of residual char
IGHAT	HAT with integrated coal gasification
IH	Sequential Combustion process in gas turbine (staged-combustion)
IPCC	Intergovernmental Panel on Climate Change
IS	Intermediate Superheating
IW	Cologne Institute for Business Research (German: <i>Institut der deutschen Wirtschaft</i> )
KRW	Kellog Rust Westinghouse (gasification process)
LP	Low Pressure
LT	Low Temperature
MCFC	Molten Carbonate Fuel Cell
MEA	Monoethanolamine
MHD	Magneto-Hydro-Dynamic
MP	Medium Pressure
PAFC	Phosphoric Acid Fuel Cell
PEMFC	Proton Exchange Membrane Fuel Cell
PF	Pulverized-Coal-Fired
PFBC	Pressurized Fluidized Bed Combustion
PPCC	Pressurized Pulverized Coal Fired Combined Cycle
PRENFLO	PREssurized ENtrained FLOW (gasification process)
Prox. Anal.	Proximate Analysis
PSA	Pressure Swing Adsorption
PTSA	Pressure/Temperature Swing Adsorption
R&D	Research and Development
REVAP	Recuperated EVAPorative (cycle), similar to HAT
RU	Refrigerating Unit
SH	Superheater
SOFC	Solid Oxide Fuel Cell
SPP	Steam Power Plant
ST	Steam Turbine
STIG	Steam Injected Gas Turbine
TIT	Turbine Inlet Temperature
TRC	Triple Rankine Cycle
TSA	Temperature Swing Adsorption
Ult. Anal.	Ultimate Analysis
USC	Ultra Supercritical Steam Cycle
VEAG	Vereinigte Energiewerke AG
VEW	Vereinigte Elektrizitätswerke Westfalen AG
VSA	Vacuum Swing Adsorption
WEC	World Energy Council
WIHYS	<u>W</u> ater Gas Shift With <u>I</u> ntegrated <u>H</u> ydrogen Carbon Dioxide <u>S</u> eparation
ad	as delivered
af	ash-free
ar	as received
dr	Dry

liq.	Liquid
maf	moisture and ash free
mf	moisture free

## SYMBOLS

Unless stated otherwise, efficiencies are plant net efficiencies in relation to the fuel energy flow

$$(\text{LHV}) \text{ of the fuel, and defined as } \eta = \frac{\text{benefit}}{\text{expenditure}} = \frac{P_{el,total} - P_{el,int}}{\dot{m}_F \cdot \text{LHV}}$$

A	Surface Area
b	Solvent loading
D	Permeability
$c_p$	Specific isobaric heat capacity
e, E	Exergy (specific, absolute)
h, H	Enthalpy (specific, absolute)
HHV	Higher Heating Value
LHV	Lower Heating Value
$k_{CO_2}$	CO <sub>2</sub> avoidance costs
$k_{el,i}$	Electricity generating costs
K	Chemical equilibrium constant, investment
l	Membrane thickness
m, $\dot{m}$	Mass, mass flow
M	Molecular weight
n	Number of moles
$\bar{n}$	Cost degression exponent
$O_{min}$	Minimum oxygen requirement
p	Pressure
P	Power
Q	Heat
R	Gas constant
s, S	Entropy (specific, absolute)
$s_{CO_2}$	CO <sub>2</sub> separation factor in gas separation process alone. Relation of mass flow of the separated CO <sub>2</sub> to the mass flow of CO <sub>2</sub> in the raw gas.
$r_{CO_2}$	CO <sub>2</sub> capture ratio, consisting of all process steps such as gas conversion and CO <sub>2</sub> separation of the gas separation process. The value of CO <sub>2</sub> capture ratio $r_{CO_2}$ is the quotient of the separated CO <sub>2</sub> molar flow and the molar amount of carbon in the fuel.
T	Temperature in K
t	Temperature in °C
V	Volume
W	Work
$w_{O_2}$	Specific work for the generation of O <sub>2</sub> (kWh/kg O <sub>2</sub> )
$w_t$	Specific gas turbine work, in relation to the air mass flow in the compressor
$x_i$	Mass fraction of component i
x	Moisture content in the steam
$y_i$	Volume fraction of component i
$\alpha$	Equivalence factor for the conversion of a supplied exergy in the steam cycle into electrical energy
$\alpha_{ij}$	Selectivity in mass separation (two indices)
$\kappa$	Adiabatic exponent
$\pi$	Compressor pressure ratio











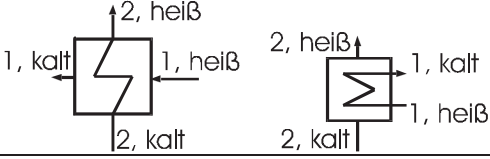


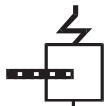







$\eta$	Energetic efficiency (in relation to LHV, if not otherwise indicated)
$\Delta$	Change in a value vs. a another value
$\Delta_r H$	Reaction enthalpy
$\Delta\bar{\eta}, \Delta\eta$	Efficiency penalty through measures for CO <sub>2</sub> capture vs. a baseline plant of the same type without CO <sub>2</sub> capture (in relation to LHV). $\Delta\bar{\eta} = \eta_{\text{Reference}} - \eta_i$
$\mathcal{E}_{CO_2}$	CO <sub>2</sub> emissions reduction
$\epsilon_{RU}$	Performance coefficient of a refrigerating unit
$\psi$	Utilization of fuel energy
$\zeta$	Exergetic efficiency
$\epsilon_i$	Mass fraction of component i







## INDICES

<i>B</i>	fuel
<i>C</i>	carbon
<i>CC</i>	combustion chamber
<i>Comp</i>	compressor
<i>el</i>	electrical
<i>f</i>	feed
<i>FG</i>	flue gas
<i>gas</i>	gaseous
<i>GT</i>	gas turbine
<i>int</i>	internal consumption
<i>crit</i>	critical point (thermodynamic)
<i>liq</i>	liquid
<i>max</i>	maximum
<i>min</i>	minimum
<i>opt</i>	optimum
<i>p</i>	permeate
<i>Reference</i>	reference power plant
<i>RRG</i>	raw gas/clean gas heat exchanger
<i>r, rev</i>	reversible
<i>S</i>	steam
<i>S</i>	state of saturation
<i>ST</i>	steam turbine
<i>t, T</i>	turbine
<i>tot</i>	total
<i>U</i>	ambient conditions
<i>wgs</i>	homogeneous water/gas reaction (CO shift reaction)
<i>Z</i>	steam extraction



## Graphical Symbols

	Circulating water (condensate, cooling water, feedwater, ...)
	Steam
	Waste water
	Air
	Combustible gases
	Non-combustible gases
	Solid fuel (hard coal or bituminous coal, brown coal or lignite)
	Other solids
	Shut-off device, throttle (open)
	Shut-off device, throttle (closed)
	Heat exchanger (heiss = hot, kalt = cold)
	Evaporator
	Heat recovery steam generator with superheater, flue gas heated
	Steam generator with superheater, coal-fired
	Steam condenser
	Fuel gasifier
	Combustion chamber
	Turbine (depending on material flow symbol: steam turbine, gas turbine, liquid fluid turbine)
	AC motor
	Generator
	Liquid pump

	Compressor, vacuum pump
	Separator
	Rotary separator, e.g. cyclone, particulates separator
	Wet separator, scrubber
	Tank with its accessories (packed column, catalytic reactor,...)
	Tank, feedwater container

## Abstract

CO<sub>2</sub> capture in power plants is one possible measure, which could potentially be used to reduce CO<sub>2</sub> emissions in the future. This work contains a summary of methods of CO<sub>2</sub> capture in power plants, which are currently under discussion. It includes an energy analysis of the individual methods, as well as an assessment of specific CO<sub>2</sub> emissions, penalties in efficiency resulting from CO<sub>2</sub> capture, additional investment required, additional electricity generation costs incurred, CO<sub>2</sub> avoidance costs and technical feasibility. The following methods of CO<sub>2</sub> capture are examined: separation of carbon dioxide from synthesis gases following CO conversion, CO<sub>2</sub> concentration in flue gas through combustion in an atmosphere consisting of oxygen and recirculated flue gas, carbon dioxide separation from flue gases, and CO<sub>2</sub> capture in power plants with fuel cells. In addition to the various power plant cycles, gas separation methods such as absorption, adsorption, membrane separation processes, and cryogenic processes are analyzed.

A comprehensive review of the literature indicates that cited levels of efficiency in power plants with CO<sub>2</sub> capture, and the efficiency penalties, are scattered over a broad range. This makes it difficult to assess differences between the various methods of CO<sub>2</sub> capture and different types of power plants. Furthermore, the majority of published studies on CO<sub>2</sub> capture in power plants fail to provide an in-depth analysis of the energetics.

Highly efficient power plants consume less primary energy and produce less CO<sub>2</sub>. At the same electrical power out, with increased efficiency, the CO<sub>2</sub> mass flow to be separated, and thus the expenditure on energy and equipment required for CO<sub>2</sub> capture, is smaller. The calculations in this study therefore focus on those power plants, which currently display the greatest efficiency potential, specifically natural gas-fired gas/steam turbine combined cycle (GTCC) power plants and integrated gasification combined cycle (IGCC) power plants.

To enable direct comparisons to be made, a number of my own calculations of power plant cycles and gas separation methods are performed under standardized conditions, and the contributions of the individual process steps to CO<sub>2</sub> capture are analyzed. The minimum expenditure required for CO<sub>2</sub> capture and the effectiveness of individual methods are examined by means of the reversible separation work and other ideal process steps. These indicate the development potential. In addition to the gas separation techniques, this study also examines CO conversion and – for processes involving concentration of CO<sub>2</sub> in the exhaust gas – cycles with CO<sub>2</sub> as a working substance, and O<sub>2</sub> supply. For processes involving CO<sub>2</sub> concentration in the exhaust gas, a selective O<sub>2</sub> supply is proposed. In a theoretical, ideal case, this would allow for capture of gaseous CO<sub>2</sub> through combustion in an atmosphere consisting of O<sub>2</sub> and recirculated CO<sub>2</sub>, without any further energy requirement.

CO<sub>2</sub> capture in coal-fired power plants, and CO<sub>2</sub> liquefaction, result in an efficiency penalty of between 6 and 14 percentage points. An evaluation of the techniques for CO<sub>2</sub> capture in coal-fired power plants demonstrates that the most favorable method, at current levels of technology, is separation of carbon dioxide from the synthesis gas of an IGCC following CO conversion. With regard to CO<sub>2</sub> capture in natural gas-fired power plants, the most suitable method, with the current state of the technology, is CO<sub>2</sub> scrubbing from the flue gas. CO<sub>2</sub> avoidance costs for CO<sub>2</sub> capture and liquefaction range from 20 to 45 US\$/t CO<sub>2</sub>. This does not include the cost of transporting and disposing of the CO<sub>2</sub>, which adds on an additional 7 to 14 US\$/t CO<sub>2</sub> (based on a pipeline length of 1000 km). Thus, CO<sub>2</sub> capture in power plants only becomes an interesting proposition in the case where global CO<sub>2</sub> emission reduction targets are greater than 10%.

# 1 INTRODUCTION

## 1.1 The Problem

As early as 1896, Arrhenius estimated the influence of atmospheric carbon dioxide ( $\text{CO}_2$ ) on the temperature of the Earth's surface [9]. The first World Climate Conference, backed by the United Nations, took place in 1979, and was followed by further conferences, which continue to the present day, all prompted by the concern that increasing concentrations of  $\text{CO}_2$  and other trace gases (such as  $\text{CH}_4$ ,  $\text{N}_2\text{O}$  and fluorocarbons) in the Earth's atmosphere could lead to global warming. The "International Energy Agency" (IEA) set up a special group (IEA Greenhouse Gas R&D) engaged on the task of reducing greenhouse gas emissions. Since 1992, this group has held a series of conferences focusing on methods for the capture and disposal of  $\text{CO}_2$ .

Of all the anthropogenic greenhouse gas emissions,  $\text{CO}_2$  makes the most significant contribution towards the greenhouse effect (Figure 1.1) [10]. Since the start of the industrial era,  $\text{CO}_2$  concentration as a proportion by volume has risen from 280 ppm to 360 ppm today. This increase in  $\text{CO}_2$  concentration has primarily been caused by the increasing combustion of fossil fuels (Figure 1.2). According to a number of predictions, global energy consumption based on fossil energy fuels will continue to climb [11, 12]. For the long term, to prevent a  $\text{CO}_2$  concentration exceeding a proportion by volume of 500 ppm, projected worldwide  $\text{CO}_2$  emissions will have to be cut by around 40% as early as the year 2025 [10, 13]. According to Schönwiese [14],  $\text{CO}_2$  emissions will have to be halved by the middle of the next century. Taking into account the lesser obligations of the Third World to reduce emissions, this would mean industrialized countries having to achieve  $\text{CO}_2$  emission reductions of 80%.<sup>1</sup>

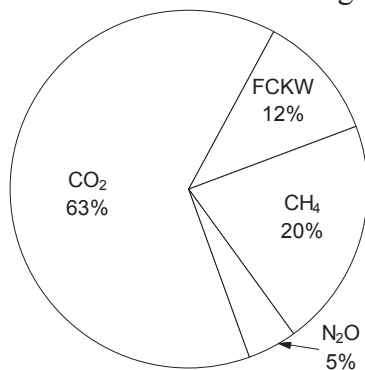


Fig. 1.1: Proportional contributions of anthropogenic greenhouse gas emissions towards climate change, allowing for effects over a period of 100 years [10]

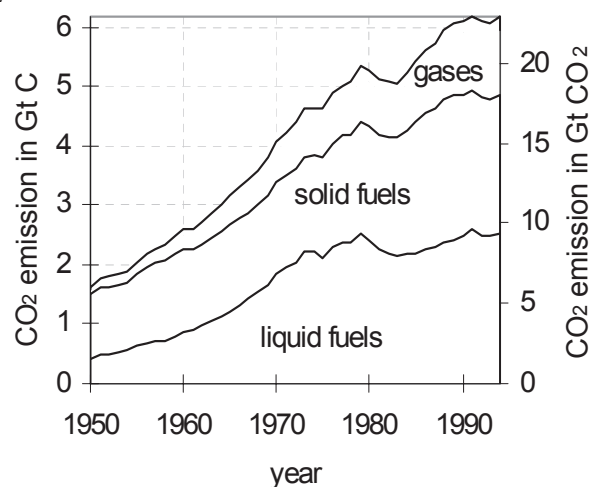


Fig. 1.2: Development of global  $\text{CO}_2$  emissions from various fossil fuels [15]

In addition to energy conservation, improvements in energy efficiency, and the use of low-carbon or carbon-free primary energy sources (nuclear fuels, renewable energies), another possible measure<sup>1</sup> is  $\text{CO}_2$  capture in power plants. This study analyzes and evaluates the possibilities of this latter measure. The  $\text{CO}_2$  separated in this process must subsequently be disposed of in a permanent manner. This disposal process is described in other studies (see Section 2.2.1) and is not dealt with in this paper.

<sup>1</sup> See also Appendix, Sections 6.1 and 6.2

## 1.2 Task Definition

The purpose of this dissertation is to analyze and compare methods of CO<sub>2</sub> capture in power plants fired with fossil fuels. This paper also provides a comprehensive overview of proposals described in the literature, and includes calculations and comparisons of the expenditure of energy and exergy in these proposals, as well as levels of efficiency and efficiency penalties.

The technical implementation of CO<sub>2</sub> capture in power plants and a comparison of the methods have already been presented in numerous publications, (e.g. [16, 17, 18]). However, no analysis of the energetics of CO<sub>2</sub> capture in power plants has yet been described, which systematically demonstrates the impact of CO<sub>2</sub> capture.

The overview of the literature presented in Chapter 2 of this work ("State of the Science and Technology") incorporates a far greater number of process variants than previous studies, and includes process data such as efficiency, CO<sub>2</sub> emissions and costs.

By combining the various concepts for the integration of CO<sub>2</sub> capture in the plant as a whole, with the different types of power plant and gas separation methods, it is possible to generate a large number of different power plant processes with CO<sub>2</sub> capture. In this study, the methods of CO<sub>2</sub> capture in power plants have been divided into five process families, taking into consideration data from the literature, as well as fundamentals of thermodynamics and process engineering:

### Grouping the Methods of CO<sub>2</sub> Capture

- In **Process Family I**, CO<sub>2</sub> is removed from synthesis gases, which are produced through coal gasification or steam reforming of natural gas. For CO<sub>2</sub> capture, the CO in the synthesis gas must be converted into CO<sub>2</sub> and H<sub>2</sub> through CO conversion with the addition of steam. Following CO<sub>2</sub>/H<sub>2</sub> separation, the hydrogen-rich fuel gas undergoes combustion with air in a gas turbine, subsequent to which the CO<sub>2</sub> is disposed of.
- **Process Family II (CO<sub>2</sub> enrichment)** comprises all those processes, in which exhaust gas consisting of CO<sub>2</sub> and steam is produced through combustion in an atmosphere of oxygen and recirculated flue gas or steam. In cycles with CO<sub>2</sub> condensation, liquid CO<sub>2</sub> can be separated without further CO<sub>2</sub> liquefaction.
- **Process Family III** includes all those combinations of power plant processes in which CO<sub>2</sub> is removed from the flue gas at the cold end.
- **Process Family IV** comprises processes such as the so-called hydrocarb process, in which carbon is removed from the fuel prior to combustion.
- **Process Family V** deals with CO<sub>2</sub> capture in power plants with fuel cells, which can be operated with combustible gases of fossil origin.

Building on a comprehensive review of the literature dealing with CO<sub>2</sub> capture in power plants (Chapter 2, "State of the Science and Technology"), this work goes on to consider the distinctive characteristics of the various combinations of different power plant types and methods of CO<sub>2</sub> capture.

The studies presented in the literature are based on very different assumptions; consequently, their results are scattered over a very broad range (Figure 1.3). For a better comparison of the studies, the data contained in the literature has been converted to come close to a set of standardized process conditions (see Chapter 2.2.8, Table 2.18).

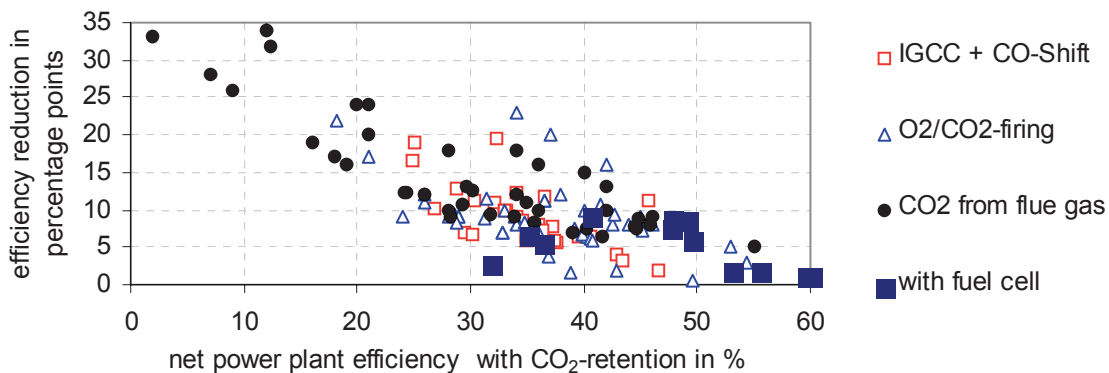


Figure 1.3: Variance of data from the literature (see Chapter 2, "State of the Science and Technology") relating to the efficiency of power plants with CO<sub>2</sub> capture, and efficiency penalties resulting from CO<sub>2</sub> capture and liquefaction.

Chapter 3 ("Energy and Exergy Analysis") determines the fundamental thermodynamic principles for the most important methods of CO<sub>2</sub> capture in power plants, and analyzes how individual process steps involved in CO<sub>2</sub> capture impact on the energy balance and exergy balance in real processes and, in some instances, in ideal processes. Detailed calculations in this study are based on standardized boundary conditions and process conditions. The core of the calculations deal with gas separation methods, chemical conversion of gases, and combined cycle power plants, which therefore also requires the thermodynamic calculation of coal gasification, gas turbines and gas/steam turbine combined cycle power plants (GTCC, also known as GUD power plants<sup>2</sup>).

In the literature (see Chapter 2, "State of the Science and Technology"), the expenditure of energy in technical installations is described. In addition to examining the processes under real conditions, this present study also determines the minimum expenditure of energy for the ideal case with reversible changes of state, and the process-related, minimal irreversibilities, and from this the minimum expenditure for CO<sub>2</sub> capture in the various integrated systems.

Cost comparisons are presented in Chapter 4 ("Economic Comparison of Power Plant Cycles with CO<sub>2</sub> Capture"). Based on estimations of required investment for the individual component groups of the power plants and for the CO<sub>2</sub> separating equipment, this chapter calculates the electricity generating costs of the power plants with CO<sub>2</sub> capture, and the CO<sub>2</sub> avoidance costs.

<sup>2</sup> GUD is a registered trademark of the Siemens company and stands for "*Gas und Dampf*" (gas and steam) power plant (GTCC).

### 1.3 CO<sub>2</sub> Capture: Definitions

Some of the terms relating to CO<sub>2</sub> capture used in this study are not particularly common, and are therefore explained below. Definitions of separation behavior and of operation conditions of gas separation methods are given in the description of the relevant process.

CO<sub>2</sub> separation, CO<sub>2</sub> separation factor  $s_{CO_2}$  : This represents the effectiveness of a gas separation method alone. The CO<sub>2</sub> separation factor  $s_{CO_2}$  refers solely to the mass flow of CO<sub>2</sub> present in the raw gas (not in the primary fuel); it is the ratio between the mass flow of separated CO<sub>2</sub> and the mass flow of CO<sub>2</sub> in the raw gas.

CO<sub>2</sub> capture, CO<sub>2</sub> capture ratio  $r_{CO_2}$  : CO<sub>2</sub> capture is the overall effect produced by gas separation and other process steps, enabling a portion of the CO<sub>2</sub> to be separated from the process as a separate mass flow and stored or used in some other manner. The CO<sub>2</sub> capture ratio  $r_{CO_2}$  is the ratio between the separated CO<sub>2</sub> mass flow rate and the mass flow rate of the carbon in the primary fuel supplied, or the CO<sub>2</sub> produced from this, respectively:

$$r_{CO_2} = \frac{\dot{n}_{CO_2,removed}}{\dot{n}_{C,fuel}} = \frac{\dot{m}_{CO_2,removed}}{\dot{m}_{C,fuel} \cdot \frac{M_{CO_2}}{M_C}} \quad (1.1)$$

In the above equation,  $\frac{M_{CO_2}}{M_C}$  is the ratio between the molecular weights of CO<sub>2</sub> and carbon.

#### Reference Power Plant:

The term "reference power plant" refers to a power plant with no CO<sub>2</sub> capture. Efficiency penalties, reductions in CO<sub>2</sub> emissions and CO<sub>2</sub> avoidance costs resulting from CO<sub>2</sub> capture are calculated relative to the reference power plant. The reference power plant can be an equivalent type of power plant (baseline power plant, see below), or alternatively any other type of power plant, or the average of a power plant park, for example.

#### Baseline Power Plant:

In this document, a baseline power plant is considered to be a reference power plant with no CO<sub>2</sub> capture, where this is equivalent in type to the corresponding power plant with CO<sub>2</sub> capture or where the power plant with CO<sub>2</sub> capture is derived from the process layout of the baseline power plant.

#### Specific CO<sub>2</sub> Emissions Reduction $\varepsilon_{CO_2}$ of a Power Plant ( $i$ ):

The specific CO<sub>2</sub> emissions reduction of a power plant ( $i$ ) is the reduction in the emitted, i.e. non-separated CO<sub>2</sub> quantity  $m_{CO_2}$ , at the same level of power  $P_{el}$  as the reference power plant without CO<sub>2</sub> capture:

$$\varepsilon_{CO_2} = 1 - \frac{\left( \frac{\dot{m}_{CO_2}}{P_{el}} \right)_i}{\left( \frac{\dot{m}_{CO_2}}{P_{el}} \right)_{reference}} \quad (1.2)$$

This equation applies to cases where the reference power plant is of the same type and uses the same fuel (baseline power plant), as well as to cases where the fuel is changed or the reference power plant is of a different type (i.e. the formula also applies in the case of an IGCC power plant with CO<sub>2</sub> capture compared to a baseline plant of the pulverized coal-fired steam type, for example, or even a gas-fired gas turbine cycle).

Since CO<sub>2</sub> capture also involves efficiency penalties, the CO<sub>2</sub> emissions reduction  $\varepsilon_{CO_2}$  differs from the CO<sub>2</sub> capture ratio  $r_{CO_2}$ . Assuming that the fuel composition remains the same, CO<sub>2</sub> emissions reduction  $\varepsilon_{CO_2}$  may be calculated from efficiency penalty  $\Delta\bar{\eta} = \eta_{reference} - \eta_i$  and CO<sub>2</sub> capture ratio  $r_{CO_2}$ <sup>3</sup>:

$$\varepsilon_{CO_2} = 1 - \frac{\eta_{reference}}{\eta_{reference} - \Delta\bar{\eta}} (1 - r_{CO_2}) \quad (1.3)$$

This equation shows that the CO<sub>2</sub> emissions reduction is affected less by efficiency penalty  $\Delta\bar{\eta}$  at high efficiency levels of the reference power plant than at low efficiency levels. In the case of  $r_{CO_2} = 0$  and negative  $\Delta\bar{\eta}$ , CO<sub>2</sub> emissions reduction is obtained merely through efficiency improvement<sup>3</sup>.

CO<sub>2</sub> avoidance costs  $k_{CO_2}$  :

CO<sub>2</sub> avoidance costs are the additional costs associated with the avoidance of CO<sub>2</sub> emissions, incurred over the planning, construction and lifetime of a measure. The CO<sub>2</sub> avoidance costs  $k_{CO_2}$  are calculated from the ratio between the increase in electricity generating costs  $k_{el,i}$  and the difference between the specific CO<sub>2</sub> emissions (relating to the electrical energy output)  $\dot{m}_{CO_2,i}$  of the reference power plant and power plant (i):

$$k_{CO_2} = \frac{k_{el,i} - k_{el,reference}}{\dot{m}_{CO_2,reference} - \dot{m}_{CO_2,i}} \quad (1.4)$$

<sup>3</sup> Efficiency penalty  $\Delta\bar{\eta}$  resulting from CO<sub>2</sub> capture is considered here as a positive value. This involves reversing the sign, when compared with other publications, in which the efficiency improvement with no CO<sub>2</sub> capture, as a measure of CO<sub>2</sub> emissions reduction, is counted as positive.



## 2 STATE OF THE SCIENCE AND TECHNOLOGY

### 2.1 Baseline Efficiencies

By improving the efficiency of a power plant, both fuel consumption and, as a result, CO<sub>2</sub> emissions, are reduced. In contrast, CO<sub>2</sub> capture requires an additional expenditure of energy, and thus causes a penalty in efficiency. However, the additional expenditure of energy associated with CO<sub>2</sub> capture becomes smaller as the efficiency of a power plant increases, since higher efficiency means lower production of CO<sub>2</sub>. For this reason, when considering the baseline power plant with no CO<sub>2</sub> capture, on which the development of a concept involving CO<sub>2</sub> capture is to be based, it is essential that this baseline power plant should achieve the highest possible level of efficiency.

Table 2.1 contains a summary of the various power plants, which have either already been introduced, as of today, or are currently under development, together with improvement measures and efficiency potentials. The most important measures for improving efficiency involve increasing steam temperatures and gas turbine inlet temperatures, and improving waste heat utilization and component efficiency [19].

Of all the power plants currently capable of being built, natural gas-fired gas turbine combined cycle (GTCC) power plants (Table 2.2) achieve the highest efficiency, lowest CO<sub>2</sub> emissions and lowest costs (Table 2.2).

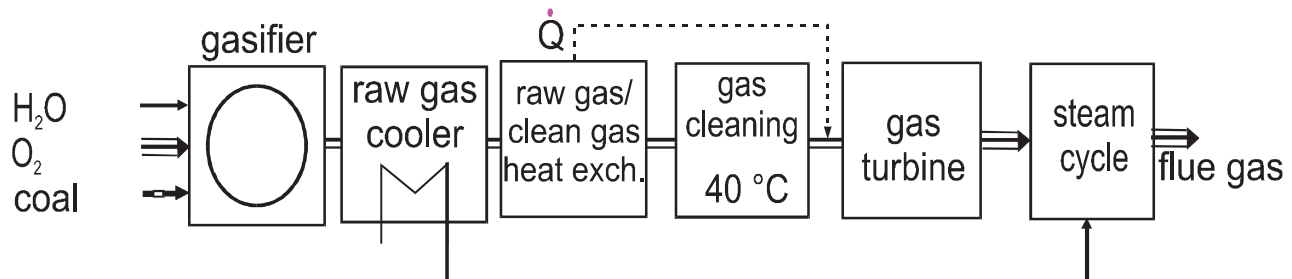


Figure 2.1: Simplified flow diagram of an integrated gasification combined cycle (IGCC) power plant with low-temperature gas cleaning

The most common coal-fired power plant is the steam power plant with pulverized coal combustion at atmospheric pressure. Coal-fired combined cycle power plant cycles with pressurized fluidized bed combustion (PFBC) are commercially viable, but display limited efficiency (43%); integrated gasification combined cycle (IGCC) power plants (Figure 2.1) are in the demonstration phase, and pressurized pulverized coal-fired combined cycle power plants are at an early stage of development. Among the coal-fired power plants, the greatest level of efficiency, at current levels of technology for coal-fired plants, is attained by the IGCC power plants. This is why a large proportion of studies on CO<sub>2</sub> capture in coal-fired power plants suggest the IGCC power plant [20]. Another advantage of the IGCC power plant, in terms of CO<sub>2</sub> capture, is that this is the only type of coal power plant, which allows CO<sub>2</sub> to be separated, prior to combustion, from a gas flow, which is not diluted with air. According to recent studies, there is now virtually no difference between the electricity generating costs of coal-fired steam power plants and IGCC power plants of the next generation, in cases where the annual utilization factor is high [21].

Table 2.1: Efficiency of current power plant types and efficiency potential stemming from possibilities for improvement and for future power plant cycles [22]<sup>4</sup>

Year of Initial Operation	Example	Operating Characteristics	Efficiency in %
<b>Natural Gas-Fired Power Plant Cycles</b>			
1998	Gas turbine simple cycle	TIT approx. 1190°C (ISO 2314) <sup>5</sup>	approx. 38-40
1997	GT with reheat		approx. 38
1998	GT with recuperation		approx. 40
1996	GT with steam injection (STIG/Cheng)		<45
>1998	Humid Air GT (HAT)		approx. 58-59
>>2000	GT with chemical recuperation (CRGT)		55-62
1998	Gas / steam turbine combined cycle power plants	TIT approx. 1190°C (ISO 2314) <sup>5</sup>	58-59
<b>Fuel cells, natural gas-fired:</b>			
1995 / >2000	PAFC / PEMFC	[23, 24]	approx. 40
>2000 / >2005	MCFC / SOFC combined cycle plant	[23, 24, 25]	55 ... >60
<b>Coal-Fired Steam Power Plants</b>			
Operational since 1998	Coal-fired steam power plant (seawater cooling system) Nordjyllandsvaerket [26]	Steam: 285 bar/580°C/580°C/580°C Feedwater preheating: 300°C Condenser pressure: 0.023 bar 10 feedwater preheating stages	47
Planned for 1999 (adjusted)	Coal-fired steam power plant (wet cooling tower system) Gelsenkirchen-Heßler[27]	Steam: 275 bar/580°C/600°C Feedwater preheating: 300°C Condenser pressure: 0.037 bar 9 feedwater preheating stages	45 to 45.5
Planned for 2001-2005	Coal-fired steam power plant (seawater cooling system) Avedoere 2 [28, 29]	Steam: 300 bar/580°C/600°C Condenser pressure: 0.023 bar	50
Planned for 2010	Coal-fired steam power plant, study [30]	Steam: 700°C	52-55
<b>Coal-Fired Combined Cycle</b>			
1994	Pressurized Fluidized Bed Combustion (PFBC) combined cycle	Gas turbine: 860°C/12 bar	36-40 (1999: >45)
>2010	Pressurized Pulverized Coal-Fired combined cycle power plant (with hot gas clean up or warm gas clean up according to heat exchanger)		>50
	Magneto Hydro Dynamic generator (MHD) + steam cycle		50-60
1993	IGCC Power plant Buggenum (NL)	TIT 1050°C (ISO 2314) <sup>5</sup>	43.2
1998	Puertollano (E)	TIT 1120°C -"	45
>1998	Study, ready for construction in 1998 [21]	TIT >1190°C -"	51.5
≥1998	IGFC (IGCC with fuel cells): PAFC (split fuel stream) / GT combined cycle plant	[31]	approx. 50
>2000	MCFC combined cycle plant	[32]	> 55
>2005	SOFC combined cycle plant	[32]	> 55
	Multiple steam cycles		50-51
	Kalina cycle		>47

There are currently two IGCC power plants in Europe: Buggenum Power Plant (253 MW,  $\eta = 43\%$ , in operation since 1993) and Puertollano (300 MW, rated efficiency 45%, in operation since 1998). Additional IGCC demonstration power plants have been constructed in the USA, thanks to a sponsorship program run by the US Department of Energy.

<sup>4</sup> Key parts of the "Combined Cycles" study were compiled during the writing of this work, such as the chapters dealing with the topics of steam power plants, wet gas clean up, the HAT cycle, multiple steam cycles, the Kalina cycle, the MHD/steam turbine combined cycle, and fuel cells.

<sup>5</sup> It is important to distinguish gas turbine inlet temperature, according to ISO 2314, from combustion chamber/firing temperature, since the influence of blade cooling is not taken into account in the latter temperature (Figure 3.1, 66).

Table 2.2: Levels of efficiency, specific CO<sub>2</sub> emissions and investment costs for power plant types currently ready for construction (off-the-shelf)

	Efficiency (LHV) in %	CO <sub>2</sub> Emissions in kg CO <sub>2</sub> /kWh	Investment in US\$/kW	Elec. Generating Costs in US\$/kWh
Steam power plant, hard coal	45-47	0.69 – 0.79	1050	0.036
IGCC, hard coal	50-52	0.62 – 0.71	1100	0.037
Gas/steam turbine combined cycle	58-59	0.32 – 0.33	510	0.027

## 2.2 Power Plants with CO<sub>2</sub> Capture

### 2.2.1 Overview

In 1977, Marchetti became the first person to put forward the idea of separating CO<sub>2</sub> from flue gases in power stations fired with fossil fuels and sinking it in the ocean [33]. A storage period of several hundred years would at least flatten out the peak of CO<sub>2</sub> concentration in the atmosphere. A wide variety of proven absorption methods are available for CO<sub>2</sub> capture; furthermore, demonstration plants, provided with absorption facilities, are in operation, and adsorption processes are under development in laboratory tests. Removing CO<sub>2</sub> by condensing it or freezing it has also been considered in some proposals.

The idea of burning fuel in an atmosphere of recirculated flue gas enriched with oxygen originated from Horn and Steinberg [34, 35]. The flue gas would then consist, primarily, of carbon dioxide and water vapor, and it would be easy to subsequently remove the water component through condensation.

When using synthesis gases from coal gasification, the option exists of removing CO<sub>2</sub> at a highly concentrated level from the fuel gas prior to combustion (this option also applies for natural gas subsequent to steam reforming). One way to achieve this is to convert the CO component of the synthesis gas, i.e. conversion of CO (with the addition of steam) into H<sub>2</sub> and CO<sub>2</sub> followed by combustion of the remaining H<sub>2</sub>-rich gas with air (thermodynamically at best in a combined cycle). The alternative possibility is separation of H<sub>2</sub> and CO using a membrane, followed by separate combustion of H<sub>2</sub> in air and CO in “technically” pure O<sub>2</sub>.

Where natural gas or biomass is to be used, Steinberg [36, 37, 38] suggests a process in which, in addition to the generation of CH<sub>4</sub> or methanol, a further variation allows for only the hydrogen component of the fuel mixture to be used as an energy supply, and for the carbon component to be stored as carbon black.

Fuel cells provide particularly advantageous conditions for CO<sub>2</sub> capture, since they already feature gas separation as part of the system, and the electrochemical oxidation is performed with the exclusion of atmospheric nitrogen.

### *Demonstration Plants*

The separation of CO<sub>2</sub> from power plant flue gases has already been demonstrated to be technically feasible. In the period between 1982 and 1986, chemical scrubbing, based on an aqueous solution with a percentage by weight of 20% monoethanolamine (MEA), was carried out in two locations: the natural gas-fired Lubbock Power Plant in Texas, USA (50 MW), and a natural gas-fired steam generator in Carlsbad (New Mexico, USA). The mass flow of CO<sub>2</sub> leaving the two plants was on a scale of 1000 t and 113 t per day, respectively. It was used to enhance oil recovery in neighboring oilfields.

Deterioration in the economic climate, coupled with lower oil prices, led to the two plants being shut down [39]. Since 1991, CO<sub>2</sub> scrubbing with a 15 to 20% MEA solution has been carried out in the 300 MW Shady Point Combined Heat and Power Station (Oklahoma, USA), and in a coal-fired steam generator of a soda ash plant in Botswana. At these sites, more than 400 t of a 99.99+% pure CO<sub>2</sub> product (dry basis) are produced each day, and are used for the food industry and in oil recovery [40, 41, 42]. In Japan and in the USA, demonstration and test plants are currently seeking to use additives to achieve a higher concentration of the MEA solution without increasing oxidation of the absorbent [43, 39].

Norway and Indonesia are both conducting projects to remove (and actually dispose of) CO<sub>2</sub> from natural gas and from gas turbine exhaust gases. On the gas production platforms of the Norwegian "Sleiper Vest" gas field, the volume fraction of CO<sub>2</sub> in the recovered natural gas is to be reduced from 9.5% to 2.5%; the separated CO<sub>2</sub> is then injected into a 250m-deep aquifer located 800 m below the ocean surface [44]. The primary motivation behind this sequestration process is the CO<sub>2</sub> tax totaling 50 US\$ per ton of CO<sub>2</sub> emitted, which applies to offshore areas of Norway. In another announced project involving the recovery of natural gas from the Indonesian "Natuna" field, the volume fraction of CO<sub>2</sub> in the recovered natural gas must be reduced from 71% to almost 0%. Exxon and Pertamina, the two companies involved in the project, intend to inject the separated CO<sub>2</sub> into a nearby aquifer [45].

### *CO<sub>2</sub> Sequestration*

Storing global, anthropogenic CO<sub>2</sub> emissions amounting to 6 Gt C, corresponding to 22 Gt CO<sub>2</sub> per year, requires global storage capacity on a scale of up to several hundred Gt of carbon. There are a variety of sinks and storage options, e.g.:

- depleted oil and gas fields, as well as enhanced oil and gas recovery through CO<sub>2</sub> injection,
- CH<sub>4</sub> recovery from coal seams by injecting CO<sub>2</sub>,
- aquifers in geological formations,
- oceans (largest capacity),
- fixation in biomasses (afforestation, biomass fuel) or
- solid CO<sub>2</sub> (dry ice) repository: storage in a thermally insulated sphere of dry ice, with a diameter of approximately 200 m (dry ice repository with limited storage period) [46].

A summary of storage capacities, storage duration and costs involved in the sequestration process is given in Table 2.3.

The Strait of Gibraltar has been proposed as a suitable ocean location for CO<sub>2</sub> sequestration, based on the fact that strong currents from the Mediterranean would thin out the CO<sub>2</sub> and transport it to deeper

regions of the Atlantic [47]. Baes [48] has suggested pumping liquid CO<sub>2</sub> into deep beds, where dissolved CO<sub>2</sub> becomes heavier than seawater and sinks; this delays its return into the atmosphere by a few hundred years. When CO<sub>2</sub> is introduced at depths > 1200 m, the density of the CO<sub>2</sub> water solution is greater than that of the surrounding seawater, with the result that the solution sinks [49]. If it is introduced at depths > 3000 m, the density of the CO<sub>2</sub> is greater than that of seawater, with the result that the CO<sub>2</sub> collects on the ocean floor. It is anticipated that the CO<sub>2</sub> would then remain on the ocean bed for more than 1000 years [50]. To avoid the danger to the biosphere posed by high carbonic acid concentrations in the ocean, one proposal is to distribute the CO<sub>2</sub> in the ocean via a pipe extending several hundred meters into the depths, which would be attached to a moving tanker [51]. With regard to the concept of sinking blocks of dry ice in the ocean depths, it is certainly possible to circumvent the associated technical problems posed by deep-sea pipelines, though these methods nevertheless emerge as being, however, very expensive and ineffective, due to the high energy consumption associated with the production process and the losses from thawing during the sinking process.

Injecting CO<sub>2</sub> into oilfields is already a popular method of enhancing oil recovery (also see Table 6.4). As well as improving oil production, CO<sub>2</sub> can also be used to recover methane from coal seams. CO<sub>2</sub> replaces CH<sub>4</sub> in the coal seam and does not get ejected with the CH<sub>4</sub>. The resulting sequestration capacity for CO<sub>2</sub> is greater than the quantity of CO<sub>2</sub> produced by the recovered CH<sub>4</sub>. The first CH<sub>4</sub>-recovery pilot plants using CO<sub>2</sub> are already in operation [52, 53]. This particular method of utilizing CO<sub>2</sub> may even potentially yield profits.

Table 2.3: Natural reservoirs and proposed additional sinks for CO<sub>2</sub> sequestration

Natural Reservoirs	Global Storage Capacity in Gt CO <sub>2</sub>		
Earth's atmosphere	2631	(with 348 ppm volume fraction of CO <sub>2</sub> )	
Dissolved in the ocean	154	(hydrocarbonate, carbonate) [60]	
Potential CO <sub>2</sub> Sinks	Global Storage Capacity in Gt CO <sub>2</sub> [54]	Storage Duration [55] in years	Storage Costs [54] in US\$/t CO <sub>2</sub>
Oceans	> 3664	> 500	1.1 (up to a depth of 500 m) 5.6 (depth of 1200-3000 m)
Aquifers		10 <sup>3</sup> - 10 <sup>6</sup>	1.2
Depleted gas and oil fields	>366	10 <sup>6</sup>	2.2
Oil recovery	238	10 <sup>6</sup>	
Afforestation	4.4 /a	10 <sup>2</sup>	>0.3
Afforestation of the entire agricultural land effective area of the Fed. Rep. of Germany [56]	0.023 /a (<10% of the CO <sub>2</sub> emissions in Germany)		
Chemicals (current market volumes) [55]	< 0.33 /a 0.006 /a	10	
Dry ice repository [46]		800 with 50% loss of CO <sub>2</sub>	130
CO <sub>2</sub> Transport in Pipelines [57]			Ocean: 0.6/100 km Land: 0.8/100 km

Aside from the storage potential in the ocean, underground locations, and gas and oil fields, a maximum of 1.5% of CO<sub>2</sub> emissions could be used for further processing to produce chemical substances. However, the lifespan of chemicals is limited, which means that storage duration is fairly low. Products,

which require CO<sub>2</sub> include uric acid, methanol, polymers, polycarbonate, polyurethane, carbamate, solvents, fuel additives and di-methyl carbonate. A larger quantity of CO<sub>2</sub> could be used to produce methanol as an alternative fuel [20]. Obviously CO<sub>2</sub> used in this way would be re-emitted during combustion of the methanol; the purpose of this measure would therefore be to create a simple storage and transport medium for hydrogen, which would have to be produced without CO<sub>2</sub> emissions.

Biological methods of CO<sub>2</sub> fixation are restricted by the size of the areas required. Fixation of the CO<sub>2</sub> from a 300 MW coal-fired steam power plant would require an area of around 200 km<sup>2</sup> of algae pools, for example [58]. Other proposals highlight the potential of increasing the natural fixation of CO<sub>2</sub> in algae or plankton in the ocean by adding nutrients [59].

In the natural, geochemical carbon cycle<sup>6</sup>, carbon dioxide dissolved in water is absorbed into silicate minerals, as part of an extremely slow-acting, energy-releasing process<sup>7</sup>, and is deposited on the floor as water-insoluble carbonate rock [60]. Silicate minerals thus act as a carbon dioxide sink. Several research studies have therefore attempted to achieve the CO<sub>2</sub> fixation, which occurs in the natural sedimentation process, in an industrial plant, with increased rates of reaction, aiming to fix the CO<sub>2</sub> in rock [61, 62].

Fixation of CO<sub>2</sub> in lime, which first has to be produced through calcination, involves CO<sub>2</sub> emissions equal to the quantity to be taken up at a later point, plus the additional emission of the CO<sub>2</sub> stemming from the primary sources of energy used for the heating process; i.e. the CO<sub>2</sub> emissions produced are greater than the CO<sub>2</sub> absorbed. However, there are some natural rocks, which are capable of chemically absorbing CO<sub>2</sub>. The problem is the mass of rock required in this process. For example, to absorb 1 kg CO<sub>2</sub> would require 1.4 kg CaO or 2.7 kg CaSiO<sub>3</sub>. Since these minerals are only found as components of natural rock, rather than in their pure form, the mass of rock to be moved is correspondingly larger.

### *CO<sub>2</sub> Liquefaction and Transport*

In all cases where CO<sub>2</sub> is to be transported, stored or further processed, it must be compressed at high pressure. As a result, it is nearly always necessary to take into consideration additional energy consumption or an additional efficiency penalty (Table 2.4). The pressure required (Table 2.5) is generally greater than the critical pressure of 73.858 (Table 2.6). The low critical temperature of 31.05 °C means that this nearly always involves liquefaction of the CO<sub>2</sub>.

Pipelines enable the transportation of large mass flows of CO<sub>2</sub>. The USA, Canada and Europe all have many years of experience in transporting CO<sub>2</sub> through pipelines several hundred kilometers long, in the context of CO<sub>2</sub> injection for the purpose of Enhanced Oil Recovery (EOR). Operation of these pipelines has been shown to make more economic sense at supercritical pressures than at lower pressures [63, 64, 65]. Depending on the pressure drop over the total distance, and the differences in elevation of the pipeline, the most suitable pipeline inlet pressure has been cited as high as 172 bar [66, 67, 70].

According to Riemer and Ormerod [68], specific transport costs lie in the range of 0.6 US\$ per t CO<sub>2</sub> and 100 km pipeline length for pipelines in the sea, and 0.8 US\$ per t CO<sub>2</sub> and 100 km pipeline length for overland pipelines.<sup>8</sup>

---

<sup>6</sup> Regarding the natural, geochemical carbon cycle, please also see Appendix, Section 6.3.

<sup>7</sup> Assuming unimpeded silicate weathering, it would take 10000 years to absorb the entire quantity of atmospheric CO<sub>2</sub>. However, hindrances involved in exchange of materials and CO<sub>2</sub> sources must also be taken into account [60].

<sup>8</sup> For sample designs of CO<sub>2</sub> pipelines, see Appendix, Section 6.4.

Table 2.4: Energy consumption for CO<sub>2</sub> compression, liquefaction and dry ice production

	Specific energy expenditure in kWh/kg CO <sub>2</sub>	Energy expenditure related to fuel utilization (coal) in % of LHV
Compression to 110 bar	0.11-0.13	~3.5
Cryogenic liquefaction	0.16 ( 25 bar, -15°C, Linde)	~5.2
Dry ice production [48]	0.26-0.42	~8.4-13.5

Table 2.5: CO<sub>2</sub> pressure for transport, storage or further processing

Pipeline Transport:	82-172 bar [69, 70]
Sequestration in the ocean:	depends on depth at which it is injected, higher density than seawater
Enhancing oil/gas recovery:	90-340 bar [71]
Methanol synthesis:	250-350 bar (BASF), 50-100 bar (S < 0.1 ppm, Lurgi)

Table 2.6: Properties of CO<sub>2</sub>

• Critical temperature	31.05°C	• Critical pressure:	73.858 bar
• Density (at STP):	1.96 kg/m <sup>3</sup>	• Triple point	-56.67°C / 0.518 bar
• Vapor pressure at 20°C:	57.3 bar	• Boiling point at 1.013 bar:	-78.2°C

## 2.2.2 Gas Separation Methods

### Methods of CO<sub>2</sub> or H<sub>2</sub> Separation

Various methods can be used to separate CO<sub>2</sub> and H<sub>2</sub>:

- Absorption
- Adsorption
- Membrane Process
- Cryogenic Engineering Processes (distillation or freezing)
- Other processes; for example, those based on a combination of dissolution processes and magnetic or electrostatic forces (electrochemical processes), or on proposed biological methods of CO<sub>2</sub> absorption using algae or bacteria.

When CO<sub>2</sub> is removed from a gas, which is under pressure, the volumetric flow through the gas turbine decreases, which causes gas turbine output to drop. In addition to the energy consumed by the gas separation process, it is therefore also necessary to take into account the reduction in gas turbine power output, or the work which would have been gained from expansion of the CO<sub>2</sub> stream (e.g. CO<sub>2</sub> removal from a synthesis gas results in a power output reduction of around 0.03 kWh per kg of CO<sub>2</sub> removed, where the gas turbine is designed for a pressure ratio of 16).

### Absorption

Absorption in liquid solvents is a standard industrial process for CO<sub>2</sub> separation, which allows high purity levels and separation factors to be achieved. Table 6.8 (Appendix) gives examples of operating data

for usual absorption techniques.

In the case of physical solvents, solubility is approximately proportional to the partial pressure of the gaseous component. In the case of chemical solvents, saturation of the solvent occurs as loading increases (Figure 2.2). In chemical absorption, after scrubbing from the raw gas, the solvent must be heated up to recover the pure  $\text{CO}_2$  (solvent regeneration). In physical absorption, it must be expanded. In a first approximation, the energy expenditure to regenerate the solvent in chemical scrubbing is proportional to the quantity of gas taken up. In physical scrubbing it is inversely proportional to the partial pressure of the gaseous component to be removed. A rule of thumb would be to use chemical scrubbing when  $\text{CO}_2$  partial pressure is lower than 10 bar, and physical scrubbing when it exceeds this figure. Since the operating temperature for chemical absorption may not be any higher than  $60^\circ\text{C}$  (and for physical absorption it is much lower), the gas to be scrubbed must be cooled to the required temperature. To facilitate comparisons, this study expresses the heat required for regeneration in terms of the lost turbine work of the extracted steam<sup>29</sup>.

Figure 2.3 shows a typical flow diagram for chemical scrubbing.

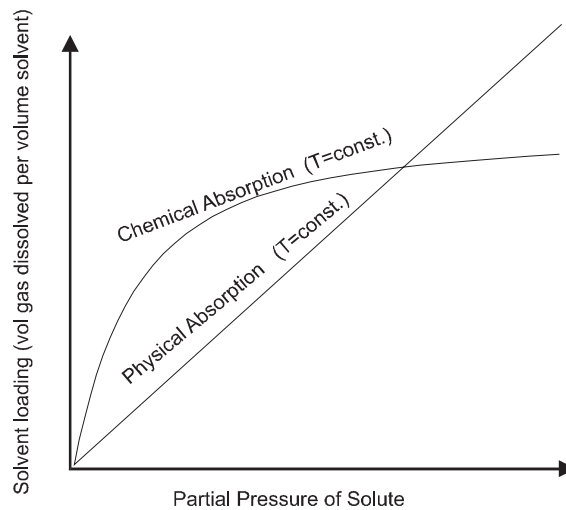


Figure 2.2: Characteristic solvent loading of chemical and physical solvents in dependence on the partial pressure of the dissolved gaseous component

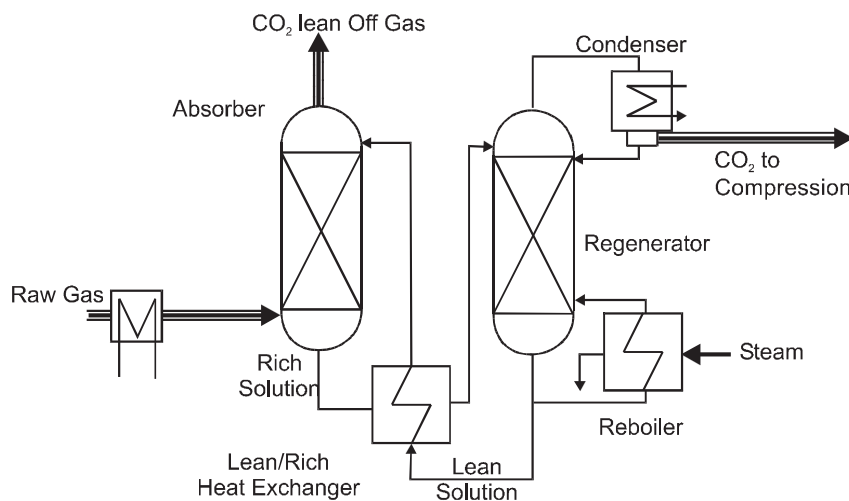


Figure 2.3: Chemical gas scrubbing process flow



## Adsorption

Adsorption of CO<sub>2</sub> in solid solvents requires an expenditure of energy for regeneration through lowering the pressure or increasing the temperature. Industrial plants for CO<sub>2</sub> adsorption are only suitable for small gas streams.

The adsorption process makes use of the different solubilities of gaseous components in a solid. Physical adsorption with regeneration through pressure reduction is referred to as pressure swing adsorption (PSA, Figure 2.4). Chemical adsorption with thermal regeneration is known as temperature swing adsorption (TSA). In addition, there are some processes where regeneration consists of a combination of lowering the pressure and increasing the temperature (PTSA).

Activated carbon or coke, carbon molecular sieves, zeolite molecular sieves or activated aluminum may be used for regenerative pressure swing adsorption. With these substances, the adsorption of CO<sub>2</sub> is greater than that of N<sub>2</sub> or O<sub>2</sub>.

Published data from laboratory and demonstration facilities are summarized in Table 6.8 of the Appendix. For CO<sub>2</sub> adsorption from synthesis gases at 13 to 21 bar, CO<sub>2</sub> separation factors of 60% to 90% are given, with levels of purity of over 99% volume fraction.

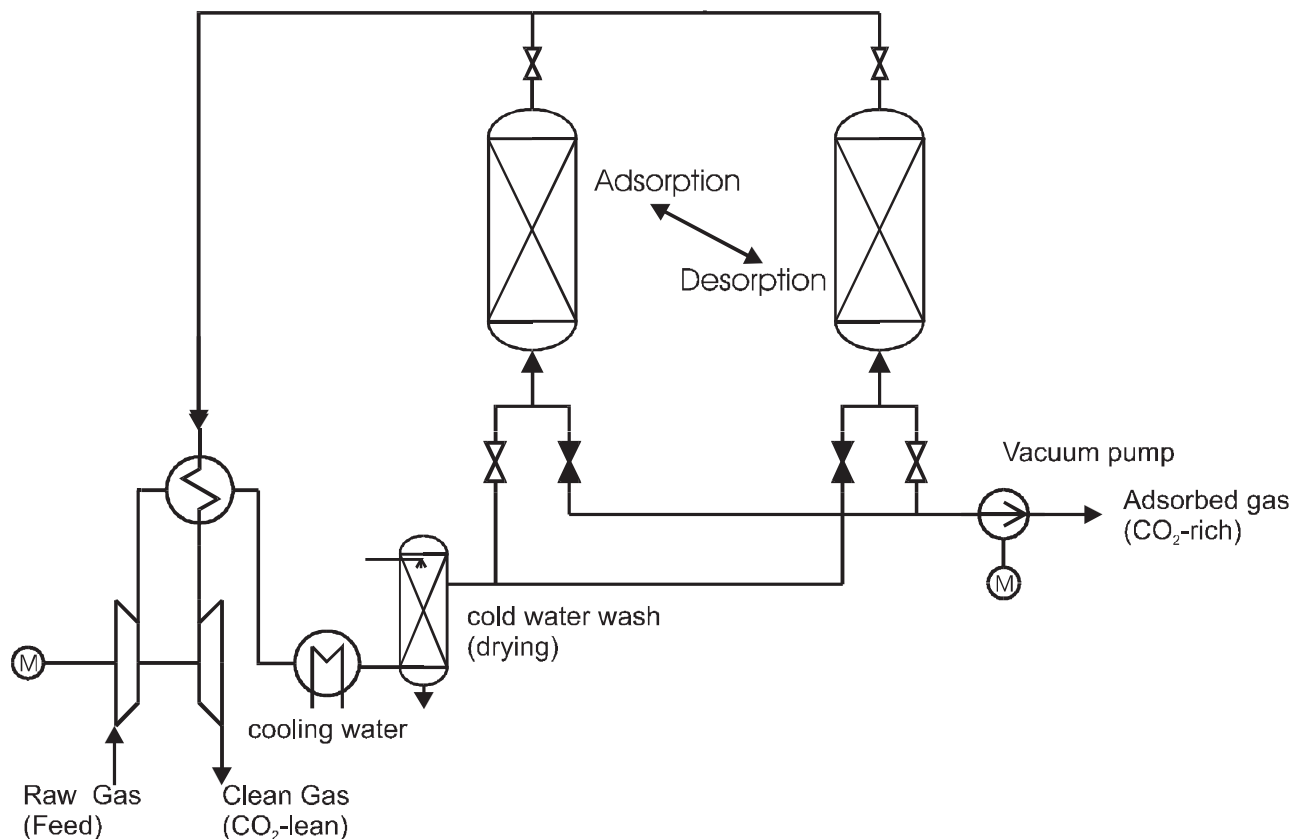


Figure 2.4: Flow diagram of a pressure swing adsorption (PSA) installation

## Membrane Processes

In a membrane process, components, which diffuse more readily, may be separated out by means of a thin layer of material under a pressure differential. Where mass transfer (permeability) is known for the individual components, mass transfer rate  $\dot{m}_{CO_2}$  of CO<sub>2</sub> may be estimated for those membranes, which primarily feature solution/diffusion transport (polymer membrane), according to Fick's Law of diffusion:

$$\dot{m}_{CO_2} = \frac{D_{CO_2} \cdot A \cdot (p_{f,CO_2} - p_{p,CO_2})}{l}, \quad (2.1)$$

where  $D_{CO_2}$  is the permeability of CO<sub>2</sub> through the membrane,  $A$  is the surface area,  $l$  is the membrane thickness and  $p_{f,CO_2}$ ,  $p_{p,CO_2}$  are the partial pressures of CO<sub>2</sub> on the feed ( $f$ ) and permeate ( $p$ ) side of the membrane.

For membranes primarily featuring mass transport through Knudsen diffusion (molecular sieve, ceramic and glass membranes), Sievert's Law applies:

$$\dot{m}_{CO_2} = \frac{D_{CO_2} \cdot A \cdot (\sqrt{p_{f,CO_2}} - \sqrt{p_{p,CO_2}})}{l}. \quad (2.2)$$

Separation (transport) behavior of a membrane is determined by selectivity  $\alpha_{ij}$ , which is defined as the ratio between the permeabilities of two components  $i$  and  $j$ :

$$\alpha_{ij} = \frac{D_i}{D_j} \quad (2.3).$$

In the case of Knudsen diffusion (molecular sieve, ceramic/ glass membranes), selectivity  $\alpha_{ij}$  is approximately determined by molecular weight  $M_i$ ,  $M_j$  of the two components  $i$  and  $j$ :

$$\alpha_{ij} = \sqrt{\frac{M_j}{M_i}}. \quad (2.4)$$

Separation behavior is often described in terms of the separation factor. The separation factor for a binary mixture consisting of H<sub>2</sub> and CO<sub>2</sub> is defined as:

$$\bar{\alpha}_{H_2/CO_2} = \frac{y_{p,H_2} \cdot y_{f,CO_2}}{y_{p,CO_2} \cdot y_{f,H_2}}, \quad (2.5)$$

where  $y$  is the amount of substance, index  $p$  is the permeate and index  $f$  is the feed.

Reducing the gas mixture to a binary system enables us to describe the mass transport in the membrane using the Weller-Stein equation [72]:

$$\frac{\dot{m}_i}{\dot{m}_j} = \alpha_{ij} \frac{\left(\frac{p_f}{p_p}\right)^{y_{fi}} - y_{pi}}{\left(\frac{p_f}{p_p}\right)(1 - y_{fi}) - (1 - y_{pi})}. \quad (2.6)$$

The amount of substance of permeated component  $i$  is then given by:

$$y_{pi} = \frac{-B + \sqrt{B^2 + 4(1 - \alpha_{ij})\alpha_{ij}\left(\frac{p_f}{p_p}\right)^{y_{fi}}}}{2(1 - \alpha_{ij})}, \quad (2.7)$$

$$\text{where } B = (\alpha_{ij} - 1)\left(\frac{p_f}{p_p}\right)^{y_{fi}} + \left(\frac{p_f}{p_p}\right) + (\alpha_{ij} - 1). \quad (2.8)$$

In addition to the quality of the membrane (permeability and selectivity), gas separation is determined by two further process parameters:

- The compression ratio of permeate to feed gas: a large pressure ratio promotes effective separation, but it also leads to a greater compressor work.
- Permeation ratio as the ratio of permeate molar flow to feed molar flow: high purity is obtained at low efficiency. If an increased separation factor is required, the permeation ratio must be increased, and product gas concentration decreases.
- The required membrane surface depends on the permeability, the desired level of efficiency and the pressure ratio. The size of the membrane apparatus is determined by the membrane surface, and the specific membrane surface by volume, which may differ significantly for different membrane types. For example, polymer membranes have low permeabilities, yet they attain the largest specific surface per unit volume when arranged in bundles of hollow fiber membranes.

As a general rule, it is simpler to separate gaseous components with small molecular weights (and possibly to use the retentate as product). This applies in particular to hydrogen removal from synthesis gases, where the result is a retentate rich in CO<sub>2</sub>, correspondingly CO.

In the case of hydrogen or CO<sub>2</sub> removal from a fuel gas, energy losses consist approximately of:

- Pressure loss:
  - The expenditure of work is caused by pressure loss in the permeating gas (permeate). This must be compensated for, either through increased pressure of the feed gas (see Figure 2.5) or through subsequent compression of the permeated gas.
- Losses through residual H<sub>2</sub> in the carbon-rich split flow:
  - additional energy requirements for O<sub>2</sub> production to burn fuel residue
  - poor usage of the released combustion enthalpy in a steam cycle.

The gas, which remains (retentate), has approximately the same pressure as the feed gas. Efficient separation requires high selectivities (ratio of permeabilities), a reasonably sized membrane surface and high permeabilities for the components to be removed. Table 6.9 (Appendix) provides an overview of the selectivities of commercial membranes.

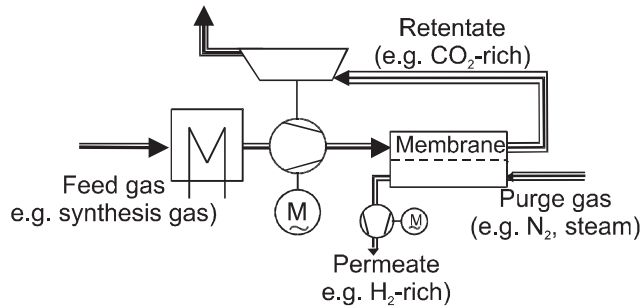


Figure 2.5: Single-stage membrane separation process

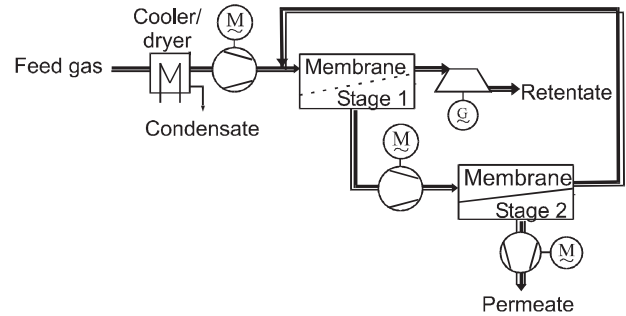


Figure 2.6: Two-stage membrane separation process

By adding a purge gas (e.g. steam or waste nitrogen from the air separation facility of an IGCC) on the permeate side, the partial pressure difference between the permeating components is increased (Figure 2.5). This allows a smaller overall pressure difference to be selected, which, in turn, reduces the energy consumption for the gas separation process. By arranging the membranes over several stages, the purity of the permeate can be increased while simultaneously the yield (separation factor) is lower (Figure 2.6)

H<sub>2</sub> removal from synthesis gases using polymer membranes has now been developed to a stage where it can nearly compete with other processes. In contrast, no competitive application is yet in sight for CO<sub>2</sub> removal from flue gases (CO<sub>2</sub>/N<sub>2</sub> separation), for which the best selectivity is currently 33, as compared to a required minimum selectivity of 200 [73]. Polymer membranes are, however, also used in the pre-separation of CO<sub>2</sub> from natural gas, for example.

## Cryogenic Processes

Direct condensation, sublimation or distillation may all be used, with or without the addition of solvents, to remove CO<sub>2</sub> from mixtures with gases, which only condense/sublime at lower temperatures. In any case, the separation process must be preceded by a drying stage to avoid blockage caused by formed ice.

In cases where CO<sub>2</sub> is the only condensable component of the gas mixture, its partial pressure is reduced by cooling it to the saturation vapor pressure (assuming an ideal gas). The highest CO<sub>2</sub> separation factor  $s_{CO_2}$  is achieved through reducing the temperature and increasing the pressure. CO<sub>2</sub> sublimates below the triple point temperature of -56.6°C.

The principal advantage of CO<sub>2</sub> removal through freezing is that, in theory, the lower sublimation pressure at lower temperatures means that it can be carried out at pressures as low as 4 or 5 bar [16]. In contrast, condensation requires significantly higher pressures to obtain lower separation factors (see also p 93).

One commercial process for CO<sub>2</sub> freezing is the "Controlled Freezing Zone" (CFZ) process designed by Exxon, in which expansion of the CO<sub>2</sub> as it emerges from nozzles causes it to sublime freely in the

chamber, after which it is thawed. One problem, which emerges with freezing using heat exchangers, is how to remove the solid CO<sub>2</sub> from the surfaces of the heat exchanger. With regard to theoretical energy consumption for the production of dry ice through freezing CO<sub>2</sub> out of flue gas (which has 13% volume fraction of CO<sub>2</sub>), Kümmel et al. [74] cite figures of 0.3533 kWh per kg of CO<sub>2</sub> for a CO<sub>2</sub> capture ratio of 80%, and 0.3768 kWh per kg of CO<sub>2</sub> for a CO<sub>2</sub> capture ratio of 90% at 4 bar, -100°C. Hendricks also suggests CO<sub>2</sub> freezing for CO<sub>2</sub> capture in liquid phase due to the advantage of lower operating pressure [16]. The CO<sub>2</sub> would then have to be thawed out in a heat exchanger.

### Oxygen Recovery from Air

The most common type of air separation is liquefaction, in accordance with the Linde method, and rectification in a double column. To achieve oxygen purity of 90% (volume fraction), the feed air must have a pressure of approximately 5 bar, which results in an oxygen product pressure slightly above ambient pressure. For the integration in IGCC power plants, air separation units have been designed with supply air having the final discharge pressure of the gas turbine compressor. The maximum air pressure, which is technically feasible currently, lies in the range of slightly more than 16 bar, with a resulting oxygen pressure of around 6 bar. The nitrogen, which becomes available at around 6 bar, is further compressed in the IGCC power plant and mixed into the fuel gas, in order to maintain the required mass flow ratios between the compressor and turbine<sup>9</sup>, and to reduce NO<sub>x</sub> prior to the gas turbine combustion chamber.

For installations dealing with up to 100 t of O<sub>2</sub> per day, pressure swing adsorption (PSA) or temperature swing adsorption (TSA) are also installed. Membrane processes in laboratory experiments have obtained 85% O<sub>2</sub> (volume fraction)[75].

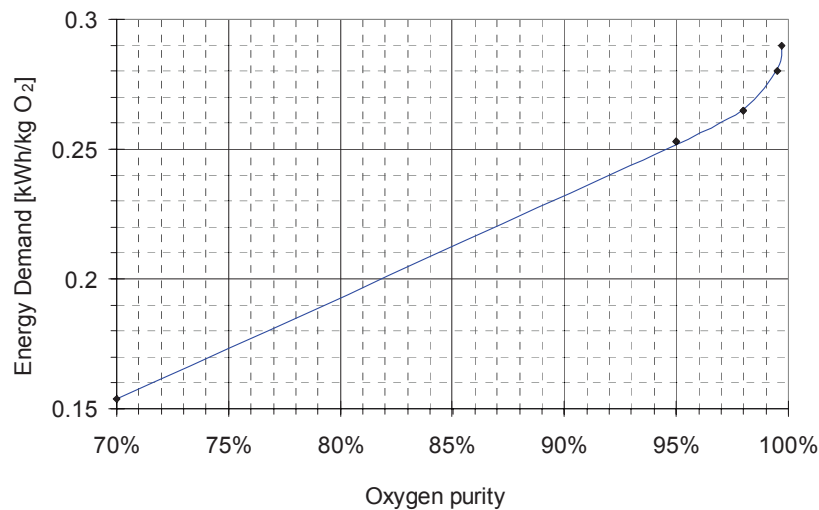


Figure 2.7: Energy expended to produce oxygen in a large-scale double column facility. Figures taken from Springmann [76].

The theoretical, reversible energy consumption for air separation is determined by separation into all the components and reversible compression of each partial pressure to the total pressure:

<sup>9</sup> Currently, all gas turbines are designed for natural gas as a fuel, i.e. the air and exhaust gas mass flows, which prevail in that type of usage must be maintained when using the gas turbine in an IGCC.

$$w_r = T_0 \sum_i \varepsilon_i R_i \ln p_{tot} / p_i \quad (2.9)$$

The reversible separation work<sup>10</sup> required to separate air into all its components is 0.01754 kWh per kg of air, or 0.0759 kWh per kg of O<sub>2</sub>. In contrast, reversible separation work, in which just O<sub>2</sub> is separated from the ambient air, requires just 0.0336 kWh per kg of O<sub>2</sub>. The work required for oxygen production occurs in the course of the cryogenic liquefaction of air utilizing the Joule-Thomson effect, in accordance with the Linde process, with the energy recovery of the cooling and liquefaction cold processes and the subsequent separation of the components through rectification. The basic separation work in a double column is constrained by the liquefaction pressure of the pure nitrogen in a condenser, on the other side of which O<sub>2</sub> is vaporized. It amounts to around 0.05 kWh per kg of air (approx. 0.215 kWh/O<sub>2</sub> with 99.5% volume fraction) [76]. Irreversibilities through heat transfer or turbulence and friction increase the work in a real installation to approx. 0.29 kWh/kg O<sub>2</sub>. The energy used in refrigeration accounts for only 10% of the overall energy demand [76].

To calculate the energy required for O<sub>2</sub> production at 1 bar with cryogenic air separation, this study uses the data given by Springmann [76], in dependence on the O<sub>2</sub> concentration according to Figure 2.7. The energy requirement shown for oxygen production by various methods refers to the production of O<sub>2</sub> at above-atmospheric pressure and subsequent work recovery through expansion of the O<sub>2</sub> to atmospheric pressure. The figures used correspond closely to data published in more recent studies (e.g. [77]).

### Summary: Gas Separation Methods

Due to the differing CO<sub>2</sub> content in synthesis gases and flue gases, a suitable method should be chosen to match the specific application. Synthesis gases mainly consist of hydrogen, carbon monoxide and carbon dioxide. Flue gases mainly consist of nitrogen and carbon dioxide. Additional data on gas separation processes is provided in the Appendix in Section 6.5.

- **CO<sub>2</sub> / H<sub>2</sub> Removal from Synthesis Gases:**

Physical absorption methods have proved themselves to be highly suitable for CO<sub>2</sub> removal from synthesis gases. They are characterized by their low energy demand for solvent regeneration. Taking the additional required heat input as a reduction in steam turbine work<sup>11</sup>, the expenditure for pumps and heat input for CO<sub>2</sub> removal in commercial processes described in the literature amounts to between 0.04 and 0.09 kWh per kg of CO<sub>2</sub> removed. Physical-chemical methods require around 0.04 to 0.07 kWh per kg of CO<sub>2</sub> removed. As a rule, chemical scrubbing is not used for pressurized gases.

Whereas synthesis gas is mostly under pressure, CO<sub>2</sub> is normally released from the desorber at ambient pressure. For this reason, this method requires an additional 0.05 to 0.08 kWh per kg of CO<sub>2</sub> removed, to compress from ambient pressure to the pressure of the synthesis gas.

Membranes used with synthesis gases are only suitable for hydrogen separation. They require high-pressure ratios. Since the carbon-rich retentate generally still has a fairly considerable calorific value, the combustible portions of the retentate have to be burnt with additional oxygen. Commercially available polymer membranes are expensive, but they are fully capable of achieving sufficiently high CO<sub>2</sub> separation factors. Taking into account the lost power from the fuel residues and the production of the oxygen

<sup>10</sup> For more details on "reversible separation work", see Section 3.4.2.

<sup>11</sup> If the heat required is calculated as a reduction in steam turbine power output through steam extraction. For more details, see Section 6.6 of the Appendix.

required to burn these residues, the energy demand for CO<sub>2</sub> capture with membranes totals 0.17 to 0.29 kWh per kg of CO<sub>2</sub> removed.

Methods employing cryogenic technologies require high pressures to perform CO<sub>2</sub> separation through direct condensation without a solvent (88 bar minimum pressure at -56°C; 592 bar minimum pressure at 0°C) in order to achieve a CO<sub>2</sub> separation factor of 90%. Moderate pressures are sufficient for CO<sub>2</sub> freezing, though extremely low temperatures are required (33.6 bar at -70°C; 88.2 bar at -57°C). For CO<sub>2</sub> removal using cryogenic technologies, in theory, only low separation factors can be obtained, and CO<sub>2</sub> freezing has still not been technologically resolved.

Adsorption of CO<sub>2</sub> or H<sub>2</sub> from synthesis gases is technically feasible using very large equipment; the energy demand of approx. 0.16 to 0.2 kWh per kg of CO<sub>2</sub> removed is higher than with physical scrubbing. In this case, too, the compressor work (of around 0.05 to 0.08 kWh per kg of CO<sub>2</sub> removed), must be considered, which is required to compress the pressure of the separated CO<sub>2</sub> to the pressure of the synthesis gas.

- **CO<sub>2</sub> removal from flue gases:**

With regard to CO<sub>2</sub> capture from flue gases, chemical absorption is the method, which achieves the greatest exergetic efficiency (see Section 0). This method has also been shown to be technically feasible. The power consumption of solvent pumps lies in the range of between 0.02 and 0.4 kWh per kg of CO<sub>2</sub> removed. To this must be added the heat requirements for solvent regeneration, amounting to between 0.5 to 1.7 kWh<sup>12</sup> per kg of CO<sub>2</sub> removed.

When using common sorbents such as amine, strict limit values for SO<sub>x</sub> must be maintained in order to minimize loss of the absorbent through corrosion. Physical solvents are not suitable, due to the low CO<sub>2</sub> concentration in flue gases.

Membranes require high-pressure ratios of more than 40 and selectivities of CO<sub>2</sub> to N<sub>2</sub> of almost 200 (not yet achieved), in order to achieve the required rates of separation and purity at competitive levels of energy consumption.

Cryogenic technology methods require pressures of more than 387 bar to directly condense CO<sub>2</sub> or temperatures below -100°C (at 11 bar) to sublime CO<sub>2</sub>. However, there are no installations available with these technical specifications.

Adsorption of CO<sub>2</sub> from flue gases is currently under development and should achieve a specific energy consumption of between 0.42 and 1.2 kWh per kg of CO<sub>2</sub> removed. Large-scale implementation fails due to the large quantities of adsorbent.

### 2.2.3 Process Family I: CO<sub>2</sub> Separation from Synthesis Gas Subsequent to CO Conversion

Synthesis gases can be produced from coal by means of coal gasification, or from natural gas through steam reforming<sup>13</sup>. They mainly consist of CO and H<sub>2</sub>. Minor quantities of other inert gases in coal gases stem from the residual gases in the oxidant and from the transport gas for coal dust sluicing. Without conversion of the CO component, a CO<sub>2</sub> capture ratio of up to around 14% can be achieved solely

---

<sup>12</sup> Enthalpy of the steam

<sup>13</sup> See pp. 22 and 23 for a description of steam reforming and CO shift conversion

through capture of the  $\text{CO}_2$  produced by coal gasification<sup>14</sup>. The efficiency penalty in this case amounts to less than 1 percentage point [78].

By converting  $\text{CO}$  to  $\text{CO}_2$  and  $\text{H}_2$  by adding steam (referred to as the 'carbon monoxide shift reaction', 'water-gas shift reaction', or 'CO shift conversion'), a concentration of  $\text{CO}_2$  can be produced in the fuel gas which is significantly higher than that produced in flue gases generated by the combustion with air of a fuel containing carbon (Figure 2.8). This makes it possible to remove  $\text{CO}_2$  with a lower expenditure of energy. However, the exergy losses caused by the required fuel conversion (CO shift reaction, steam reforming for natural gas) result in a further energy demand. This process is therefore only advantageous if the energy required for CO shift conversion and  $\text{CO}_2$  removal from the synthesis gas is lower than that required for  $\text{CO}_2$  removal from a flue gas diluted with atmospheric nitrogen.

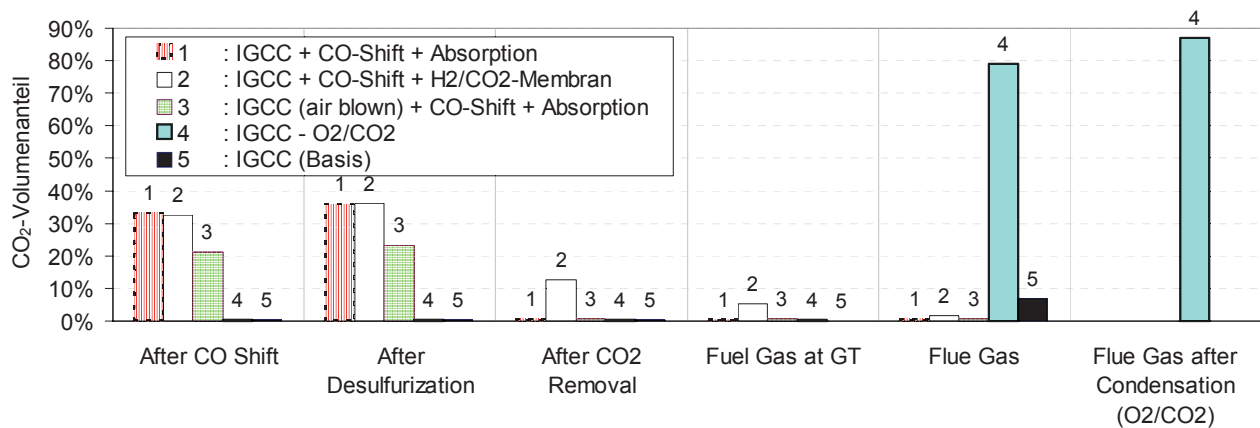


Figure 2.8:  $\text{CO}_2$  volume fractions after various process steps in a baseline IGCC, in an IGCC power plant with CO conversion (CO shift reaction) and  $\text{CO}_2$  scrubbing or with an  $\text{H}_2/\text{CO}_2$  membrane, and in an IGCC power plant with a  $\text{CO}_2$  gas turbine (combustion in an atmosphere of oxygen and recirculated exhaust gas).

Following CO shift conversion, cooling and desulfurization, the  $\text{CO}_2$  can be separated and the carbon-lean, cleaned fuel gas can be delivered into a gas turbine cycle or a fuel cell. Figure 2.9 illustrates the difference between two process arrangements: the first with a clean gas CO shift reaction (clean gas CO conversion), and the second with a raw gas CO shift reaction (raw gas CO conversion) (see also p 24). The CO shift reaction causes the  $\text{CO}_2$  volume fraction to increase from almost zero to approx. 30% (Figure 3.35, Section 3.5.1), and the  $\text{H}_2$  volume fraction to increase from approx. 30% to approx. 50%.

<sup>14</sup> The maximum value is only obtained in a coal gasification process with coal slurry charging, i.e. with low exergetic efficiency.



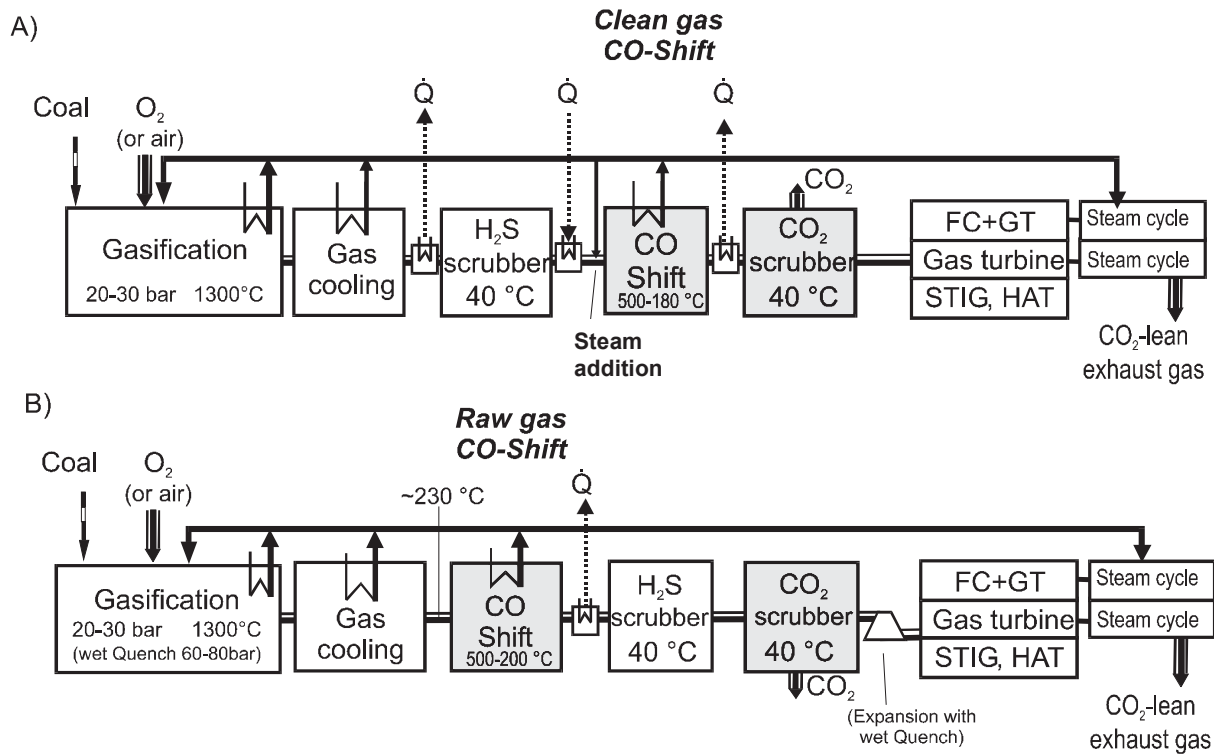


Figure 2.9: Flow diagram of an IGCC power plant using the raw gas heat recovery method to generate steam, with CO conversion (CO shift reaction) and CO<sub>2</sub> scrubbing:  
 A) Clean gas CO shift reaction, B) Raw gas CO shift reaction<sup>15</sup>.

After the CO shift reaction, the fuel gas primarily consists of CO<sub>2</sub> and H<sub>2</sub>. It is therefore necessary to differentiate between two different ways of increasing CO<sub>2</sub> concentration, i.e. either by removing CO<sub>2</sub> or by removing H<sub>2</sub>. If CO<sub>2</sub> is removed, the gas turbine is operated with the remaining H<sub>2</sub>-rich gas (combustion in air) and the previously separated CO<sub>2</sub> is liquefied. If H<sub>2</sub> is removed (separation using membranes), a portion of the combustible components remain in the mixture with the concentrated CO<sub>2</sub>. This portion can subsequently be burnt with technically pure oxygen to avoid fuel losses. The separated, H<sub>2</sub>-rich portion of the gas is burnt with air in the gas turbine combustion chamber.

### 2.2.3.1 Raw Gas Conversion

To remove CO<sub>2</sub> prior to combustion, coal gas and natural gas must be converted into H<sub>2</sub> and CO<sub>2</sub>, the former via the CO shift reaction and the latter through steam reforming and the CO shift reaction.

The **CO shift reaction** (CO shift conversion, water-gas shift reaction) is the exothermic conversion of carbon monoxide and steam into CO<sub>2</sub> and hydrogen:



The exothermic CO shift reaction causes the heating value of one mole of CO (282.98 kJ/mol) to be reduced by 14.5% to the heating value of one mole of hydrogen (241.82 kJ/mol).

<sup>15</sup> In the case of raw gas cooling through direct quenching with water, raw gas CO shift reaction is preferred.

**Steam reforming**<sup>16</sup> refers to the endothermic conversion of hydrocarbons and steam into carbon monoxide and hydrogen, in this case using the example of the steam reforming of methane:



The overall reaction consisting of steam reforming and CO shift reaction of methane and steam into CO<sub>2</sub> and H<sub>2</sub> is endothermic, when taken as a whole:



Endothermic steam reforming, and the subsequent exothermic CO shift reaction of methane and steam, causes the fuel energy flow (LHV) to be increased by 20.6% from 802.34 kJ for one mole of CH<sub>4</sub> to 4 x 241.82 kJ = 967.28 kJ for 4 moles of H<sub>2</sub>.

Higher hydrocarbons can also be converted through similar reactions:



....



To achieve a high CO<sub>2</sub> capture ratio, high CO or CH<sub>4</sub> conversion is required. This can only be achieved with a high excess of water in relation to the stoichiometric reaction. The enthalpy of vaporization delivered with the excess steam contributes significantly to the exergy losses in the CO shift reaction and steam reforming. Additionally, exergy losses occur during cooling of the synthesis gas subsequent to the CO shift reaction, due to condensation of the excess steam component, even if part of the enthalpy of vaporization expended can be recovered via the heat exchanger.

### *Potential For Improvement*

By increasing the number of reaction stages, heat recovery can be improved and the excess of steam can be reduced.

If the reaction products (CO<sub>2</sub>, H<sub>2</sub>) of the CO shift reaction or steam reforming are removed during the reaction, then, in accordance with the Le Chatelier-Braun principle (law of mass action), conversion of the reaction educts (CO, CH<sub>4</sub>, H<sub>2</sub>O) increases, or, alternatively, less steam need be supplied.

Using a combination of a membrane and catalyst, for example, the hydrogen produced during CO shift reaction/steam reforming is separated off, thereby allowing increased CO conversion to be achieved with a low expenditure of energy on steam injection (WIHYS process, see page 31). Other possibilities are, for example, membrane reactors for steam reforming (laboratory tests [103, 104]), or a combination of a CO shift reaction and CO<sub>2</sub> adsorption with limestone or dolomite as a catalyst and absorbent (see Section 3.5.2).

<sup>16</sup> Aside from the process of steam reforming described above, reforming in petrochemical processes refers to a process of catalyst-supported chemical conversion, without additives, effected through a combination of isomerization, aromatization and ring formation.

## Operating Conditions for CO Conversion

In the temperature range between 950°C and 1000°C, a CO shift reaction with synthesis gases takes place at a sufficiently rapid pace even without a catalyst [79]. At lower temperatures, the speed of the reaction is slower, in accordance with Arrhenius' Law, though the Le Chatelier Principle means that more CO is converted at lower temperatures in the exothermic CO shift reaction before the state of chemical equilibrium is reached. In industrial applications, catalysts have long been employed at reaction temperatures of between 180°C and 500°C.

In practice, a state is reached after the converter corresponding to an equilibrium temperature, which lies around 10 to 20 K above the reaction temperature. Pressure losses are between 0.18 and 0.3 bar [79]. For reasons of cooling, equipment size and energy utilization, large-scale conversion processes employ a multistage CO shift reactor with different temperature stages (Figure 2.10).

CO shift reactors are classified according to temperature range, and according to the sensitivity of the catalysts to impurities, in particular to sulfur compounds [80, 81, 82]:

- Catalytic clean gas CO shift conversion:
  - catalyst is sensitive to impurities, i.e. desulfurization required prior to CO shift conversion,
  - advantage: high rate of conversion is possible at low end temperatures,
  - disadvantage: reheating required subsequent to wet desulfurization; in the case of wet desulfurization, the water vapor component of the gas condenses, it must subsequently be humidified; high excess of steam required,
  - maximum CO conversion: approx. 99% (2-stage).
- High temperature CO shift conversion:
  - operating temperature: 300°C to 530°C,
  - rapid conversion/smaller volume, full conversion not possible,
  - catalyst types: Ni/Cr oxide, Fe/Cr oxide,
  - minimal molar ratio of steam to CO: > 2 - 2.2;
  - sulfur tolerance: mass fraction <0.03%.
- Low temperature CO shift conversion:
  - operating temperature: 180°C to 270°C,
  - 2nd stage after HT-CO shift conversion, virtually full CO conversion possible,
  - catalyst types: Cu/Zn oxide,
  - operating temperature: 180°C to 270°C,
  - minimal molar ratio of steam to CO: > 2 - 2.2;
  - sulfur tolerance: volume fraction < 0.1 ppm.

- Catalytic raw gas CO shift conversion:
  - requires sulfur-resistant catalyst; simultaneously partial COS hydrolysis; often requires two-stage execution (HT/LT).
  - advantage: better use of enthalpy (thermal component) and humidity of the raw gas after Venturi scrubbing (higher inlet temperature and raw gas humidity than in clean gas CO shift conversion after wet scrubbing). This also results in lower costs.
  - disadvantage: lower CO conversion rate than with low temperature clean gas CO shift conversion - this latter process may need to be incorporated downstream (combined raw gas/clean gas CO shift conversion).
  - maximum CO conversion: approx. 95% (2 stage).
  - operating temperature: 230°C to 500°C.
  - catalyst: CoMo/Al oxide.
  - same catalysts for all reactor stages.
  - minimal molar ratio of steam to CO: > 1.8 - 2.

If a wet scrubber working at low temperatures is used for desulfurization, the gas must consequently be reheated prior to the clean gas CO shift reaction. Due to the condensing of the water component, it must also be humidified to a greater extent than is necessary in the case of a raw gas CO shift reaction prior to cold scrubbing. This distinction does not apply if a hot, dry desulfurization technique is used, such as an iron oxide bed [83] or a zinc oxide bed [84].

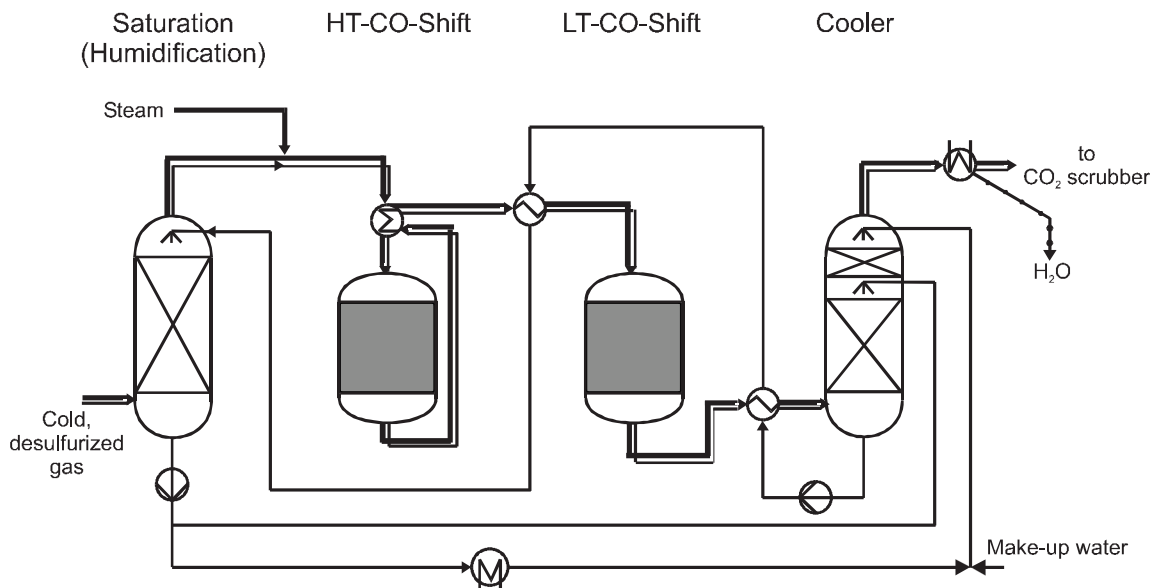


Figure 2.10: Typical arrangement of a two-stage clean gas CO shift conversion process with a cooler-saturator system for heat recovery and for reducing the amount of make-up steam [85, 20]

To set the required proportion of water, the chemical industry frequently employs a cooler-saturator cycle, which utilizes the recovered heat within the "CO shift reactor" system (Figure 2.10). Brand [85], for example, has investigated heat integration with a two-stage CO shift reactor.

In cases where the raw gas is cooled by injecting water (direct quenching), the steam content may be sufficient for the CO shift reaction without the addition of extra steam [79, 86]. At the same time, direct quenching with water results in a greater exergy loss than that found in raw gas heat recovery with external steam generation.

### Operating Conditions for Steam Reforming

According to the Le Chatelier Principle, a high rate of CH<sub>4</sub> conversion is achieved in the endothermic reforming reaction through high temperatures, low pressures and high water excess. Since it is also true that CO conversion in the exothermic CO shift reaction is favored by low temperatures, a further CO shift stage at low temperature must be incorporated downstream in order to achieve the fullest possible conversion of CH<sub>4</sub> to CO<sub>2</sub>. This means heating prior to steam reforming, subsequent cooling for the CO shift reactor and re-cooling for the case of wet CO<sub>2</sub> scrubbing. Heat recovery is only possible to a limited extent, meaning that the heating and cooling processes cause further exergy losses on top of the exergy lost through chemical conversion.

Steam reforming generally takes place at temperatures of between 800°C and 900°C. Pre-reforming can be carried out at temperatures between 325°C and 600°C. Compared to the stoichiometric, molar ratio of steam to methane of 2, the ratio of steam to methane required for commercial catalysts is at least twice as high (4 to 5). In practice, the catalytic reforming reaction results in a composition similar to that achieved with an equilibrium temperature reduced by 5 K.

The typical process stages for steam reforming, CO conversion and CO<sub>2</sub> separation are:

- Desulfurization to prevent poisoning of the catalysts,
- Steam reforming in tubular fixed-bed reactors with Cr/Ni catalysts,
- CO shift reactor (HT + LT stage) and
- H<sub>2</sub>/CO<sub>2</sub> separation.

In a similar manner to the CO shift reaction, a membrane reactor may also be used for steam reforming, allowing the excess of steam, and potentially the reaction temperature, to be reduced.

#### 2.2.3.2 Processes with Coal Gasification

In processes involving oxygen-blown gasification, there are two methods which are suitable for removing CO<sub>2</sub> from a synthesis gas converted through a CO shift process: physical absorption and, as a future option, concentration of CO<sub>2</sub> through removal of H<sub>2</sub> using membranes. For air-blown gasification processes, it is also possible to use physical-chemical absorption techniques, due to the lower CO<sub>2</sub> partial pressure. At the current stage of development, only absorption scrubbing has been proven on an industrial scale; membrane techniques with high selectivity and permeability, and the required resistance to corrosion, are still at the stage of laboratory testing. Adsorption processes are less suitable for this application due to the quantities of adsorbent required, and high energy requirements [87].

The majority of IGCC processes discussed in the literature, which incorporate CO conversion (CO shift reaction) and CO<sub>2</sub> removal, use a raw gas CO shift. For a CO<sub>2</sub> capture ratio of between 80% and 96%, 90% to 95% of the CO is converted via a CO shift reaction, and 91% to 99.8% of the CO<sub>2</sub> is removed from the converted gas (Table 2.7). The processes described in the literature differ primarily in terms of

the different gas turbine efficiencies, on which they are based, meaning that any comparison of efficiencies is made on the basis of non-standardized levels of technology. For this reason, it makes more sense to compare efficiency penalties resulting from CO<sub>2</sub> capture.

According to various literature sources, CO conversion, CO<sub>2</sub> removal and liquefaction reduce the net efficiency of an IGCC power plant by between 7 and 13 percentage points (Table 2.7).

Table 2.7: Data on CO<sub>2</sub> capture in an IGCC power plant with CO conversion (all gasification procedures are O<sub>2</sub>-blown, except for nos. 8, 11 and 13)

Gasification Method Reference		Gas Separation Method	CO <sub>2</sub> Removal/ Capture			CO <sub>2</sub> Emissions (CO <sub>2</sub> liquid) in kg CO <sub>2</sub> /kWh	Efficiency Penalty Δη (percentage points)		Efficiency (CO <sub>2</sub> liquid) in %
			CO conversion in %	Separation factor of scrubbing in %	Capture ratio in %		CO <sub>2</sub> at 1 bar	CO <sub>2</sub> at 110 bar	
Physical absorption									
Raw gas CO shift conversion									
1	Texaco + direct quenching with water [86, 88]	Selexol	95	99	90	0.019 Baseline 0.89	4.5	7	29.5
2	Texaco [17]	Selexol	90	91	79	0.137	(4*)	(7*)	37.0
3	HTW [87]	Purisol	90	98	86.6	0.13	approx. 3.5	approx. 6.8	38.2
4	(British Coal) [89]	phys. scrubbing	not spec.	not spec.	90	0.1 Baseline 0.79	approx. 6.4	approx. 10	33.0
5	(British Coal) [89]	seawater	not spec.	not spec.	90	0.1 Baseline 0.79	approx. 8		35.0
Clean gas CO shift conversion									
6	PRENFLO [20]	Rectisol	91.2	98.1	88	0.10 Baseline 0.69	6.2	10.7	36.0
7	Shell [16, 71, 90]	Selexol	98	98-99	96	0.04 Baseline 0.76	approx. 4.0	7.3 .. 7.7	36.3
8	KRW (air-blown) + hot gas desulfurization[91]	Glycol methanol	95	95	90	0.16 0.20 Baseline 0.745	3.5 14.5	6.5 16.6	35.0 24.9
9	KRW (O <sub>2</sub> -blown) [91]	Glycol	95	95	90	0.277 Baseline 0.8	1.9	3.3%	35.2
Raw gas CO shift conversion + chemical absorption									
10	(British Coal) [89]	aqueous amine	not spec.	not spec.	90	0.1 Baseline 0.79	approx. 7.4	approx. 11	32.0
11	"British Coal Topping Cycle" (air-blown) [89]	aqueous amine	not spec.	not spec.	87	0.1	approx. 9	approx. 12	34
12	Shell [81]	DEMEA	95	99.8	94.6	0.057 Baseline 0.756	6.6	9.8	33.2
13	KRW (air-blown) + hot gas desulfurization[91]	MEA K <sub>2</sub> CO <sub>3</sub>	95	95	90	0.19 0.18 Baseline 0.84	9.4 7.8	12.9 11.3	28.7 30.3
Raw gas CO shift conversion + membrane (H <sub>2</sub> separation)									
14	HTW [87]	membrane				not spec.	>4	>8.5	< 36.5
15	British Coal [89]	metal membrane Separation factor <sup>17</sup> ≈200	not spec.	not spec.	90	0.1 Baseline 0.79	approx. 4.5	approx. 8	35
16	Shell [92, 93]	ceramic membrane Separation factor <sup>17</sup> ≈25	90	88 (H <sub>2</sub> ) >95 (H <sub>2</sub> )	96.6 "-"	0.030 0.028	approx. 7 approx. 4	approx. 11.5 approx. 8.5	34.5 37.5
17	KRW (O <sub>2</sub> -blown) [91]		95	95	90	0.457 Baseline 0.8	6.0%	8.5%	30.7
Combined clean gas CO shift conversion + membrane (H <sub>2</sub> separation)									
18	PRENFLO [94]	ceramic membrane Separation factor <sup>17</sup> ≈25	90.1	80 (H <sub>2</sub> )	79.6	0.178 Baseline 0.75	3.9 3.3	7.9 7.3	38.8 39.4 (with hot gas clean up)
Without CO <sub>2</sub> conversion: separation only of CO <sub>2</sub> component from coal gasification process									
19	Texaco [78]	chem. abs.	0.00	99	14.4	0,63	< 1	< 2	46.4

\* my own estimates

<sup>17</sup> See equation 2.5 (p 15).

## CO<sub>2</sub> Removal Using Physical Absorption

A high CO<sub>2</sub> partial pressure favors removal via physical absorption [95]. Hence, physical scrubbing to remove CO<sub>2</sub> is also proposed for the majority of the power plant cycles with CO conversion described in the literature. Using combined, selectively acting solvents, CO<sub>2</sub> and H<sub>2</sub>S can be removed simultaneously and recovered separately at high levels of purity.

Fluor Daniel Inc. carries out investigations for EPRI [86, 88] examining CO<sub>2</sub> capture in the case of coal gasification with coal slurry feed (approx. 50 bar) and raw gas cooling through direct quenching with water according to the Texaco method (Table 2.7: No. 1). Poor raw gas heat recovery means that even the baseline process displays a low level of efficiency. After cooling by direct quenching, the raw gas has an extremely high water vapor content. To reduce the water content, and to ensure that its enthalpy of vaporization is not lost through cooling and condensing prior to desulfurization, a raw gas CO shift process is used. Using this process arrangement, no additional steam is required for the CO shift reaction, which means that, in principle, it is possible to achieve an efficiency penalty (in this case, 4.5 percentage points<sup>18</sup>), which is smaller than that incurred with raw gas cooling via a steam generator.

In all other studies, the heat from the raw gas cooling process is used to generate steam, in which cases the proportion of water vapor in the raw gas is extremely small (approx. 1% volume fraction at a gasification temperature of 1300°C). For this reason, it is necessary to increase the water content up to a ratio of H<sub>2</sub>O to CO of 1.4 to 2 through humidification and additional steam injection prior to the CO shift reaction. The water component, which remains following CO conversion, is condensed no later than the point where the gas is cooled to the CO<sub>2</sub> scrubber working temperature, causing further exergy losses attributable to CO conversion.

According to KEMA [17], the high operating pressure in a Texaco gasification process (approx. 80 bar, with steam generation in the raw gas cooler) allows a water content of approx. 30% volume fraction to be achieved subsequent to Venturi scrubbing at temperatures of around 230°C (Table 2.7: No. 2). This reduces the need for additional steam injection, resulting in an efficiency penalty calculated at 4 percentage points<sup>18</sup>.

In the work of Pruscek et al. [20] (Table 2.7: No. 6), relating to gasification according to the PRENFLO method with raw gas cooling via the steam generator, the water component required for CO conversion in the desulfurized gas is introduced largely via the saturator, meaning that only a small additional amount is required to be injected directly as steam prior to CO conversion. The efficiency penalty comes to 6.2 percentage points<sup>18</sup>.

In a study by British Coal [89] (Table 2.7: No. 5), the physical absorption of CO<sub>2</sub> in seawater is also investigated. Since the seawater simultaneously serves as a solvent and as a sequestration site, neither solvent regeneration nor compression work for the separated CO<sub>2</sub> is required. Since CO<sub>2</sub> will leak out again if introduced at ocean depths <2000 m, a large-diameter seawater pipeline extending to great depths (> 2000 m) would be required. The efficiency penalty resulting from pump work and pressure build-up (with a CO<sub>2</sub> capture ratio  $r_{CO_2}$  of 90%) is cited at 8 percentage points. However, the low solubility of CO<sub>2</sub> in water means that giant tower scrubbers are required, as well as feed and drainage systems for the seawater (see also my own calculations in Section 3.4).

---

<sup>18</sup> CO<sub>2</sub> gaseous at 1 bar, excluding liquefaction





larger proportion of H<sub>2</sub>. For this reason, it is more advantageous simply to remove the H<sub>2</sub> component with a membrane and to burn in pure oxygen the residual fuel, which remains with the CO<sub>2</sub>. At low temperatures of up to approx. 100°C, polymer membranes can be used. At higher temperatures, ceramic membranes are required, though these display lower selectivity. For temperatures in the range between 350°C and approx. 700°C, metal membranes (e.g. palladium) can be used; however, these achieve high selectivities for H<sub>2</sub>, meaning that it is virtually only the H<sub>2</sub> component, which is removed. Since palladium membranes are too expensive for large-scale industrial use, metal membranes are being developed, in which an extremely thin metal film is deposited on a ceramic base material. Since membranes, which meet the requirements of power plant technology (e.g. in terms of corrosion resistance and separation behavior), are still at the development stage, virtually all the studies base their research on selectivities and permeabilities, which will be achievable in the future.

According to ECN [92, 93] (Table 2.7: No. 15), a gas separation procedure using a membrane with a separation factor<sup>20</sup> of 25 for H<sub>2</sub> to CO<sub>2</sub>, and a pressure ratio between feed and permeate of 3.2, can separate out 88% of the H<sub>2</sub>, after hot gas clean up at 350°C and CO conversion. The H<sub>2</sub> component, which remains in the retentate, is liquefied and disposed of together with the CO<sub>2</sub>. The separated H<sub>2</sub>-rich gas stream is burnt in a gas turbine. An efficiency of 34.5% is obtained, including CO<sub>2</sub> liquefaction. Recovery of the residual H<sub>2</sub> in the retentate can boost the efficiency of the power plant to 37.5%. This corresponds to an efficiency penalty of 7, or 4, percentage points<sup>18</sup>, respectively, when set against a comparable baseline power plant. According to British Coal (Table 2.7: No. 16), an efficiency penalty of 4 percentage points<sup>18</sup> can be achieved, inclusive of CO<sub>2</sub> liquefaction, using a metallic membrane after the raw gas CO shift to separate out the H<sub>2</sub> with an anticipated future separation factor<sup>20</sup> of 200 for H<sub>2</sub>/CO<sub>2</sub> [89]. At approx. 250°C, and with a pressure ratio between feed and permeate of approx. 1.33, the H<sub>2</sub> partial pressure in the permeate is lowered by mixing in excess N<sub>2</sub> from the air separation unit as a purge gas (Figure 2.11). Subsequent to desulfurization, the CO<sub>2</sub> component of the retentate is liquefied through condensation, and the remaining mixture of inert gases and H<sub>2</sub> is fed into the gas turbine together with the separated H<sub>2</sub>.

### Combination of CO Shift Reaction and Gas Separation

If a portion of the products (H<sub>2</sub>; CO<sub>2</sub>) is removed during the CO shift reaction, its partial pressure drops and the chemical equilibrium shifts to the product side. For the CO shift reaction, this means a higher rate of CO conversion and, at the same time, a lower excess of steam. The reduced excess of steam means that less steam has to be added, so that exergy losses become lower.

A combination of catalytic CO conversion and a ceramic membrane for removing H<sub>2</sub> is being developed by ECN and tested in an application known as the WIHYS process in an IGCC power plant, as part of the JOULE II program [94] (Table 2.7: No. 18). With a low molar ratio of steam to CO of 1.28, a reactor exit temperature of 500°C, a ratio of feed to permeate pressure of around 1.7, and a selectivity of H<sub>2</sub> to CO<sub>2</sub> of 15, 90% of the CO is converted and 80% of the H<sub>2</sub> is removed. 80% of the carbon in the feed coal is retained in the retentate. A conventional CO shift reactor would require a higher excess of steam and a lower reaction end temperature. The addition of nitrogen from the air separation unit causes the H<sub>2</sub> partial pressure on the permeate side to be reduced to less than a third of the overall pressure, thereby improving the separation behavior of the membrane. The H<sub>2</sub>, which remains in the retentate, is burnt with a small proportion of other combustible components, with the addition of pure oxygen, and the

<sup>20</sup> See equation (2.5) (p 15).

enthalpy of combustion is used for the steam turbine process. Since the gas separation process works at high temperatures, the efficiency penalty with hot desulfurization is lower than with wet H<sub>2</sub>S scrubbing.

Apart from membrane reactors, the combination of a CO shift reaction and CO<sub>2</sub> adsorption is also a feasible method of reducing the energy expended on CO<sub>2</sub> capture. In this study, an efficiency penalty, due to CO conversion/CO<sub>2</sub> adsorption with CaO, of 12.5 percentage points was calculated for an IGCC power plant (see Section 3.5.2). More favorable reaction conditions for CO shift conversion and CO<sub>2</sub> adsorption from coal gas, or for basic CO<sub>2</sub> adsorption from flue gases, emerge for a mixture of limestone and dolomite. CO shift conversion and CO<sub>2</sub> adsorption should be performed at between approx. 300°C and 350°C, basic CO<sub>2</sub> adsorption at between 200°C and 350°C, and desorption at around 650°C. According to Heesink [96], a heat exchanger can limit further heat requirements to 0.38 kWh per kg of CO<sub>2</sub>. In this case, power plant efficiency would be reduced by approx. 10 to 15 percentage points. According to Ito and Makino [97], at temperatures of between 150°C and 300°C, zeolites can also act simultaneously as a catalyst for CO conversion and an adsorbent for CO<sub>2</sub>. The advantage over MgO/CaO would be the fact that zeolite does not need to be heated to high temperatures for desorption, since the PSA principle can be applied.

### **Air-Blown Gasification**

Subsequent to processing in an air-blown gasifier, coal gas is diluted with N<sub>2</sub>; therefore, the concentration of CO<sub>2</sub> and of H<sub>2</sub> in the synthesis gas following CO shift conversion is lower than that obtained after O<sub>2</sub>-blown gasification. For this reason, literature sources also suggest chemical absorption as a suitable CO<sub>2</sub> separation method, as well as physical absorption [98, 91].

In the case of an IGCC power plant with an air-blown KRW gasifier [91] (Table 2.7: Nos. 8, 13) or of the "British Coal Topping Cycle" (Table 2.7: No. 11), an IGCC power plant with partial gasification [98], desulfurization can be achieved by adding lime to the fluidized bed combustion process, which means that cooling prior to a stage of wet desulfurization is no longer necessary. However, the fact that cooling is required prior to wet CO<sub>2</sub> scrubbing eliminates the advantage (as compared against the baseline case) of hot desulfurization in the fluidized bed. Although the KRW gasification process apparently achieves virtually complete carbon conversion, the "British Coal Topping Cycle" requires subsequent combustion of the residual char, with 20% to 30% of the original proportion of carbon, in a separate fluidized bed, which means that, to perform CO<sub>2</sub> capture, a second CO<sub>2</sub> scrubbing stage must be incorporated in the flue gas of the fluidized bed combustion process.

#### **2.2.3.3 Processes with Natural Gas Reforming**

Since temperatures of between 800°C and 900°C are required for steam reforming of a fuel gas containing hydrocarbons, a portion of the fuel gas is used for reformer heating. The combustion of a portion of the fuel for these reformer heating purposes causes the majority of the exergy losses attributable to CO<sub>2</sub> capture. Whereas coal gasification is still required even without CO<sub>2</sub> capture, in order to render the coal usable for the gas turbine processes, steam reforming in a natural gas-fired power plant is not actually required unless CO<sub>2</sub> capture is being performed. Thus, in contrast to coal gasification, the exergy losses associated with steam reforming, together with CO conversion and gas separation, are entirely attributable to CO<sub>2</sub> capture.

The separation of  $\text{CO}_2$  and  $\text{H}_2$  after steam reforming is performed at significantly lower temperatures than the steam reforming process. This means that the synthesis gas produced must be cooled prior to gas separation. The heat from the gas cooling process is normally used to generate steam (Figure 2.12).

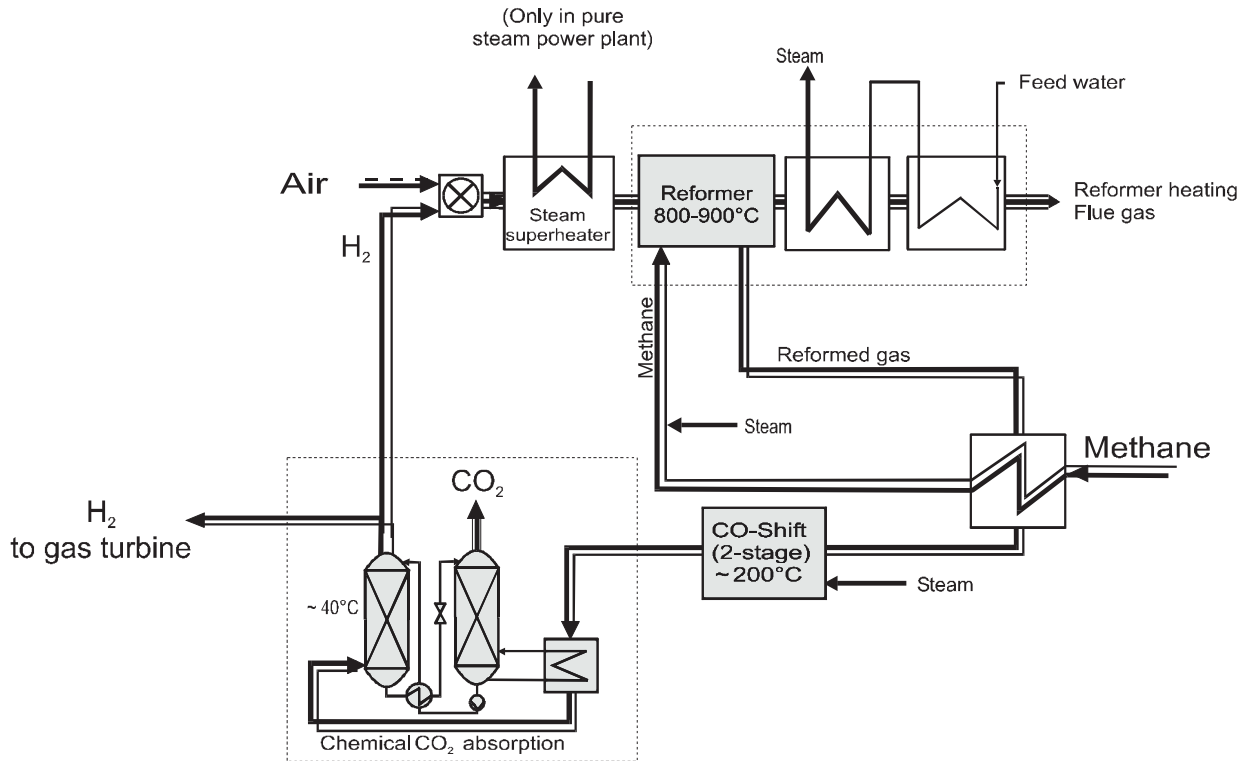


Figure 2.12: Flow diagram of a natural gas reforming process with downstream CO conversion and  $\text{CO}_2$  removal (chemical absorption in this example) and external reformer heating with carbon-lean gas

There are relatively few cases in the literature of  $\text{CO}_2$  separation after natural gas steam reforming and CO conversion (see Table 2.8 for data). In any event, exergy losses occur in this case due to:

- combustion of a portion of the fuel for reformer heating purposes,
- temperature differences in the heat exchange (heating of the reformer, cooling prior to gas separation),
- steam reforming,
- CO conversion including steam losses and
- $\text{H}_2/\text{CO}_2$  separation.

Through steam reforming at 800°C to 900°C, with a moderate excess of steam, only a part of the natural gas can be converted, which means that it is difficult to achieve a  $\text{CO}_2$  capture ratio of 90%, even with high rates of CO conversion in the water-gas shift reaction, and a high  $\text{CO}_2$  separation factor  $s_{\text{CO}_2}$  in the  $\text{CO}_2$  scrubbing stage.

In the majority of process arrangements, which have been proposed, the reformer is heated externally through combustion of an  $\text{H}_2$ -rich fuel gas (Figure 2.12). In a purely steam power plant, the thermal enthalpy of the hot, reformed gas can be used for steam superheating (Table 2.8: No. 1). In this case, the

efficiency penalty due to CO<sub>2</sub> capture is cited as being approx. 4 percentage points<sup>21</sup> [99]. Similar to the manner in which heat from the raw gas cooling process is used in the IGCC, only a small portion of the thermal enthalpy of the hot synthesis gas in gas/steam turbine combined cycle power plants can be transferred to the gas turbine, subsequent to reforming, to be exploited at the high efficiency of the combined cycle. For this reason, the efficiency penalty due to reforming, CO shift conversion and CO<sub>2</sub> separation in a gas/steam turbine combined cycle power plant is greater than in a purely steam power plant. According to Hille [100], this efficiency penalty amounts to 14.5 percentage points<sup>21</sup> (Table 2.8: No. 2).

Table 2.8: Data on CO<sub>2</sub> capture in natural gas-fired processes subsequent to steam reforming and CO conversion

No.	Power Plant Type Reference	Reformer Heating	CO <sub>2</sub> Removal/Capture			CO <sub>2</sub> Emissions (with CO <sub>2</sub> liquefaction) in kg CO <sub>2</sub> /kWh	Efficiency Penalty $\Delta\eta$ (in percentage points)		Efficiency (with CO <sub>2</sub> liquefaction) in %
			Method	Separation factor of scrubbing in %	Capture ratio in %		CO <sub>2</sub> at 1 bar	CO <sub>2</sub> at 110 bar	
1	Steam plant [99]	external with H <sub>2</sub>	distillation	not spec.	90	0.059	approx. 4	6.8	30
2	Gas/steam turbine combined cycle [100]	external with H <sub>2</sub> (890°C)	MDEA (phys.-chem.)	90.9	56	0.167	14.5	15.8	36.5
3	Gas/steam turbine combined cycle [101]	internal	chem. scrubbing	not spec.	approx. 90	not spec.	not spec.	approx. 9	50
4	CRGT plant (see Sec. 3.5.3)	external with H <sub>2</sub>	phys.-chem. scrubbing	90	83.5	0.07	11.3	13	44.0

In a "chemically recuperated" gas turbine (CRGT) (Table 2.8: No. 4), the reformer is heated by hot gas turbine exhaust gas, rather than by additional fuel (see Section 3.5.3 for calculations). Due to the lower exhaust gas temperatures, the reforming temperature is lower than in steam reforming heated by direct firing. Accordingly, there is also a lower conversion of hydrocarbons. To achieve higher conversion rates, additional combustion is required (Figure 3.62). Since the reformer is heated using waste heat, the resulting efficiency penalty of approx. 11 percentage points is less than that obtained through arranging an externally heated steam reformer and CO<sub>2</sub> separation process prior to a gas/steam turbine combined cycle.

A significant drop in exergy losses is achieved by heating the natural gas, which is to be reformed, solely through internal partial combustion, while mixing in hot gas turbine exhaust gas (Figure 2.13, Table 2.8: No. 3) [101]. The portion of fuel gas burnt in this process reduces the mass flow of the gas components, which are to be converted via steam reforming and CO shift reaction, and also reduces the associated exergy losses, as compared to cases where the reformer is heated by an external source using H<sub>2</sub>. In addition, the enthalpy of the hot gas turbine exhaust gas, mixed in for the combustion process, reduces the amount of fuel required for reformer heating. With this method of reformer heating through internal partial combustion, CO<sub>2</sub> capture and CO<sub>2</sub> liquefaction only reduce the efficiency of a gas/steam turbine combined cycle by 9 percentage points. Estimated costs lie slightly below those incurred by steam reforming with external heating. By comparing various gas/steam turbine combined cycles, namely those with CO<sub>2</sub> separation subsequent to steam reforming, those with combustion in an

<sup>21</sup> CO<sub>2</sub> gaseous at 1 bar, excluding liquefaction.

atmosphere of  $O_2/CO_2$ , and those with  $CO_2$  removal from the flue gas, it can be seen that the smallest reductions in efficiency are attributable to  $CO_2$  separation subsequent to steam reforming and CO conversion with internal partial combustion [101, 102].

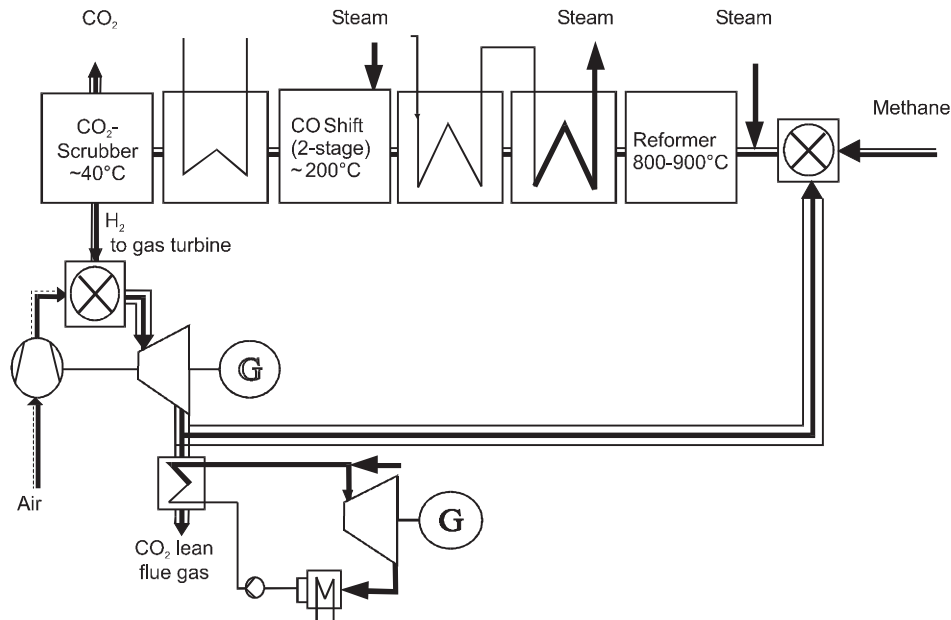


Figure 2.13: Flow diagram of a gas/steam turbine combined cycle with steam reforming (heated by internal partial combustion) and subsequent CO conversion and  $CO_2$  separation

By using a membrane reactor, which combines steam reforming, CO shift reaction and  $H_2$  separation, the chemical equilibrium could be shifted in such a way, that sufficient methane conversion becomes possible even at lower temperatures. Experiments with a palladium/silver membrane reactor have been described by Jørgensen et al. [103]. A  $CH_4$  conversion rate of 60% was achieved at a pressure of 10 bar using a purge gas. Moritsuka [104] suggests the use of a ceramic membrane reactor.

## 2.2.4 Process Family II: Carbon Dioxide Concentration in the Exhaust Gas

By burning fuel in an atmosphere consisting of oxygen and  $CO_2$  or steam, with the exclusion of other inert gases, it is possible to produce an exhaust gas consisting only of  $CO_2$  and  $H_2O$ .

Depending on the way in which the oxygen is supplied, a distinction may be made between processes involving:

- production of a high-purity oxygen gas by means of air separation (Figure 2.14) or
- oxygen delivery through direct, selective mass transport from the ambient air through to the reaction (p 40).

The second method eliminates both the energy required to generate the pure oxygen, and the exergy losses resulting from the mixing process with the fuel and the recirculated flue gas. While oxygen production through air separation is a proven process, there are only a few laboratory investigations, which are currently experimenting with selective processes to generate oxygen for combustion.

The temperature of combustion is adjusted by recirculating the CO<sub>2</sub> to the combustion chamber. The CO<sub>2</sub>-rich flue gas may be drawn off either at high pressure prior to the gas turbine, or at low pressure prior to entering the compressor. If the gas is extracted prior to the gas turbine, the thermal enthalpy of the hot CO<sub>2</sub> must be incorporated in the subsequent steam cycle. Since the thermal enthalpy of the hot CO<sub>2</sub>, at high temperatures after the gas turbine combustion chamber, is used less efficiently in the steam cycle than in the combined cycle, it is preferable to remove the CO<sub>2</sub> at low pressure, following expansion in the gas turbine (providing that the compressor pressure ratio in the gas turbine and the steam cycle are set to optimal performance levels, and that the gas temperature is significantly higher than the temperature of the steam).

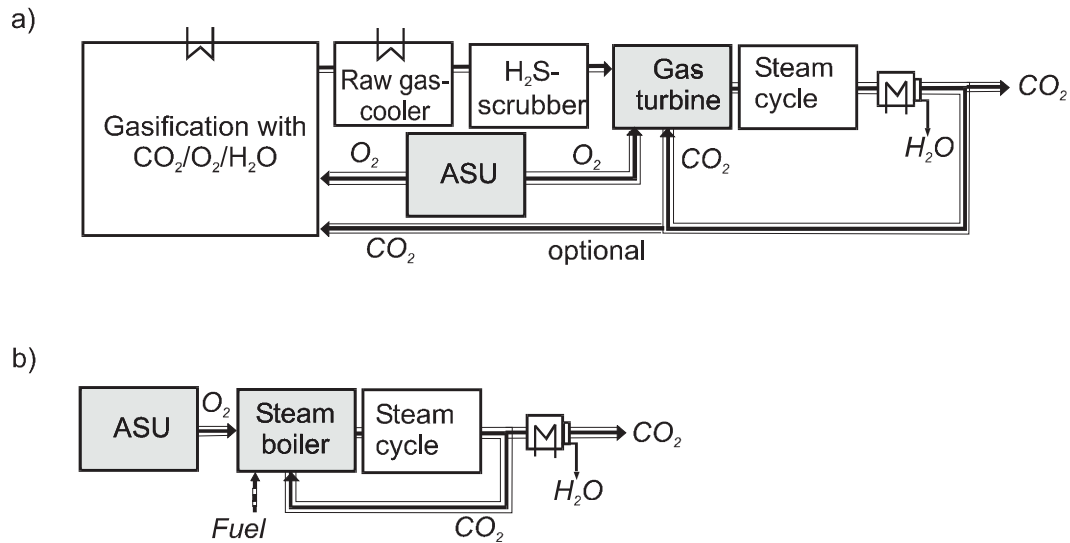


Figure 2.14: Basic principles of a power plant process with combustion in an atmosphere consisting of pure oxygen and recirculated CO<sub>2</sub>. (a) IGCC power plant, (b) Steam power plant.

This process group practically eliminates the emission of CO<sub>2</sub> into the atmosphere. Minor emissions of CO<sub>2</sub> are caused by dissolution of the CO<sub>2</sub> in the condensate from the exhaust gas cooling stage, and in the condensate from the CO<sub>2</sub> compression process. In addition, CO<sub>2</sub> is also absorbed in the desulfurization process, and is released with the waste gas from the Claus plant. Furthermore, leakages may occur in the compressor and pumps, as well as in the combustion chamber. Overall, however, well over 99% of the CO<sub>2</sub> is retained. Other CO<sub>2</sub> capture techniques are also susceptible to these potential CO<sub>2</sub> leakages and emissions.

The characteristics of combustion, in an atmosphere consisting of recirculated waste gas (CO<sub>2</sub>) and pure oxygen, have already been investigated in the course of various research experiments. Descriptions of experiments involving coal combustion are provided, for example, by Weller and Rising [105], Wolsky [106], Abele [107] and Roberts [108]. Experiments involving natural gas combustion are described by Kimura et al. [109]. In spite of smaller intrusions of air, CO<sub>2</sub> volume fractions of over 90% were achieved with a residual oxygen content of 3% to 4% (volume fraction) [108].

### CO<sub>2</sub> as a Turbine Working Fluid

In a similar manner to operation with air, a gas turbine, in accordance with the Joule cycle, can also be driven with CO<sub>2</sub>, or a mixture of CO<sub>2</sub> and H<sub>2</sub>O, as the working fluid. In the Joule cycle, the changes of state are above the critical point, in a region in which CO<sub>2</sub> approximates the behavior of an ideal gas.

Since the properties of CO<sub>2</sub> differ substantially from those of air, it will be necessary to develop a new gas turbine for processes, which use CO<sub>2</sub> as a working fluid, which has been adapted to satisfy these modified characteristics. There are currently no gas turbines of this type available or under development.

Compared to the use of air as a working fluid, the main changes in physical characteristics for a working fluid primarily consisting of CO<sub>2</sub> are as follows [110]:

- 7% to 12% smaller isentropic exponent,
- heat capacity: -17% at 1 bar/15°C, +20% at 30 bar/15°C, +9% at 1 to 30 bar/1000°C,
- approx. 22% lower speed of sound,
- higher density,
- approx. 48% to 38% lower kinematic viscosity,
- approx. 58% to 92% higher Reynold's number and
- a critical temperature, which lies closer to ambient temperature ( $T_k = 31.05^\circ\text{C}$ ).

The fact that these physical characteristics differ from those of air has the following consequences for the gas turbine cycle:

- higher mass flow in gas turbines,
- lower specific compression and expansion work,
- higher turbine exit temperature (Figure 2.15),
- maximum efficiency of the Joule cycle at significantly higher pressure ratios (Figure 3.70) and
- changes to optimal blade shape, turbine and compressor diameter, and number of stages. Bammert and Mukherjee [111], for example, have described the design of a CO<sub>2</sub> gas turbine in great detail.

A standard gas turbine (Joule/Brayton process with air as a working fluid) is not suitable for operation using CO<sub>2</sub> as a working fluid (or can only be used with a significant penalty in performance and efficiency), unless changes are made to blade shape, flow area and the number of stages [112].



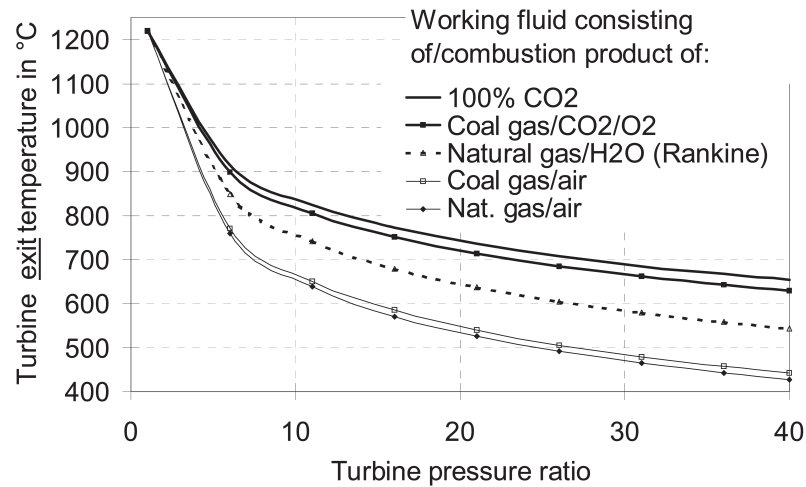


Figure 2.15: Turbine exit temperature calculated for different working fluids in dependence on pressure ratio at a turbine inlet temperature of 1200°C<sup>22</sup>.

### Special CO<sub>2</sub> Working Cycles

Aside from the Joule cycle, which is situated far in the supercritical region ( $p_{max} \ll p_{crit}$ ) throughout, there are a number of other cycles suited to the use of CO<sub>2</sub> as a working fluid, which, in particular, make use of the lower compression work close to the critical point of CO<sub>2</sub> (73.858 bar, 31.05°C). Cycles of this type, with moderate pressure ratios, but high overall pressures, adapted to operation with CO<sub>2</sub> as a working fluid, could potentially achieve greater efficiency and more cost-effective designs than today's standard gas turbines and gas/steam turbine combined cycle power plants.

In conjunction with the development of alternative working cycles for nuclear power stations, detailed research -- even to the extent of detailing the structural design of the turbines -- was carried out, between 1967 and 1975, on cycles using pure CO<sub>2</sub> as a working fluid [111, 113, 114, 115]. In these studies, the upper process temperature was limited to a maximum of 800°C. Several proposals were even published on processes with internal combustion and a working fluid resulting from this consisting of CO<sub>2</sub> and steam [116, 117].

In order to achieve low compressor work, it is advantageous to select the lowest pressure close to critical pressure. With the resulting high pressures of around 73.858 bar, together with the high densities, there is greater heat transfer, which means that it was advantageous to utilize regenerative heat transfer from the hot gas after the turbine to the compressed cold gas. In terms of cycles, which use CO<sub>2</sub> as a working fluid, it is important to differentiate between:

- supercritical processes ( $p_{min} > 73.858$  bar),
- subcritical processes ( $p_{min} < 73.858$  bar),
- processes with or without condensation ( $p_{min} < 73.858$  bar,  $T_{min} < 31.05$ °C)

and process improvements due to

- split flow compression,

<sup>22</sup> Calculated with real gas factors in accordance with Redlich-Kwong-Soave.

- an intercooled compressor,
- intermediate superheating (via heat exchanger) or reheating (via internal combustion, sequential combustion chambers).

Increasing the lower operating pressure of a Joule gas turbine cycle to a level above the critical pressure results in the Feher cycle (Figure 2.16), which operates entirely in the supercritical region. In the Gohstjejn cycle, compression of the working fluid occurs subcritically in the liquid region following condensation, whereas expansion occurs in the supercritical region (Figure 2.17).

Due to the differing heat capacities on the high-pressure and low-pressure sides in the recuperator, and the consequent difference in enthalpy flow rates, the heat-up range on the high-pressure side is lower than the cooling range on the low-pressure side. Partial compression allows the enthalpy flow rates to be balanced out (Schabert cycle = Feher cycle + partial compression; entirely supercritical; Sulzer cycle = Gohstjejn cycle + partial compression). Improved heat transfer has a positive effect on efficiency.

Though partial compression improves efficiency, it also simultaneously reduces specific work, and more equipment is required due to the additional compressor. According to Gašparovic [114], processes involving partial compression, or processes with additional compressors required for other purposes, are less suitable for practical applications than the Feher or Gohstjejn cycle. Bammert and Mukherjee [111] come to a different conclusion for a process limited to 520°C: they rule out the Feher and Gohstjejn cycles, and only compare processes with partial compression (Schabert cycle, Schabert cycle with additional intermediate superheating, Sulzer cycle with reheating). Although the Sulzer cycle with reheating does, in fact, achieve the highest efficiency in the comparison test, the Schabert cycle with reheating is selected as the most favorable in terms of both structural design and economic viability.

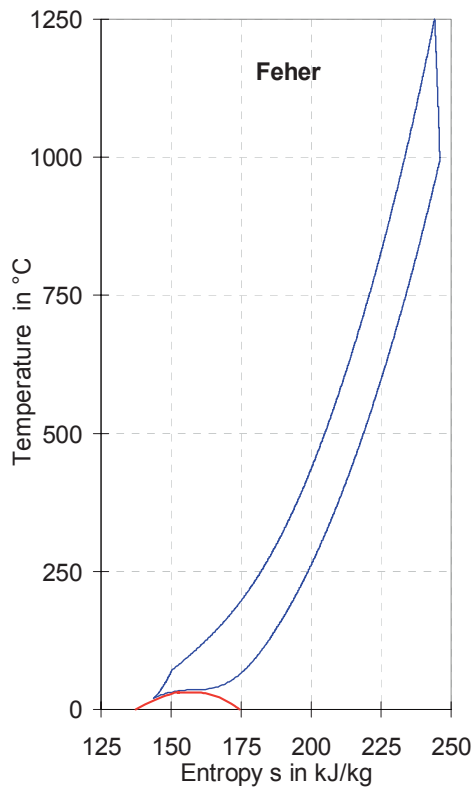


Figure 2.16: T-S diagram of the Feher cycle (entirely supercritical)<sup>23</sup>

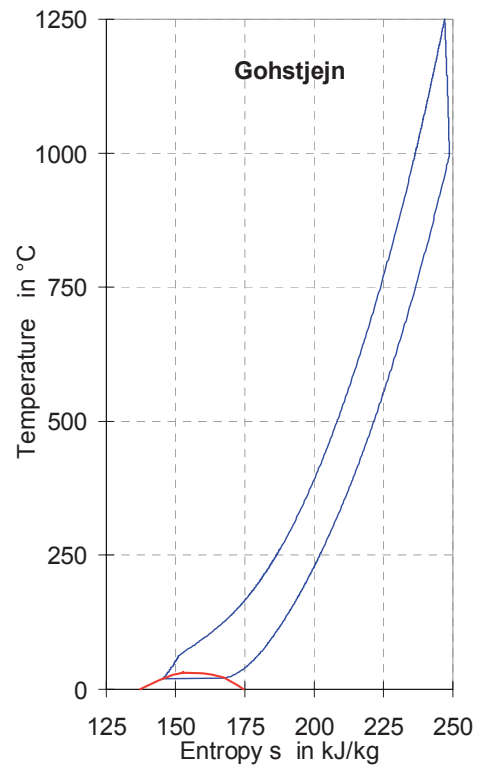


Figure 2.17: T-S diagram of the Gohstjejn cycle (condensation;  $p_{min} < p_{crit}$ ,  $p_{max} > p_{crit}$ )<sup>23</sup>

Iantovski [117] proposes a 'quasi'-combined cycle in the form of a Joule cycle (gas turbine: TIT 1300°C, 60 bar/4 bar) with a Rankine cycle (steam turbine: 240 bar, 600°C/60 bar, 20°C) in a partially subcritical, partially supercritical process with recuperators, but without partial compression (see Section 3.6.5, p 127). In the version with reheat (sequential combustion), this is referred to as the "MATIANT" cycle (MAThieu and IANTovski [118]).

All cycles with condensation (Gohstjejn/Sulzer/"MATIANT" cycles) require a coolant to be available, at all times, at a sufficiently low temperature (31.05°C minus the pinch point in the condenser), which can be difficult to achieve in hot areas. In the case of fully or partially condensing working fluids, savings can also be made on the compression work for CO<sub>2</sub> liquefaction.

The "Graz cycle" is a mix between the (H<sub>2</sub>O) Rankine cycle and a CO<sub>2</sub> gas turbine cycle with steam injection [119]. The exhaust gas emerges from the final expansion stage, which is arranged downstream from the gas turbine waste heat recovery stage, at a temperature of around 30°C, with the result that virtually no exhaust gas heat losses occur. Nevertheless, high exergy losses in the steam injection process in the combustion chamber mean that claimed efficiencies of over 60% (TIT 1400°C) seem somewhat dubious.

<sup>23</sup> Values for pure CO<sub>2</sub> according to IUPAC [163].

### Oxygen Delivery

One theoretical possibility for delivering oxygen to the combustion process is ambient air oxidation of metals with reduction of the oxide in the combustion chamber at high temperatures. This would avoid the energy required for air separation. Jody et al. [120] suggest using barium. Ishida [121] proposes an arrangement in which a gas turbine is driven by exothermic oxidation of nickel at 1300°C. Methane is burnt with the oxygen atom of the nickel oxide in a second combustion chamber. The net reaction is exothermic, and, again, a combustion chamber temperature of 1300°C should be reached. The turbine is driven by the waste gas, consisting of steam and CO<sub>2</sub>, which arises in this process; the reduced nickel is fed into the first combustion chamber (Figure 2.18). In this case, the difference in oxygen partial pressure between air and fuel (in this example, methane, 0% volume fraction of O<sub>2</sub>) serves as a driving potential for the mass transfer of O<sub>2</sub>. The overall achievable efficiency is supposed to be higher than that achieved by any other gas-fired cycle with the same turbine inlet temperature; in the case of gaseous CO<sub>2</sub> capture, it is even, theoretically, supposed to be higher than that achieved in combined cycles with combustion in air and without CO<sub>2</sub> capture. The possibility of high efficiencies can be explained by lower exergy losses in the combustion process through intermediate reactions with Ni/NiO [122].

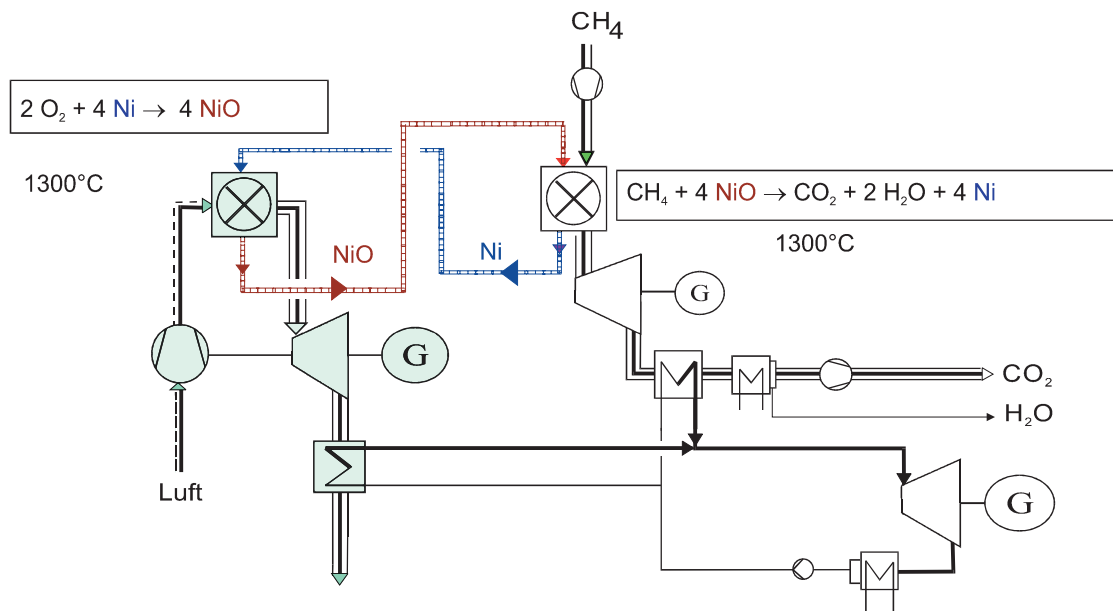


Figure 2.18: Gas turbine cycle with O<sub>2</sub> supplied by Ni/NiO (according to [121])

### Coal-fired Cycles

According to data from the literature, steam power plants display an efficiency penalty due to CO<sub>2</sub> capture of between 5 and 7 percentage points (Table 2.9), caused by oxygen production in the air separation units and flue gas recirculation. CO<sub>2</sub> liquefaction reduces efficiency by a further 3.6 to 4.8 percentage points. In some proposals, no desulfurization or nitrogen removal is envisaged, while other processes integrate not only desulfurization and nitrogen removal, but also the recovery of residual oxygen.

Descriptions of coal-fired combined cycles in the literature are limited to gas/steam turbine combined cycles. The majority of the proposals deal with IGCC power plants (Table 2.10, No. 1-10; 12) or MHD/steam turbine combined cycles (Table 2.10, No. 12-14). Relatively few of the proposals examine gas turbines operated directly with flue gas from the coal combustion process (Table 2.10, No. 11).

In addition to the changes in the combustion process and the gas turbine cycle, it is also necessary to provide the air separation unit (ASU) in an IGCC power plant with a separate air compressor. It only remains to provide an interface to the combined cycle through use of the enthalpy of the hot, compressed air prior to the air separation unit to preheat the feed water.

Table 2.9: Data from the literature for steam power plants featuring an air separation unit and flue gas recirculation

Source	DESOX / DENOX	Oxygen Purity Volume Fraction in %	Energy Expended on O <sub>2</sub> Production (in kWh/kg O <sub>2</sub> )	Power Plant η in % (CO <sub>2</sub> 1 bar)	Δ η CO <sub>2</sub> gas. / liq. (percentage points)	
Horn, Steinberg [34, 35]	-	98	0.228	34.4	5.6	9.2
McMullan et al. [123]	-	not spec.	not spec.	30.9	8.5	13.0
Herzog et al. [124]	-	95	0.221	28.9 to 30.9	6	10.8
IEA GHG [18]	-	99	not spec.	32.8	7.0	11
Allam, Spilsbury [125]	distillation of entire exhaust gas, O <sub>2</sub> recovery	99.5	not spec.	32.6	5.4	9.4
Bower et al. [98]	absorption/condensation	not spec.	not spec.	25 to 33	5.0-8.0	9.0-12.0

The nitrogen byproduct cannot be used in the power plant. Rendering the coal mills inert can only be achieved by using CO<sub>2</sub>-rich recirculated waste gas instead of N<sub>2</sub> (as used in a conventional IGCC), in order to avoid dilution of the fuel gas and exhaust gas. The only oxidant worth considering in this case is high-purity oxygen, in order to prevent the fuel gas and flue gas becoming diluted with atmospheric nitrogen and other inert gas components of the air.

In contrast to a conventional IGCC power plant, it is possible, in this case, using a heat exchanger, to utilize the waste heat from the raw gas to preheat the compressed gas turbine working fluid, since there is no danger of it igniting even if leakages in the heat exchanger were to occur, or if the fuel gas were to flow into the recirculated flue gas. A preheating process of this type is proposed by Wessel [137] (Table 2.10, No. 8) and, due to the fact that much of the heat from the raw gas cooling process can be used in the gas turbine, it results in high efficiency levels for an IGCC power plant with ASU and flue gas recirculation, as compared to other designs in which heat from the raw gas cooling process is used to generate steam.

In coal gasification, the large supply of CO<sub>2</sub> can be used to replace the gasification medium of steam with CO<sub>2</sub> (Table 2.10, No. 8-10). The main problem of CO<sub>2</sub>/O<sub>2</sub>-blown gasification is that gasification with CO<sub>2</sub> (Boudouard Reaction) takes around three times longer to run its course than gasification with H<sub>2</sub>O (water-gas reaction) [126]. Similar results have been obtained in experiments performed by van Heek [127], Teggars et al. [128], Azuma et al. [129] and Köhl et al. [130]. Further investigations into gasification using CO<sub>2</sub> have been performed at Delft University [131] and at CPERI [146]. Even the addition of catalysts did not serve to improve the difference in reaction rates between CO<sub>2</sub> and H<sub>2</sub>O [132].

Knoche et al. [138] choose CO<sub>2</sub> as a gasification medium, in order to reduce the exergy losses of gasification (Table 2.10, No. 9). In an idealized process, with CO<sub>2</sub>/O<sub>2</sub>-blown gasification and a three-stage CO<sub>2</sub> gas turbine with different recuperators (with no subsequent steam cycle), an exergy loss of 42.4% is calculated, corresponding to an overall exergetic efficiency of 57.6%.

According to Boeddicker [110] (Table 2.10, No. 10), where process conditions are otherwise identical, the efficiency obtained through CO<sub>2</sub>/O<sub>2</sub>-blown gasification of hard coal is greater than that obtained using H<sub>2</sub>O/O<sub>2</sub>-blown gasification by up to 0.8 percentage points. In contrast, according to Ruyck et al. [146], CO<sub>2</sub>/O<sub>2</sub>-blown gasification of lignite reduces the efficiency of an IGCC power plant by more than

one percentage point. According to Boeddicker [110], the specific useful work of the IGCC power plant is 5.7% higher in the case of H<sub>2</sub>O/O<sub>2</sub> gasification than with CO<sub>2</sub>/O<sub>2</sub>-blown gasification.

According to data from the literature, the efficiency penalty in IGCC power plants due to oxygen production in combination with a CO<sub>2</sub> gas turbine cycle (Joule cycle) lies between 6 and almost 9 percentage points, excluding CO<sub>2</sub> liquefaction (Table 2.10).

The efficiency of a pressurized pulverized coal-fired combined cycle with a gas turbine directly driven by hot, cleaned flue gas (TIT 1300°C) is reduced to 45.2%, excluding CO<sub>2</sub> liquefaction, i.e. 6.9 percentage points lower than that of the baseline power plant [139] (Table 2.10, No. 11).

Table 2.10: Data from the literature for coal-fired combined cycles (IGCC, PPCC, MHD) with combustion in an O<sub>2</sub>/CO<sub>2</sub> atmosphere

No.		Gasification Method <sup>(24)</sup>	Gas Turbine (TIT / $\pi$ )	Steam Cycle (pressure stages)	Oxygen Purity Volume Fraction in %	O <sub>2</sub> Production in kWh/kg O <sub>2</sub>	$\eta$ (CO <sub>2</sub> 1 bar) in %	$\Delta\eta$ CO <sub>2</sub> gas./ liq. in percentage points
<b>IGCC: H<sub>2</sub>O/O<sub>2</sub>-blown gasification, Joule gas turbine cycle</b>								
1	van Steenderen [133]	Texaco	1050°C / 11 1050°C / 20	3 + IH	gasifier: 95 GT: 98	not spec.	34.5 34.9	8.5 / 10 8.1 / 9.1
2	Pruschek et al., [20], Boeddicker [110]	PRENFLO	1190°C / 16.2 1190°C / 30 1190°C / 46	3 + IH	95	0.445 <sup>(25)</sup>	39.1 39.9 40.2	7.5 / 10.7 6.8 / 10.0 6.5 / 9.7
3	McMullan et al. [123]	partial gasification + PFBC	1000°C / 20	1 + IH	not spec.	not spec.	33.2	11.0 / 15.7
4	Pak et al. [134]	not spec.	STIG: 1250°C / 60 30bar/0.5bar	--	not spec.	0.2379	31.1	----
5	Koetzler et al.[17]	Texaco Shell	1050°C / 20 1050°C / 22	1 + IH 2 + IH	98	0.37 <sup>(25)</sup> 0.36 <sup>(25)</sup>	38.5 39.5	$\approx 4 / 7.5$ <sup>(26)</sup> $\approx 3-4 / 7-7.5$ <sup>(26)</sup>
6	Shao et al.[135]		1140°C/15.6	not spec.	not spec.	combined with CO <sub>2</sub> liquefaction	36.6 (CO <sub>2</sub> liq.)	- / $\approx 6-8$
7	Pechtl [136]	not spec.	STIG, not spec.	--	not spec.	not spec.	39	--
<b>IGCC: CO<sub>2</sub>/O<sub>2</sub>-blown gasification, Joule gas turbine cycle</b>								
8	Wessel [137]	Entrained flow (dry feed)	1150°C / 30	2+ IH	not spec.	0.35 <sup>(25)</sup>	42.8	(0.4 / 4.5) <sup>(27)</sup>
9	Knoche et al. [138]	not spec.	4-stage compression / 3-stage combustion	--	not spec.	not spec.	(49.6) <sup>(28)</sup>	-- <sup>(2)</sup>
10	Pruschek et al., [20], Boeddicker [110]	PRENFLO	1190°C / 16.2 1190°C / 30 1190°C / 46	3 + IH	95	0.445 <sup>(25)</sup>	39.9 40.5 40.7	6.8 / 10.0 6.2 / 9.2 6.0 / 9.0
<b>Pressurized Pulverized Coal-fired Combined Cycle (PPCC), Joule gas turbine cycle, hot gas clean up (1300°C)</b>								
11	Leithner [139]	--	1300°C / 15	1 + IH	not spec.	not spec.	45.2	7.2 / 12.1
<b>MHD/steam turbine combined cycle</b>								
12	Davison, Eldershaw [140, 141]	--	(MHD) 2563°C / 8	1 + IH	99.5	0.288	42.6	8.1 / 12.4
13	Goldthorpe et al. [89]	--	(MHD) not spec.	not spec.	not spec.	not spec.	$\approx 44$	$\approx 6 / 9$
14	McMullan et al. [123]	--	(MHD) not spec.	1+ IH	not spec.	not spec.	41.6	8.6 / 11.9
<b>IGCC: H<sub>2</sub>/CO membrane separation, separate combustion of H<sub>2</sub> and CO, Joule gas turbine cycle</b>								
15	Hendriks, Blok [142]	Texaco / Shell	1260°C/14.5	2 + IH	99.5	0.28	37.1 39.6	3.7 / 6.8 4.0 / 7.0

<sup>(24)</sup> All with raw gas cooler/steam generator

<sup>(25)</sup> Including O<sub>2</sub> compression.

<sup>(26)</sup> Baseline IGCC estimated.

<sup>(27)</sup> Baseline IGCC with raw gas cooler as steam generator; in the case of CO<sub>2</sub> capture with raw gas/air heat exchanger.

<sup>(28)</sup> Efficiency estimated from exergy losses.

In the case of an MHD/steam turbine combined cycle power plant with combustion in an O<sub>2</sub>/CO<sub>2</sub> atmosphere, the efficiency penalty is greater than with CO<sub>2</sub> removal from the flue gas, due to the fact that a considerable portion of the enthalpy of combustion can only be utilized after the MHD channel, due to dissociation of CO<sub>2</sub> at the high temperatures in the combustion chamber (around 1800°C) [140, 141] (Table 2.10, No. 12-14).

### IGCC Power Plant with H<sub>2</sub>/CO Separation and Separate Combustion in Two Gas Turbine Cycles

With coal gas, around one-third of the combustion oxygen is used for the oxidation of the hydrogen component. By burning the hydrogen component separately with air, less energy is required to generate O<sub>2</sub> for combustion of the carbon-containing components of the fuel. According to a proposal from Hendricks and Blok [142], hydrogen is removed from a cleaned coal gas, using a membrane, and is then burnt with air in a gas/steam turbine combined cycle (Figure 2.19; Table 2.10: No. 15). The retentate, which remains behind the membrane, primarily consists of CO and a small quantity of CO<sub>2</sub> and inert gas components. This retentate is burnt with recirculated flue gas, with the addition of oxygen, in a second gas turbine cycle, from which highly-concentrated CO<sub>2</sub> can be removed subsequent to condensation of the combustion water. The efficiency penalties in this process, as compared to the baseline IGCC power plant without CO<sub>2</sub> removal, arise from the energy required for additional oxygen production and the separation work of H<sub>2</sub> and CO in the membrane, which is mainly caused by the pressure drop across the membrane. Based on a membrane with a selectivity for CO to H<sub>2</sub> of 60, Hendricks and Blok calculate an efficiency penalty for this process, in comparison to the baseline IGCC power plant, amounting to nearly 4 percentage points, or nearly 7 percentage points if CO<sub>2</sub> liquefaction is included.

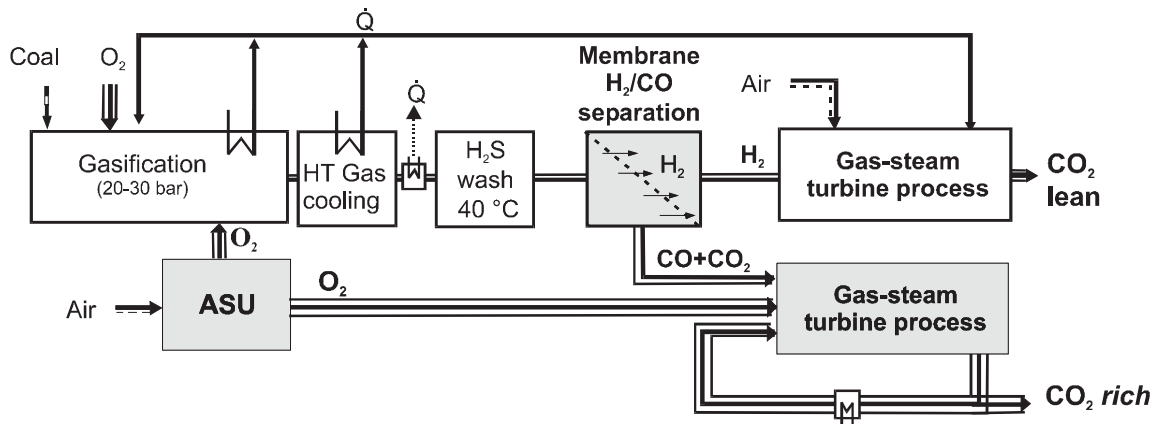


Figure 2.19: IGCC power plant with separate combustion of carbon-containing synthesis gas components excluding inert gases

### Gas-Fired Processes

The highest plant efficiency given in the literature for processes involving combustion in oxygen-enriched, recirculated flue gas is cited by Iantovski [117, 147], who gives a figure of 54.3% for a 'quasi-combined' cycle specially adapted to the characteristics of CO<sub>2</sub>-rich flue gas, and capture of CO<sub>2</sub> in its liquid form (for recalculations see Section 3.6.5, p 127ff). For combined cycles with a Joule gas turbine

cycle and subsequent steam cycle, efficiency penalties of between 6 and 8.5 percentage points are cited; in accordance with current gas turbine technologies, this corresponds to efficiencies of between 49% and 55% (see Table 2.11 for an overview of the literature).

Table 2.11: Data from the literature for gas-fired cycles with CO<sub>2</sub> as a working fluid and oxygen supplied via air separation

Source	G	T (TIT / )	Steam Cycle (pressure stages)	Oxygen Purity Volume Frac- tion O <sub>2</sub> in %	O <sub>2</sub> Production in kWh /kg O <sub>2</sub>	(CO <sub>2</sub> 110bar) in %	CO <sub>2</sub> gas. / liq. percentage points
Steam power plant							
Syed et al. [143]		--	not spec.	90	not spec.	28.7	5.8 / 8.3
Gas/steam turbine combined cycle							
Bolland, Sæther [144]		not spec./ 30	2	95	0.42 **	41.4	8.0 / 10.7
van Steenderen [133]		1050°C / 11 1050°C / 20	3 +IH	98	not spec.	42.7 44.0	6.9 / 9.3 5.6 / 8.0
Shao, Golomb [135]		1140°C / 15.6	not spec.	not spec.	combined with CO <sub>2</sub> liquefaction	45	( 6.5/9.0)
GT cycle with evaporation (REVAP)							
de Ruyck [145, 146]		1200°C / 80 (40 bar/0.5 bar)	--	100	not spec.	46	5.8 / 8.3
H <sub>2</sub> O-CO <sub>2</sub> Rankine cycle (water/steam injection in combustion chamber, only H <sub>2</sub> O condensed and recirculated)							
Bolland, Sæther [144]		900°C / 1333 (200/0.15bar)	1 95		0.42 ** 34.	0	-
Iantovski et al. [117]		750°C / 480 (240/30/5/0.5 bar)	2 x intermediate heating	not spec.	0.3	36.7 (TIT 1300°C: 42.7)	-
CO <sub>2</sub> /H <sub>2</sub> O Feher cycle (with basic intermediate cooling and intermediate heating)							
Iantovski et al. [117]		1300°C / 100	--	not spec.	0.3	42 - 53 *	(7-18/9.5-20.5)
CO <sub>2</sub> /H <sub>2</sub> O quasi-combined ("MATIANT") cycle							
Iantovski et al. [147]		1300°C / 4/ 15 (240/60/4 bar)	-- not	spec.	0.2 **	54.3	2 / 6

\* min. temperature difference at recuperator: a) 70 K b) 170 K

\*\* incl. O<sub>2</sub> compression

### 2.2.5 Process Family III: CO<sub>2</sub> Separation from Flue Gases

As shown in Section 3.4.2, the energy required for CO<sub>2</sub> separation from a flue gas is dependent on the concentration of CO<sub>2</sub> in the flue gas and the gas separation method selected. In the case of steam power plants, there is a greater concentration of CO<sub>2</sub> in the flue gas than in cycles with gas turbines. However, in terms of CO<sub>2</sub> separation processes, the resulting slightly lower expenditure on gas separation cannot compensate for the less favorable efficiency of steam power plants in comparison to combined cycle power plants. Furthermore, CO<sub>2</sub> concentration in a coal-fired cycle is always greater than that of a natural gas-fired cycle of a similar type, which means that the energy expended on CO<sub>2</sub> separation is slightly lower. However, CO<sub>2</sub> removal from the flue gas is still an attractive option in natural gas-fired combined cycles, since the other methods of CO<sub>2</sub> capture involve high energy consumption.

A simple method to increase CO<sub>2</sub> concentration in the exhaust gas of gas turbine cycles -- and thus to reduce theoretical separation work -- is to recirculate a portion of the flue gas. According to Bolland and Sæther [144], this method can be used to increase the volume fraction of CO<sub>2</sub> concentration in the flue gas of a natural gas-fired gas turbine from between 3% and 3.5% to around 5.5% volume fraction, which, however, only has the effect of improving efficiency by 0.1 percentage points, as compared to the case of CO<sub>2</sub> removal without flue gas recirculation (Table 2.13: No. 5b).



The results obtained from a study of the literature, dealing with coal-fired and natural gas-fired power plants with CO<sub>2</sub> removal from the flue gas, are summarized in Tables 2.12 and 2.13.

Table 2.12: Data from the literature on CO<sub>2</sub> capture from flue gases in coal-fired cycles

No.	Source	CO <sub>2</sub> Separation Method	CO <sub>2</sub> Capture Ratio in %	CO <sub>2</sub> Emissions	Efficiency Penalty $\Delta\eta$ in percentage points		Efficiency (LHV) in %	Specific Investment	CO <sub>2</sub> Avoidance Costs
					in kg CO <sub>2</sub> /kWh	CO <sub>2</sub> at 1 bar			
<b>Steam Power Plants</b>									
1	Kümmel et al. [74]	freezing under pressure	80 - 90	0.136-0.253	10-12	--	26 - 28	not spec.	not spec.
2	Blok et al. [148], Hendriks et al. [71]	chem. absorption (MEA)	90	0.115	8.3	11.6	31.7	1691 1828* =Baseline+822	32
3	Herzog et al. [124]	a) chem. absorption (MEA) b) distillation c) membrane (2 stage, polymer) d) phys. absorption (seawater)	90 90 80 --	0.17-0.42 0.2-1.76 0.35-0.7 --	16-20 19-34 17-26 14-19	12-14 15-29 13-22 10-15	11 - 23 (6 - 20) 13 - 22 (20 - 25)	not spec.	not spec.
4	Smelser et al. [154]	chem. absorption (MEA)	90	0.085	8.9-9.0		27.9-28.0	1871-2185 2070-2297*	not spec.
5	Bower et al. [98]	chem. absorption (aqueous amine)	90	0.13	8	11.9	30.0	not spec.	not spec.
6	Koetzler et al. [17]	a) chem. absorption (column) b) chem. absorption (membrane apparatus)	a)86.2 b)86.4	a)0.105 b)0.103	≈11	13.9	a)32.6 b)33.0	a) 1752 1877*	41
7	McMullan et al. [123]	chem. absorption (MEA)	86.1	0.123	7.6	10.6	30.7	1843*	not spec.
<b>Hybrid IGCC+PFBC (Topping Cycle)</b>									
8	Bower et al. [98]	chem. absorption (aqueous amine)	90	0.1	7.9	11.9	38.1 GT: 1170°C/16	not spec.	not spec.
9	McMullan et al. [123]	chem. absorption (MEA)	87.0	0.102	7.3	10.4	36.9 GT: 1000°C/20	1741*	not spec.
<b>MHD/Steam Turbine Combined Cycle</b>									
10	McMullan et al. [123]	chem. absorption (MEA)	88.2	0.075	5.3	8.0	44.9	1633*	not spec.

\* incl. CO<sub>2</sub> compression

Table 2.13: Data from the literature on CO<sub>2</sub> capture from flue gases in natural gas-fired cycles

Nr.	Source	CO <sub>2</sub> Separation Method	CO <sub>2</sub> Capture Ratio in %	CO <sub>2</sub> Emissions	Efficiency Penalty		Efficiency (LHV) in %	Specific Investment	CO <sub>2</sub> Avoidance Costs
					in percentage points				
				in kg CO <sub>2</sub> /kWh	CO <sub>2</sub> at 1 bar	CO <sub>2</sub> at 110 bar	CO <sub>2</sub> at 1 bar	in US\$/kW	US\$/t CO <sub>2</sub>
<b>Steam power plants</b>									
1	Hansen [149]	a) chem. absorption (MEA) b) distillation c) membrane	80	not spec.	8 5 32	10 7 34	38 41 14	not spec.	not spec.
<b>Gas/steam turbine combined cycle</b>									
2	Miller et al. [150]	chem. absorption (25-30% MEA)	55 -60	0.3-0.4	8.5	10	35.5 - 43.5	646-822 <sup>c)</sup>	k. A.
3	Blok et al. [148], Hendriks et al. [71]	chem. absorption (MEA)	90	0.048	4.5	6.6	43.5	941 <sup>c)</sup>	k. A.
4	Hansen [149]	a) chem. absorption (MEA) b) distillation c) electrochemical d) membrane	80	k. A.	11 13 7 < 0	13 15 9 < 0	44 42 48 < 0	not spec.	not spec.
5	Bolland, Sæther [144]	chem. absorption (MEA) a) standard b) flue gas recirculation (65%)	a)88.5 b)88.6	0.0128 0.0127	5.5 5.4	7.6 7.5	46.7 46.6 GT: 1060°C/11	a) 845 885 <sup>c)</sup> b) 1525 <sup>p)</sup>	not spec.
6	Koetzier [17]	a) chem. absorption (column) b) chem. absorption (membrane apparatus)	a)77.4 b)77.6	a)0.086 b)0.085	7.0 6.1	8.4 8.5	a)46.5 b)47.4 GT: 1050°C/11	a) 873 927 <sup>c)</sup> 1007 <sup>p)</sup>	38.3
<b>HAT cycle</b>									
7	Rao et al. [151]	chem. absorption ECONAMINE FG	k. A.	0.085- 0.090	5	not spec.	55 GT: 1300°C	not spec.	not spec.

As well as the energy required to compress and liquefy CO<sub>2</sub>, the separation of CO<sub>2</sub> involves some further work: depending on the gas separation method, this may involve compressor work (membrane, adsorption, physical absorption), cooling work (distillation, freezing) or heat for solvent regeneration (e.g. through the provision of extraction steam). Whereas, in all other methods, mechanical/electrical internal energy requirements for compression or refrigeration directly reduce power plant output, the reduction in electrical output in the case of chemical absorption is also determined by the manner in which the heat demand for solvent regeneration is integrated.

Literature sources almost always cite chemical absorption as the most appropriate method (with the lowest energy consumption) of removing CO<sub>2</sub> from flue gases, which have a low CO<sub>2</sub> concentration (Table 2.12: No. 2-11; Table 2.13: No. 1-7). Since up to 2/3 of the low-pressure steam mass flow (2-5 bar) of the turbine is consumed for the purpose of solvent regeneration, the low-pressure turbine section must be adjusted accordingly. Using chemical absorption, CO<sub>2</sub> can be captured at a higher level of purity, with a CO<sub>2</sub> capture ratio of over 90%. The equivalent electrical energy consumption<sup>29</sup>, comprising pump work and heat consumption, lies between 0.28 and 0.4 kWh/kg of CO<sub>2</sub>, whereby less energy is required for higher concentrations of the chemically reactive absorbent in the solvent. Some solvents (e.g. aqueous amine) require an effective desulfurization stage to be incorporated upstream, in order to keep down the costs incurred by oxidation of the absorbent.

As an example, 80% of the CO<sub>2</sub> can be absorbed from the flue gas of a natural gas-fired gas/steam turbine combined cycle using CO<sub>2</sub> scrubbing with an aqueous MEA solution. After the heat recovery steam generator, the flue gas must be cooled from around 100°C to approx. 40°C. After MEA scrubbing, it

<sup>29</sup> If heat requirements are calculated as a reduction in steam turbine output through steam extraction. Also see Appendix, Section 6.6.

must then be heated up again to approx. 60°C. The solvent regenerator is heated using steam extracted from the steam turbine, at 4 bar, which is subsequently released as condensate at approx. 109°C.

Low CO<sub>2</sub> partial pressure means that physical absorption is not a suitable method for removing CO<sub>2</sub> from power plant flue gases, unless seawater is used as a solvent (Table 2.12: No. 3d). Although energy expenditure would be lower if regeneration were to be omitted, seawater is still not a suitable CO<sub>2</sub> solvent, since the low solubility of CO<sub>2</sub> in water would require large quantities of water to be transported, and the pump work associated with this would exceed the energy requirements of other processes [152] (see also Section 3.4, p 84).

Low-temperature fractional distillation of a flue gas can be used to achieve high purity levels of the separated CO<sub>2</sub>. Specific electrical energy consumption lies between 0.6 and 1 kWh per kg of CO<sub>2</sub> removed, higher than the figure for chemical scrubbing [152]. Theoretically, direct freezing of CO<sub>2</sub> would consume 0.35 to 0.38 kWh per kg of CO<sub>2</sub> [74] (Table 2.12: No. 1); however, this is virtually impossible to perform from a technical point of view, since the cooling surfaces freeze up.

Using currently available polymer membranes, it is not possible to achieve sufficient purity of the separated CO<sub>2</sub> (only around 30% volume fraction is obtained) [153]. A two-stage membrane module can increase the capture ratio and, at the same time, improve CO<sub>2</sub> purity. However, the energy consumed in the course of flue gas compression approximates the gross power output of the entire plant [124] (Table 2.12: No. 3c; Table 2.13: No. 4d). According to van der Sluis et al. [73], membrane modules will require a selectivity between CO<sub>2</sub> and N<sub>2</sub> of at least 200 to 1, if they are to compete with other methods of CO<sub>2</sub> capture from flue gases.

The final method of removing CO<sub>2</sub> from flue gases is chemical absorption. For a CO<sub>2</sub> capture ratio (or separation factor, since in this case  $r_{CO_2} = s_{CO_2}$ ) of between 80% and 90%, literature sources cite efficiency penalties of between 8 and 13 percentage points for coal-fired steam power plants, and between 5.5 and 11 percentage points for gas/steam turbine combined cycle power plants. It should be noted, however, that the specific work per kg of separated CO<sub>2</sub> is much higher in gas-fired power plants.

According to [154], CO<sub>2</sub> capture should only reduce the availability of the power plant by approx. 0.75%.

## 2.2.6 Process Family IV: Carbon Separation

Another possible way of avoiding CO<sub>2</sub> emissions is to remove the carbon from the fuel. Since the carbon can then no longer be used as a fuel, it only makes sense to apply this method to fuels containing a high proportion of hydrogen.



Table 2.14: Energy utilization, and specific CO<sub>2</sub> emissions, with maximum C capture from the fuel, for different fuel mixtures and end products

Fuel Mixture/ Chemical Reaction	Fuel Utiliza- tion $\psi^*$ in %	Specific CO <sub>2</sub> emissions** in kg CO <sub>2</sub> /kWh of fuel produced			Power Plant Effi- ciency*** in %
		primary fuel mix	absolute	minus CO <sub>2</sub> from bio- mass	
<b>Methanol synthesis ("Hydrocarb" process, according to Steinberg et al. [36, 37, 38])</b>					
Biomass + methane ( $\dot{m}_{LHV} = 1.65 : 1$ )	58.2 / 60.9	0.311	0.248	-0.128	33.8
CH <sub>(1.44)</sub> O <sub>(0.66)</sub> + 0.34 CH <sub>4</sub> → 0.68 C + 0.66 CH <sub>3</sub> OH					
Biomass + oil ( $\dot{m}_{LHV} = 0.82 : 1$ )	42.1 / 46.3	0.289	0.248	-0.128	24.4
CH <sub>(1.44)</sub> O <sub>(0.66)</sub> + 0.7 CH <sub>(1.7)</sub> → C + 0.66 CH <sub>3</sub> OH					
Biomass + hard coal ( $\dot{m}_{LHV} = 0.3:1$ )	42.6 / 44.4	0.335	0.248	0	19.0
0.32 CH <sub>(1.44)</sub> O <sub>(0.66)</sub> + CH <sub>(0.8)</sub> O <sub>(0.1)</sub> → C + 0.32 CH <sub>3</sub> OH					
Hard coal only	36 / 40	0.33	0.248	0.248	20.8
<b>Synthesis gas production</b>					
Biomass + methane	69.9 / 71.6	0.311	0.21	-0.11	40.5
CH <sub>(1.44)</sub> O <sub>(0.66)</sub> + 0.34 CH <sub>4</sub> → 0.68 C + 0.66 CO + 1.32 H <sub>2</sub>					
Biomass + oil	50.6 / 54.4	0.289	0.21	-0.11	29.3
CH <sub>(1.44)</sub> O <sub>(0.66)</sub> + 0.7 CH <sub>(1.7)</sub> → C + 0.66 CO + 1.32 H <sub>2</sub>					
Biomass + hard coal	39.3 / 42.7	0.335	0.21	0.00	22.8
0.32 CH <sub>(1.44)</sub> O <sub>(0.66)</sub> + CH <sub>(0.8)</sub> O <sub>(0.1)</sub> → C + 0.32 CO + 0.64 H <sub>2</sub>					
<b>Hydrogen production (100% C retention)</b>					
Biomass only	3.2 / 3.5	0.351	0.00	-10.92	1.9
CH <sub>(1.44)</sub> O <sub>(0.66)</sub> → C + 0.66 H <sub>2</sub> O + 0.06 H <sub>2</sub>					
Biomass + methane	24.7 / 26.9	0.311	0.00	-0.89	14.3
CH <sub>(1.44)</sub> O <sub>(0.66)</sub> + 0.34 CH <sub>4</sub> → 1.34 C + 0.66 H <sub>2</sub> O + 0.74 H <sub>2</sub>					
Biomass + oil	31.7 / 36.1	0.289	0.00	-0.50	18.4
CH <sub>(1.44)</sub> O <sub>(0.66)</sub> + 0.7 CH <sub>(1.7)</sub> → 1.7 C + 0.66 H <sub>2</sub> O + 1.31 H <sub>2</sub>					
Biomass + hard coal	12.4 / 14.2	0.335	0.00	-0.66	7.2
0.32 CH <sub>(1.44)</sub> O <sub>(0.66)</sub> + CH <sub>(0.8)</sub> O <sub>(0.1)</sub> → 1.32 C + 0.3112 H <sub>2</sub> O + 0.3192 H <sub>2</sub>					
<b>Notional net calorific values/gross calorific values</b>					
Fuel	LHV in MJ/kmol	kg CO <sub>2</sub> /kWh (LHV)		HHV in MJ/kmol	
Biomass (CH <sub>(1.44)</sub> O <sub>(0.66)</sub> )	451.2	0.351		484.8	
Methane (CH <sub>4</sub> )	802.34	0.197		890.36	
Oil (CH <sub>(1.7)</sub> )	785	0.2		787.7	
Hard coal CH <sub>(0.8)</sub> O <sub>(0.1)</sub>	479.6	0.33		485.7	
Methanol (CH <sub>3</sub> OH)	638.5	0.248		726.5	
H <sub>2</sub>	241.82	-		285.83	
CO	282.98	0.55		282.98	
C (graphite)	393.51	0.40		393.51	

$$* \quad \psi = \frac{\dot{m}_{B, produced} LHV_{o, produced} (without C)}{\dot{m}_{F, in} LHV_{o, in}}$$

\*\* after combustion

\*\*\* with optimum chemical conversion process; possible heat recovery or additional internal consumption have not been taken into consideration.

If the fuel produced is burnt in a gas/steam turbine combined cycle with an efficiency of 58%, the efficiency penalty due to C-retention and methanol production lies between 24 and 26 percentage points. If the synthesis gas is produced directly for conversion into electrical energy, the efficiency penalty ranges between 17 and 23 percentage points (Table 2.14).

### 2.2.7 Process Family V: CO<sub>2</sub> Capture with Fuel Cells

There are several possible methods of CO<sub>2</sub> capture associated with fuel cells, depending on the type of fuel cell used:

- Removing the carbon component from the fuel gas prior to the fuel cell (PEMFC, PAFC, MCFC, SOFC), Figure 2.21.a, .b or
- Separating the residual fuel and CO<sub>2</sub> in the anode exhaust gas, Figure 2.22, Figure 2.23.

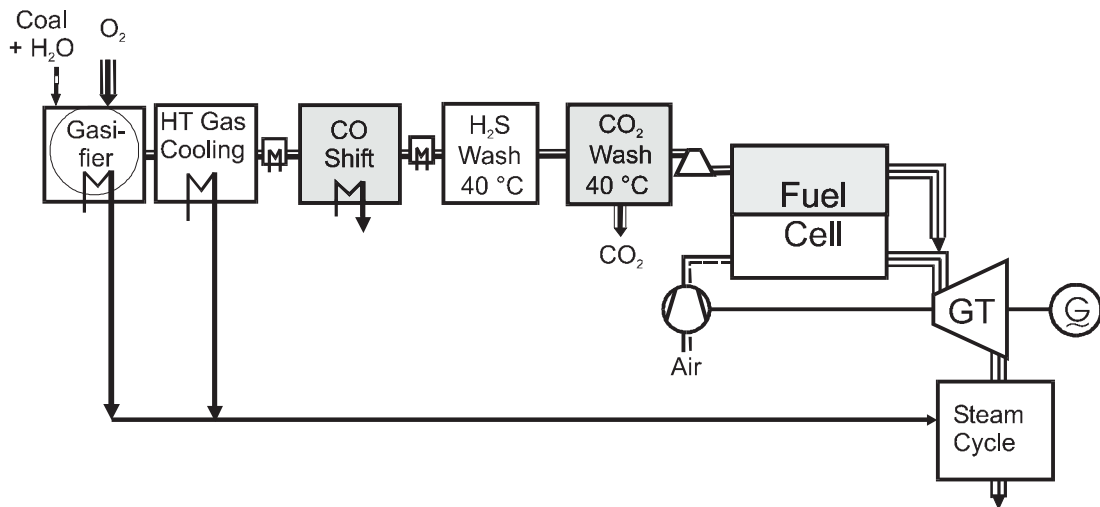


Figure 2.21.a: Gasification and CO shift with CO<sub>2</sub> removal prior to the fuel cell (PEMFC, PAFC, MCFC, SOFC)

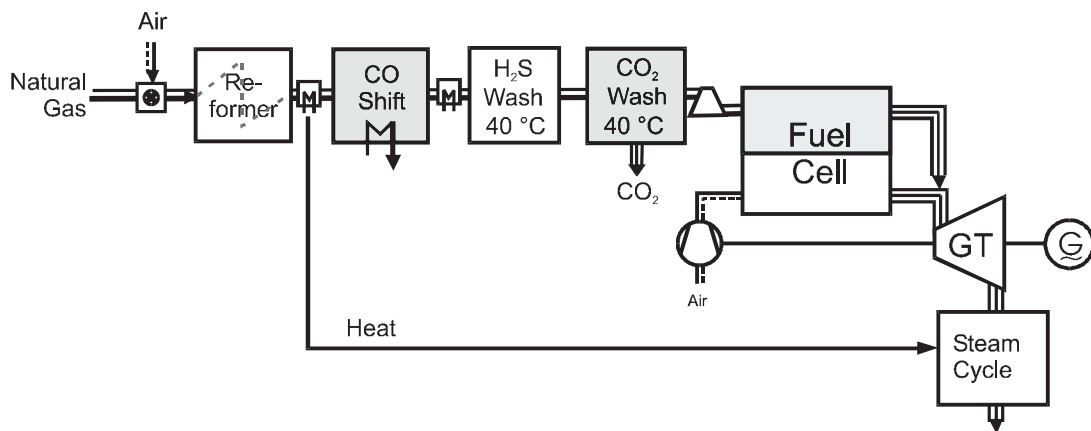


Figure 2.21.b: Natural gas reforming and CO shift with CO<sub>2</sub> removal prior to the fuel cell (PEMFC, PAFC, MCFC, SOFC)

In the first method, the fuel cell is operated with pure H<sub>2</sub> and the conversion work corresponds to the processing of the fuel described in "Process Family I". Since hydrogen production anyway represents a necessary component of the operation of a PEMFC or PAFC, the efficiency penalty incurred with these types of fuel cell is conditional solely on the energy required for CO<sub>2</sub> removal. Due to the high working temperatures associated with MCFC and SOFC, CO shift conversion and steam reforming take place internally, after fuel gas humidification, to at least a partial extent. Using a process arrangement featuring anode exhaust gas recirculation or afterburning for preheating purposes, fuel gas conversion is avoided for operation without CO<sub>2</sub> capture. In the case of the first method of CO<sub>2</sub> capture for these types of fuel cell, the efficiency penalty can be calculated in accordance with the expenditures cited for "Process Family I".

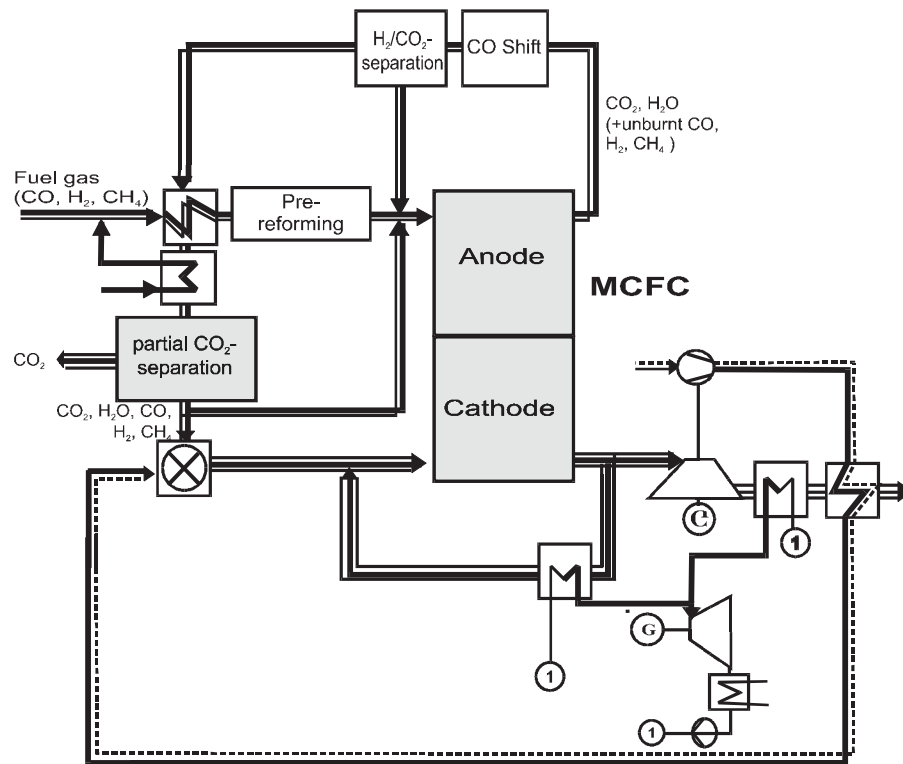


Figure 2.22: Flow diagram of an MCFC with removal of CO<sub>2</sub> from the anode exhaust gas. Due to the operating characteristics of the MCFC, it is necessary to mix a portion of the CO<sub>2</sub> into the cathode intake air.

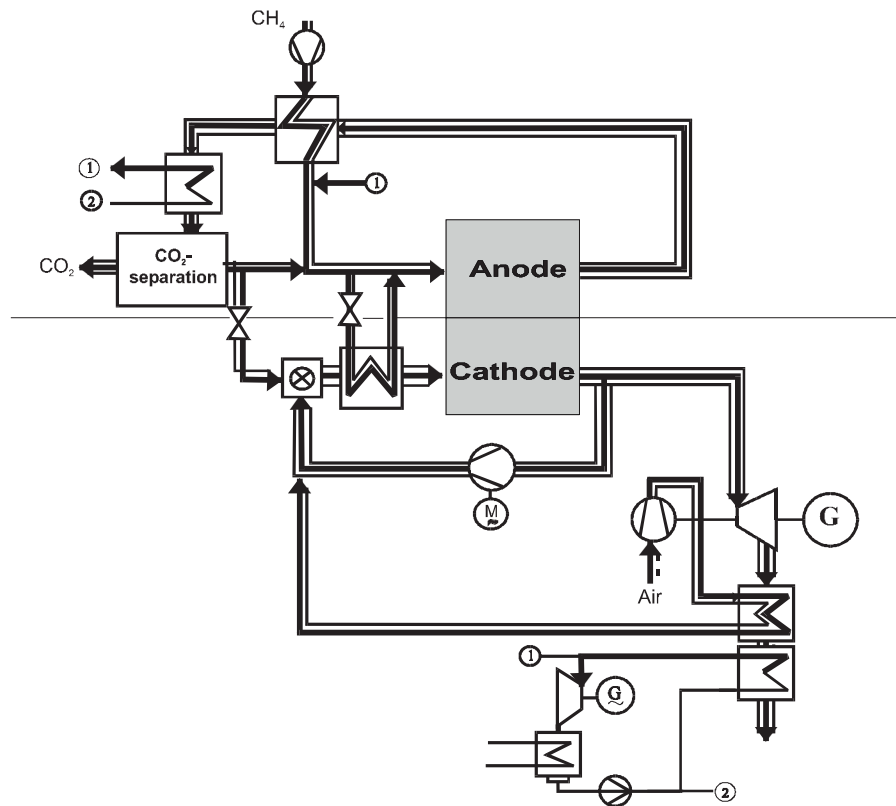


Figure 2.23: Flow diagram of a natural gas-fired SOFC with removal of CO<sub>2</sub> from the anode exhaust gas

In the second method, the fuel cell could be described as functioning as a gas separation apparatus, since the fuel gas is oxidized in the fuel cell without mixing with atmospheric nitrogen and without requiring any work for oxygen production. In fact, the oxidation process in the fuel cell represents a suppressed mixing of the reaction product with the ambient air (i.e. the anode exhaust gas is not mixed with nitrogen) and, in the case of MCFC and SOFC, the selective transport of O<sub>2</sub> (and CO<sub>2</sub> with the MCFC), and, in the case of PAFC and PEM, selective removal of the hydrogen at the cathode, where water is produced. In this method, CO<sub>2</sub> capture work essentially consists of the separation of non-burned components (mainly H<sub>2</sub>) and CO<sub>2</sub> in the anode exhaust gas. Since PEM fuel cells are extremely sensitive to CO, it is necessary to convert virtually all of the CO to CO<sub>2</sub> (or to CH<sub>4</sub> through methanation) before the fuel cell stage. In some cases in the literature, the theoretical energy advantage of gas separation with a high level of concentration in the anode exhaust gas is abandoned, in favor of simple utilization of the residual fuel to heat the cathode air, and the CO<sub>2</sub> produced is removed from the cathode exhaust gas [25].

In the case of high-temperature fuel cells, in addition to the electrochemical reaction of H<sub>2</sub> with oxygen ions to form water (and, in part, of CO to CO<sub>2</sub>), catalyst-supported CO shift and hydrocarbon reforming also take place. Since not all the fuel can be converted, the anode exhaust gas consists of steam, CO<sub>2</sub> and non-burned fuel. For CO<sub>2</sub> capture, the residual fuel must be separated out, and the water component must be removed through condensation. There are various possible ways of simplifying the CO<sub>2</sub> capture process:

- subsequent (downstream) CO shift, separation of the CO<sub>2</sub> and H<sub>2</sub> which are produced, and return of the H<sub>2</sub> to the anode (best utilization of fuel, most expensive solution),



- afterburning of the anode exhaust gas with oxygen from the air separation unit of a coal gasification unit, utilizing this partly to preheat the cathode air, and separation of CO<sub>2</sub> and H<sub>2</sub>O through condensation from the anode exhaust gas, or
- afterburning of the anode exhaust gas, utilizing this to preheat the cathode air, and removal of the CO<sub>2</sub> from the cathode exhaust gas.

Due to the way in which an MCFC functions, sufficient CO<sub>2</sub> must be mixed into the cathode gas. The CO<sub>2</sub> concentration in the cathode exhaust gas should be expected to be higher than that in the intake air. It may therefore make sense to mix all of the burnt anode exhaust gas into the cathode and remove the CO<sub>2</sub> from the cathode exhaust gas.

Table 2.15: Concentrations and CO<sub>2</sub> absorption rate at the cathode of the MCFC, taken from various studies.

Source	No. in Table 2.16	Cathode Inlet	Cathode Exhaust Gas	Operating Pressure in bar	CO <sub>2</sub> Absorption Rate in %	CO <sub>2</sub> capture
		Volume fraction of CO <sub>2</sub> (%)				
MCFC, coal gasification IEA-GHG [25]	2	8.9	5.0	3	60	before anode
MCFC, coal gasification IEA-GHG [25]	3	6.3	3.3	3	50	from anode exhaust gas
MCFC, natural gas re-forming IEA-GHG [25]	8	6.5	2.8	3	60	before anode
MCFC, direct firing with natural gas IEA-GHG [25]	9	16.1	5.1	1	74	from cathode exhaust gas
MCFC, coal gasification Doctor et al. [155]	4	9.1	0.85	10	92	from anode exhaust gas

Precise analysis of CO<sub>2</sub> capture in fuel cells requires knowledge of the electrochemical conversion of individual gas components for different gas compositions and fuel cell operating states. For example, CO<sub>2</sub> absorption in the cathode of the MCFC is a decisive factor for the remaining CO<sub>2</sub> emissions after the cathode. Table 2.15 shows the wide differences in CO<sub>2</sub> absorption in the cathode under different operating conditions, which are used as a basis in various literature sources. The fact that fuel cells are in such an early stage of development means that exact data is hard to obtain; this study therefore limits its scope to a comparison of the data from the literature, rather than providing a separate analysis in Section 3.

For coal gasification power plants, cycles with PAFC, MCFC and SOFC are described in the literature (see Table 2.16: No. 1-7). With coal gasification, CO shift and a CO<sub>2</sub> capture ratio of 68.5%, an efficiency rating of 40.6% can be achieved in a combined cycle consisting of a PAFC and a subsequent steam cycle, including CO<sub>2</sub> liquefaction [31] (Table 2.16: No. 1). With the combination of an MCFC and a steam cycle in a similar configuration, a CO<sub>2</sub> capture ratio of 68% and an efficiency of only approx. 35%, including CO<sub>2</sub> liquefaction, can be achieved [25] (Table 2.16: No. 2). According to IEA-GHG [25] (Table 2.16: No. 3), CO<sub>2</sub> removal from the anode exhaust gas (following combustion with O<sub>2</sub> without CO conversion) holds no potential for improvement, when compared to variations with CO<sub>2</sub> removal from the coal gas prior to the fuel cell (Table 2.16: No. 2). With afterburning of the anode exhaust gas of an MCFC with air, and subsequent CO<sub>2</sub> scrubbing, the efficiency in a plant with

integrated coal gasification and a subsequent steam cycle is even lower, according to a study performed by Doctor et al. [155] (Table 2.16: No. 4). The low efficiencies of these cited MCFC power plants can primarily be traced back to poor fuel conversion, of around 75%, in the fuel cell, and further exergy lost through the cooling of the hot, afterburnt anode exhaust gas prior to CO<sub>2</sub> scrubbing. Improved efficiencies for MCFC with coal gasification and subsequent steam cycle are obtained with CO conversion in the anode exhaust gas and H<sub>2</sub> recirculation to the anode [156] (Table 2.16: No. 5). By using a ceramic membrane, it is stated that between 88% and 95% of the H<sub>2</sub> can be removed from the anode exhaust gas (converted through a CO shift reaction) and recirculated. Assuming CO conversion of 90% in the CO shift reaction and fuel conversion of 75% with a single pass through the MCFC, this would mean a reduction in residual fuel energy in the anode exhaust gas of 25% of the fuel gas energy before the anode, to between approx. 3.6% and 5.2%. Improved utilization of the fuel gas and hot gas separation are the explanation behind the achievable efficiencies of between 47.7% and 53.2%, including CO<sub>2</sub> liquefaction and depending on the H<sub>2</sub> separation factor, achieved with a CO<sub>2</sub> capture ratio of 68.5%, according to the study by Jansen et al. [156]. With a similar process arrangement, McMullan et al. [32] (Table 2.16: No. 6) calculates an efficiency of 49.6% for an IGCC power plant with MCFC and a CO<sub>2</sub> capture ratio of 87.9%. Without CO<sub>2</sub> capture and liquefaction, the efficiency rating is 5.9 percentage points higher. For a corresponding process arrangement of an IGCC power plant with SOFC (Table 2.16: No. 7), and a CO<sub>2</sub> capture ratio of 98.8% from the anode exhaust gas after CO conversion, McMullan et al. [32] cite an efficiency of 47.8%, corresponding to an efficiency penalty of 8.7 percentage points when compared to the IGCC power plant with SOFC without CO<sub>2</sub> capture. Due to the early stage of development of the SOFC, McMullan et al. assume a lower efficiency for the SOFC than for the MCFC.

All the cases of MCFC in combination with coal gasification are based on a maximum feasible CO<sub>2</sub> capture ratio of between around 70% and 88%. A large portion of the remaining CO<sub>2</sub> emissions stem from the emissions of the MCFC cathode, which requires increased CO<sub>2</sub> concentrations at the cathode for correct functioning. The CO<sub>2</sub> absorbed at the cathode of the MCFC varies between 50% and 92% in the various studies (Table 2.15). It is possible that the CO<sub>2</sub> emissions may be subject to further uncertainty due to deviations in CO<sub>2</sub> absorption at the cathode.

In the case of MCFC operation using natural gas, with an efficiency of 49.0% (including CO<sub>2</sub> liquefaction), the variant which features CO<sub>2</sub> removal subsequent to reforming and CO conversion is inferior to a gas/steam turbine combined cycle with CO<sub>2</sub> scrubbing from the flue gas [25]. At the same time, this process allows less than 60% of the CO<sub>2</sub> to be separated. With a CO<sub>2</sub> capture ratio of 90%, removal of CO<sub>2</sub> from the cathode exhaust gas of an MCFC results in a power plant efficiency of 55.5%, including CO<sub>2</sub> liquefaction, which is marginally higher than that achieved in a gas/steam turbine combined cycle with CO<sub>2</sub> scrubbing from the flue gas. With an efficiency of 59.7%, including CO<sub>2</sub> liquefaction, with a CO<sub>2</sub> capture ratio of approx. 90%, a combined cycle power plant with SOFC featuring afterburning of the anode exhaust gas with air, and subsequent gas turbine and heat recovery steam cycle stages, in which 90% of the CO<sub>2</sub> arising in the process is washed out of the cathode exhaust gas, is far superior to all other methods of CO<sub>2</sub> capture, at least from the point of view of efficiency [25].

Investment costs for PAFC and MCFC are estimated to be substantially higher than for other types of power plant. This is why the CO<sub>2</sub> avoidance costs cited in the literature, relating to IGCC power plants or gas/steam turbine combined cycle power plants, are so high. The only case where the costs are comparable with the costs incurred in other gas/steam turbine combined cycle power plants is that of CO<sub>2</sub> capture with a natural gas-operated SOFC.

Table 2.16: Data from the literature on power plant systems with fuel cells, CO<sub>2</sub> capture and liquefaction

No	Type of power plant, literature source	CO <sub>2</sub> capture	FC operating conditions (temp./ pressure)	Efficiency (LHV) in %	Efficiency penalty due to CO <sub>2</sub> capture and liquefaction (percentage points)	CO <sub>2</sub> emissions in kg CO <sub>2</sub> / kWh	CO <sub>2</sub> capture ratio in %	Investment in US\$/kW	CO <sub>2</sub> avoidance costs in US\$/t of CO <sub>2</sub>
1	Coal gasification + PAFC Campbell et al. [31]	before anode (CO shift + scrubbing)	200°C / 1 bar	40.6	9.0	0.254	68.5	4310 (1995) 2100 (future)	---
2	Coal gasification + MCFC IEA-GHG [25]	before anode (CO shift + scrubbing)	650°C / ≈ 1 bar **	35.2	not spec.	0.306	68	3303	65
3	Coal gasification + MCFC IEA-GHG [25]	from anode exhaust gas, (after combustion with O <sub>2</sub> )	650°C / ≈ 1 bar **	36.3	not spec.	0.217	76	2925	40.4
4	Coal gasification + MCFC Doctor et al. [155]	from anode exhaust gas (scrubbing)	700°C / 10 bar	31.7	2.3 liquefaction + 0.4 CO <sub>2</sub> scrubbing + x other	0.195	81	2666	
5	Coal gasification + MCFC Jansen et al. [156]	H <sub>2</sub> separation from anode exhaust gas after CO shift	650°C / 4 bar	47.7 - 53.2	> 2	0.0228 (+0.15-0.16 from cathode exhaust gas *)	68.5	IGCC x 1.2-1.4	
6	Coal gasification + MCFC McMullan et al. [32]	CO <sub>2</sub> separation from anode exhaust gas after CO shift		49.6	5.9	0.08	87.9	3820	30 (own calculation)
7	Coal gasification + SOFC McMullan et al. [32]	CO <sub>2</sub> separation from anode exhaust gas after CO shift		47.8	8.7	0.008	98.8	3820	35 (own calculation)
8	Natural gas reforming + MCFC IEA-GHG [25]	before anode (reforming + CO shift + scrubbing)	650°C / ≈ 1 bar **	49.0	not spec.	0.177	58	2153	117
9	Direct natural gas-fired MCFC IEA-GHG [25]	from cathode exhaust gas (scrubbing)	650°C / ≈ 1 bar **	55.5	not spec.	0.034	91	1955	55.4
10	Direct natural gas-fired SOFC IEA-GHG [25]	from cathode exhaust gas (scrubbing)	1000°C / ≈ 6 bar **	59.7	not spec.	0.034	90	1637	39.8
<i>Baseline IGCC power plant according to IEA-GHG [25] (does not conform to current state of the technology)</i>									
	IGCC without CO <sub>2</sub> capture	---	---	41.9	---	0.791	---	1811	---
	Gas/steam turbine combined cycle plant without CO <sub>2</sub> capture	---	---	52.0	---	0.406	--	840	---

\* according to my own estimations, a maximum limit of 70%-80% of the CO<sub>2</sub> can be absorbed at the cathode, meaning that additional emissions should be expected in this case.

\*\* MCFC: ΔT≈40 K, 85% fuel utilization, SOFC: ΔT≈380 K, 85% fuel conversion

## 2.2.8 Review of the Literature with Conversion to a Common Basis

The power plants with CO<sub>2</sub> capture described in the literature display widely differing levels of technology, in terms of factors such as gas turbine inlet temperature and live steam temperature, for example, as well as differing ambient conditions. This causes significant discrepancies in the efficiencies described.

By using simple conversion equations, it is possible to convert the efficiencies obtainable with CO<sub>2</sub> capture to the same level of baseline power plant (modern steam power plant, or gas/steam turbine combined cycle power plant with currently achievable gas turbine inlet temperature) and the same energy requirements for CO<sub>2</sub> liquefaction, assuming an identical final pressure. CO<sub>2</sub> avoidance costs are calculated based on the assumption of standard costs for the baseline power plant (Table 2.2, p 8), and further investment according to the literature sources.

However, some of the processes described in the literature are no longer currently available, some cannot even be performed with current technologies. To a certain extent, information on the efficiencies and CO<sub>2</sub> avoidance costs is therefore speculative.

## Efficiency Conversions and Estimates

### *Conversion to an IGCC Power Plant with Improved Combined Cycle (Without CO<sub>2</sub> Capture)*

The efficiency of GTCC power plants has improved significantly over the last few years. When comparing different processes, it is therefore important to assess efficiency on the basis of comparable individual efficiencies. The following equation provides a first approximation for the conversion of IGCC efficiency  $\eta_{IGCC,0}$  (without CO<sub>2</sub> capture), in dependence on the efficiency of the gas/steam turbine combined cycle  $\eta_{GTCC,0}$  on which this is based, to achievable efficiency  $\eta_{IGCC,1}$  using an improved gas/steam turbine combined cycle power plant with efficiency  $\eta_{GTCC,1}$ :

$$\eta_{IGCC,1} = \eta_{IGCC,0} \frac{\eta_{GTCC,1}}{\eta_{GTCC,0}} \quad (2.16).$$

The following equation applies to CO<sub>2</sub> emissions:

$$\dot{m}_{CO_2,1} = \dot{m}_{CO_2,0} \frac{\eta_{GTCC,0}}{\eta_{GTCC,1}} \quad (2.17).$$

### *Power Plants with CO<sub>2</sub> Separation from the Flue Gas, CO<sub>2</sub> Liquefaction*

By relating the additional energy requirements for CO<sub>2</sub> separation (or the penalty in output caused by CO<sub>2</sub> separation) to the heating value of the fuel employed, efficiency  $\eta_{PP,CO_2}$  of the power plant with CO<sub>2</sub> separation can be calculated from efficiency  $\eta_{Basis}$  of the baseline power plant without CO<sub>2</sub> separation, as follows:

$$\eta_{PP,CO_2} = \eta_{Basis} - \overline{\Delta\eta} \quad (2.18)$$

where 
$$\overline{\Delta\eta} = \frac{\text{(additional internal consumption) or (reduction in output)}}{\dot{m}_F LHV_F}$$

If the energy expenditure for CO<sub>2</sub> capture consists solely of the energy expended on gas separation, with specific energy expenditure  $w_{CO_2}$  related to mass flow  $\dot{m}_{CO_2}$  of the separated CO<sub>2</sub>, efficiency penalty  $\overline{\Delta\eta}$  is calculated from:

$$\Delta\eta = \frac{m_{CO_2} W_{CO_2}}{m_F LHV_F} \quad (2.19)$$

and efficiency  $\eta_{PP,CO_2}$  of the power plant with CO<sub>2</sub> separation is approximated from:

$$\eta_{PP,CO_2} = \eta_{Basis} - \frac{m_{CO_2} W_{CO_2}}{m_F LHV_F} \quad (2.20)$$

### Power Plants with Combustion in an Atmosphere of O<sub>2</sub>/CO<sub>2</sub>

In power plants featuring combustion in an atmosphere of oxygen and recirculated exhaust gas or steam, additional energy is required to generate the oxygen. Based on the assumption that a working cycle, which uses CO<sub>2</sub> as a working fluid, has the same cycle efficiency as a cycle using air as a working fluid, efficiency  $\eta_{PP,O_2/CO_2}$  of the power plant with CO<sub>2</sub> capture is approximated by:

$$\eta_{PP,O_2/CO_2} = \eta_{Basis} - \frac{O_{min} W_{O_2}}{m_F LHV_F} \quad (2.21)$$

where:  $O_{min}$  minimum oxygen required,  $W_{O_2}$  specific work to generate O<sub>2</sub>,  $m_F$  mass flow of fuel,  $LHV_F$  heating value of the fuel,  $\eta_{Basis}$  efficiency of the baseline power plant without CO<sub>2</sub> capture

### IGCC Power Plants with CO Conversion and CO<sub>2</sub> Capture

For an IGCC power plant with CO conversion and subsequent CO<sub>2</sub> separation, it is not possible to estimate the efficiency of the power plant with CO<sub>2</sub> capture directly from that of the baseline power plant, since the efficiency is influenced not only by internal consumption for the gas separation process, but also by the CO<sub>2</sub> conversion process. The relationships involved in determining the efficiency of the IGCC with CO<sub>2</sub> capture are illustrated by the following equation:

$$\begin{aligned} \eta_{IGCC,CO_2} = & \eta_{CG} \eta_{CO-shift} \eta_{GTCC} \\ & + [(1 - \eta_{CG} \eta_{CO-Shift}) - c_G] c_1 \eta_{HT} + [(1 - \eta_{CG} \eta_{CO-Shift}) - c_G] (1 - c_1) c_2 \eta_{steam} \\ & - m_{CO_2} \eta_{turbine} RT_u \ln \left( \frac{P_{GT}}{P_u} \right) - w_{int} - w_{int,CO_2} \end{aligned} \quad (2.22)$$

where:

$\eta_{CO-Shift}$  : efficiency of the CO shift (95 to 97%);

$\eta_{CG}$  : ratio of fuel energy flow (HHV/HHV) or cold gas "efficiency", see equation 3.12, p 74;

$\eta_{GTCC}$  : efficiency of the gas/steam turbine combined cycle power plant;

$\eta_{Steam}$  : efficiency of the steam cycle;

$\eta_{HT}$  : efficiency in the utilization of heat from the raw gas cooling stage in the steam cycle;

$w_{int} = W_{int} / (m_{Coal} LHV_{Coal})$  : specific internal consumption

$$w_{\text{int},\text{CO}_2} = - \frac{m_{\text{CO}_2} w_{\text{CO}_2}}{m_{\text{Coal}} \text{LHV}_{\text{Coal}}} : \text{ internal consumption of the CO}_2 \text{ separation process;}$$

$w_{\text{CO}_2}$  : specific work required to separate a kg of CO<sub>2</sub>;

$c_G$  : enthalpy for the gasification steam requirement related to the coal energy;

$c_1$  : constant representing the proportion of the heat from the raw gas cooling stage, which is used in the steam cycle;

$c_2$  : proportion of the heat from the raw gas cooling stage, which is transferred from the raw gas to the clean gas. Since ratio of fuel energy flows  $\eta_{CG}$  does not include the exergy expenditure for gasifying agent (H<sub>2</sub>O) and oxidant (O<sub>2</sub>), this expenditure must be taken into account in the values for  $c_2$  and specific internal consumption  $w_{\text{int}}$  and adjusted to the specific application under examination.

The third from last term approximately describes the lost expansion work of the separated CO<sub>2</sub>. Values for the constants are given in Table 2.17.

Table 2.17: Constants used for approximate estimation of the efficiency of an IGCC

Gasification temperature	in °C	1300	1200	1100	1000	900
Ratio of gross heating value (cold gas efficiency)	in %	88.0	89.1	90.2	91.1	91.8
Heat from raw gas cooling to HRSG	in % *	6.0	4.9	3.8	2.5	0.9
Heat from raw gas cooling to clean gas preheating	in % *	4.8	4.8	4.7	4.7	4.7
Heat from raw gas cooling to saturator heating	in % *	1.6	1.7	1.9	2.5	3.9
$\eta_{HT}$ (Efficiency of the heat from the raw gas cooling process in the steam cycle) in %		47	47	47	47	47
$c_G$ (Gasification steam)	in % *	1.7	2.0	2.6	3.7	6.1
$c_1$ (Steam produced from heat from the raw gas cooling process) in %		52.5	48.0	42.0	33.0	15.1
$c_2$ (Heat from raw gas cooling to the clean gas)	in %	55.8	63.3	74.5	95.0	142.6
$w_{\text{int}}$ (ASU, DESOX,...)	in %	1.3	1.2	1.2	1.2	1.1
$w_{\text{int},\text{CO}_2}$ (Internal consumption of the CO <sub>2</sub> separation process) in %		1.0 - 1.7	1.0 - 1.7	1.0 - 1.7	1.0 - 1.7	1.0 - 1.7

\* based on the fuel energy flow (LHV) of the feed coal

## Evaluation and Comparison

A comprehensive assessment of the different processes may be performed on the basis of technical/economic operating data (e.g. costs, efficiency, emissions, simple operation), and social criteria, such as acceptance on the part of the local population and decision-makers in energy supply companies and the political arena. By evaluating and weighting the individual criteria, the different designs may be ranked according to their suitability (e.g. see [157]<sup>30</sup>). The scope of this present study is restricted to the evaluation of individual, objectively assessable, technical criteria. Specifically, these are:

- specific CO<sub>2</sub> emissions,
- efficiency with and without CO<sub>2</sub> capture,
- efficiency penalties, or specific energy expended on reducing CO<sub>2</sub> emissions, respectively (establishing the contributions of the individual steps in the process),
- increase in specific investment due to CO<sub>2</sub> capture,

<sup>30</sup> Criteria compiled and weighted by R. Pruschek and G. Göttlicher, among others.

- increase in electricity generating costs<sup>31</sup> caused by CO<sub>2</sub> capture,
- CO<sub>2</sub> avoidance costs and
- technical feasibility.

The achievable CO<sub>2</sub> capture ratio and the incorporation of CO<sub>2</sub> liquefaction are two of the most important boundary conditions in a standardized comparison of CO<sub>2</sub> capture processes.

Efficiency penalties due to CO<sub>2</sub> capture, and the specific additional energy requirements of CO<sub>2</sub> capture, are primarily dependent on the method and the level of technology of the CO<sub>2</sub> capture process, and only depend to a small degree on the efficiency of the baseline power plant<sup>32</sup>. The efficiency penalty can thus be viewed as a characteristic variable for energy expenditure.

Table 2.18 shows the results of the conversion process, where the baseline power plants are converted to a standardized level of technology of the steam power plant, the IGCC power plant and the gas/steam turbine combined cycle power plant, and where the specific energy requirements of CO<sub>2</sub> liquefaction, related to the CO<sub>2</sub> mass flow, are the same in all cases. The occasionally inconsistent discrepancies between the data (e.g. the efficiency penalties due to combustion in an atmosphere of oxygen and recirculated CO<sub>2</sub> in a natural gas-fired steam power plant are different from those in a natural gas-fired gas/steam turbine combined cycle) are due to the fact that the data is based on literature sources which differ by up to approx. 30%.

### *Specific CO<sub>2</sub> Emissions (kg CO<sub>2</sub>/kWh)*

The only way of achieving virtually complete avoidance of CO<sub>2</sub> emissions is through combustion in an atmosphere of O<sub>2</sub>/CO<sub>2</sub>. In all other processes, the maximum CO<sub>2</sub> capture ratio that can be achieved with a reasonable amount of work done only amounts to around 95%. CO<sub>2</sub> separation from the flue gas of a coal-fired power plant (steam power plant or IGCC), or CO<sub>2</sub> separation following CO conversion in an IGCC power plant, can serve to reduce specific CO<sub>2</sub> emissions to between one-quarter and one-fifth of the CO<sub>2</sub> emissions of a natural gas-fired gas/steam turbine power plant without CO<sub>2</sub> capture. With CO<sub>2</sub> capture, the specific CO<sub>2</sub> emissions of a natural gas-fired power plant again lie below those of the coal-fired power plant, in accordance with the lower carbon content of the fuel.

### *Efficiency With and Without CO<sub>2</sub> Capture*

The highest efficiencies with CO<sub>2</sub> capture are achieved by high-temperature fuel cell power plants. Setting aside fuel cells for the time being as a "future option", the natural gas-fired gas/steam turbine combined cycle power stations and the coal-fired IGCC power stations display the greatest efficiency, as is the case with the baseline power plants. In IGCC power plants, the most advantageous method, from the point of view of energy expenditure, is CO<sub>2</sub> capture after CO conversion, closely followed by combustion in an atmosphere of O<sub>2</sub>/CO<sub>2</sub>.

In the case of natural gas-fired gas/steam turbine combined cycle power stations, literature sources cite both CO<sub>2</sub> separation from the flue gas, and CO<sub>2</sub> separation subsequent to reforming with internal partial combustion and CO conversion as the most advantageous methods. According to the results from Table 2.18, CO<sub>2</sub> separation from flue gases ranks slightly higher than CO<sub>2</sub> separation subsequent to reforming with internal partial combustion and CO conversion.

<sup>31</sup> Electricity generating costs calculated according to the annuity method, see Appendix, Section 6.7 [180].

<sup>32</sup> In spite of this, the baseline power plant needs to display high efficiency, since this is the only way to create a small ratio between power output penalties caused by CO<sub>2</sub> capture and gross electricity generation, and thereby to make the additional costs low.

Several processes can be ruled out due to their low efficiencies: namely, processes with CO<sub>2</sub> adsorption, CO<sub>2</sub> separation from synthesis gases following gasification with air or following direct quenching of the raw gas with water, STIG processes with combustion in an atmosphere of O<sub>2</sub>/CO<sub>2</sub> and Rankine cycles with internal combustion, as well as processes with CO<sub>2</sub> separation subsequent to externally heated reforming or CO<sub>2</sub> separation from flue gases using a membrane process.

### *Specific Expenditure of Energy on Reducing CO<sub>2</sub> Emissions / Efficiency Penalty*

In this case, too, high-temperature fuel cell power plant cycles again achieve the lowest energy requirements related to avoided CO<sub>2</sub> emissions, followed by CO<sub>2</sub> separation from synthesis gases after CO conversion in an IGCC power plant (if adsorption, air-blown gasification and raw gas cooling through direct quenching with water are excluded), and IGCC power plants with combustion in an O<sub>2</sub>/CO<sub>2</sub> atmosphere. The variation featuring H<sub>2</sub>/CO separation and combustion of just the CO portion in an O<sub>2</sub>/CO<sub>2</sub> atmosphere also achieves low specific energy expenditure.

In the case of natural gas-fired processes, the specific expenditure of energy on reducing CO<sub>2</sub> emissions is significantly higher than that required in all the coal-fired processes. However, the efficiency penalty due to CO<sub>2</sub> capture in natural gas-fired processes is smaller, since the CO<sub>2</sub> mass flow to be separated is substantially smaller overall. Specific energy expenditure on CO<sub>2</sub> capture from the flue gas, and with combustion in an O<sub>2</sub>/CO<sub>2</sub> atmosphere, lies slightly below that of CO<sub>2</sub> separation with reforming with internal partial combustion and CO conversion.

CO<sub>2</sub> adsorption after CO conversion in an IGCC, CO<sub>2</sub> separation subsequent to externally heated reforming and CO conversion, and the Rankine cycle with internal combustion (working fluid: mixture of H<sub>2</sub>O and burner gas) all require a significantly higher expenditure of energy than that of the other cases.

### *Increase in Specific Investment Due to CO<sub>2</sub> Capture*

The additional investment for CO<sub>2</sub> capture stems from the efficiency/output penalties and the additional equipment required for CO<sub>2</sub> capture. Overall, CO<sub>2</sub> capture increases specific investment by between 20% and 40%, if processes with low efficiencies or high expenditures of energy are disregarded. The lowest relative increase in investment caused by CO<sub>2</sub> capture occurs in the case of CO<sub>2</sub> capture in power plants using fuel cells, followed by gas/steam turbine combined cycle power plants with flue gas scrubbing, and CO<sub>2</sub> capture using membranes from the synthesis gas of an IGCC power plant subsequent to CO conversion. For CO<sub>2</sub> capture through combustion in an atmosphere of O<sub>2</sub>/CO<sub>2</sub>, the investment required increases slightly more than in the case of CO<sub>2</sub> separation from synthesis gases after CO conversion in an IGCC. In the case of fuel cell power plants, however, the costs of the baseline power station are already extremely high, and, at the same time, the efficiency penalties are lower than in the other cases, meaning that the additional investment required for CO<sub>2</sub> capture will be less significant overall. No significant difference was found between natural gas-fired and coal-fired processes in terms of the increase in additional costs due to CO<sub>2</sub> capture.

### *Increase in Electricity Generating Costs Due to CO<sub>2</sub> Capture*

According to the results given in Table 2.18, electricity generating costs rise by between approx. 20% and 40% in the case of CO<sub>2</sub> separation from the synthesis gas of an IGCC power plant following CO conversion. For combustion in an O<sub>2</sub>/CO<sub>2</sub> atmosphere, this figure ranges between around 30% to over 50%, and for CO<sub>2</sub> capture from flue gases it ranges from 40% to over 60%. In spite of this, thanks to higher efficiencies overall, natural gas-fired combined cycle power plants achieve lower electricity generating costs than coal-fired power plants.



### *CO<sub>2</sub> Avoidance Costs*

CO<sub>2</sub> avoidance costs (Equation 1.4) depend heavily on the choice of reference power plant. In Table 2.18, two instances of reference power plants are given.

If CO<sub>2</sub> avoidance costs are related to the emissions of a baseline power plant of the same type, they can be seen to be significantly higher in the case of natural gas-fired processes with reforming or combustion in an atmosphere of O<sub>2</sub>/CO<sub>2</sub>, than in the case of coal-fired processes. The lowest costs, amounting to between 16 and 35 US\$ per ton of CO<sub>2</sub> avoided, are achieved with CO<sub>2</sub> separation from synthesis gases following CO conversion in an IGCC power plant (where possible with hot gas desulfurization), in a steam power plant with combustion in an O<sub>2</sub>/CO<sub>2</sub> atmosphere, and with flue gas scrubbing following a gas/steam turbine combined cycle. The costs of CO<sub>2</sub> capture with fuel cells in coal-fired processes are much higher.

If CO<sub>2</sub> avoidance costs are related more generally to a coal-fired steam power plant as a reference power plant, the change to a fuel with a lower carbon content (in the case of natural gas-fired power plants), and the simultaneously lower specific investments, make the CO<sub>2</sub> avoidance costs much lower. In the case of CO<sub>2</sub> separation from the flue gas, these costs even turn out to represent a net cost saving as compared to a coal-fired steam power plant without CO<sub>2</sub> capture (though this excludes transport and disposal costs), meaning that the CO<sub>2</sub> avoidance costs become negative.

To evaluate CO<sub>2</sub> capture without the factor of the change in fuel, the reference power plant must be operated with the same fuel as the power plant with CO<sub>2</sub> capture. Analyzed in this way, CO<sub>2</sub> capture from natural gas-fired power plants would no longer be favorable.

### *Technical Feasibility.*

At current levels of technology, gas/steam turbine combined cycle power plants, steam power plants and IGCC power plants with CO<sub>2</sub> capture via flue gas scrubbing can all be built, as can IGCC power plants with CO<sub>2</sub> scrubbing subsequent to CO conversion. In contrast, membranes for CO<sub>2</sub> separation, and membrane reactors which combine H<sub>2</sub>/CO<sub>2</sub> separation with CO conversion or reforming, are not yet available for large-scale industrial use in power plants. Fuel cell power plants are still in the development stage; no implementation of MHD processes is yet in sight. In principle, the current state of combustion technology and O<sub>2</sub> generating technology means that processes involving combustion in an atmosphere of O<sub>2</sub>/CO<sub>2</sub> are feasible, though there is still a lack of a CO<sub>2</sub> gas turbine. Development of CO<sub>2</sub> gas turbines would have to be stimulated by concrete demand. This would involve new technical challenges due to the higher pressure ratios of CO<sub>2</sub> gas turbines as compared to today's gas turbines.

### *Summary*

With the current state of the technology, the following designs have been proven to be advantageous: in the case of coal-fired processes, designs involving CO<sub>2</sub> separation from synthesis gases following CO conversion in an IGCC power plant and, in the case of natural gas-fired power plants, designs involving CO<sub>2</sub> separation from flue gases in gas/steam turbine combined cycle power plants. Fuel cell power plants will only provide a realistic alternative in the future if costs are reduced.

Table 2.18: Data comparison of processes (converted to a common technical basis). Costs based on assumptions for component groups (see Section 4). Costs of MHD and IGCC hybrid investment according to data from the literature. All costs exclude pipelines and sequestration

1) Investment	1	2	3	4	3	1	2	3	4	5	6	
2) CO <sub>2</sub> emissions											Reference power plant:	
3) Efficiency	Baseline power plant				with CO <sub>2</sub> capture						Baseline power plant	Steam PP, η=45%
4) Electricity generating costs	(same type of power plant)										Baseline power plant	η=45%
5) Specific power consumption to reduce CO <sub>2</sub> emissions	without CO <sub>2</sub> capture				gas.	CO <sub>2</sub> liq.			liq.	gas. / liq.	liq.	
6) CO <sub>2</sub> avoidance costs	US\$/kW	kg CO <sub>2</sub> /kWh	η in %	US\$/kWh	η in %	US\$/kW	kg CO <sub>2</sub> /kWh	η in %	US\$/kWh	kWh/kg CO <sub>2</sub>	US\$/t CO <sub>2</sub>	US\$/t CO <sub>2</sub>
Process Family I:												
IGCC + CO conversion/ reforming + CO conversion												
Dir. quenching with water, phys. abs.	967	0.78	40.2	0.052	35.9	1300	0.099	31.9	0.067	0.293	11 / 23	27
Phys. abs.	1112	0.62	51.5	0.050	47.3	1436	0.075	42.8	0.063	0.300	11 / 23	18
Phys. abs. (seawater)	1112	0.63	51.5	0.050	---	1470	0.095	43.1	0.064	0.299	26 / 26	20
Chem. abs.	1112	0.63	51.5	0.050	44.3	1649	0.047	40.3	0.070	0.370	23 / 35	28
Membrane, hot gas clean up	1112	0.61	52.4	0.050	48.2	1336	0.020	44.2	0.060	0.262	7 / 16	12
Membrane reactor	1112	0.63	51.5	0.050	47.6	1384	0.155	43.6	0.061	0.311	11 / 23	18
Distillation	1112	0.63	51.5	0.050	45.2	1573	0.121	41.2	0.067	0.378	21 / 35	27
Adsorption	1112	0.63	51.5	0.050	35.3	2236	0.135	31.3	0.094	0.722	64 / 88	73
Air-blown gasification, chem. abs.	947	0.67	48.0	0.047	39.7	1547	0.178	35.7	0.071	0.476	31 / 48	36
Natural gas-fired cycles (reformer, CO conversion)												
Steam power plant	1049	0.46	45.0	0.062	35.0	1417	0.053	33.3	0.085	0.623	42 / 54	50
GTCC (reform. externally heated)	510	0.35	59.0	0.040	44.5	936	0.225	42.8	0.061	1.476	139 / 171	20
GTCC (reform.: internal partial combustion)	510	0.35	59.0	0.040	51.8	760	0.062	50.0	0.051	0.514	32 / 40	-1
Process Family II: combustion in an O <sub>2</sub> /CO <sub>2</sub> atmosphere												
Steam power plant	1049	0.72	45.0	0.052	40.0	1414	0.007	35.6	0.067	0.296	11 / 23	23
DFCC	1134	0.61	52.5	0.050	45.0	1754	0.007	40.6	0.073	0.374	24 / 37	30
MHD + steam cycle	1170	0.64	50.2	0.052	41.6	1902	0.007	37.2	0.079	0.408	28 / 43	39
IGCC hybrid (+ PFBC)	945	0.67	48.0	0.047	40.0	1726	0.007	35.6	0.075	0.390	29 / 43	34
IGCC (O <sub>2</sub> /H <sub>2</sub> O-blown.)	1112	0.63	51.5	0.050	46.5	1613	0.007	42.1	0.068	0.296	18 / 29	24
IGCC (O <sub>2</sub> /H <sub>2</sub> O-blown) / STIG	1112	0.84	38.4	0.057	32.6	1901	0.007	28.2	0.088	0.320	22 / 37	52
IGCC (CO <sub>2</sub> /H <sub>2</sub> O-blown)	1112	0.63	51.5	0.050	46.7	1609	0.007	42.3	0.068	0.290	18 / 29	23
IGCC, H <sub>2</sub> /CO membrane	1112	0.63	51.5	0.050	47.4	1668	0.048	43.4	0.069	0.269	21 / 32	26
Natural gas-fired cycles												
Steam power plant	1049	0.46	45.0	0.062	39.0	1375	0.007	37.1	0.078	0.390	26 / 36	38
GTCC	510	0.35	59.0	0.040	51.0	914	0.007	49.1	0.056	0.490	40 / 47	6
Gas turbine cycle with evaporation	505	0.35	59.0	0.040	47.2	1002	0.007	45.3	0.061	0.677	53 / 62	14
Rankine cycle with internal combustion	510	0.35	59.0	0.040	38.5	2022	0.007	36.6	0.096	1.102	150/165	64
Process Family III: CO <sub>2</sub> separation from the flue gas												
Steam power plant, distillation	1049	0.78	45.0	0.052	37.8	1920	0.190	33.8	0.082	0.389	36 / 52	59
Steam power plant, chem. absorption	1049	0.78	45.0	0.052	37.4	1721	0.102	33.4	0.078	0.364	25 / 39	43
Steam power plant, membrane	1049	0.78	45.0	0.052	32.0	1870	0.514	28.0	0.087	0.816	74 / 134	180
MHD + steam cycle, chem. abs.	1170	0.78	50.2	0.052	44.9	1706	0.077	40.9	0.071	0.257	17 / 27	31
IGCC hybrid (+ PFBC), chem. abs.	945	0.67	48.2	0.047	40.9	1514	0.092	36.9	0.069	0.392	25 / 38	28
Natural gas-fired cycles												
Steam power plant, chem. abs.	1049	0.46	45.0	0.062	38.0	1471	0.042	36.3	0.082	0.458	37 / 47	45
GTCC + chem. abs.	510	0.35	59.0	0.040	53.5	594	0.045	51.8	0.046	0.396	13 / 19	-9
HAT + chem. abs.	488	0.35	59.0	0.039	55.0	724	0.088	53.3	0.048	0.361	27 / 35	-5
Process Family V: CO <sub>2</sub> capture with fuel cells												
IG-PAFC+CO shift, (future costs)	1503	0.78	50.5	0.061	44.6	2098	0.279	40.6	0.082	0.351	52 / 93	70
IGCC MCFC (exhaust gas scrubbing)	3318	0.58	55.5	0.108	53.6	3700	0.081	49.6	0.120	0.209	6 / 26	108
IGCC SOFC (exhaust gas scrubbing)	3188	0.57	56.5	0.104	51.8	3772	0.0081	47.8	0.123	0.274	16 / 34	101
Natural gas-fired cycles												
MCFC (exhaust gas scrubbing)	1361	0.35	58.5	0.054	57.3	1953	0.034	55.5	0.071	0.160	26 / 31	29
SOFC (exhaust gas scrubbing)	1134	0.33	62.7	0.047	61.5	1628	0.034	59.7	0.061	0.161	20 / 24	14

### 3 ENERGY AND EXERGY ANALYSIS

The overwhelming majority of published studies and investigations, which deal with the various possible methods of CO<sub>2</sub> capture in power plants, do not include any detailed analysis of the energetics. In particular, investigations into how individual process steps in CO<sub>2</sub> capture influence efficiency penalties and the energy required for CO<sub>2</sub> capture, and analysis of the minimum energy required for CO<sub>2</sub> capture, could open up new horizons in the systematic evaluation of the thermodynamic qualities of different processes, and the possible ways of minimizing the energy expended on CO<sub>2</sub> capture.

Table 3.1: How individual process steps contribute to efficiency penalties in the various CO<sub>2</sub> capture processes (see the "Introduction" Section for definitions of the process families)

Process family:	I				II				III			IV	V			
	coal fired CO Shift +				natural gas fired Reforming/CO-Shift +				Combustion in O <sub>2</sub> /recirculated flue gas	Combustion in O <sub>2</sub> /steam	CO/H <sub>2</sub> -separatio (2 GT)	C-removal prior to combustion	PAFC	MCFC	SOFC	
	+ Physical absorption	+ Chemical absorption	+ Adsorption	+ Membrane	+ Physical absorption	+ Chemical absorption	+ Adsorption	+ Membrane			Chemical absorption	Membranes	CO <sub>2</sub> freezing			
<b>Chemical conversion</b>																
CO-Shift	X	X	X	X	X	X	X	X								Basis (X) (X)
Reforming					X	X	X	X								Basis (X) (X)
C-separation													X			
<b>Pressure losses</b>																
CO-Shift/Reformer	x	x	x	x	x	x	x	x							x	(x) (x)
Absorber	x	x			x	x					x		x		x	
Adsorber			x				x								(x)	(x) (x)
Membrane			X	X				X			X				(X)	
Flue gas recirculation									x							(x) (x)
<b>Gas separation</b>	Energiebedarf: E= electric work Q=heat P=pressure loss F=fuel loss															
CO <sub>2</sub> -separation	E	Q	P/E/Q		E	Q	P/Q				Q	P	E		P/E	P/E P/E
H <sub>2</sub> -separation			P/E/Q	P / F			(P/Q)	P			P				(P/E)	(P/E) (P/E)
O <sub>2</sub> -separation									E	E						
<b>Influence on cycle characteristics</b>																
Gasifying agent									(CO <sub>2</sub> )	(CO <sub>2</sub> )						
Turbine working fluid									CO <sub>2</sub>							
Bottoming stem cycle: influence of steam/water extraction (heat consumption)	x	Xx	x	x	x	Xx	x	x			X					
Changes in fuel conversion									MHD						(x +)	(x +) (x +)
CO <sub>2</sub> -liquefaction	X	X	X	X	X	X	X	X	X	X	X	X	X	X	X	X X

Efficiency penalties due to CO<sub>2</sub> capture in power plants are caused by the energy requirements of individual process steps (e.g. heat and/or compressor work for solvent regeneration in gas scrubbing, pressure losses), and by exergy losses (e.g. through temperature differences in heat transfer, or in fuel conversion processes involving a CO shift reaction or steam reforming). In some cases, CO<sub>2</sub> capture results in process data being changed slightly; for example, the composition of the raw gas in a gasification process using CO<sub>2</sub> as a gasification substance, combustion in a CO<sub>2</sub>-rich atmosphere in a high-temperature combustion chamber, or gas turbine characteristics in cases where the fuel or working fluids are changed. The potential contributions to efficiency penalties caused by CO<sub>2</sub> capture, which are examined in the following investigations into complete plant cycles, are marked in Table 3.1. Expenditure required for CO<sub>2</sub> compression and liquefaction must be added in addition.

Due to the high carbon content of coal, CO<sub>2</sub> capture in coal-fired power plants results in a greater CO<sub>2</sub> emissions reduction than in natural gas-fired power plants. At current levels of technology, the coal-fired plant, which achieves the highest levels of efficiency, is the IGCC power plant, which also allows for the possibility of separating the CO<sub>2</sub> from the fuel gas. For this reason, the following calculations primarily focus on CO<sub>2</sub> capture in an IGCC.

### 3.1 Calculation Methods in the Energy and Exergy Analysis of Power Plant Systems

To calculate power plant cycles, and the individual components of these cycles, including gas separation, a computer program was developed for use in a spreadsheet program, allowing a variety of tasks to be solved in a flexible manner.

The calculations are based on:

- Steam tables according to IFC67 [158]<sup>33</sup>: functions for liquid water, superheated steam, wet steam, saturation line;
- Physical characteristics of ideal gases according to Hougen et al. [160]<sup>34</sup>: heat capacity, enthalpy, entropy, wet bulb temperature, speed of sound, adiabatic exponent;
- Exergy according to the environment model developed by Baehr and Schmidt [161];
- Physical characteristics of coal.

The most important calculation routines, designed to calculate work/power output, temperatures and compositions, and exergy and exergy losses, comprise the following:

- Steam turbines (isentropic expansion), pumps, steam/water mixture;
- Compression, expansion of gases (polytropic/isentropic expansion);
- Gas humidifier ("saturator"; it is assumed that the water exit temperature is equivalent to the wet bulb temperature<sup>35</sup> of the incoming gas);
- Gas separation: reversible separation work, membrane model according to Shindo[162];
- stoichiometric combustion;
- Chemical equilibrium reactions: CO shift reaction, reforming (partial reaction towards the equilibrium is simulated through deviations of the reaction temperature);
- Coal gasification:
  - compositions of the delivered coal mix subsequent to ash recirculation,
  - coal gasification,
  - integrated gas production with ASU, raw gas cooler, gas cleaning, gas humidification, reheating (optionally with CO shift and CO<sub>2</sub> scrubbing or membrane);
- Integrated gas turbine module (optionally with capacity to define the optimum pressure ratio for maximum efficiency or maximum specific work, optional blade cooling).

<sup>33</sup> With the functions for the steam tables according to IFC67, uncertainties of up to 1% arise, primarily at the boundaries of numerical regions (phase changes, numerical boundary changes); these uncertainties can even be as high as 6.5% in extreme cases close to the critical point [158]. During the preparation of this paper, a more precise formulation with a higher rate of accuracy was published [159].

<sup>34</sup> Numerical formulations of physical characteristics always deviate from the given values at boundaries. The accuracy of the formulations of physical characteristics employed here for ideal gases for the current heat capacity lie, on average, between 0.24% and 0.57%, depending on the gas component (Appendix, Table 6.6).

<sup>35</sup> aka: wind chill temperature

For processes involving the condensation of CO<sub>2</sub> or changes of state close to the critical point of CO<sub>2</sub> (Table 2.6), real gas behavior must be taken into account. For these kinds of changes of state with pure CO<sub>2</sub>, functions were created to calculate the CO<sub>2</sub> steam tables according to IUPAC [163]. The ASPEN-plus simulation program was used for process simulations with mixtures.

### 3.1.1 Calculations for Gas Turbines

For a simple gas turbine cycle, the compressor, combustion chamber and turbine components are calculated. Pressure loss in the combustion chamber is also taken into account in this calculation, as well as the option of a simple model for blade cooling air (Figure 3.1). The given values and calculated values are summarized in Table 3.2.

Table 3.2: Initial parameters and calculated values for the simple gas turbine cycle

Parameters	Calculated Values
<ul style="list-style-type: none"> <li>• Turbine inlet temperature according to ISO 2314</li> <li>• Compressor pressure ratio</li> <li>• Polytropic compressor and turbine efficiency</li> <li>• Pressure loss in the combustion chamber</li> <li>• Air: composition, temperature and pressure</li> <li>• Fuel: mass flow, composition, temperature and pressure</li> </ul>	<ul style="list-style-type: none"> <li>• Efficiency of the gas turbine (in relation to LHV, HHV, exergy)</li> <li>• Combustion chamber temperature prior to blade cooling (combustion temperature)</li> <li>• Turbine exit temperature (<math>T_{off}</math> in Figure 3.1)</li> <li>• Temperature after compressor</li> <li>• Mass flow of intake air</li> <li>• Flue gas: mass flow and composition</li> <li>• Compressor and turbine output</li> <li>• Exergy losses: compressor, combustion chamber, turbine blade cooling, total</li> <li>• Exergy of exhaust gas, compressor intake air, fuel</li> <li>• Specific total work, related to mass flow of intake air</li> </ul>

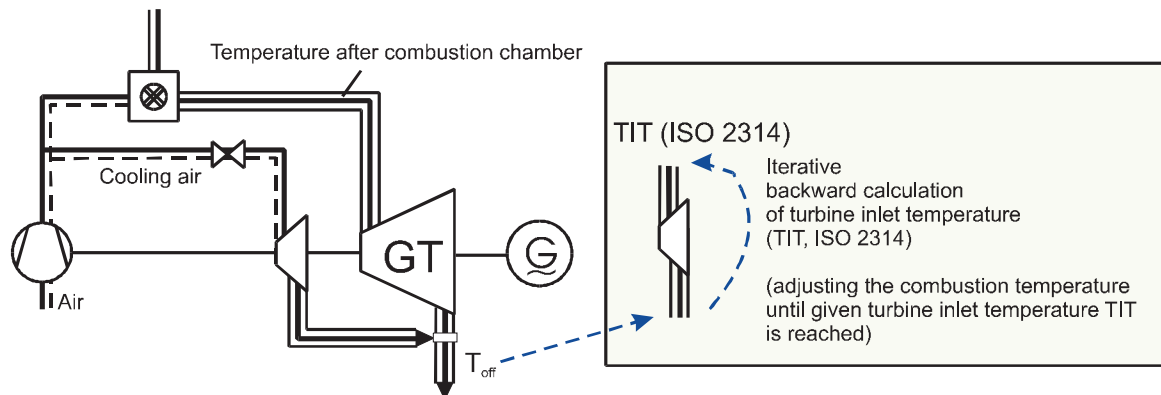


Figure 3.1: Process flow simulating a simple gas turbine cycle.

### 3.1.2 Calculations for the Heat Recovery Steam Cycle

The process arrangement of a heat recovery steam cycle is very elaborate. In order to adapt to the sources of heat and heat sinks used in each case (waste gas enthalpy flow, heat from raw gas cooling, steam extraction), it requires the variation of a number of parameters (adjustment of flue gas cooling curve, Figure 3.2). Since this study required the calculation of so many different processes, the output of the heat recovery steam cycle was determined using a simplified method, rather than by calculating a detailed heat recovery steam cycle each time.

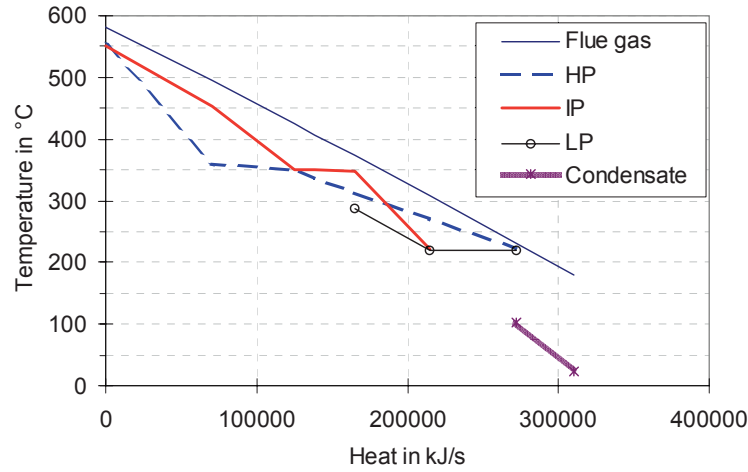


Figure 3.2: Flue gas cooling curve of the heat recovery steam cycle according to Figure 3.4

If exergetic efficiency  $\zeta_{HRSG}$  of the downstream heat recovery steam cycle is defined as the ratio of power used  $P_{ST}$  to useful difference in exergy  $\Delta E$  (e.g. between the exergy of the flue gas at the turbine exit and at the stack after the heat recovery steam generator)

$$\zeta_{HRSG} = \frac{P_{ST}}{\Delta E} \quad (3.1)$$

and exergetic efficiency  $\zeta_{HRSG}$  is taken as being constant, the output of the steam turbine is proportional to the useful difference in exergy. The exergetic efficiency is used to calculate the proportion of the exergy supplied or released, which is converted into electric work, or which results in a reduction in work, respectively.

For the tests carried out here, it proved to be practical to introduce two further exergetic efficiencies in addition to the equivalence factor for the utilization of the hot gas turbine exhaust gas; namely, efficiencies for the import of saturated steam and the export of hot feed water.

The exergies supplied and released are split into:

- $\Delta e_{HRSG}$  useful flue gas exergy (exergy of enthalpy<sup>36</sup>),
- $\Delta e_{HT}$  exergy of the enthalpy<sup>36</sup> from the balance of imported and exported steam or high-temperature heat (e.g. from raw gas cooling) and
- $\Delta e_{LT}$  exergy of the enthalpy<sup>36</sup> from the balance of imported and exported feed water, or low-temperature heat.

The output of the heat recovery steam cycle comprises:

$$P_{ST} = \zeta_{HRSG} \Delta e_{HRSG} \dot{m}_{HRSG} + \zeta_{HT} \Delta e_{HT} \dot{m}_{HT} + \zeta_{LT} \Delta e_{LT} \dot{m}_{LT} \quad (3.2)$$

where:

$\zeta$  : exergetic efficiency for the conversion of the exergy supplied or released in the steam cycle into electrical energy

HRSG : gas turbine exhaust gas,

HT: steam import/export,

<sup>36</sup> 'Exergy of enthalpy' (= only the thermal portion of the exergy, excluding fuel exergy or mixing exergy):  $e_h = \Delta h - T_u \Delta s$  according to Baehr [161], aka contact exergy [174].

$L_T$ : hot feed water import/export.

The useful flue gas exergy was taken to be the difference in exergy between the exhaust gas temperature at the inlet of the waste heat steam boiler and 100°C as the minimal exit temperature after the waste heat steam boiler:

$$\Delta e_{HRSG} = (e_{RG}(T_{FG}, p_a) - e_{FG}(T_{Stack}, p_a)) \quad (3.3)$$

With use of the hot gas turbine exhaust gas, this gives an electric output of:

$$P_{ST} = \zeta_{HRSG} \cdot \Delta e_{HRSG} \dot{m}_{HRSG} \quad (3.4)$$

A more detailed waste heat steam cycle according to Figures 3.4 and 3.2 was calculated to obtain a more precise determination of the exergetic efficiencies in utilizing the exergy flows supplied and released in the waste heat steam cycle. For utilization of the flue gas exergy in a three-pressure heat recovery steam cycle (evaporation at three different pressures), according to Figure 3.4, an exergetic efficiency  $\zeta_{HRSG}$  of 87.0% was calculated.

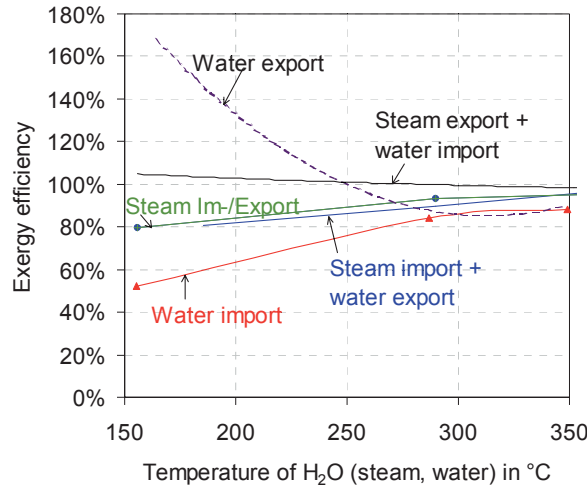


Figure 3.3: Exergetic efficiency  $\zeta_{HRSG}$  for evaluating exergy utilization with heat consumption and heat supply in the heat recovery steam cycle

The output of a heat recovery steam cycle in an IGCC power plant is also influenced by the steam or hot feed water imported from, or exported to, the gasifier island. For a temperature range of 150°C to 350°C, changes in steam turbine output were calculated for saturated steam consumption, saturated steam supply and hot water consumption and supply, as well as for cases involving steam import/export, in which the corresponding mass flow of hot feed water is recirculated. The exergetic efficiencies for the conversion of the exergy supplied and released in the heat recovery steam cycle were determined from these calculations (Figure 3.3).

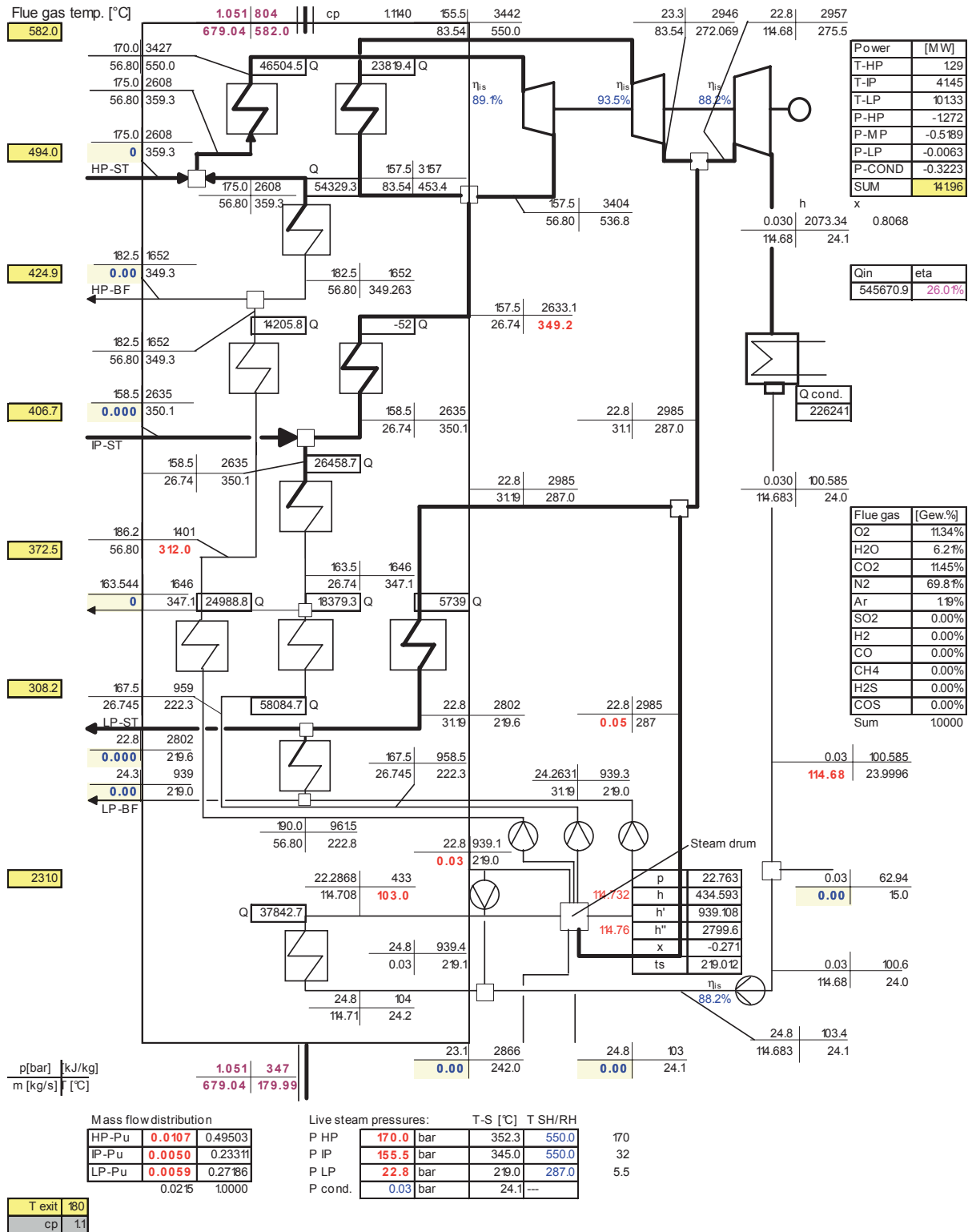


Figure 3.4: Process diagram of the heat recovery steam cycle

*Application to Gas/Steam Turbine Combined Cycle Power Plants*

By working on the simplified basis of an ideal gas with constant isentropic exponent and a simple gas turbine without pressure losses in the combustion chamber, and calculating the heat recovery steam cy-



cle with the help of exergetic efficiency  $\zeta_{HRSG}$  for utilization of the enthalpy of the gas turbine exhaust gas, the power output of the steam turbine  $P_{ST}$  can be calculated as follows:

$$P_{ST} = \zeta_{HRSG} \Delta \dot{E} = \zeta_{HRSG} c_p \left[ (T_{GT,exit} - T_{Stack}) - T_a \ln \frac{T_{GT,exit}}{T_{Stack}} \right] \quad (3.5).$$

The efficiency of the gas/steam turbine combined cycle may be expressed as:

$$\eta_{GTCC} = \frac{P_{GT} + P_{ST}}{h_3 - h_2} = \frac{\theta \eta_{Comp} \eta_T \left( 1 - \frac{1}{\varphi} \zeta \right) - (\varphi - 1) + \zeta_{HRSG} c_p \left[ (T_{GT,exit} - T_{Stack}) - T_a \ln \frac{T_{GT,exit}}{T_{Stack}} \right]}{\eta_{Comp} (\theta - 1) - (\varphi - 1)} \quad (3.6)$$

where:

$$\theta = \frac{T_{Combustor}}{T_a}, \quad \zeta = \left( \frac{1}{1 - \frac{\Delta p_{CC}}{p_{Comp}}} \right)^{\frac{\kappa-1}{\kappa}}, \quad \varphi = \pi^{\frac{\kappa-1}{\kappa}} \quad (3.7),$$

$\Delta p_{CC}$  = pressure loss in the combustion chamber,  $p_{Comp}$  = pressure after gas turbine compressor,

$\pi$  = compressor pressure ratio,

$\eta_{Comp}$  = compressor efficiency (isentropic),  $\eta_T$  = turbine efficiency (isotropic).

As shown in Figure 3.5, the energetic efficiency and the specific useful work of the combined cycle power plant increase with a higher exergetic efficiency  $\zeta_{HRSG}$  of the heat recovery steam cycle. At the same time, the pressure ratio drops at the point of maximum efficiency.

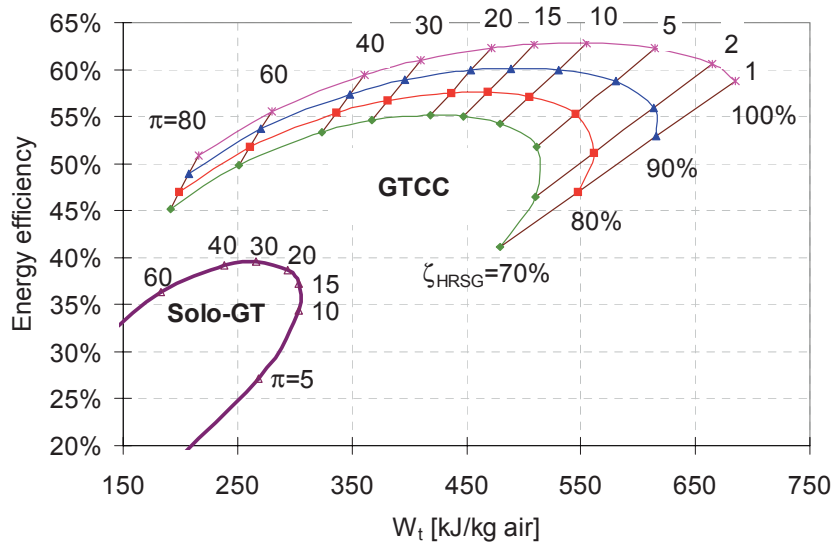


Figure 3.5: Efficiency and specific work of a simple gas turbine and gas/steam turbine combined cycle power plant at different pressure ratios and exergetic efficiencies  $\zeta_{HRSG}$  of the heat recovery steam cycle. Turbine inlet temperature 1190°C (ISO 2314).

### 3.1.3 Calculations for Coal Gasification

Coal gasification involves the production of a synthesis gas consisting primarily of carbon monoxide and hydrogen. The fundamental reactions of coal gasification are presented in Table 3.3. In the case of autothermic gasification, oxygen acts as an oxidant for the exothermic combustion reaction. In allothermic gasification, the energy required for gasification can theoretically also be delivered from an external source via a heat exchanger. Steam is used as the gasification agent, which reacts with carbon in the water-gas shift reaction to form CO and H<sub>2</sub>. The Boudouard reaction and the hydrogasification reaction only play a minor role in coal gasification if steam is used as the gasification agent. The gasification products are converted further by means of the water-gas shift reaction and the methane-forming reaction.

For the simulation of coal gasification, after entering the gasification temperature, the coal and the temperature of the gasification steam and oxygen, the raw gas composition, and the mass flows of the oxidant (O<sub>2</sub>, air), of the gasification agent (H<sub>2</sub>O) and of the raw gas produced are calculated from the chemical equilibrium and the energy balance, as are the efficiencies of the coal gasification process (see below).

- Input data:
  - Composition of coal, oxidant, transport gas (nitrogen),
  - Gasification temperature, gasification pressure,
  - Temperature and pressure of coal, oxidant, transport gas (nitrogen), H<sub>2</sub>O at reactor inlet
  - Mass flow of coal, dissipation of heat through gasifier wall cooling,
  - Particulates clean up (separation of residual carbon and ash in cyclone dust separator and filter, recirculation to the gasifier).
- Values calculated for:
  - Fuel composition and mass flow at gasifier inlet of a mixture of fresh coal and ash recirculated from the cyclone dust separator and filter,
  - Energy balance of all gaseous, liquid and solid material flows delivered and removed.
  - Reaction equilibrium and conversion:
 

partial combustion	$C + 1/2 O_2$	$\rightarrow CO$	(conversion $n_1$ in mol),	(3.8)
water-gas (steam-carbon) reaction	$C + H_2O$	$\rightarrow CO + H_2$	(conversion $N_2$ in mol),	(3.9)
methane-forming reaction	$C + 2 H_2$	$\rightarrow CH_4$	(conversion $n_3$ in mol),	(3.10)
CO shift reaction	$CO + H_2O$	$\rightarrow CO_2 + H_2$	(conversion $n_{wgs}$ in mol).	(3.11)
  - Conversion of sulfur into H<sub>2</sub>S and COS, formation of HCl (assuming conversion of the entire amount of S and Cl),
  - Exergy losses.

Table 3.3: Basic reactions of coal gasification

Partial combustion $C + 1/2 O_2 = CO$ ← increase of pressure	→ <i>close to equilibrium</i> -123.1 kJ/mol
Combustion $C + O_2 = CO_2$ = pressure-independent =	→ <i>close to equilibrium</i> -393.6 kJ/mol
Boudouard reaction $C + CO_2 = 2 CO$ ← increase of pressure    increase of temperature →	→ <i>equilibrium reached at low CO<sub>2</sub> concentrations</i> +159.9 kJ/mol
Heterogeneous shift reaction $C + H_2O = CO + H_2$ ← increase of pressure    increase of temperature →	→ <i>close to equilibrium</i> +118.5 kJ/mol
Hydrogasification reaction $C + H_2 = CH_4$ ← increase of temperature    increase of pressure →	→ <i>equilibrium not reached (dependent on volatile matter)</i> -87.5 kJ/mol
(Homogeneous) CO shift reaction $CO + H_2O = H_2 + CO_2$ ← increase of temperature = pressure-independent =	→ <i>close to equilibrium</i> -40.9 kJ/mol
Methane-forming reaction $CO + 3 H_2 = CH_4 + H_2O$ ← increase of temperature    increase of pressure →	→ <i>equilibrium not reached</i> -205.9 kJ/mol

Molar conversion  $n_1$ ,  $N_2$ ,  $n_3$  and  $n_{wgs}$  is calculated iteratively with the aid of the equilibrium constants and the energy balance (Figure 3.6). It determines the composition of the raw gas (Figure 3.7) and the mass flows (Figure 3.8). All seven of the fundamental reactions of coal gasification presented in Table 3.3 may be combined from these four reactions. A partial reaction equilibrium as proposed by Steiner [164] is assumed for the methane forming reaction. For the CO shift reaction (water-gas shift reaction), a partial equilibrium is simulated through raising the reaction temperature by 300 K.

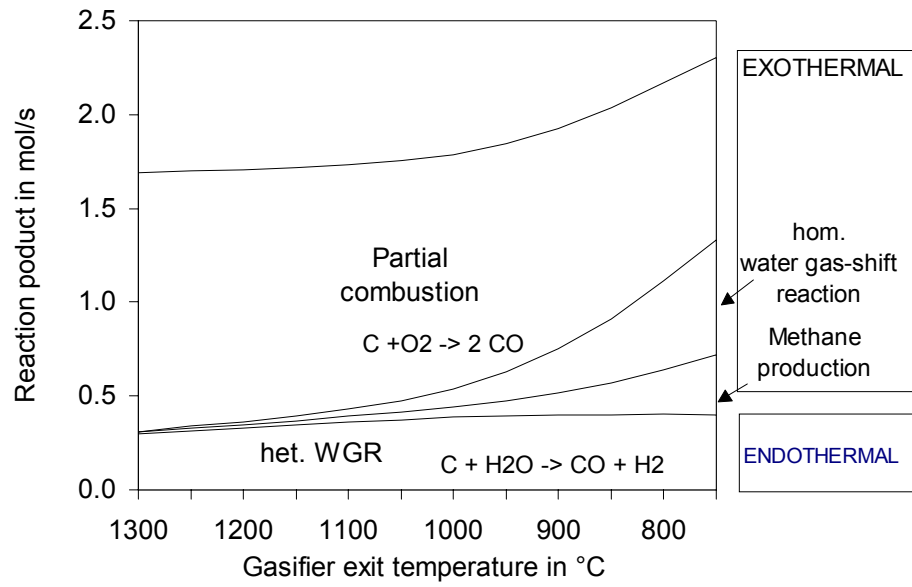


Figure 3.6: Molar conversion of the individual reactions in dependence on gasification temperature

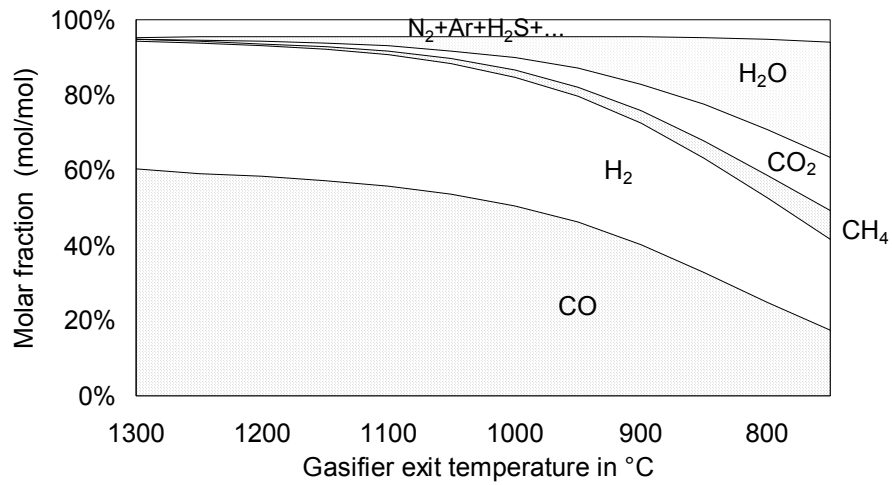


Figure 3.7: Composition of the raw gas

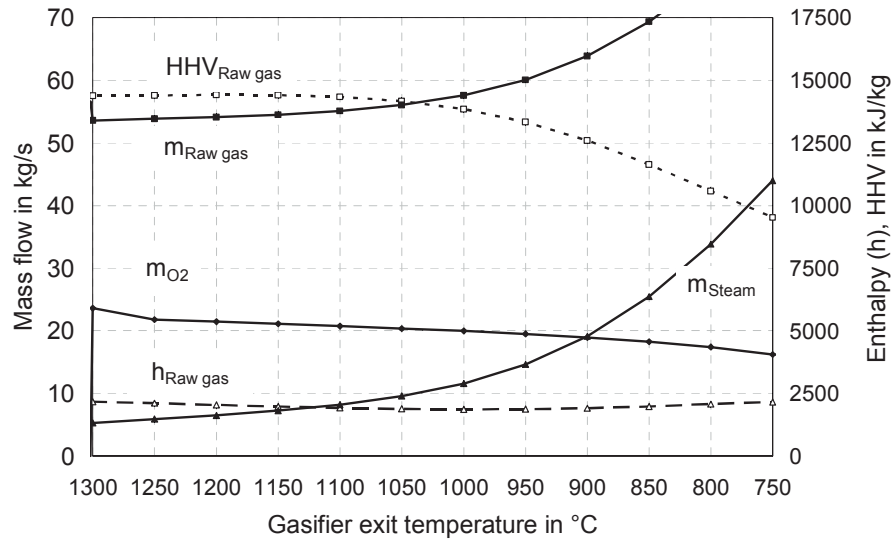


Figure 3.8: Supplied mass flows of gasification medium ( $H_2O$ ) and oxidant ( $O_2$ ), as well as enthalpy and gross heating value of the raw gas produced

Three different efficiencies are used to evaluate coal gasification in this case:

- Cold gas " efficiency"  $\eta_{CG}$  (proper thermodynamic term: ratio of fuel energy flow (HHV)):

$$\eta_{CG} = \frac{\dot{m}_{Raw\ gas} HHV_{Raw\ gas}}{\dot{m}_{Coal} HHV_{Coal}} \quad (3.12)$$

This value is not suitable for energetic or exergetic evaluation of the overall process, since it does not take into consideration the auxiliary energy required for gasification (steam, oxygen, ...).

- Exergetic efficiency of the gasification process (hot raw gas at gasifier exit):

$$\xi_{Exergy(hot\ Raw\ gas)} = \frac{\dot{E}_{Raw\ gas, hot} + \dot{E}_{Steam, exit, 1} - (\dot{E}_{Feed\ water, in, 1} - \dot{E}_{N_2} - \dot{E}_{O_2} + \dot{E}_{Gasifying\ steam})}{\dot{E}_{Coal}} \quad (3.13)$$

- Exergetic efficiency of gas generation (gasifier island) including raw gas cooling (cooled raw gas, excluding gas cleaning and reheating) and the balance of the steam generated:

$$\xi_{Exergy(cooled\ raw\ gas)} = \frac{\dot{E}_{Raw\ gas, 500^\circ C} + \dot{E}_{Steam, out, 2} - (\dot{E}_{feed\ water, in, 2} - \dot{E}_{N_2} - \dot{E}_{O_2} + \dot{E}_{Gasification\ steam})}{\dot{E}_{Coal}} \quad (3.14)$$

in which:  $\dot{E} = Exergy\ flow\ [kJ / s]$ ,

$$\dot{E}_{Steam, exit, 1} = \dot{E}_{Steam\ from\ gasifier\ wall\ cooling} ,$$

$$\dot{E}_{Feed\ water, in, 1} = \dot{E}_{Feed\ water\ to\ gasifier\ wall\ cooling} ,$$

$$\dot{E}_{Steam, exit, 2} = \dot{E}_{Steam\ from\ gasifier\ wall\ cooling} + \dot{E}_{Steam\ to\ Raw\ gas\ cooler} ,$$

$$\dot{E}_{Feed\ water, in, 2} = \dot{E}_{Feed\ water\ to\ gasifier\ wall\ cooling} + \dot{E}_{Feed\ water\ to\ Raw\ gas\ cooler} .$$

The exergetic efficiencies take into consideration all exergy flows supplied and released. The exergy of the materials is made up of the chemical and the thermal exergy components.

### 3.1.4 Calculations for an IGCC Power Plant

The calculation for an IGCC power plant is divided into three areas:

- gas generation,
- gas turbine (Section 3.1.1) and
- heat recovery steam cycle (Section 3.1.2).

The process arrangement, on which the calculations are based, is shown in Figure 3.9.

As well as the energy and exergy analysis of coal gasification, the calculation of gas generation also includes the balances of raw gas cooling, Venturi scrubbing, desulfurization, gas humidification, and reheating, as well as oxygen supply and the mixing of nitrogen from the ASU into the cleaned fuel gas.

An exergetic efficiency of 7% is assumed in calculating the electrical internal consumption of the desulfurization plant.

The calculation of oxygen production by means of air separation is simplified by the assumption that energy expenditure  $w_{O_2}$  is required to produce 1 kg of  $O_2$  at 1 bar with an  $O_2$  volume fraction of  $y_{O_2}$ , as expressed in the following equation (see Figure 2.7; p 18):

$$w_{O_2} = 0,3868 (y_{O_2} - 0,21) e^{0,00021/(1-y_{O_2})} - 0,0357 \quad (\text{in kWh/kg } O_2 \text{ at 1 bar}) \quad (3.15)$$

For example, to produce  $O_2$  with a purity of 95% volume fraction, solving the equation results in an energy requirement of 0.25 kWh per kg  $O_2$  at 1 bar. It is also necessary to take into account the energy required to further compress the oxygen to the gasification pressure, and to compress the nitrogen (mixed into the clean gas) to the pressure required prior to the combustion chamber. If air is used for the gasification process, both oxygen production and the admixing of nitrogen may be omitted from the calculations. Nitrogen admixing is omitted in the case of IGCC cycles with combustion in an atmosphere of  $O_2/CO_2$ .

After deducting the heat/enthalpy flows released and consumed in the gas generation process at varying temperatures, the heat values  $\dot{Q}_{LT}$ ,  $\dot{Q}_{HT}$  transferred to the heat recovery steam cycle (Figure 3.9) are determined from the energy balance and exergy analysis, as are their exergies, the exergy losses in the individual process steps and the exergetic efficiency of the gas generation process.

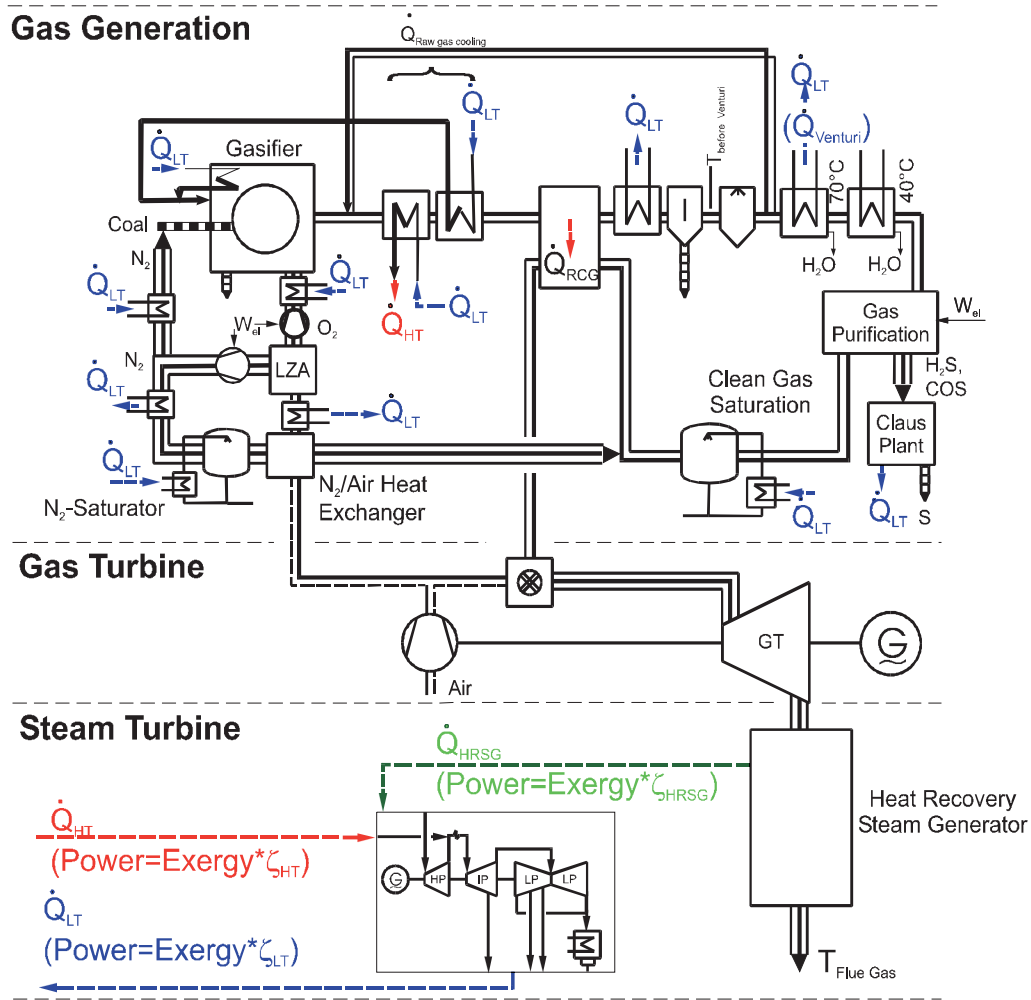


Figure 3.9: Model for calculating an IGCC power plant

To calculate gas generation with CO<sub>2</sub> capture, special program modules were designed, which determine energy conversion, exergy conversion and substance conversion in the gas generation process with raw gas CO shift and CO<sub>2</sub> capture (see process diagram in Figure 2.10). The heat required to humidify the raw gas prior to CO conversion, and the useful component of the lost heat from CO conversion, both play a part in determining heat value  $\dot{Q}_{HT}$  given off in the heat recovery steam cycle, extracted heat value  $\dot{Q}_{LT}$ , and their exergies. The CO<sub>2</sub> capture is simulated either through the exergetic efficiency of the gas separation process with input of the separation factor, or through a membrane calculation<sup>37</sup> with input of the relative permeabilities of all the gas components, the pressure ratios and the quantity of permeating gas.

### 3.1.5 Baseline Case for Performing Calculations for an IGCC Power Plant

Calculations of IGCC power plants are based on more recent studies prepared for an IGCC power plant, ready for construction in 1998, which uses an entrained flow gasification process (PRENFLO) and a gas turbine with a turbine inlet temperature of 1250°C (ISO 2314); these studies were carried out as part of a

<sup>37</sup> Membrane model according to Shindo [162]

project sponsored by the European Commission [20]. The gasifying installation is operated with oxygen (95% volume fraction  $O_2$ ) as an oxidant. It achieves a carbon conversion rate of 99.6% and a cold gas "efficiency" (Equation 3.12) of 87.2% at a gasifier exit temperature of 1300°C. Raw gas cooling basically consists of a steam generator and a raw gas/clean gas heat exchanger for reheating the cleaned fuel gas to around 360°C. The air separation unit is fully integrated, i.e. the air required is included in the compression process of the gas turbine compressor, and a portion of the nitrogen is re-mixed into the generated fuel gas prior to the gas turbine combustion chamber. The nitrogen and the cleaned fuel gas are humidified with the required water component in the saturator, prior to mixing, at the lowest possible temperature. The saturator columns are heated with hot water.

Under the ambient conditions stated, the IGCC power plant achieves an efficiency of 51.5% (exergetic efficiency: 47.4%) with a gas turbine inlet temperature of 1250°C. The largest exergy losses result from combustion of the generated gas in the gas turbine combustion chamber, gasification and partial combustion of the coal in the gasifier, and heat transfer in the raw gas cooler and the heat recovery steam cycle (Figure 3.10).

To conform with legal limit values for  $NO_x$  emissions without using additional nitrogen oxide reduction measures, it is necessary to observe a minimum water content in the clean gas, in dependence on the gas temperature, in conformance with the guidelines issued by the gas turbine manufacturer. The equation used in this case to describe the dependence of the water content on the fuel gas temperature is as follows:

$$x_{H_2O, fuel\ gas} = 0,1946 \cdot 10^{-6} \cdot t_{fuel\ gas}^2 + 0,719168 \cdot 10^{-4} \cdot t_{fuel\ gas} + 0,0992476 \quad (3.16)$$

where:  $x_{H_2O, fuel\ gas} = \frac{m_{H_2O}}{m_{fuel\ gas}}$  and  $t_{fuel\ gas}$  in °C.



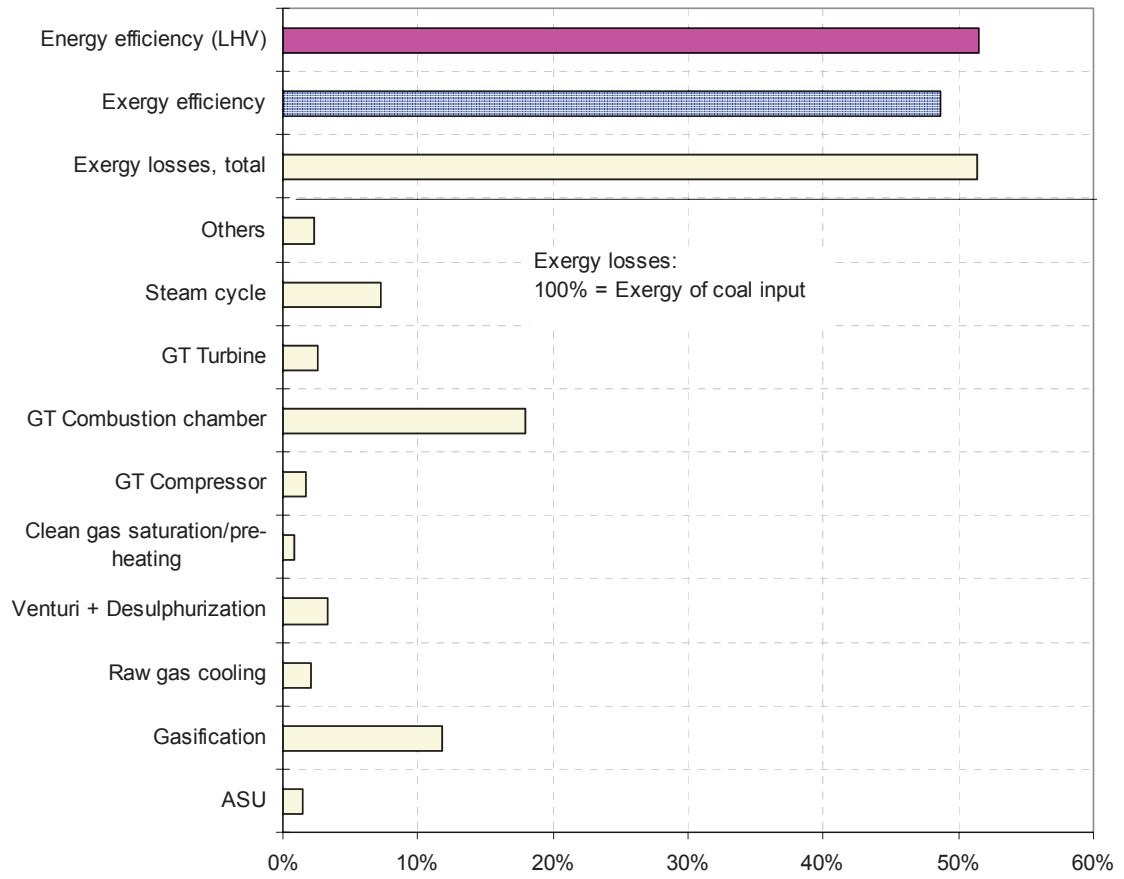


Figure 3.10: Exergy losses in an IGCC power plant (gasification at 1302°C, TIT 1250°C)

### 3.2 Boundary Conditions and Process Data

Table 3.4: Ambient conditions

Ambient temp.	20°C
Ambient pressure	1.013 bar
Air	
Rel. humidity	80.0%
	Mass Fractions
O <sub>2</sub>	22.88%
H <sub>2</sub> O	1.16%
CO <sub>2</sub>	0.05%
N <sub>2</sub>	74.65%
Ar	1.27%

Table 3.5: Gas turbine data

Compressor pressure ratio	17.8
TIT (ISO 2314)	1250°C
Compressor efficiency (polytropic)	89.7%
Turbine efficiency (polytropic)	89.7%
Pressure loss in combustion chamber	2.6%
Pressure at gas turbine exit	1.06 bar

Table 3.6: Data on heat recovery steam cycle

Steam circuit	
Min. waste gas temp.	75°C
Difference in temp. between hot waste gas and steam	30 K
Exergetic efficiency (gas turbine waste heat)	87.0%
Exergetic efficiency for HT heat (steam from raw gas cooling)	90.0%
Exergetic efficiency for LT heat (feedwater)	125.0%
Max. permissible temp. of the steam	580°C
	Vapor States
LP steam	163.8°C / 6.3 bar
MP steam	245.9°C / 35.2 bar
HP steam	365.0°C / 180 bar
LP feedwater	154.1°C / 11 bar
MP feedwater	245.8°C / 39 bar
HP feedwater	358.4°C / 190 bar

Table 3.7: Coal gasification data

Gasifier exit temperature	in °C	1302
Gasification pressure	in bar	29.0
Residual moisture after coal drying	in %	1.2
Exerget. efficiency of desulfurization	in %	7.0
Degree of desulfurization	in %	99.0
Pressure drop at gasification island	in bar	1.2
Temperature prior to Venturi scrubbing	in °C	288
Temp. of clean gas	in °C	375
Moisture in clean gas		Equation (3.16)
C conversion, single pass	in %	97.0
Ash to slag	in %	57.01
C to slag	in %	1.98
Residual ash in filter cake	in %	24.25
Residual C in filter cake	in %	11.11
Gasifier wall cooling:		
Cooling, related to ( $HHV \cdot \dot{m}_{Coal}$ )	in %	0.659
Difference in pressure (gasifier/GT comb. chamber)	in bar	11.0

Table 3.8: Composition of coal, oxygen for gasification and transport nitrogen

Coal	Pittsburgh No.8	Gasification Oxygen		Transport Nitrogen	
	Mass fractions in %		Volume fraction in %		Volume fraction in %
C	76.56 (mf)	O <sub>2</sub>	95.0	O <sub>2</sub>	0.64
H	5.26 (mf)	H <sub>2</sub> O	0.0	H <sub>2</sub> O	0.00
O	5.88 (mf)	CO <sub>2</sub>	0.0	CO <sub>2</sub>	0.00
N	1.44 (mf)	N <sub>2</sub>	1.7	N <sub>2</sub>	99.01
S	3.00 (mf)	Ar	3.4	Ar	0.35
Cl	0.06 (mf)			N <sub>2</sub> /coal (kg/kg)	0.0578
Ash	7.80 (mf)	Temp. in °C	200	Temp. in °C	as for coal
Volatile matter	39.15 (mf)	Pressure in bar	33.8	Pressure in bar	40
H <sub>2</sub> O	5.50 (raw) 1.2 (dried)				
LHV (mf)	31438 kJ/kg				
HHV (mf)	32613 kJ/kg				

Table 3.9: Source data for CO<sub>2</sub> capture

CO <sub>2</sub> capture ratio $r_{CO_2}$	in %	88.0
CO conversion in CO shift reaction	in %	91.2
CO <sub>2</sub> separation factor $s_{CO_2}$ in scrubber	in %	96.9
Exerget. efficiency of CO <sub>2</sub> scrubbing	in %	30.5

For details of influencing factors in the calculation of electricity generating costs, see Table 4.2, p 143.

### 3.3 CO<sub>2</sub> Compression and Liquefaction

Liquefaction of CO<sub>2</sub> may be performed using cryogenic techniques, or through intercooled compression and subsequent cooling to ambient temperature. The results of an example calculation for multi-stage compression ranging from 1 bar to a maximum of 200 bar, with intercooling to 30°C, are shown in Figure 3.11.

Since CO<sub>2</sub> is a highly corrosive medium, the water content must be reduced to less than 60% of the saturation state [165]. In the case of intercooled compression, a portion of the moisture is removed through condensation; however, it is still necessary to provide a further drying stage after the final compressor stage (e.g. using triethylene glycol, glycerol, activated aluminum, silicate gel or molecular sieves) [65]. The small quantity of water involved means that the energy expended in the drying process is negligible in comparison to the compression work.

For the purposes of the conversion process and simulations in this study, CO<sub>2</sub> final pressure after liquefaction is assumed to be 110 bar. The costs and additional energy expenditure, which is required to overcome pressure loss in transporting CO<sub>2</sub> through a pipeline, increase in dependence on the discharged CO<sub>2</sub> mass flow and the pipeline length; they are nevertheless independent of the power plant cycle and do not therefore fall within the mandate of this study.

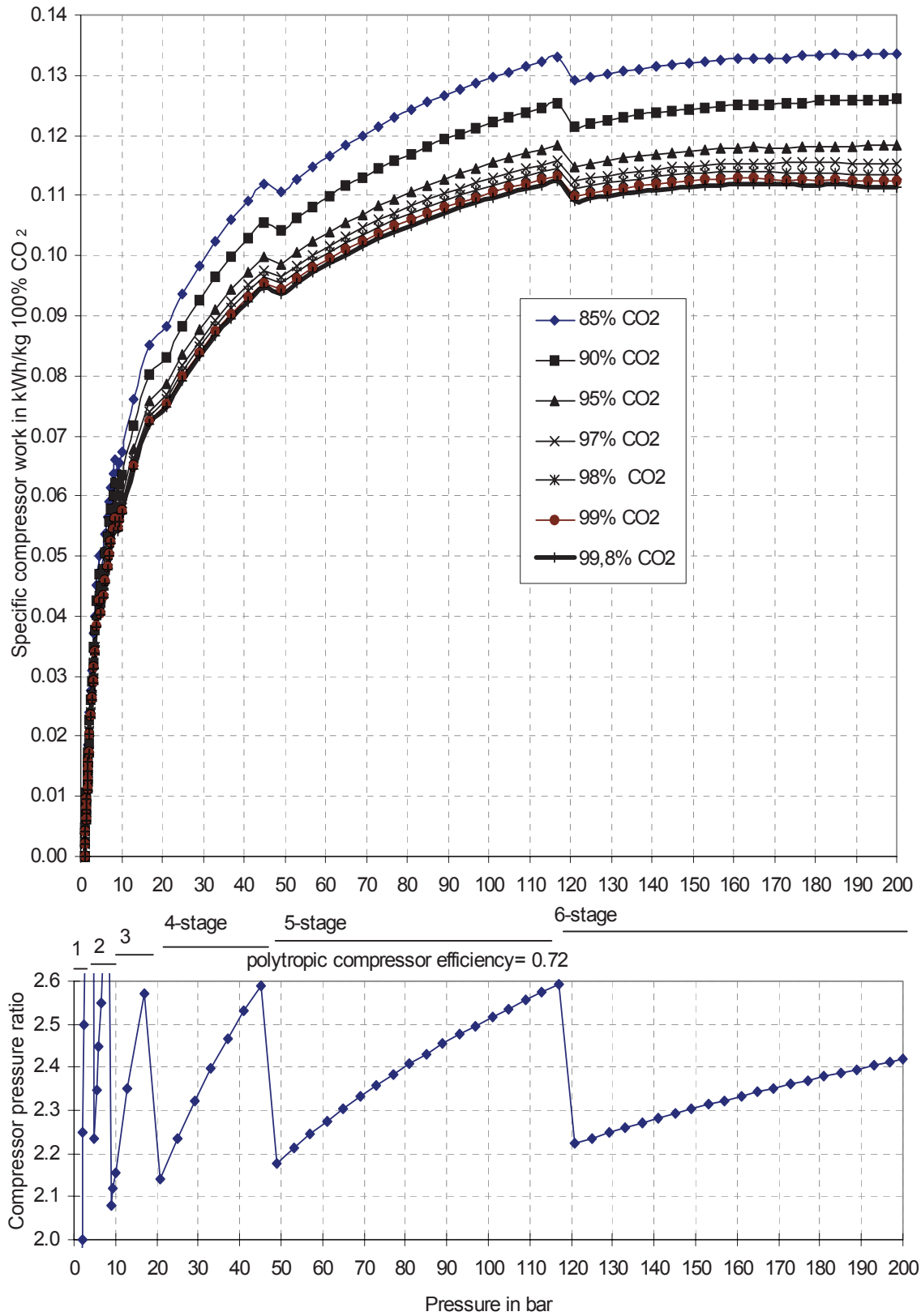


Figure 3.11: Compressor work in intercooled compression of CO<sub>2</sub>. The compression stages and the corresponding pressure ratios are shown in the lower diagram. Intercooling: 30°C, polytropic compressor efficiency: 72%. Calculated using ASPENplus and real gas factors according to Redlich-Kwong-Soave.

Using Pittsburgh No.8 coal, and with a CO<sub>2</sub> capture ratio of 90%, the efficiency penalty resulting from CO<sub>2</sub> liquefaction in this case equals 3.1 percentage points. With a CO<sub>2</sub> capture ratio of 100%, it rises to 3.9 percentage points. CO<sub>2</sub> liquefaction in natural gas-fired cycles with a CO<sub>2</sub> capture ratio of 90% reduces efficiency by 2.0 percentage points.

### 3.4 Gas Separation

The energy required for CO<sub>2</sub> separation in physical and chemical absorption processes is calculated using information on solubility for different solvents, and the exergetic efficiency of the scrubbing process is determined through a comparison between the theoretical work required for gas separation (reversible separation work) and data from the literature concerning energy requirements for gas scrubbing procedures, on the basis of typical gas compositions. For adsorption methods and membrane separation techniques, the results of calculations are shown, which also calculate the composition of the exhaust gases. For the calculations in Section 3.4, the example gas compositions presented in Table 3.10 are used.

Table 3.10: Composition of the gases compared (volume fractions in %)

	Air	Coal gas (O <sub>2</sub> blown entrained flow gasification)		Flue gases		
Fuel	--	Coal	Coal	Coal	Coal	Natural gas
Type of plant (syngas)	--	IGCC (95% CO conversion)	IGCC (raw gas)	Steam power plant	IGCC	Combined cycle
O <sub>2</sub>	20.47			6.13	11.90	13.74
H <sub>2</sub> O	2.30	0.10	2.12	1.10	7.00	7.20
CO <sub>2</sub>	0.03	40.50	1.49	11.10	8.08	3.20
N <sub>2</sub>	76.29	3.70	6.05	72.00	72.07	74.90
Ar	0.91		0.96	9.67	0.95	0.98
H <sub>2</sub>		54.00	28.78			
CO		1.80	59.66			
CH <sub>4</sub>		0.01	0.01			
H <sub>2</sub> S			0.92			

#### 3.4.1 Estimated Energy Requirements of Gas Separation Processes

##### Physical absorption of CO<sub>2</sub> with methanol at low temperatures (similar to Rectisol process)

Working on assumptions designed to simplify the calculation (disregarding product purities, cooling work and heating work), an estimated first approximation of the energy required for solvent regeneration in the form of pump work for recirculation of the solution  $P_{pump}$  is given by:

$$P_{pump} = \dot{V}_{Solvent} \frac{\Delta p}{\eta_{pump}}, \quad (3.17)$$

where  $\Delta p$  is the pressure drop between absorption and desorption and  $\eta_{pump}$  is the efficiency of the pump.

Solvent circulation  $\dot{V}_{Solvent}$  can be estimated if solvent charge  $b_{Solvent}$  (in  $\frac{m^3_{Solut}}{m^3_{Solvent} \text{ bar}}$ ), in dependence on pressure, is known:

$$\dot{V}_{Solvent} = b_{Solvent} \Delta p \quad (3.18)$$

Part of the solvent pump conveying work can be recovered by a pressure drop in a hydraulic turbine.

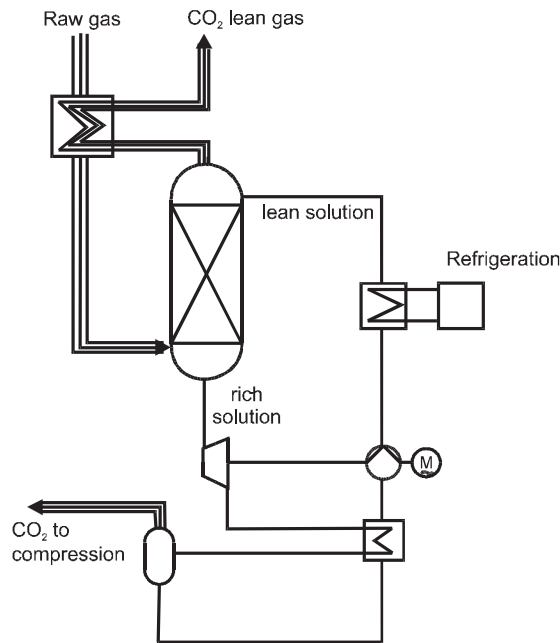


Figure 3.12: Flow diagram for calculating physical absorption from synthesis gases

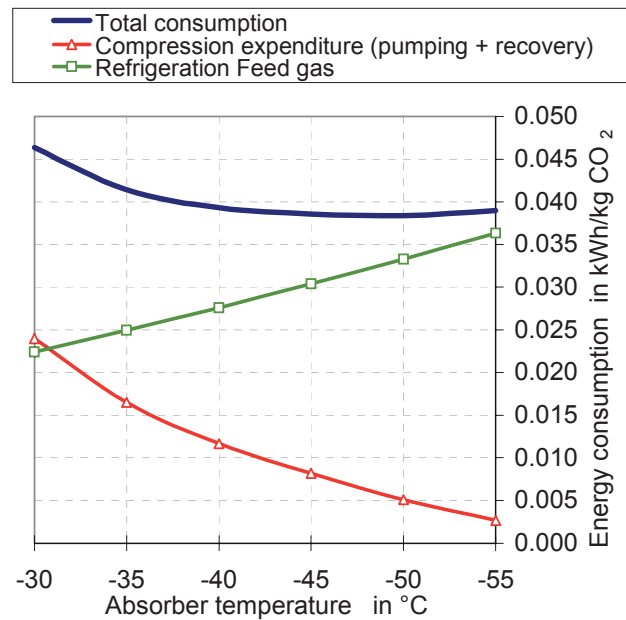


Figure 3.13: Proportion of total energy consumption represented by pumping and refrigerating work for a physical CO<sub>2</sub> scrubbing process with methanol in dependence on the absorber temperature (for information on assumptions and partial results, see Appendix, Table 6.10).

CO<sub>2</sub> solubility increases as the temperature drops, meaning that solvent recirculation and energy consumption decrease. The refrigerating energy<sup>38</sup> to be applied is kept to a minimum through cold recovery.

Using these formulae, calculations are performed for the required solvent recirculation and the pump work for CO<sub>2</sub> separation from a coal gas following CO conversion according to the flow diagram shown in Figure 3.12. The solubility coefficients of CO<sub>2</sub> in methanol were taken from Landolt-Börnstein [166]. As absorption temperature sinks, so too does the pump work required to circulate the solvent, as a consequence of the increasing solubility of CO<sub>2</sub> in methanol; at the same time, however, more refrigerating energy is required (Figure 3.13). The most advantageous absorber temperature to achieve the lowest energy consumption is around -60°C in this example. In real processes, the operating temperature of the absorber lies between -70°C and -30°C.

<sup>38</sup> Efficiency of refrigerating unit  $\eta_{RU} = 35\%$ , performance coefficient  $\epsilon_{RU} = \eta_{RU} / \eta_{Carnot}$  (see Appendix, Table 6.10, for calculation of values).

### CO<sub>2</sub> Absorption Using Seawater as a Solvent

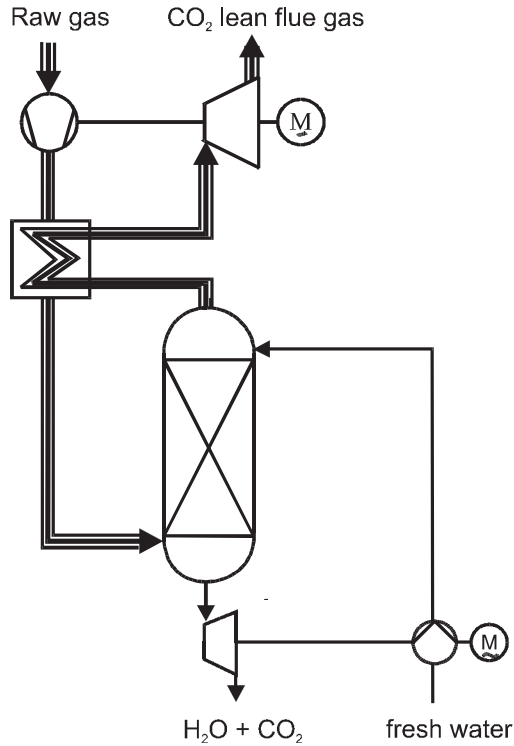


Figure 3.14: Flow diagram of physical absorption with seawater

If seawater<sup>39</sup> is used to scrub CO<sub>2</sub> out of flue gases or synthesis gases, then solvent regeneration is no longer required. The low solubility of CO<sub>2</sub> in seawater makes it necessary to use high pressures or large quantities of solvent. Working on the assumption that the pump and compressor work can be partially recovered using turbines, in accordance with the flow diagram shown in Figure 3.14, energy consumption primarily occurs as a result of the irreversibilities in the pumps, compressors and turbines, and of the lost expansion work of the compressed CO<sub>2</sub> component in the raw gas, in the case of a pressurized raw gas.

Calculation of the pump work and the recoverable hydraulic work shows the optimum absorption pressure to achieve minimal energy consumption as lying between 15 and 20 bar (Figure 3.15). Pressure losses in the supply and disposal pipes are not taken into account in this calculation. The energy consumption for all the gas compositions considered is greater than that of the standard absorption processes. Furthermore, the large quantity of water involved (approx. 100 kg water per kilogram CO<sub>2</sub> in the case of a synthesis gas after CO

conversion, or between 350 and 930 kg water per kg CO<sub>2</sub> in the case of flue gases) means that expensive pipe layouts and absorption columns with large diameters are required.

<sup>39</sup> Calculations are based on the solubility of CO<sub>2</sub> in water according to IUPAC [167].

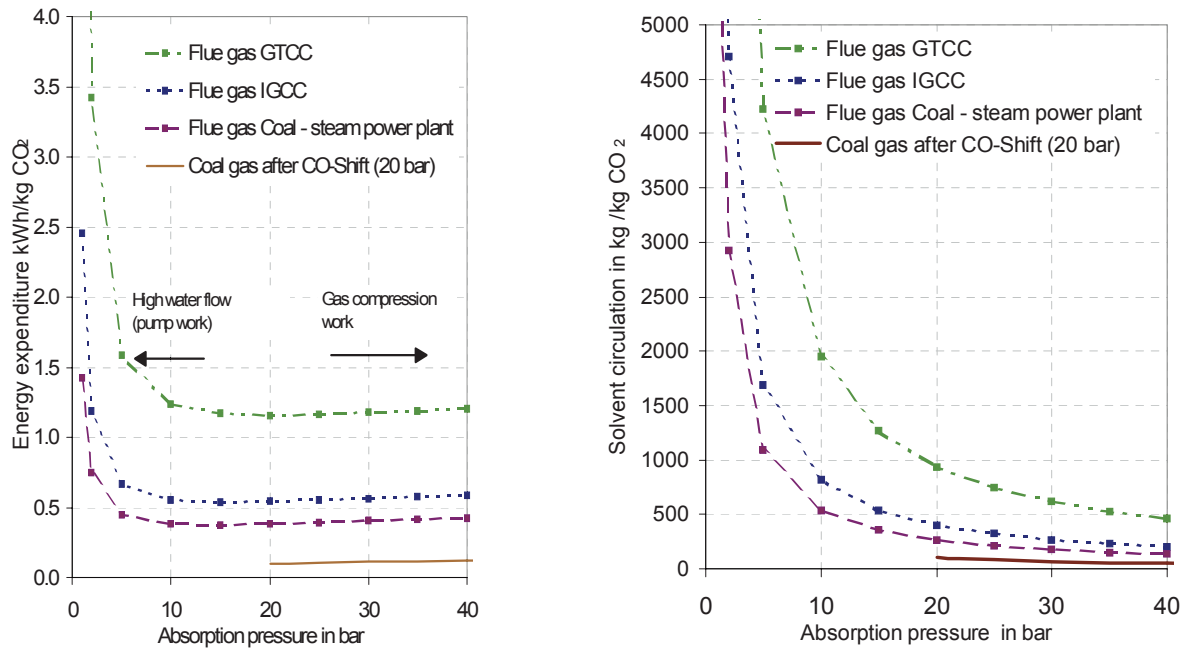


Figure 3.15: Energy required to separate 90% of the CO<sub>2</sub> from various gases, using seawater at 20°C as a solvent (for process data and partial results, see Appendix, Table 6.11).

### Chemical CO<sub>2</sub> Scrubbing

Approximately 80% of the energy required in chemical scrubbing occurs in the regeneration of the solvent [168], which is synonymous with desorption of the components to be separated. The following formula applies for a simplified estimate [168]:

$$\text{Energy for regeneration} = \left\{ \begin{array}{l} \textit{enthalpy of reaction} \\ + \textit{thermal enthalpy component of the solution (heating)} \\ + \textit{enthalpy of vaporization of the vaporized water} \\ + \textit{enthalpy of vaporization of the vaporized absorbent} \\ + \textit{pump and compressor work} \end{array} \right. \quad (3.19)$$

In this case, the enthalpy of reaction represents the lower boundary of the energy expenditure for chemical scrubbing, since it is always required to break the chemical bond of the dissolved gas with the absorbent (MEA, DIPA, DEA, K<sub>2</sub>CO<sub>3</sub>, ...). A skilful process arrangement can ensure that the heat supplied to heat up the charged solution can be kept to a minimum (e.g. through heat recovery via the solvent heat exchanger (Figure 2.3)). The absolute enthalpy of vaporization, and the proportions of the absorbent and the water required as a solvent for the absorbent, which evaporate during regeneration, are dependent on the steam pressure and on the temperature in the desorber, respectively. From this, it is possible to approximate the amount of water/absorbent, which is evaporated proportionally with the desorbed gas<sup>40</sup>.

An estimation of the overall energy expenditure comprising these various components is shown in Figure 3.16. In these assessments, the reaction enthalpy represents a proportion of between 19% and 37% of the total energy consumption (see also Appendix, Table 6.12).

<sup>40</sup> Assisting desorption by lowering the pressure (flash), and lowering the partial pressure through stripping with an inert gas (e.g. water vapor), are not considered here.



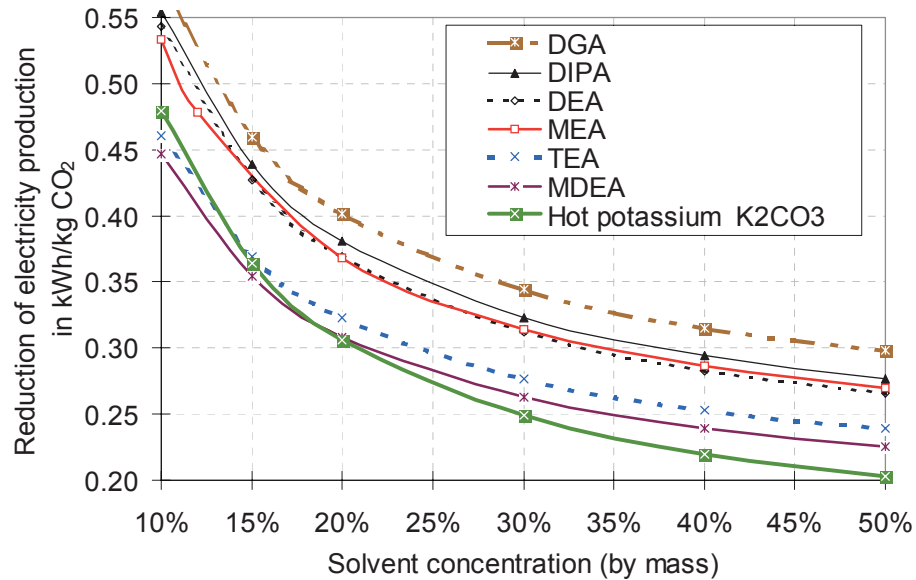


Figure 3.16: Energy consumption for chemical CO<sub>2</sub> scrubbing, calculated in terms of the reduction in electricity production (for information on assumptions and partial results, see Appendix, Table 6.12).

### CO<sub>2</sub> Separation in a PSA Plant Using Zeolite 5A<sup>41</sup>

The energy required for gas separation in a PSA plant comprises:

- Increasing the pressure of the raw gas to the absorption pressure, utilizing the pressure potential of the clean gas (not required for synthesis gases),
- Evacuation to desorption pressure, e.g. using a water-ring pump,
- Pressure build-up in the column to adsorption pressure after desorption.

Impurities in the product are caused by:

- simultaneous adsorption of several components and
- the dead volume of the columns.

The charge is calculated using adsorption isothermals according to Figure 3.17, and the multi-component equilibrium according to Myers and Prausnitz [170]. For the sake of simplicity, these calculations are performed with isothermal adsorption and desorption at 20°C. (For assumptions, see Table 3.11).

Firstly, steam is adsorbed on the zeolite, then CO<sub>2</sub> and, only much later, CO, N<sub>2</sub>, O<sub>2</sub>, and, finally, H<sub>2</sub> (Figure 3.17). Prior condensing of the water component can improve the CO<sub>2</sub> separation process.

<sup>41</sup> Results for CO<sub>2</sub> separation with a PSA plant stem from a dissertation (Adorni [169]) written under my supervision during the writing of this work.

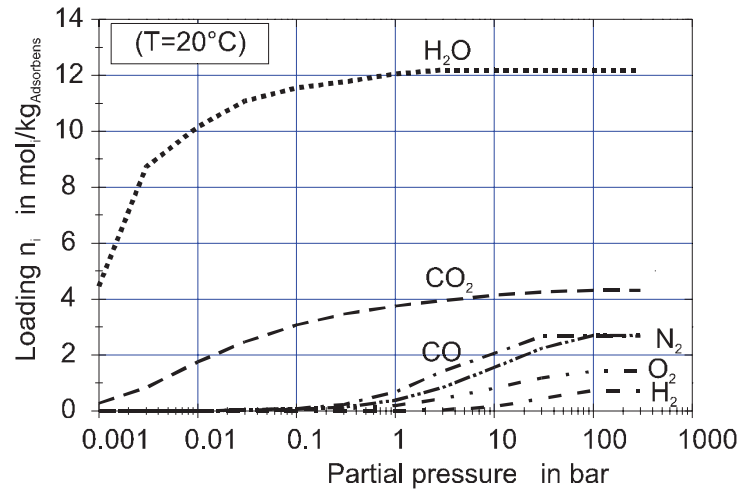


Figure 3.17: Adsorption isotherms of the pure components for zeolite 5A molecular sieve at 20°C <sup>42</sup>

Table 3.11: Assumptions on which the example PSA calculation is based

Desorption pressure	in bar	0.3
Flue gas pressure	in bar	1
Syngas pressure	in bar	24
Adsorption and desorption temperature	in °C, (isothermal)	20
CO <sub>2</sub> separation factor $s_{CO_2}$ (total, three PSA plants in sequence) in %		80

Calculation of a PSA process comprises:

- Selecting the adsorption pressure,
- Calculating the amount of adsorbent, among other factors from the raw gas volume flow and composition, adsorption pressure, residence time, the form of the adsorbent,
- Calculating the empty volumes of the columns, the number of columns and the pressure loss,
- Adsorption: calculating the adsorbed quantities of the individual components,
- Desorption: calculating the quantities which remain in the adsorbent,
- Calculating the energy expended on increasing pressure, evacuation and pressure build-up.

In comparison to CO<sub>2</sub> separation from the flue gases of a natural gas-fired combined cycle power plant, an IGCC power plant or a coal-fired steam power plant, CO<sub>2</sub> separation from the synthesis gas of an IGCC plant after CO conversion consumes the lowest amount of energy and requires the smallest quantity of adsorbent (Figure 3.18, Table 3.12). More than 80% of the higher energy expenditure required for CO<sub>2</sub> separation from flue gases is caused by the pressure build-up. Moreover, the amount of adsorbent required for CO<sub>2</sub> separation from flue gases is unacceptably large.

To achieve greater levels of purity, it is necessary to connect up several PSA plants in sequence. The diagram in Figure 3.20 was generated from a series of calculated values, which enable the product purities and the specific separation work for PSA plants connected in sequence with zeolite 5A (Figure 3.19) and with a CO<sub>2</sub> separation factor ( $s_{CO_2}$ ) of 93% per column to be evaluated in dependence on the CO<sub>2</sub> content of the raw gas.

<sup>42</sup> Data for CO and H<sub>2</sub> based on Kapoor et al. [171], data for CO<sub>2</sub> and N<sub>2</sub> based on Burkert [172], data for H<sub>2</sub>O based on Gerhartz [79], data for O<sub>2</sub> interpolated from figures for N<sub>2</sub> and H<sub>2</sub>.

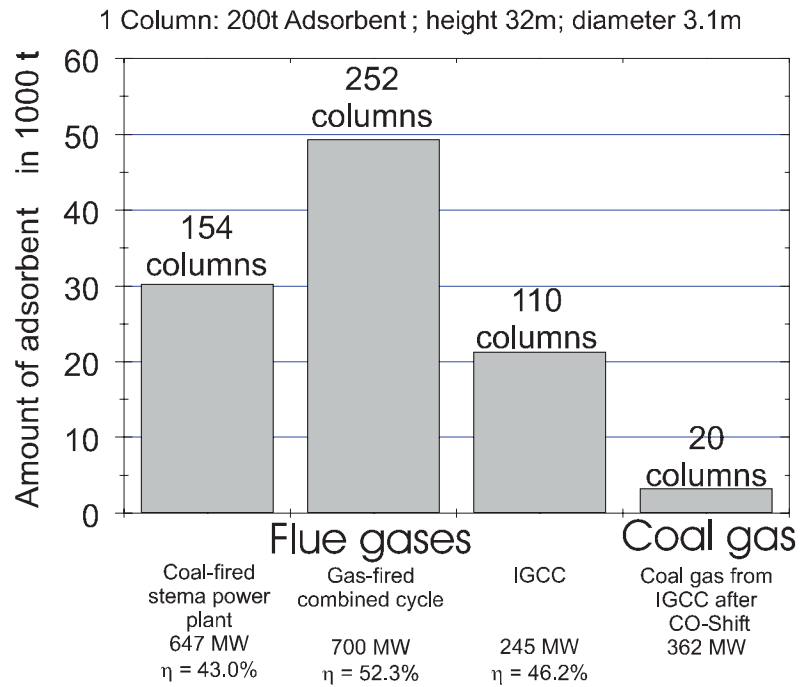


Figure 3.18: Comparison of amount of adsorbent for 80% CO<sub>2</sub> separation factor  $s_{CO_2}$  with zeolite 5A

Table 3.12: Impact on power plant efficiency (CO<sub>2</sub> separation factor 80%, zeolite 5A)

	Efficiency penalty resulting from CO <sub>2</sub> capture $\Delta\eta$ in %	CO <sub>2</sub> mass fraction in the gas in %	Specific separation work in kWh/kg CO <sub>2</sub>
Flue gases			
Gas-fired combined cycle	7.8	4.94	1.28
Integrated coal gasification plant	21.4	11.70	0.72
Coal-fired plant	13.9	17.14	0.42
Synthesis gas			
Coal gas from IGCC after CO shift	6.0	82.02	0.21

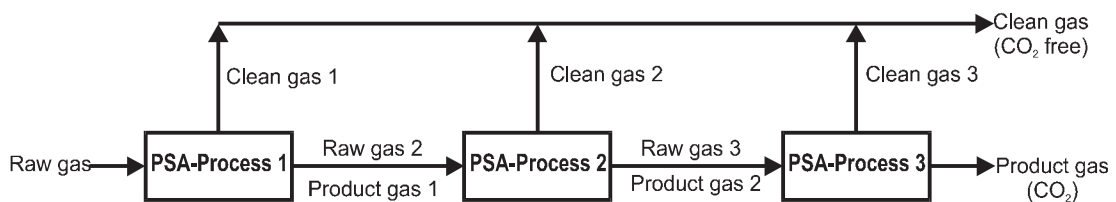


Figure 3.19: Three PSA processes connected in sequence to increase purity of product gas (CO<sub>2</sub>).

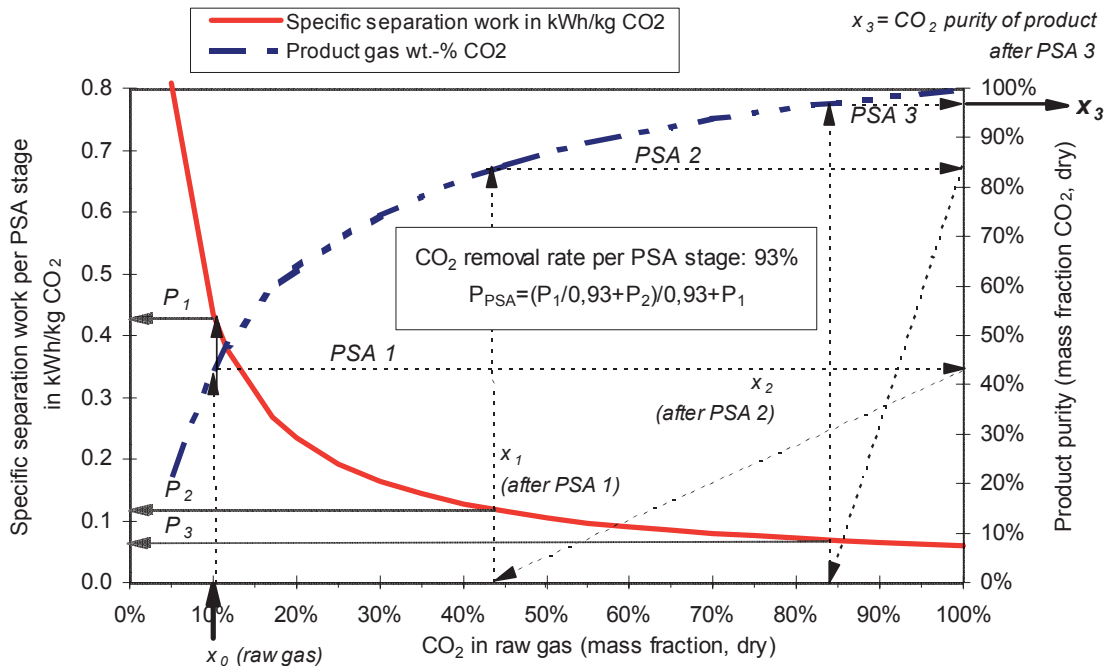


Figure 3.20: Specific separation work and CO<sub>2</sub> product purity with PSA plants connected in sequence using zeolite 5A (Figure 3.19). The separation factor per PSA plant is laid down as 93%.

Example for Figure 3.20: raw gas with CO<sub>2</sub> mass fraction  $x_0$  of 10%. After the first stage, purity is  $x_1 \approx 43\%$ , after the second stage  $x_2 \approx 86\%$  and after the third stage  $x_3 \approx 99.3\%$ . Thus, the specific work of the complete, three-stage plant is:  $P_{\text{PSA}} = (P_1/0.93 + P_2)/0.93 + P_3 \approx 0.7$  kWh/kg CO<sub>2</sub>.

## Membranes

The following example calculations for single-stage membrane modules use the process described by Shindo et al. [162] and Stern et al. [173]. The CO<sub>2</sub> capture ratio in all cases is 90%. In situations where permeabilities were unknown, selectivity  $\alpha_{ij}$  was calculated from the ratio of the mole masses. To calculate the gas separation process with membranes, with known permeabilities, it is necessary to take into consideration the gas transfer equations and the mass balances corresponding to the variable composition over the membrane surface in the various flow models (countercurrent flow, co-current flow, cross-current flow).

### *H<sub>2</sub>/CO<sub>2</sub> Separation with Synthesis Gases*

This first example of H<sub>2</sub> separation from a coal gas after CO conversion is based on the assumption that the enthalpy of combustion from subsequent combustion of the retentate is used in a steam cycle, while the hydrogen-rich permeate is used in a gas/steam turbine combined cycle with a higher efficiency. The largest component of the energy expenditure for H<sub>2</sub> separation consists of the compressor work/the pressure loss of the permeate and the reduced output resulting from fuel loss in the retentate (Figure 3.21). Simulations show that, as selectivity increases, the pressure ratio between the feed and permeate side of the membrane, which is most favorable in terms of energy expenditure, becomes lower (Figure 3.22). A higher H<sub>2</sub> separation factor should be aimed for (Figure 3.23).

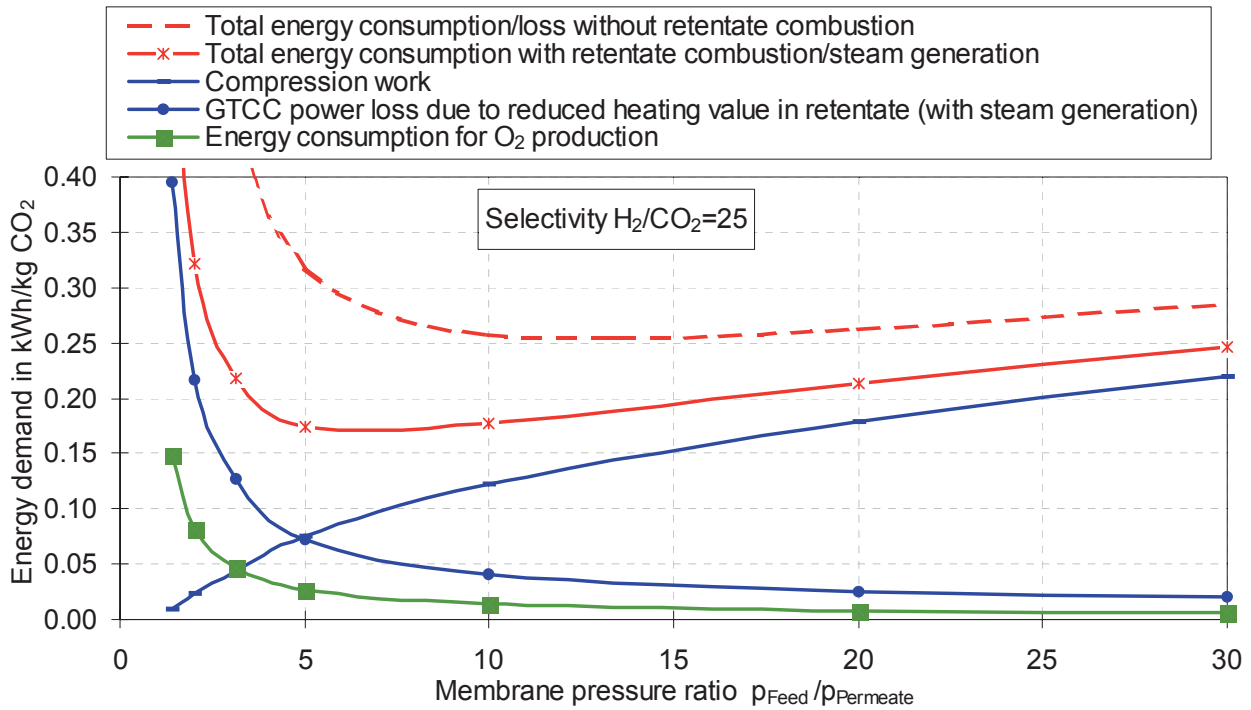


Figure 3.21: Composition of the energy expenditure on  $H_2/CO_2$  separation with a  $CO_2$ -rich coal gas after CO shift (excluding losses from CO shift)

### *H<sub>2</sub>/CO Separation With Synthesis Gases*

In a second example, a membrane is used to separate the hydrogen from a coal gas primarily consisting of  $H_2$  and CO. The hydrogen is then utilized in a gas turbine cycle. The retentate is burnt in a second, semi-closed gas turbine cycle with the same efficiency, supplied with oxygen. In this case, the energy used in capturing the  $CO_2$  is primarily determined by the compressor work involved. Consequently, the lowest energy expenditure is achieved by selecting the smallest possible pressure ratio in the membrane (Figure 3.24, Figure 3.25).

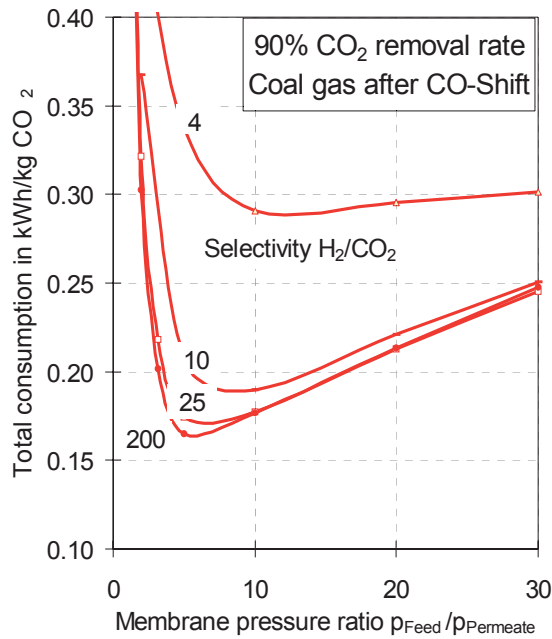


Figure 3.22: Total energy expended on  $H_2/CO_2$  separation with a  $CO_2$ -rich coal gas after CO shift, (incl. subsequent combustion of the retentate with heat recovery, without losses from CO shift).

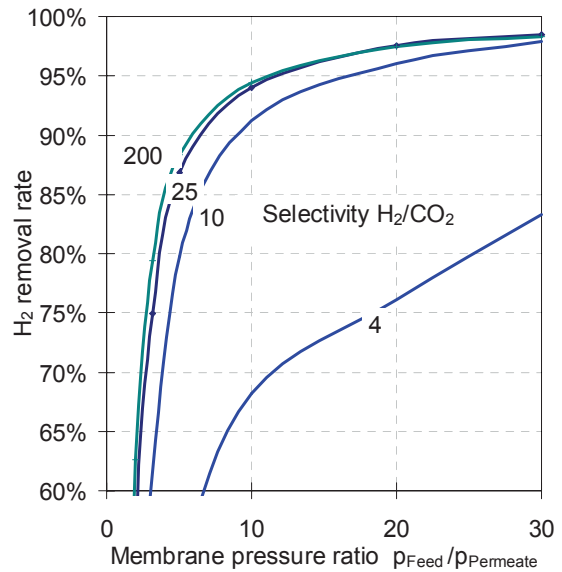


Figure 3.23:  $H_2$  separation factor achieved (pertaining to Figure 3.22).

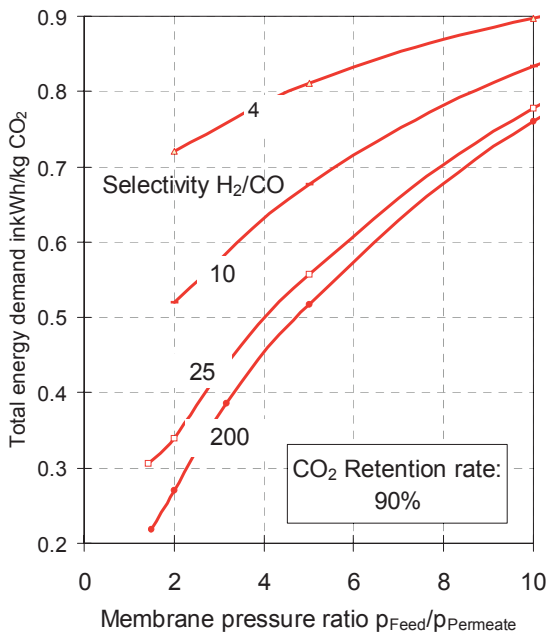


Figure 3.24: Total energy expended on  $H_2/CO$  separation of a coal gas (incl.  $O_2$  production for gas turbine cycle with combustion in an atmosphere of  $O_2/CO_2$ , assuming that both gas turbine cycles display the same efficiency).

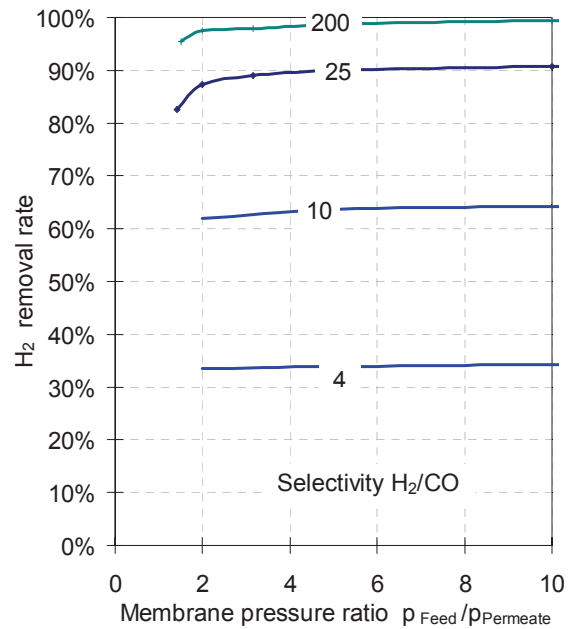


Figure 3.25:  $H_2$  separation factor achieved (pertaining to Figure 3.24).

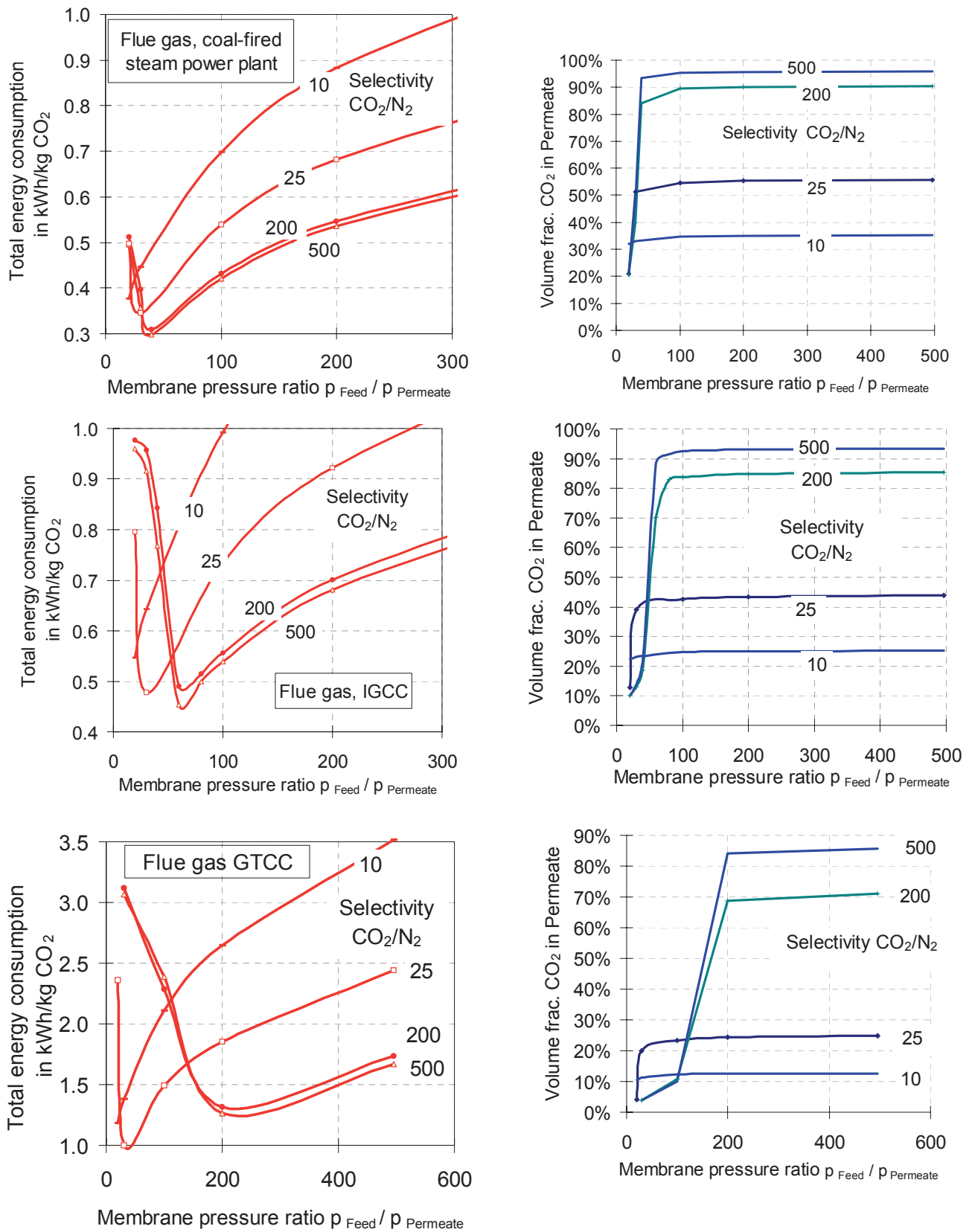


Figure 3.26: Energy consumption and CO<sub>2</sub> purity in the permeate for CO<sub>2</sub> separation from flue gases (coal-fired steam power plant, IGCC, gas/steam turbine power plant) with a CO<sub>2</sub> capture ratio of 90%

### CO<sub>2</sub> Separation from Flue Gases

In CO<sub>2</sub> separation from flue gases (Figure 3.26), a portion of the compression work required in this process can be recovered through retentate expansion. As CO<sub>2</sub> concentration increases (GTCC→IGCC→coal-fired steam power plant), the amount of energy required for CO<sub>2</sub> separation decreases. An optimum pressure ratio in terms of energy expenditure can also be obtained in this process; in contrast to the situation of hydrogen separation from synthesis gas, this optimum pressure ratio becomes larger as selectivity increases. Although higher selectivity significantly improves the purity of the separated CO<sub>2</sub>, it has little influence on energy requirements.

### Condensation and Sublimation of CO<sub>2</sub> from Flue Gases and Synthesis Gases

The CO<sub>2</sub> separation factor  $s_{CO_2}$  in the condensing or subliming of CO<sub>2</sub> from synthesis gases or flue gases is dependent on saturation or sublimation pressure  $p_s$ , total pressure  $p$  and molar fraction  $y_i$ :

$$s_{CO_2} = 1 - \left( \frac{y_{N_2} + y_{O_2}}{y_{CO_2}} \cdot \frac{p_s(T)}{p - p_s(T)} \right) \quad (3.20)$$

Equation 3.20 clearly shows that, aside from a low temperature, high overall pressure together with a high initial content of CO<sub>2</sub> also play an important role in achieving a high rate of separation. The pressures and temperatures required to achieve a CO<sub>2</sub> separation factor of 90% are shown in Figure 3.27.

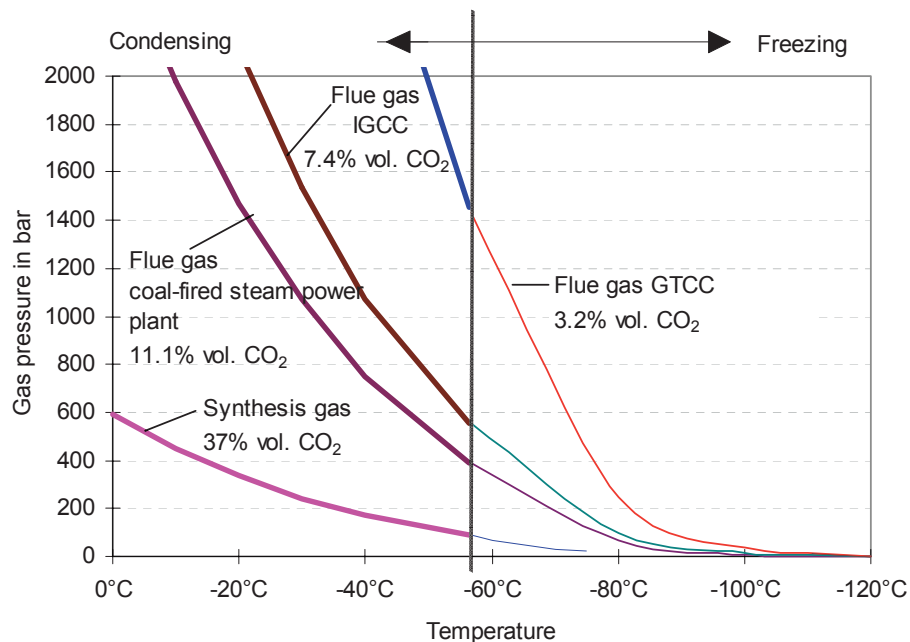


Figure 3.27: Pressure required to capture 90% of the CO<sub>2</sub> through condensing/freezing<sup>43</sup>.

For an exergetic efficiency of 35%<sup>44</sup> for the refrigerating unit, a polytropic efficiency of 85% for the compressor and turbine, and heat recovery with a pinch point of 40 K, the energy required to con-

<sup>43</sup> Calculated from steam and sublimation pressure of CO<sub>2</sub> according to IUPAC [163].

<sup>44</sup> The efficiencies were assumed to be constant over the temperature range.



dense/freeze out 90% of the CO<sub>2</sub> from the example gases was calculated according to Table 3.10 (Figure 3.28, Figure 3.29). If the freezing of CO<sub>2</sub> were technically feasible, the energy consumption involved would be lower than that of condensing, where a great deal of compressor work is required to achieve the high pressure required.

The process data for the calculation is summarized in the Appendix in Tables 6.14 to 6.17

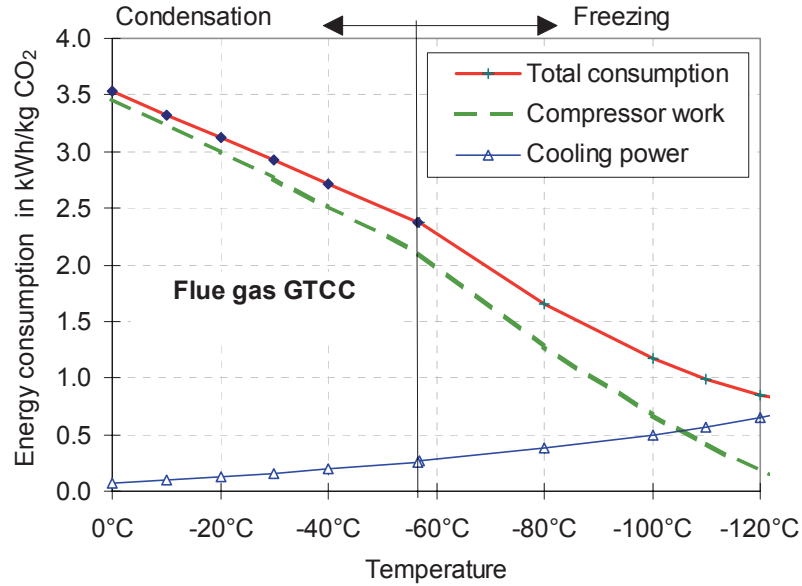


Figure 3.28: How energy consumption is divided up in the condensation/sublimation of 90% of the CO<sub>2</sub> from the flue gas of a gas/steam combined cycle.

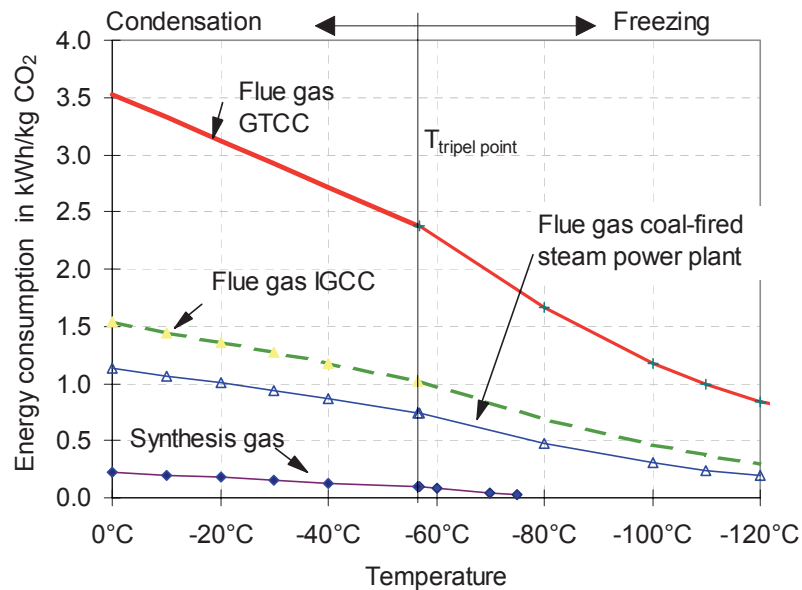


Figure 3.29: Energy required for condensation/sublimation of 90% of the CO<sub>2</sub> from various gases.

### 3.4.2 Reversible Separation Work and Exergetic Efficiency of Technical Gas Separation Processes

The exergetic efficiency  $\zeta_{sep}$  of a gas separation process is here defined as the ratio of reversible separation work to actual work, plus isothermal compression of the separated gas to the total pressure of the raw gas feed<sup>45</sup>:

$$\zeta_{sep} = \frac{w_r}{w_{real} + x_i R_i T_0 \ln p_{tot} / p_{desorber}} = \frac{x_i R_i T_0 \ln p_{tot} / p_i}{w_{real} + x_i R_i T_0 \ln p_{tot} / p_{desorber}} \quad (3.21).$$

In this equation,  $i$  is the gas component to be separated,  $x_i$  is the mass fraction,  $R_i$  is the gas constant,  $w_{real}$  is the specific energy requirement of the gas separation process,  $w_r = x_i R_i T_0 \ln p_{tot} / p_i$  is the reversible separation work (see below) and  $x_i R_i T_0 \ln p_{tot} / p_{desorber}$  is the isothermal compression work to compress separated gas from desorption pressure  $p_{desorber}$  to total pressure  $p_{tot}$  of the raw gas.

In real gas separation processes, the pressure of the separated gas is generally significantly lower than that of the supplied raw gas; to enable comparisons to be made with reversible separation work, it is therefore necessary to add on the energy required to compress the separated gas to the total pressure of the raw gas. Otherwise, in certain cases (for example, those where CO<sub>2</sub> is separated from a synthesis gas, which is under pressure, and is then released at ambient pressure), energy would actually be yielded in the reversible case with high CO<sub>2</sub> partial pressures.

Exergetic efficiency  $\zeta$  of a gas separation procedure provides an empirical parameter for a specific separation process, which, with minimal data, and without precise knowledge of the gas separation procedure, enables a first evaluation to be made for any separation task from the ideal separation work.

Exergetic efficiency  $\zeta$  of physical and chemical scrubbing, and of adsorption and membrane separation processes, is presented in the following sections, and is used for the simulation of CO<sub>2</sub> separation with scrubbing.

#### Reversible Separation Work

In cases with adiabatic mixing of streams, entropy flow  $\Delta \dot{S}_{V,mix} = \Delta \dot{S}_{irr}$  is produced irreversibly, which leads to exergy loss  $\Delta \dot{E}_{V,mix} = T_U \Delta \dot{S}_{V,mix}$ . To separate a stream into streams of differing concentration, it is necessary to expend, at minimum, the value of the exergy loss of the mixture  $\Delta \dot{E}_{V,mix}$ . This gives a minimal, reversible separation work  $w_r$  of:

$$w_r = \Delta \dot{E}_{V,mix} = T_U \left( \dot{S}_{mix} - (\varepsilon_1 \dot{S}_1 + \varepsilon_2 \dot{S}_2) \right) \quad (3.22)$$

This is synonymous with the difference in exergy between the exergy of the total mixture prior to gas separation, and the sum of the partial volumes of the separated components and of the residue, which remains, in each case at the overall pressure of the mixture. In contrast to the process of separating out individual components, reversible separation work done to separate ideal gases into  $n$  different streams is defined by the isothermal compression to be applied to all the  $n$  separated gas components to take them from their respective partial pressure to the total pressure:

<sup>45</sup> The gas is denoted as raw gas or feed prior to entering the gas separation process.

$$w'_r = T_0 \sum_{i=1}^n x_i R_i \ln(p_{tot} / p_i) \quad (3.23)$$

where:  $x_i$  mass fraction of separated gas component  $i$   
 $R_i$  individual gas constant  
 $p_i$  partial pressure,  $p_{tot}$  absolute pressure.

Working on the assumption that the work of expansion, which is to be applied owing to the reduced volume of the remaining gas, is drawn from the environment, reversible separation work  $w_r$  to separate an individual component  $i$  can be reduced to:

$$w_r = x_i R_i T_0 \ln(p_{tot} / p_i) \quad (3.24)$$

The reversible separation work for a component should not be confused with the minimum work of a separation process, which is conditional on the system (e.g. as in air separation, where this system-contingent separation work is often indicated by the reversible separation work to separate air into all its individual components) [76].

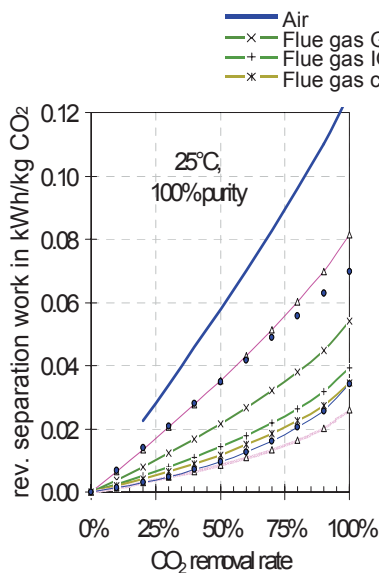


Figure 3.30: Reversible separation work in dependence on CO<sub>2</sub> separation factor<sup>46</sup>

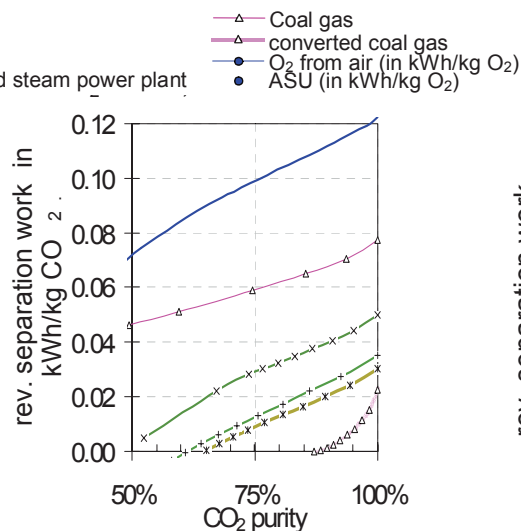


Figure 3.31: Reversible separation work in dependence on CO<sub>2</sub> purity (volume fractions)<sup>46</sup>

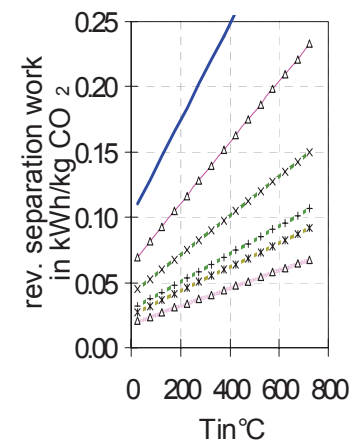


Figure 3.32: Influence of gas temperature on reversible separation work<sup>46</sup> (isothermal compression)

In accordance with Equation 3.24, minimum separation work increases, as concentration in the initial mixture of the components, which are to be separated, decreases. Thus, the work required to separate CO<sub>2</sub> from gases increases in accordance with CO<sub>2</sub> concentration in the following sequence: coal gas after CO conversion (40% vol fraction CO<sub>2</sub>), flue gases (11% to 3% vol fraction CO<sub>2</sub>) and air (0.03% vol fraction CO<sub>2</sub>) (Table 3.13). Transport of the emitted CO<sub>2</sub> through the atmosphere and removal of the CO<sub>2</sub> from air would therefore theoretically require between two and six times more energy compared with direct CO<sub>2</sub> separation. In the case of synthesis gases, CO<sub>2</sub> can also be enriched by removing H<sub>2</sub>. The energy expended on H<sub>2</sub> separation, together with the energy required to produce O<sub>2</sub> for combustion in an atmosphere of O<sub>2</sub>/CO<sub>2</sub> (Table 3.13), cannot be directly compared with the work required for CO<sub>2</sub> separation, but must instead be viewed in relation to the proportion of carbon as compared to H<sub>2</sub>, and the

<sup>46</sup> See Table 3.10 for information on gas compositions.

minimum oxygen requirements, respectively. Rising separation factors, product purity and gas temperature ( $T_0$ ) increase the reversible separation work (Figure 3.30 to Figure 3.32).

Table 3.13: Reversible separation work  $w_r$  for CO<sub>2</sub>, H<sub>2</sub> and O<sub>2</sub> separation with various gas compositions according to Table 3.10

	Coal gas after	Air	Flue gases:		
	CO shift		Coal-fired steam power plant	IGCC power plant	Gas/steam turbine combined cycle plant (GTCC)
Feed gas					
Volume fraction of CO <sub>2</sub> in %	40.5	0.032	11.1	8.1	3.2
Mass fraction of CO <sub>2</sub> in %	87.1	0.049	17.1	11.7	4.9
<i>Reversible Separation Work</i>					
CO <sub>2</sub> separation in kWh/kg CO <sub>2</sub>	0.026	0.142	0.048	0.055	0.069
H <sub>2</sub> separation in kWh/kg H <sub>2</sub> in kWh/kg CO <sub>2</sub>	0.4354 ≅0.0266	-	-	-	-
O <sub>2</sub> separation in kWh/kg O <sub>2</sub>		0.0336	-	-	-

### Exergetic Efficiency $\zeta$ of Technical CO<sub>2</sub> Separation Installations

The overview of exergetic efficiency  $\zeta_{sep}$  for various gas separation processes, which is presented in Table 3.14, was compiled on the basis of data from the literature concerning gas composition, separation factors and energy requirements. In the case of H<sub>2</sub>/CO<sub>2</sub> separation from synthesis gases, the highest exergetic efficiencies are obtained through physical absorption methods and membrane separation methods, followed by physical-chemical scrubbing. The differences in energy expenditure of physical scrubbing processes are caused by the different solvents used.

Among the processes for separating CO<sub>2</sub> from pressurized synthesis gases, the highest exergetic efficiency, of up to 31%, is obtained using physical scrubbing, followed by an efficiency of 22% for physical-chemical scrubbing and 14% for chemical scrubbing.

In the case of CO<sub>2</sub> separation from flue gases, chemical scrubbing achieves the highest exergetic efficiency, at up to 21%. The exergetic efficiency of chemical scrubbing deteriorates as the concentration of amine in the aqueous solution decreases.

In the case of membrane processes and adsorption, exergetic efficiency is heavily dependent on the composition of the gas.

In this study, calculations of the internal consumption of physical scrubbing are based on an exergetic efficiency of 30.5%. Membrane separation processes are interpreted on the basis of a special simulation method.

According to the energy consumption calculated using Equation 3.15, the exergetic efficiency of O<sub>2</sub> production via air separation is around 19%<sup>47</sup>, if only the O<sub>2</sub> generated is counted as a product.

<sup>47</sup> Baehr [161] calculates an exergetic efficiency of 9.1% for the Linde process. However, this value relates to the production of liquid air, not to the production of gaseous O<sub>2</sub> as described in this study. The exergy of liquid air is approx. 693 kJ/kg, which is more than five times higher than the figure of 124.6 kJ/kg for gaseous O<sub>2</sub>, at 25°C and 1 bar. According to Bosnjakovic and Knoche [174], air separation units obtain an exergetic efficiency of 33%. In contrast to the values stated above, this figure includes the exergy of all the products, i.e. also that of the nitrogen stream.

Table 3.14: Operating data and exergetic efficiencies of CO<sub>2</sub> and H<sub>2</sub> separation processes (80% to 90% CO<sub>2</sub> capture ratio)

Process / Solvent	Specific Expenditure of Energy kWh/kg CO <sub>2</sub>		Total Pressure P <sub>tot</sub> in bar	Volume Fraction of CO <sub>2</sub> in %	Exergetic Efficiency in % $\zeta_{sep} = \frac{\text{reversible sep. work}}{\text{work done}}$
	without expansion losses <sup>48</sup>	with expansion losses <sup>49</sup>			
Physical Scrubbing (CO <sub>2</sub> separation from pressurized synthesis gas after CO shift)					
	0.04-0.09	0.09-0.14	approx. 24	approx. 36	20-31
Physical/Chemical Scrubbing (CO <sub>2</sub> separation from pressurized synthesis gas and CO <sub>2</sub> -rich flue gases)					
Adip (DIPA & MDEA)	0.07	0.15	approx. 130	approx. 36	approx. 18 <sup>50</sup> (20 <sup>51</sup> )
Activated MDEA	0.04	0.09	approx. 24	approx. 36	approx. 29 <sup>50</sup> (32 <sup>51</sup> )
Chemical Scrubbing (CO <sub>2</sub> separation from flue gas)					
Amine					
MEA 12% aqueous sol., mass frac.	0.55	=	approx. 1.2	approx. 11.0	approx. 9 <sup>50</sup> (11 <sup>51</sup> )
MEA 20% aqueous sol., mass frac.	0.35	=	approx. 1.2	approx. 11.0	approx. 14 <sup>50</sup> (17 <sup>51</sup> )
MEA 30% aqueous sol., mass frac.	0.23	=	approx. 1.2	approx. 11.0	approx. 21 <sup>50</sup> (25 <sup>51</sup> )
Inorganic Scrubbing					
Benfield and variants	0.42	=	approx. 1.2	approx. 11.0	approx. 8 <sup>50</sup> (10 <sup>51</sup> )
Flexsorb	0.43	0.5	approx. 60	approx. 36	approx. 5-6 <sup>50</sup> (6-7 <sup>51</sup> )
Membrane Processes					
H <sub>2</sub> sep. from synthesis gas <sup>52</sup> (selectivity H <sub>2</sub> /CO <sub>2</sub> = 4-200)	--	0.17-0.29 <sup>53</sup>	approx. 24	approx. 40 (H <sub>2</sub> ) approx. 36 (CO <sub>2</sub> )	25-32
CO <sub>2</sub> sep. from flue gas Coal-fired steam plant	0.3 - 0.4	=	approx. 1.2	approx. 11.0 approx. 7.4 approx. 3.2	10-14
IGCC power plant (coal)	0.45 - 0.55	=			6.5-8
Gas/steam turbine plant (GTCC - natural gas) (selectivity CO <sub>2</sub> /N <sub>2</sub> = 10-200)	1 - 1.3	=			1.5 - 2
Adsorption (PSA/TSA)					
CO <sub>2</sub> sep. from synthesis gas	0.16-0.2	0.2-0.25	approx. 24	approx. 36	8-12
CO <sub>2</sub> sep. from flue gas Coal-fired steam plant	0.4	=	approx. 1.2	approx. 11.0	9
IGCC power plant (coal)	0.7	=			5
Gas/steam turbine plant (GTCC - natural gas)	1.2	=			1.5

<sup>48</sup> With high feed gas pressure and low separated gas pressure.<sup>49</sup> Incl. compensation for pressure loss of separated gas stream through isothermal compression of the separated gas to the total pressure of the raw gas (where  $\eta_{\text{isotherm}}=100\%$ ).<sup>50</sup> Work done = (consumption of electrical energy) + (drop in steam turbine performance due to steam extraction)<sup>51</sup> Work done as exergy of the steam.<sup>52</sup> Incl. fuel losses and oxygen production, excl. losses due to CO shift reaction.<sup>53</sup> Corresponds to 1.1 – 1.4 kWh/kg H<sub>2</sub>

### 3.5 Process Family I: CO<sub>2</sub> Separation From Synthesis Gas After CO Shift

Efficiency penalties due to CO<sub>2</sub> capture in processes with coal gasification, CO conversion and CO<sub>2</sub>/H<sub>2</sub> separation are primarily caused by<sup>54</sup>:

- Exergy losses in CO conversion (exergetic efficiency of CO conversion approx. 90% to 95%, efficiency penalty approx. 2 to 3 percentage points<sup>54,55</sup>),
- Energy required for gas separation (regeneration, pressure losses). The resulting efficiency penalty is approx. 2.5 to 3 percentage points<sup>54,55</sup>)
- Reduction in gas turbine power output corresponding to the expansion work of the separated CO<sub>2</sub> volume flow<sup>56</sup> (efficiency penalty approx. 0.8 percentage points<sup>54,55</sup>)

In cases where figures are available for total CO<sub>2</sub> capture ratio to be achieved  $r_{CO_2,tot}$ , and for CO<sub>2</sub> separation factor  $s_{CO_2,scrubbing}$  in the gas scrubbing process, related to the CO<sub>2</sub> component in the converted synthesis gases, required CO conversion  $r_{CO}$  in the CO shift reaction may be calculated from:

$$r_{CO} = \frac{r_{CO_2,tot}}{s_{CO_2,scrubbing} \cdot r_{C-conversion,gasifier}} \quad (3.25)$$

#### 3.5.1 CO Conversion, Steam Reforming

The expenditure of exergy in the CO conversion process consists of exergy  $\dot{E}_{rawgas}$  of the raw gas supplied, exergy  $\dot{E}_{H_2O}$  of the water/steam supplied, and exergy  $\dot{E}_{Q,heat}$  of the heat used for saturator heating. With useful exergy  $\dot{E}_{converted\ gas}$  of the converted gas (the gas after the CO shift reaction) and useful component  $\dot{E}_{Q,use}$  of the heat released, the exergetic efficiency of the CO shift reaction may be defined as:

$$\zeta_{CO\ shift} = \frac{\dot{E}_{rawgas} + \dot{E}_{H_2O} + \dot{E}_{Q,heat}}{\dot{E}_{converted\ gas} + \dot{E}_{Q,use}} \quad (3.26)$$

The energy efficiency of the CO shift is:

$$\eta_{CO\ shift} = \frac{\dot{H}_{rawgas} + \dot{H}_{H_2O} + \dot{H}_{Q,heat}}{\dot{H}_{converted\ gas} + \dot{H}_{Q,use}}$$

The highest exergetic efficiencies through CO conversion can only be achieved in an ideal case, if, starting from the highest possible temperature, the heat released as the temperature drops is used continuously, and thus at the maximum possible temperature, and if no more water is supplied than that which may actually be converted at each specific moment in time. In an example of a 19-stage CO shift reactor, CO conversion of 90% and exergetic efficiency of around 97% (related to overall expenditure

<sup>54</sup> Derivation of values in following sections.

<sup>55</sup> Values for 90% CO<sub>2</sub> separation

<sup>56</sup> In the majority of cases involving CO<sub>2</sub> separation, the CO<sub>2</sub> produced is released at approximately ambient pressure. Since the partial pressure of the CO<sub>2</sub> in the fuel gas prior to separation is significantly higher, expansion work would be available in the reversible case (ideal case). This is why it is necessary to take into account the reduction in the amount of work gained through expansion of the fuel gas, from which the CO<sub>2</sub> component has been removed.

and gain) are obtained using a raw gas from an oxygen-blown gasification process involving a step-by-step drop in temperature from 1000°C to 100°C with simultaneous, stepwise heat recovery and addition of the minimum quantity of steam required (Figure 3.33 to Figure 3.35). The exergy of the synthesis gas after CO conversion is reduced to 90.5% of the raw gas. Excluding heat recovery, the exergetic efficiency is 90%. The fuel energy flow (LHV) is reduced to 91% of the initial value. The ratio of total energy gain (fuel energy flow (LHV) + thermal enthalpy) to the minimum, overall energy expenditure (enthalpy flow of the raw gas including fuel energy flow (LHV) and steam) is around 86%.

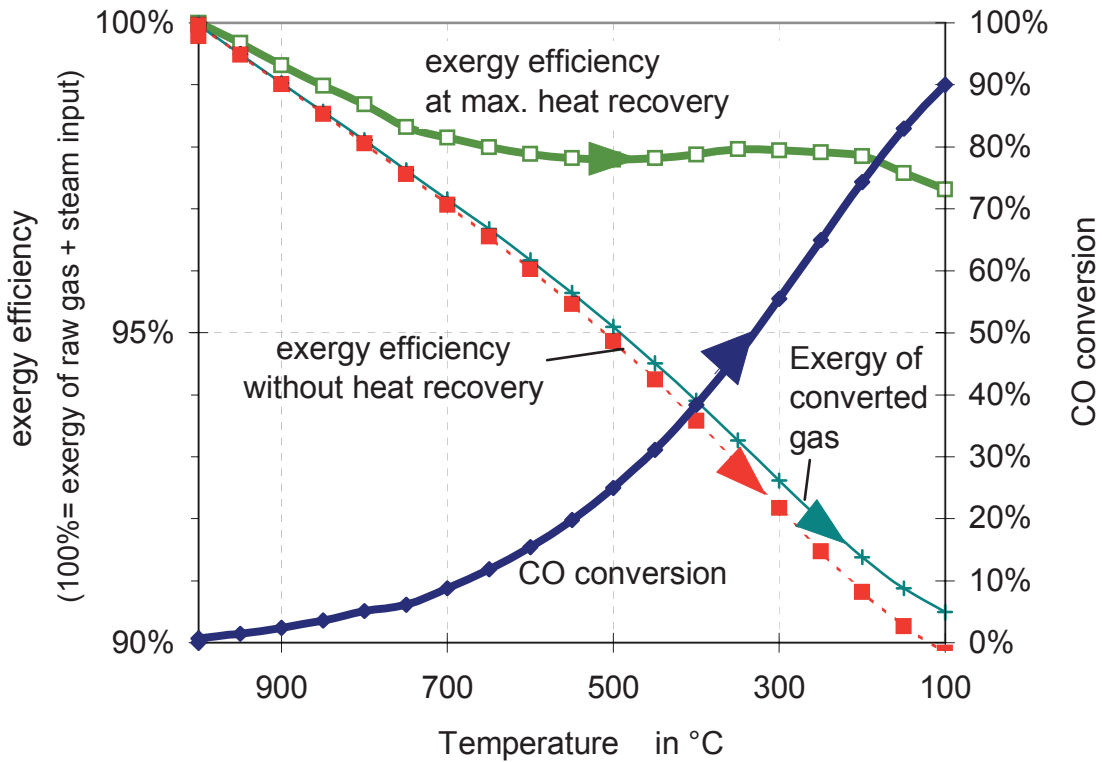


Figure 3.33: "Ideal" CO shift with continuous heat recovery and addition of steam: exergetic efficiency and CO conversion achieved<sup>57</sup>.

<sup>57</sup> Volume fractions of the components of the raw gas from oxygen-blown coal gasification: 2.12% H<sub>2</sub>O; 1.49% CO<sub>2</sub>; 6.05% N<sub>2</sub>; 0.96% Ar; 28.8% H<sub>2</sub>; 59.6% CO; 0.01% CH<sub>4</sub>; 0.92% H<sub>2</sub>S. Reaction pressure: 25 bar.

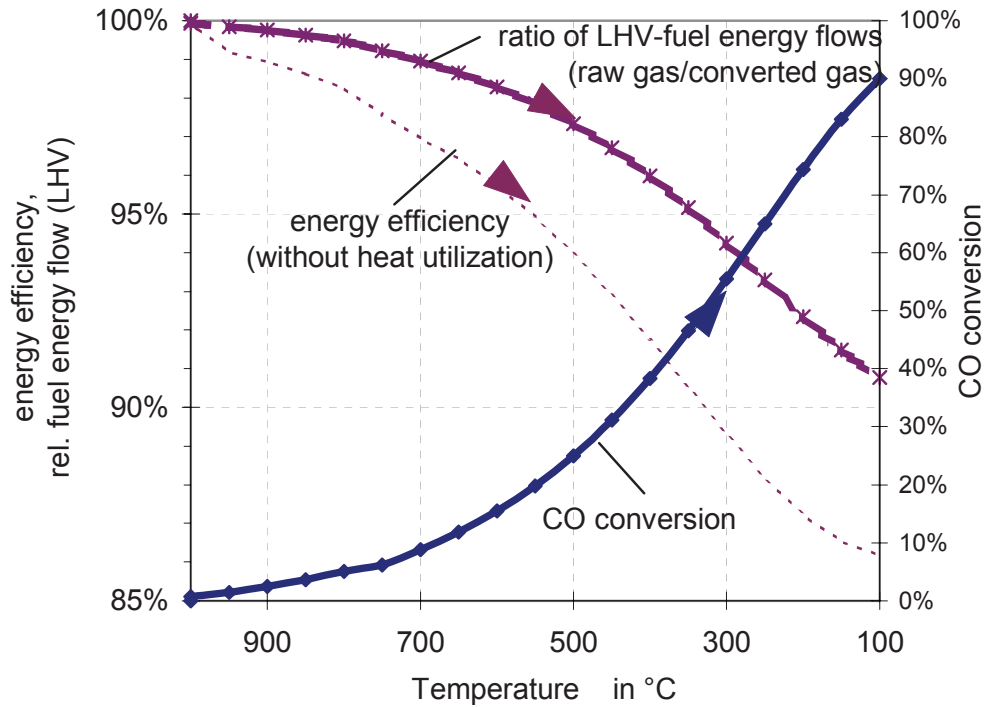


Figure 3.34: "Ideal" CO shift with continuous heat recovery and addition of steam: energy efficiency, reduction in fuel energy (ratio of fuel energy flows, LHV) and CO conversion achieved<sup>57</sup>.

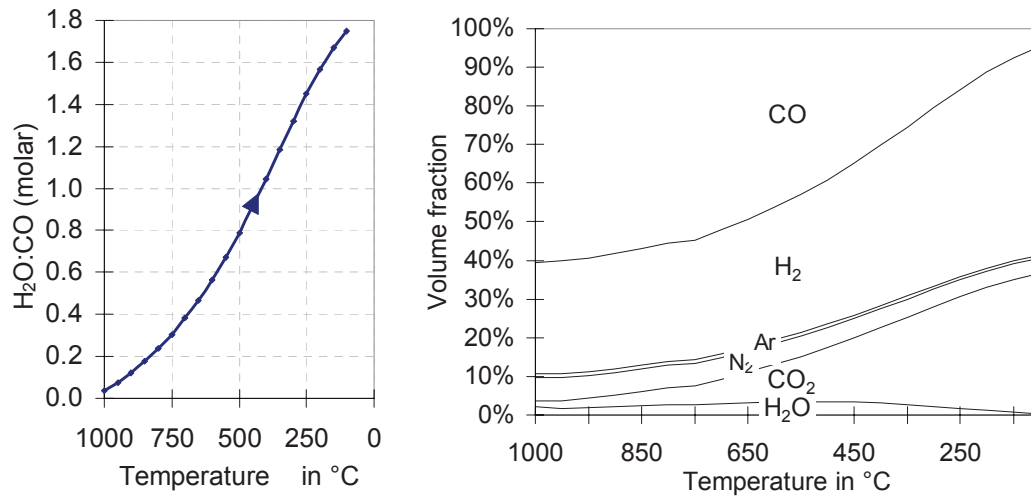


Figure 3.35: Development of the molar ratio of  $\text{H}_2\text{O}$  to  $\text{CO}$  and volume fraction of the gas components in relation to reaction temperature for an "ideal" CO shift according to Figure 3.33, Figure 3.34

In a real case (Figure 3.36), the number of reaction stages is restricted to between one and three, which means that a far higher excess of steam is required, and that the reaction enthalpy can only be used at low temperatures. As CO conversion and temperature increase, so too do the required steam excess (Figure 3.36, left) and the exergy losses (Figure 3.36, right).



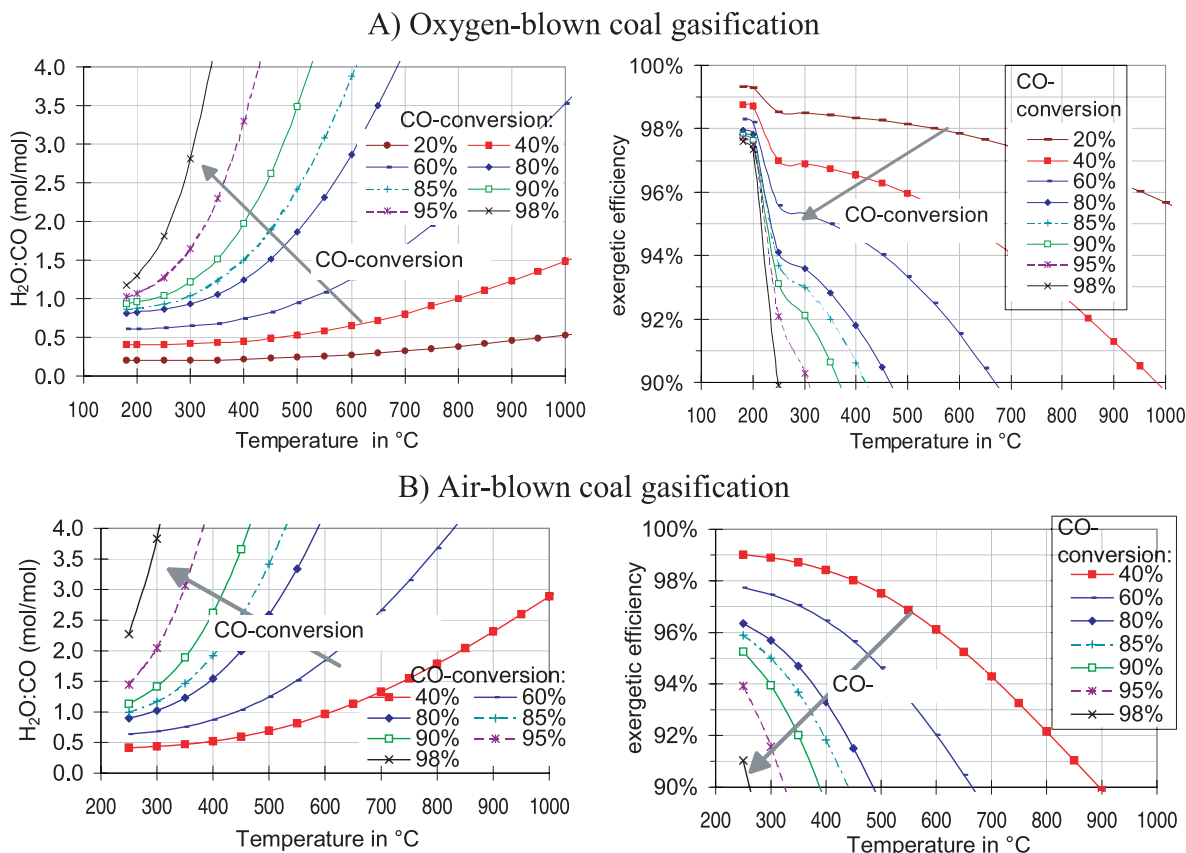


Figure 3.36: Required molar ratio of H<sub>2</sub>O:CO and exergetic efficiency with CO shift after A) oxygen-blown and B) air-blown coal gasification<sup>58</sup>

Cooling to the point of condensation after CO conversion causes, with a reactor temperature of 400°C, a further exergy loss of approx. 4%, related to the exergy supplied (Figure 3.37). Hot-gas cleaning avoids these exergy losses since it does not involve condensation.

In contrast, in steam reforming (Figure 3.38) steam excess and exergy losses become larger, as the temperature drops and CH<sub>4</sub> conversion increases.

<sup>58</sup> Volume fractions of raw gas components:

A) 2.12% H<sub>2</sub>O; 1.49% CO<sub>2</sub>; 6.05% N<sub>2</sub>; 0.96% Ar; 28.8% H<sub>2</sub>; 59.6% CO; 0.01% CH<sub>4</sub>; 0.92% H<sub>2</sub>S.

B) 7.33% H<sub>2</sub>O; 9.8% CO<sub>2</sub>; 45.5% N<sub>2</sub>; 0.59% Ar; 14.0% H<sub>2</sub>; 22.1% CO; 0.89% CH<sub>4</sub>; 0.1% H<sub>2</sub>S.

Assumptions: exit temperature= entry temperature; reaction pressure: 25 bar; steam added at saturation temperature.

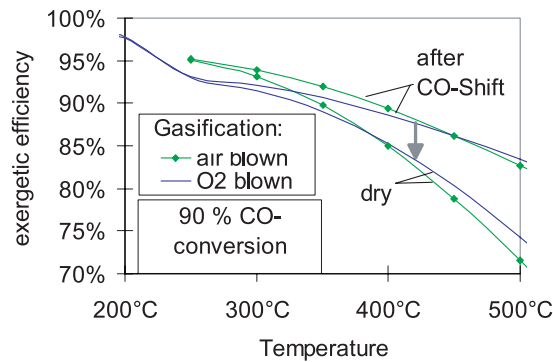


Figure 3.37: Comparison of the exergetic efficiencies for wet coal gas after CO shift and for the same gas after drying (or later water condensation, respectively) with 90% CO conversion

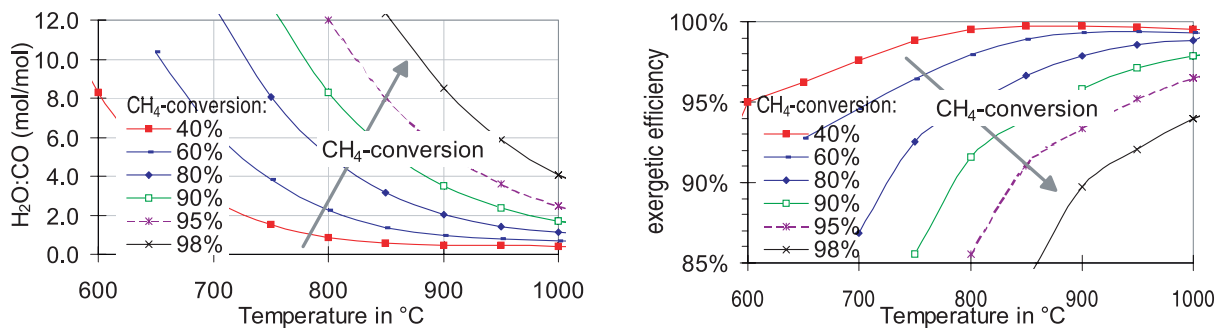


Figure 3.38: Steam excess and exergetic efficiency in steam reforming (100% methane, 25 bar, without subsequent CO shift)

### 3.5.2 Processes with Coal Gasification

The possibilities for CO<sub>2</sub> capture in IGCC power plants with CO conversion were calculated for the process arrangement of an IGCC power plant described in Figure 3.9, with the additional incorporation of CO conversion and H<sub>2</sub>/CO<sub>2</sub> separation. In accordance with Equation 3.25, required CO conversion is calculated in dependence on a given CO<sub>2</sub> capture ratio and the CO<sub>2</sub> separation factor of the gas separation process. The entire gas stream is fed through all the stages of the CO<sub>2</sub> capture process.

#### 3.5.2.1 CO<sub>2</sub> Separation Using Physical Scrubbing

Table 3.15 shows comparative calculations for an IGCC power plant with and without CO<sub>2</sub> separation by means of physical scrubbing (Rectisol), after CO conversion, for 1995 and for the most recently updated figures of 1998 [21]. Recalculation of the figures with modified process conditions (e.g. lower steam content in the clean gas, optimized raw gas heat recovery and greater efficiency of the gas turbine components) shows that the efficiency penalty with the capture of gaseous CO<sub>2</sub> amounts to approx. 5.6 percentage points (Table 3.15). In this process, oxygen with a purity of 95% vol fraction is used as an oxidant in the gasification stage.

Table 3.15: Operating data for an IGCC power plant with CO<sub>2</sub> capture from coal gas after CO shift according to Pruscek et al. [20], and re-calculation of the IGCC power plant with CO<sub>2</sub> capture for this study based on most recent figures ("IGCC 1998").

		IGCC, (updated 1995 [20])		IGCC, updated 1998 (ambient temp. 8°C)	
		Baseline	with CO <sub>2</sub> capture (CO <sub>2</sub> gaseous)	Baseline [21]	with CO <sub>2</sub> capture (CO <sub>2</sub> gaseous)
CO <sub>2</sub> emissions, absolute	in kg/s	72.9	8.4	77.9	8.7
	in kg/kWh	0.69	0.09	0.62	0.086
Coal energy used	in MJ/s	811.2	876.1	874.8	891.7
Natural gas (for drying coal)				0.9	0.9
Gross output of gas turbine	in MW	238.8	234.1	302.3	277.1
	steam turbine	in MW	177.7	170.2	177.3
Internal consumption	in MW	37.8	49.1	28.8	42.8
of which gas separation	in %	3	24	<5	25
Net output	in MW	378.6	355.2	450.8	408.6
Net efficiency	in %	46.7	40.5	51.5	45.8
O <sub>2</sub> for gasification (volume fraction of O <sub>2</sub> in %)		85		95	
Conversion to ambient temp. of 20°C				51.1	45.4

Greater exergetic efficiency of the CO<sub>2</sub> scrubbing process reduces separation work and improves IGCC efficiency. Figure 3.39 shows the different levels of exergetic efficiency and the corresponding efficiency penalty for different gas separation processes.

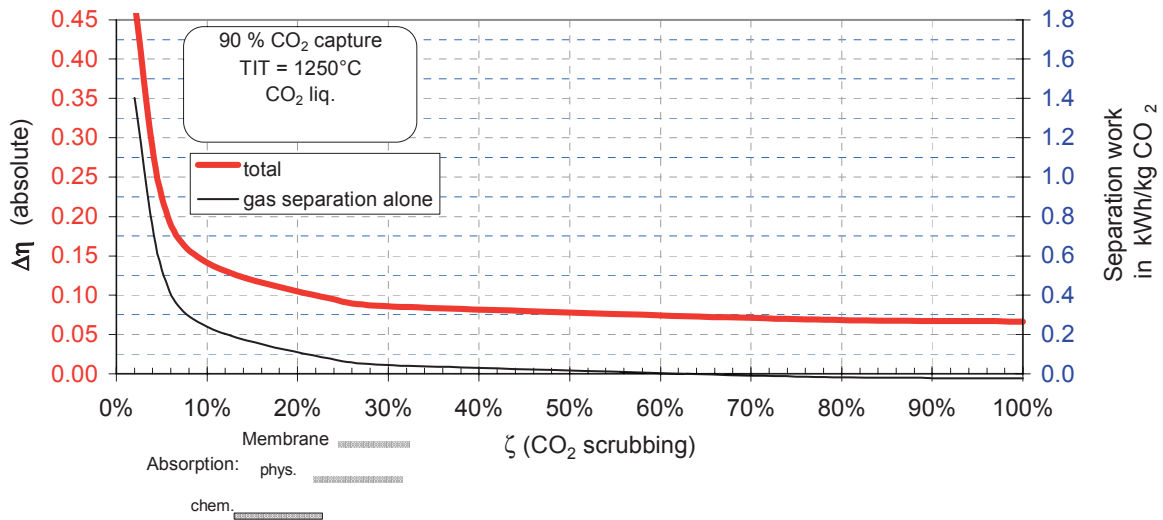


Figure 3.39: Influence of the exergetic efficiency of CO<sub>2</sub> scrubbing on the efficiency penalty and specific separation work at CO<sub>2</sub> capture ratio of 90% (TIT 1250°C)

For the following calculations with CO<sub>2</sub> separation by means of physical scrubbing, an exergetic efficiency of 30.5% is assumed when calculating the internal electrical consumption of the gas scrubbing process.

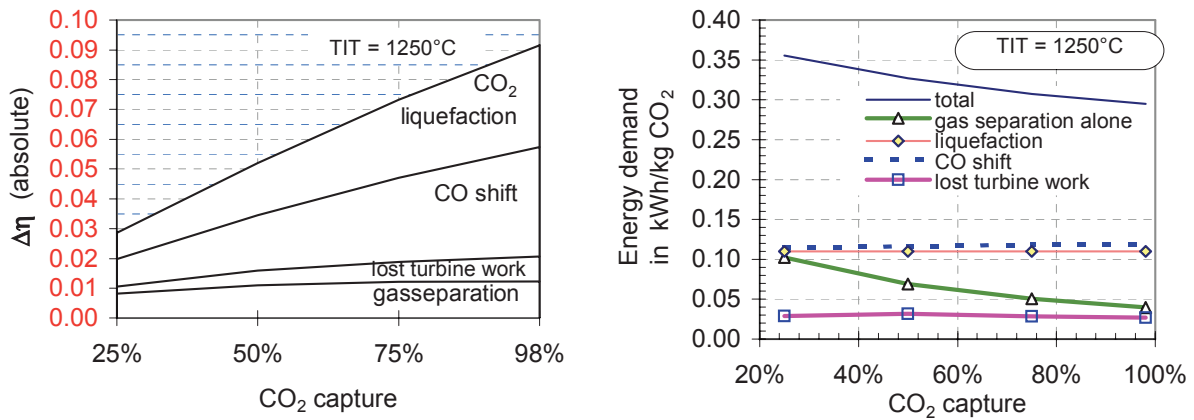


Figure 3.40: How the CO<sub>2</sub> capture ratio influences the contribution made by individual steps in the CO<sub>2</sub> capture process towards the efficiency penalty and specific energy requirements (exergetic efficiency of the scrubbing process: 30.5%).

At a high CO<sub>2</sub> capture ratio, a high level of CO conversion must be achieved; this increases the concentration of CO<sub>2</sub>, and the specific energy required for gas separation drops (Figure 3.40, right). Specific energy expenditure is virtually independent of CO<sub>2</sub> capture ratio  $r_{CO_2}$  for all other process steps. This makes it more advantageous to strive for a high CO<sub>2</sub> capture ratio in a split stream, than to remove only a small portion of CO<sub>2</sub> from the total stream. Figure 3.41 shows the achievable reduction in CO<sub>2</sub> emissions and the lower efficiencies associated with this.

The largest component of energy expenditure in CO<sub>2</sub> capture is caused by CO<sub>2</sub> liquefaction, followed by CO conversion, gas separation and lost turbine work resulting from the CO<sub>2</sub> which is not expanded in the gas turbine (Figure 3.40, left and Figure 3.42).

At higher CO<sub>2</sub> capture ratios, exergy losses increase, primarily due to the higher exergy of the separated CO<sub>2</sub>, and the greater energy requirement in the CO<sub>2</sub> scrubbing process (Figure 3.42).

Increasing the gas turbine inlet temperature has the effect, above all, of reducing exergy losses in the gas turbine combustion chamber, while simultaneously causing gas turbine power output and overall efficiency to increase (Figure 3.43, Figure 3.44). Losses due to CO<sub>2</sub> capture, related to the exergy of the feed coal, remain virtually unchanged (Figure 3.45).

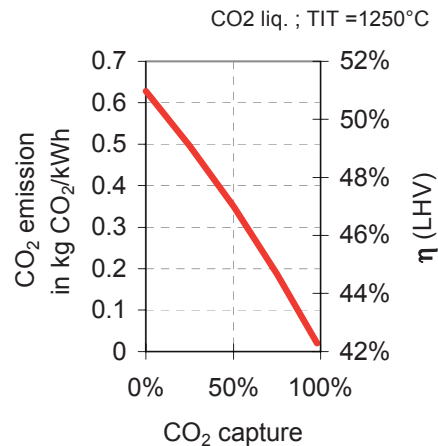


Figure 3.41: How the CO<sub>2</sub> capture ratio influences the efficiency penalty and specific CO<sub>2</sub> emissions (exergetic efficiency of the scrubbing process: 30.5%).

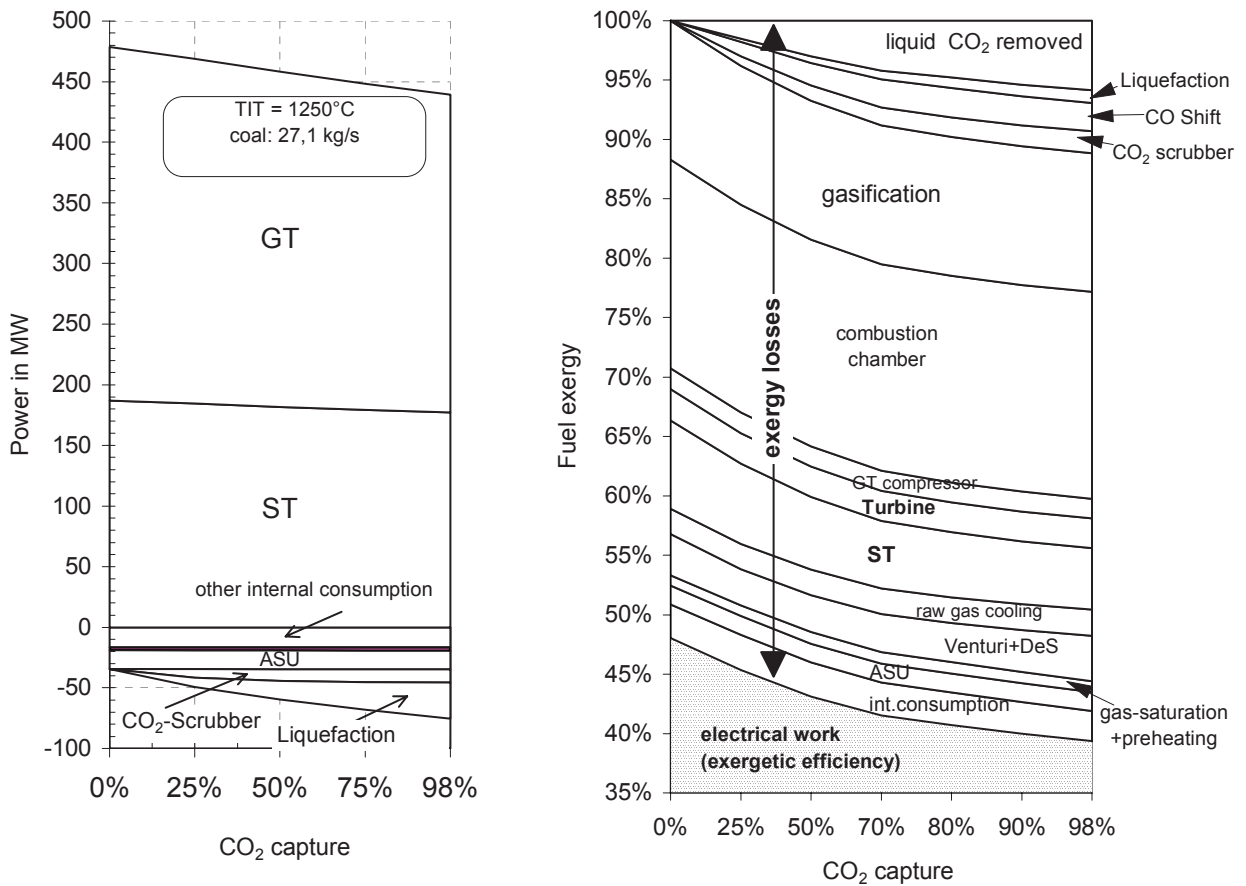


Figure 3.42: Change in output and changes in exergy conversion as a result of increasing the CO<sub>2</sub> capture ratio (exergetic efficiency of scrubbing: 30.5%, TIT 1250°C)

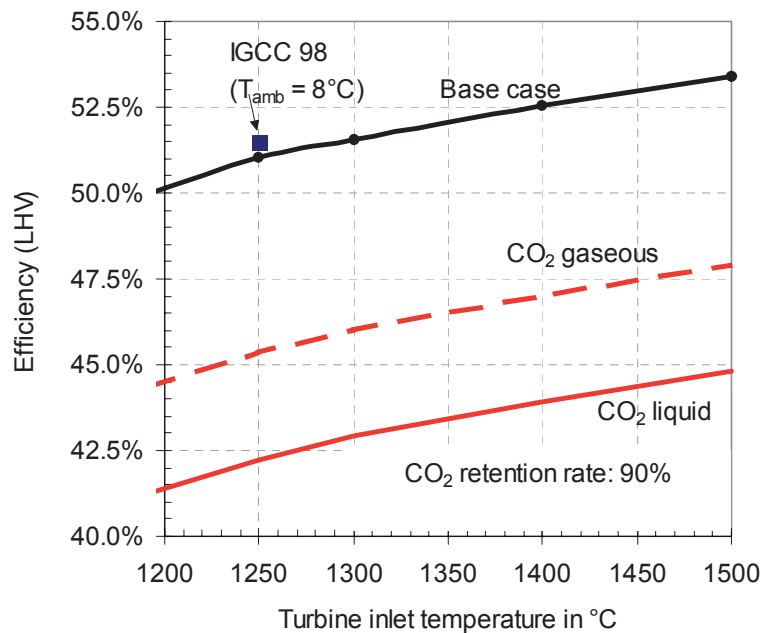


Figure 3.43: Efficiency of an IGCC power plant with CO<sub>2</sub> capture in dependence on gas turbine inlet temperature

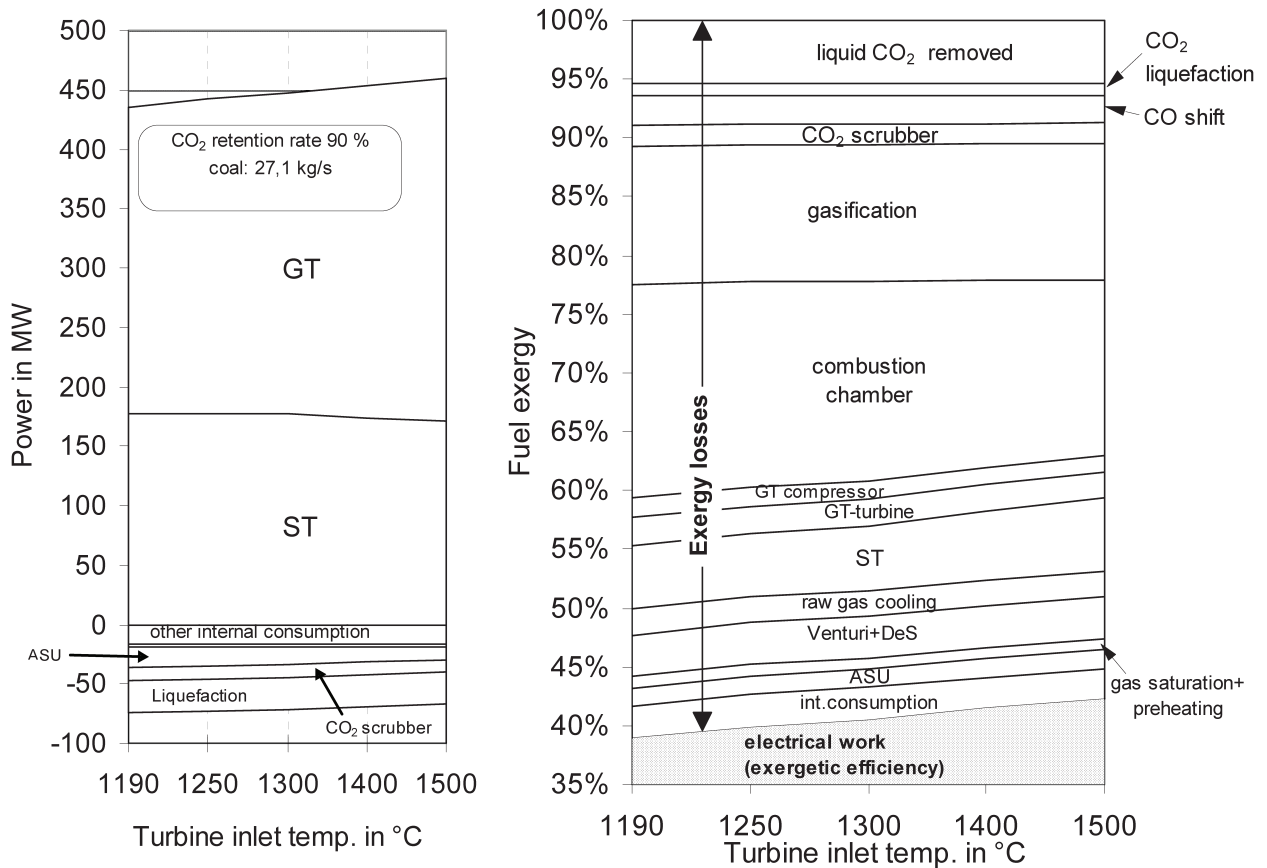


Figure 3.44: Change in output and changes in exergy conversion as a result of changes to the gas turbine inlet temperature (at a CO<sub>2</sub> capture ratio of 90%)

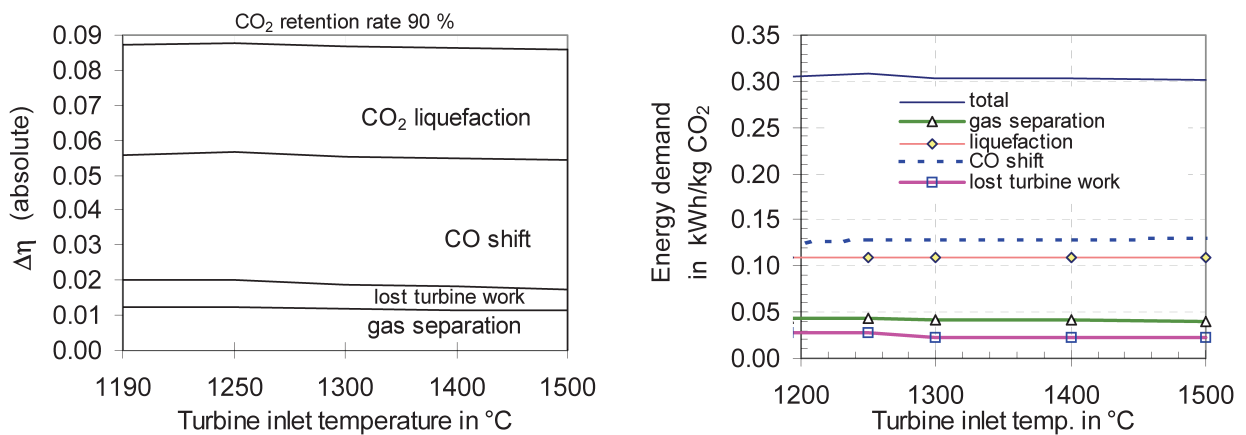


Figure 3.45: How the individual process steps contribute towards efficiency penalties and specific energy consumption, in dependence on gas turbine inlet temperature.

The gas turbine pressure ratio in these calculations has been optimized to achieve maximum specific work of the gas turbine, in correspondence with the modified conditions. At an increased CO<sub>2</sub> capture ratio, the CO<sub>2</sub> content in the flue gas decreases and the optimum pressure ratio becomes smaller (Figure 3.46). Increasing the turbine inlet temperature causes the optimum pressure ratio to become larger.

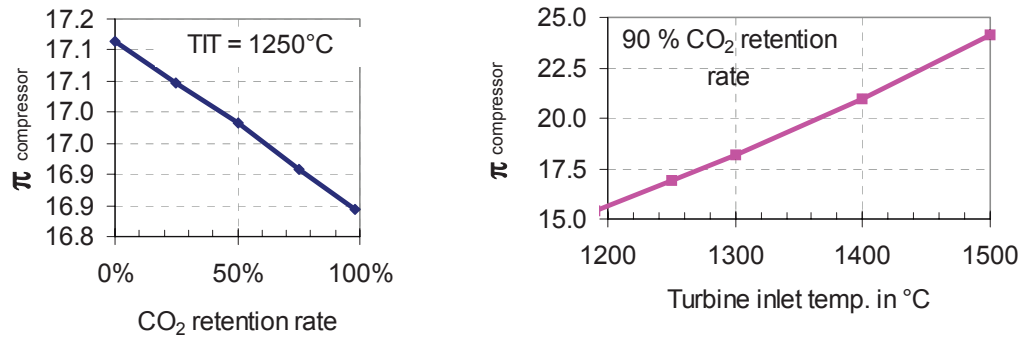


Figure 3.46: Changing the gas turbine pressure ratio for maximum IGCC efficiency, with CO<sub>2</sub> capture ratio and gas turbine inlet temperature

Table 3.16: Operating parameters and results for IGCC power plants with O<sub>2</sub>-blown gasification and CO<sub>2</sub> separation by means of physical scrubbing after CO shift, with variation of CO<sub>2</sub> capture ratio  $r_{\text{CO}_2}$

<b>Assumptions</b>					
Gasification temperature in °C	1302				
Gasification pressure in bar	34	35	36	39	42
<b>Gas turbine inlet temperature (ISO 2314)</b>	<b>1190</b>	<b>1250</b>	<b>1300</b>	<b>1400</b>	<b>1500</b>
Compressor pressure ratio of the gas turbine	15.4	16.9	18.2	21.0	24.1
CO <sub>2</sub> capture ratio in %	90				
CO <sub>2</sub> separation factor in scrubbing process (synthesis gas after CO shift) in %	99				
exergetic efficiency $\zeta$ of CO <sub>2</sub> scrubbing in %	30.5				
CO conversion in %	91.27				
<b>Results:</b>					
<b>Output and Internal Consumption</b>	in MW (positive = delivery of electric power, negative = consumption)				
Coal energy supplied (LHV)	874.9	874.9	874.9	874.9	874.9
Gas turbine	258.00	264.65	269.83	279.33	287.77
<i>Steam from GT waste heat</i>	<i>157.90</i>	<i>158.49</i>	<i>157.89</i>	<i>154.62</i>	<i>151.58</i>
<i>Steam from raw gas cooling</i>	<i>27.4</i>	<i>27.6</i>	<i>27.8</i>	<i>28.1</i>	<i>28.5</i>
<i>Low temperature raw gas cooling</i>	<i>-6.3</i>	<i>-6.4</i>	<i>-6.4</i>	<i>-6.6</i>	<i>-6.8</i>
<i>Steam for drying coal</i>	<i>-0.5</i>	<i>-0.5</i>	<i>-0.5</i>	<i>-0.5</i>	<i>-0.5</i>
<i>Feedwater for gasification</i>	<i>-1.6</i>	<i>-1.6</i>	<i>-1.6</i>	<i>-1.6</i>	<i>-1.6</i>
$\Sigma$ Steam turbine output	$\Sigma$ 177.1	$\Sigma$ 177.7	$\Sigma$ 177.2	$\Sigma$ 174.1	$\Sigma$ 171.2
O <sub>2</sub> +N <sub>2</sub> compression for gasification	-16.7	-15.3	-14.2	-12.4	-10.6
CO <sub>2</sub> scrubbing	-10.9	-10.8	-10.6	-10.2	-9.8
Desulfurization	-2.8	-2.8	-2.7	-2.6	-2.6
Other internal consumption	-16.7	-16.7	-16.7	-16.7	-16.7
CO <sub>2</sub> compression/liquefaction at 110 bar	-27.41	-27.40	-27.40	-27.38	-27.37
Net output in MW	360.6	369.5	375.4	384.1	392.0
<b>Power plant net efficiencies in %</b>					
LHV (CO <sub>2</sub> liquid)	41.2%	42.2%	42.9%	43.9%	44.8%
LHV (CO <sub>2</sub> gaseous)	44.3%	45.4%	46.0%	47.0%	47.9%
HHV (CO <sub>2</sub> liquid)	39.6%	40.6%	41.2%	42.2%	43.0%
Exergy (CO <sub>2</sub> liquid)	38.9%	39.9%	40.6%	41.5%	42.3%
<b>CO<sub>2</sub> emissions in kg CO<sub>2</sub>/kWh (with retention of liquid CO<sub>2</sub>)</b>	<b>0.081</b>	<b>0.079</b>	<b>0.078</b>	<b>0.076</b>	<b>0.075</b>

### 3.5.2.2 H<sub>2</sub>/CO<sub>2</sub> Separation With Membrane Separation Processes

For the simulation of an IGCC power plant with CO conversion and H<sub>2</sub> separation using a membrane, it is assumed that the permeate is burnt in a gas turbine (with air) and the retentate is burnt in a further gas turbine in an O<sub>2</sub>/CO<sub>2</sub> atmosphere (Figure 3.47). The waste heat from both of these gas turbines is used in the heat recovery steam cycle. Subsequent to the membrane stage, both gas streams - the permeate and the retentate - are compressed to the pressure required by their respective gas turbine (see Table 3.18 for details of pressure ratios). To allow comparisons to be made, power output values were calculated for cases where the residual fuel of the retentate is only used for steam generation, or is not used at all.

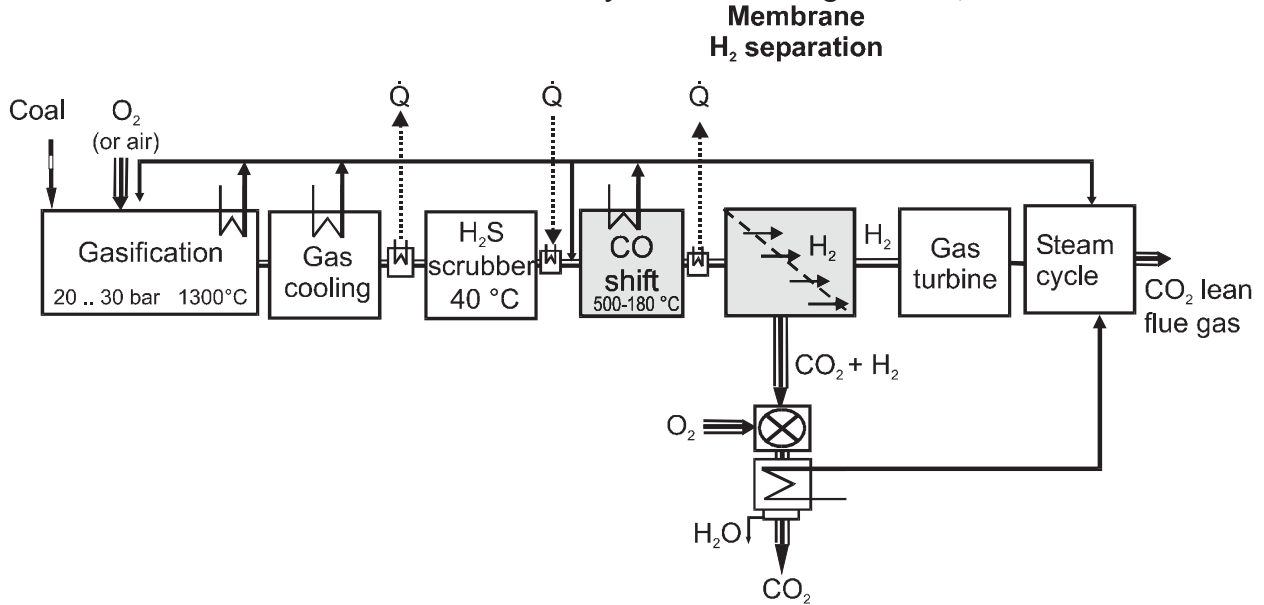


Figure 3.47: Flow diagram of an IGCC power plant with CO conversion, H<sub>2</sub> separation using a membrane and subsequent combustion of the retentate

Mass transfer in the membrane was calculated using a membrane model developed by Shindo et al. [162]. Preliminary investigations (Figure 3.24, Figure 3.25) determined that the pressure ratio of the membrane should be set at 5 to 1 (feed to permeate pressure) (for boundary conditions, see Table 3.18 to Table 3.17).

In determining permeability  $D$ , it is assumed that Knudsen diffusion is present. For the gas separation process, relative permeability  $\bar{D}_i$  (related to permeability  $D_{H_2}$  of H<sub>2</sub>) is calculated from selectivity  $\alpha_{H_2,CO_2}$  and molecular weight  $M_i$ :

$$\bar{D}_i = \frac{D_i}{D_{H_2}} = \alpha_{H_2,CO_2} \frac{\sqrt{\frac{M_{CO_2}}{M_{H_2}}}}{\sqrt{\frac{M_i}{M_{H_2}}}}, \text{ where } \bar{D}_{H_2} = 1 \text{ and } \bar{D}_{CO_2} = 1 \quad (3.27)$$

Since the required membrane surface is not realized in this case, absolute permeability is not required.

At higher CO<sub>2</sub> capture ratios, more fuel remains in the retentate (Figure 3.48), meaning that more O<sub>2</sub> must be produced for subsequent combustion. At the same time, less permeate must be compressed to the pressure prior to the gas turbine combustion chamber. Overall, the efficiency penalty becomes larger as the CO<sub>2</sub> capture ratio increases, but the specific separation work related to the separated CO<sub>2</sub> mass flow becomes smaller (Figure 3.49, Figure 3.50). If the residual fuel in the retentate is not used, CO<sub>2</sub>



separation and liquefaction cause efficiency to be reduced by up to 17 percentage points. By making use of the residual fuel in the retentate, power plant efficiency can be improved by approx. 7 percentage points (and by a further 0.5 percentage points if it is used in a gas/steam turbine combined cycle with combustion in an atmosphere of O<sub>2</sub>/CO<sub>2</sub>).

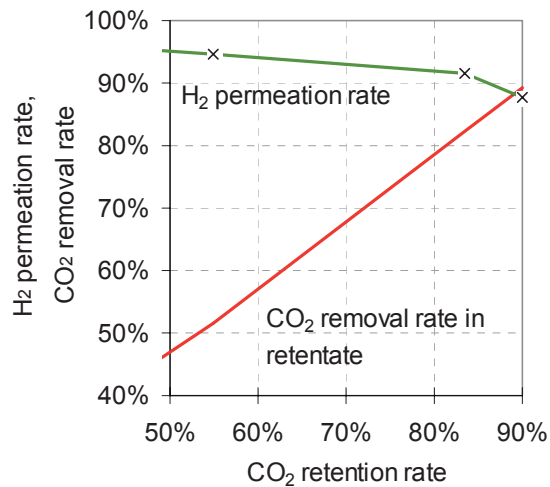


Figure 3.48: H<sub>2</sub> permeation rate and CO<sub>2</sub> separation factor in the retentate in the membrane, in dependence on the CO<sub>2</sub> capture ratio

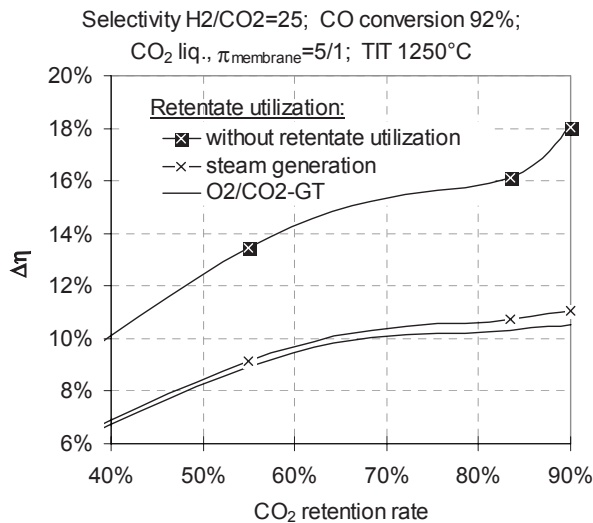


Figure 3.49: Changes in the efficiency penalty of an IGCC due to CO conversion, CO<sub>2</sub> separation using a membrane and CO<sub>2</sub> liquefaction, in dependence on the CO<sub>2</sub> capture ratio

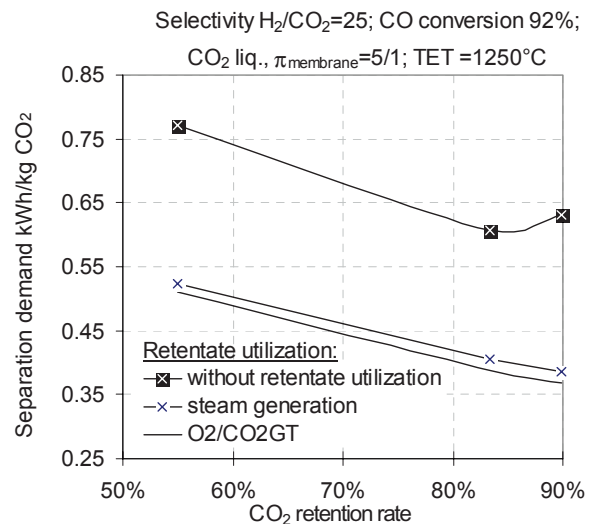


Figure 3.50: Specific energy expended on CO<sub>2</sub> capture incl. CO conversion and CO<sub>2</sub> liquefaction (cf. Figure 3.49: efficiency penalty).

Higher membrane selectivity reduces both the membrane pressure ratio required to achieve the same CO<sub>2</sub> capture ratio, and the residual fuel content in the retentate (Table 3.17). This makes the exergy of the retentate, and the work required to subsequently compress the permeate, smaller. In the following paragraphs, various efficiencies are calculated, ranging from efficiencies provided by currently available membranes, which achieve H<sub>2</sub> to CO<sub>2</sub> selectivities of 25, up to future efficiencies with a conceivable design of metal membranes capable of achieving selectivities of 1000.

With the best possible utilization of the residual fuel in the retentate, an increase in selectivity from 25 to 1000 would boost efficiency by approx. 2.1 percentage points to achieve a total of 42.2%, including CO<sub>2</sub> liquefaction (Figure 3.51, Figure 3.52). At low rates of selectivity, the retentate is used, subsequent to combustion in an O<sub>2</sub>/CO<sub>2</sub> atmosphere, in a (CO<sub>2</sub>) gas/steam turbine combined cycle, instead of being used just for producing steam. At a selectivity of 1000, the combustion heat is no longer sufficient for high gas turbine inlet temperatures, meaning that the residual fuel in the retentate will subsequently be burnt, and the heat will only be able to be used for steam generation.

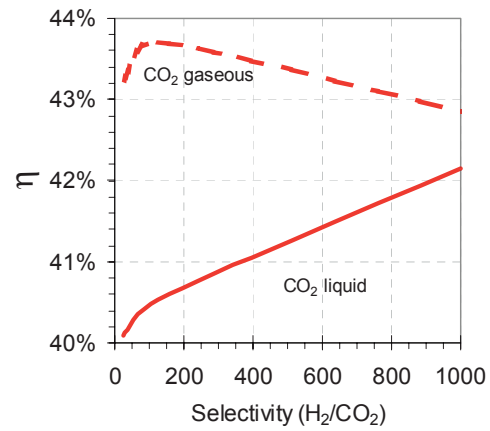


Figure 3.51: How the efficiency of the IGCC changes with selectivity of the H<sub>2</sub>/CO<sub>2</sub> membrane.

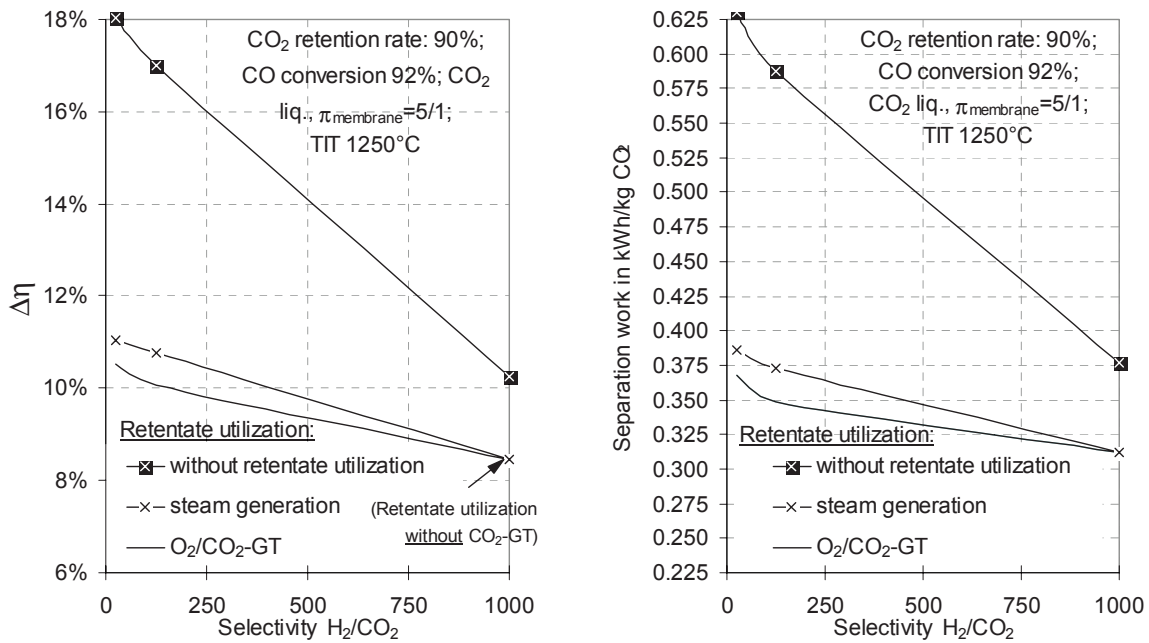


Figure 3.52: Efficiency penalty for an IGCC and separation work for CO<sub>2</sub> separation using a membrane after CO conversion and CO<sub>2</sub> liquefaction, with various ways of utilizing the residual fuel in the retentate, in dependence on membrane selectivity.

In order to demonstrate the proportional contribution of the individual process steps towards the efficiency penalty, a comparison has been drawn between the results of calculations for the basic IGCC, for an IGCC power plant with CO conversion, but without H<sub>2</sub>/CO<sub>2</sub> separation, and for an IGCC power plant with CO conversion and membrane (Figure 3.53). The contributions of the subsequent compression of the permeate and CO<sub>2</sub> liquefaction are determined by internal consumption. Since the retentate from a membrane with a selectivity of 1000 occurs at a high pressure, in the case of subsequent combustion without expansion, the CO<sub>2</sub> compression work in this case is reduced.

In comparison to CO<sub>2</sub> separation after CO conversion using a scrubbing process, the efficiencies achievable with currently available membranes are lower (Figure 3.54). This is because gas separation proc-

esses using membranes require production of O<sub>2</sub> to allow utilization of the residual fuel of the retentate, in addition to the separation work (primarily permeate compression). The process is also impaired by the fact that the gasification pressure can only be optimized for one of the two gas turbines (using air or CO<sub>2</sub> as a working fluid, respectively), which results either in the occurrence of additional compressor/expansion losses, or in one of the gas turbines working at an unfavorable pressure ratio. Thus, for example, additional compression of the retentate corresponding to the higher pressure ratio of the compressor of the O<sub>2</sub>/CO<sub>2</sub> gas turbine ( $\pi = 65$ ) reduces the performance of the IGCC power plant by approx. 1.5 percentage points.

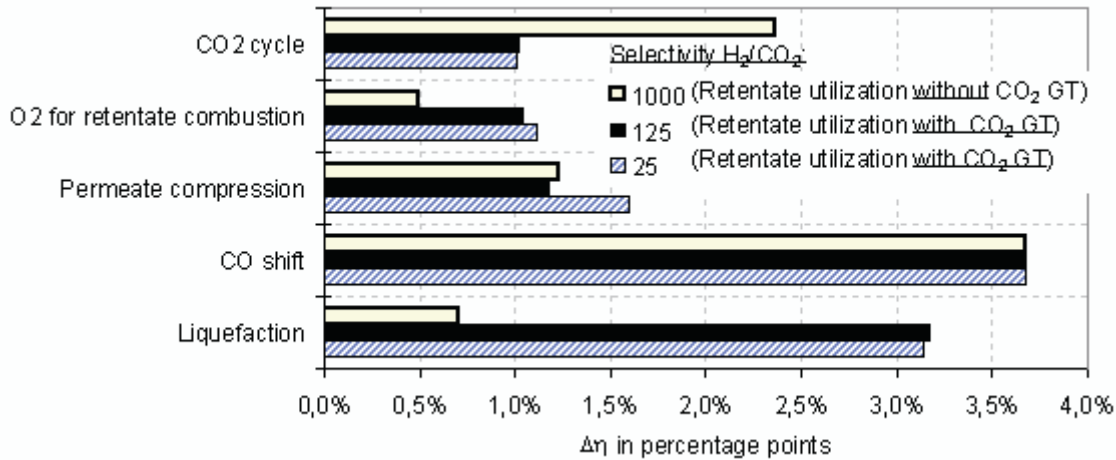


Figure 3.53: Contributions of the individual process steps towards the efficiency penalty at different membrane selectivities<sup>59</sup>

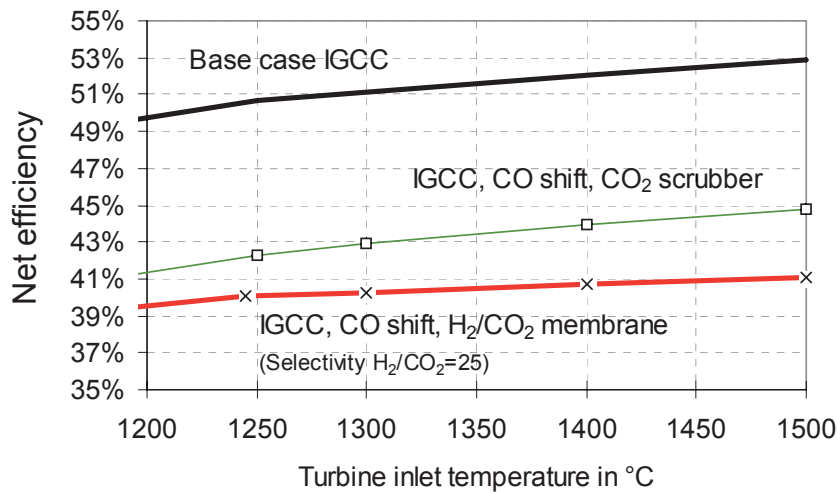


Figure 3.54: Change in the efficiency of the baseline IGCC power plant and the IGCC power plant with CO<sub>2</sub> capture using a membrane<sup>59</sup> or scrubbing after CO shift conversion, as gas turbine inlet temperature is increased.

<sup>59</sup> Utilization of the residual fuel in the retentate through additional combustion in O<sub>2</sub>/CO<sub>2</sub>, expansion in a gas turbine and waste heat recovery for the steam cycle.

Table 3.17: Data on the membrane and the IGCC power plant featuring CO conversion and H<sub>2</sub> separation using a membrane (with variation of the CO<sub>2</sub> capture ratio  $r_{CO_2}$  and membrane selectivity)

<b>Assumptions</b>					
Gas turbine inlet temperature (ISO 2314)	1250°C				
Permeation ratio (ratio of molar flow rates from permeate to feed) in %	<b>74</b>	<b>60</b>	<b>55</b>	57.8	58.6
CO conversion in %	92			92	92
Pressure ratio (permeate/feed)	0.2			0.29	0.44
Selectivity H <sub>2</sub> /CO <sub>2</sub>	25	25	<b>25</b>	<b>125</b>	<b>1000</b>
For relative permeabilities, see Table 3.19					
<b>Results:</b>					
CO <sub>2</sub> capture ratio (incl. CO, CH <sub>4</sub> , COS) in %	55.0	83.4	89.9	90.8	93.49
CO <sub>2</sub> separation factor (retentate excl. CO, CH <sub>4</sub> , COS) in %	51.5	82.3	89.3	90.3	93.6
H <sub>2</sub> permeation in %	94.7	91.6	87.8	89.3	99.4
Mass fractions in retentate in %					
CO <sub>2</sub>	86.50	89.02	89.14	89.28	90.1
H <sub>2</sub>	0.65	0.66	0.89	0.77	0.04
CO	8.98	5.90	5.46	5.42	5.28
CH <sub>4</sub>	0.14	0.19	0.20	0.21	0.22
Retentate mass flow in kg/s	31.7	38.4	46.9	71.4	73.4
Mass fractions in permeate in %					
CO <sub>2</sub>	82.9	69.3	60.0	57.6	45.4
H <sub>2</sub>	11.9	26.2	36.0	38.7	51.5
CO	0.3	0.2	0.2	0.1	0.1
CH <sub>4</sub>	0.3	0.3	0.2	0.2	0.2
Permeate mass flow in kg/s	41.3	18.1	12.6	11.9	10.0
<b>Output and internal consumption</b> in MW (positive = delivery of electric power, negative = consumption)					
Coal energy supplied (LHV)	874.9	874.9	874.9	874.9	874.9
Gas turbine 1 (working fluid: air)	252.07	233.38	221.57	224.92	248.0
GT 2 (working fluid: CO <sub>2</sub> ), incl. retentate compression	32.62	43.94	54.65	51.05	<i>w/o GT 2</i>
<i>Steam from GT waste heat (GT 1)</i>	<i>141.5</i>	<i>134.2</i>	<i>127.8</i>	<i>130.0</i>	<i>145.3</i>
<i>Steam from GT AHK (combustion. in O<sub>2</sub>/CO<sub>2</sub> atmos., GT 2)</i>	<i>12.9</i>	<i>14.8</i>	<i>20.6</i>	<i>18.4</i>	<i>19.8*</i>
<i>Steam from raw gas cooling</i>	<i>23.8</i>	<i>26.9</i>	<i>27.9</i>	<i>27.8</i>	<i>27.0</i>
<i>Low temperature raw gas cooling</i>	<i>-12.7</i>	<i>-7.7</i>	<i>-6.4</i>	<i>-6.2</i>	<i>-5.8</i>
<i>Steam for drying coal</i>	<i>-0.5</i>	<i>-0.5</i>	<i>-0.5</i>	<i>-0.5</i>	<i>-0.5</i>
<i>Feedwater for gasification</i>	<i>-1.6</i>	<i>-1.6</i>	<i>-1.6</i>	<i>-1.6</i>	<i>-1.6</i>
Σ Steam turbine	Σ 163.4	Σ 166.2	Σ 167.9	Σ 168.0	Σ 184.3
O <sub>2</sub> +N <sub>2</sub> compression for gasification	-22.76	-22.76	-22.76	-22.76	-22.76
ASU for GT 2 (addition of O <sub>2</sub> at 1 bar prior to compressor)	-5.7	-7.9	-9.7	-9.1	-4.34
Permeate compression	-18.52	-15.17	-13.95	-10.25	-10.74
Desulfurization	-2.78	-2.78	-2.78	-2.78	-2.78
Other internal consumption	-16.66	-16.66	-16.66	-16.7	-16.7
CO <sub>2</sub> compression/liquefaction at 110 bar	-16.80	-25.49	-27.47	-27.75	-6.2*
Net output	364.8	352.8	350.8	354.7	368.8
<b>Power plant net efficiencies</b> in %					
LHV (CO <sub>2</sub> liquid)	41.7	40.3	40.1	40.5	42.2
LHV (CO <sub>2</sub> gaseous)	43.6	43.2	43.2	43.7	42.9
HHV (CO <sub>2</sub> liquid)	40.1	38.7	38.5	39.0	40.5
Exergy (CO <sub>2</sub> liquid)	39.4	38.1	37.9	38.3	39.8
CO <sub>2</sub> emissions in kg CO <sub>2</sub> /kWh (retention of liquid CO <sub>2</sub> )	0.348	0.133	0.079	0.071	0.045

\* With a selectivity of 1000, the heating value of the retentate is too low for utilization in a gas turbine.

Table 3.18: Assumed pressure ratios of the gas turbine compressor, with a working fluid of air or CO<sub>2</sub>

Gas turbine inlet temperature	GT compressor pressure ratio	
	Working fluid: air	Working fluid: CO <sub>2</sub> (see Table 3.24)
1190°C	16.1	50
1250°C	17.5	65
1300°C	19.0	100
1400°C	22.1	150
1500°C	25.6	200

Table 3.19: Relative permeability of the individual gas components in the case of Knudsen diffusion, Eq. (2.4)

Selectivity H <sub>2</sub> /CO <sub>2</sub>	25	125	1000
O <sub>2</sub>	0.0469	0.0094	0.0012
H <sub>2</sub> O	0.0625	0.0125	0.0016
CO <sub>2</sub>	0.0400	0.0080	0.0010
N <sub>2</sub>	0.0501	0.0100	0.0013
Ar	0.0420	0.0084	0.0010
SO <sub>2</sub>	0.0332	0.0066	0.0008
H <sub>2</sub>	1.0000	1.0000	1.0000
CO	0.0017	0.0001	0.0000
CH <sub>4</sub>	0.0663	0.0133	0.0017
H <sub>2</sub> S	0.0455	0.0091	0.0011
COS	0.0342	0.0068	0.0009

### CO<sub>2</sub> Absorption by Seawater

If, instead of physical scrubbing, which has energy requirements of 0.05 kWh per kg of separated CO<sub>2</sub> (Figure 3.45), seawater is used as an absorbent, which has energy requirements of 0.061 kWh per kg of separated CO<sub>2</sub> (Figure 3.15), the efficiency penalty due to gas separation only increases from around 1.4 percentage points (Figure 3.45) to around 1.7 percentage points. This would produce an overall efficiency penalty of approx. 5.2 percentage points. Since no CO<sub>2</sub> liquefaction is then required, the efficiency penalty caused by absorption with seawater is lower than that caused by physical absorption and CO<sub>2</sub> liquefaction. However, the large mass flow rates of water involved mean that CO<sub>2</sub> absorption with seawater still does not represent an attractive alternative (see page 29 ff.).

### Combined CO Shift Reaction / Adsorption

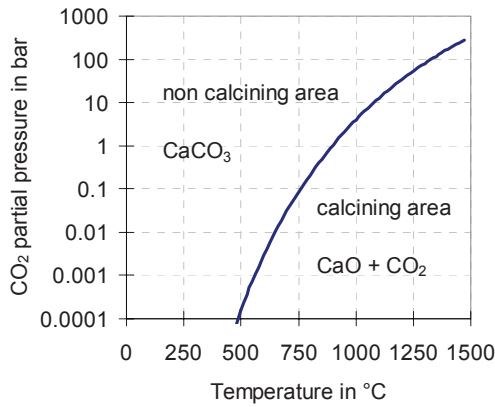
Calcium oxide and magnesium oxide can simultaneously act as a catalyst for the CO shift reaction and an absorbent for CO<sub>2</sub> separation. Calcium oxide reacts with CO<sub>2</sub> exothermically to form calcium carbonate:



Experiments described in the literature show a CO<sub>2</sub> capture ratio of over 99% for coal gas to CaO at 660°C [175]. To regenerate the absorbent, heat must be supplied for the reverse reaction (calcination) at a high temperature, corresponding to the chemical equilibrium of the calcination reaction, or a virtual vacuum must be achieved (Figure 3.55).

The theoretical, minimum energy requirement for CO<sub>2</sub> adsorption and regeneration with CaO is calculated from the difference in exergy  $\Delta e$  of the heat supplied and the heat released:

$$\Delta e = (T_u / T_{adsorption} - T_u / T_{regeneration}) \cdot \Delta_r H \quad (3.29)$$



Calcination (CaO regeneration) [176]:

$$K_{CaO} < p_{CO_2} \quad (\text{bar})$$

$$\log_{10} K_{CaO} = -8684,6 / T(K) + 7,423 \quad (3.30)$$

Figure 3.55: Conditions of equilibrium for calcination

Using the temperatures given in Table 6.18 (Appendix), a minimum exergy loss with coal gas of around 7.4 percentage points is calculated, related to the heating value of the coal used, or, with an exergetic efficiency of the overall process of 40%, an efficiency penalty of around 3 percentage points. In fact, with higher temperatures and lower pressure, further losses must also be expected, especially for the regeneration process (e.g. due to fuel consumption, vacuum pump work, oxygen for combustion). Based on estimated values of energy expenditure and possible recovery of energy for CO<sub>2</sub> separation from the cleaned coal gas of an IGCC power plant according to Figure 3.56, an efficiency penalty of 12.5 percentage points is calculated, with a CO<sub>2</sub> capture ratio of 99.9% (Appendix, Table 6.18).

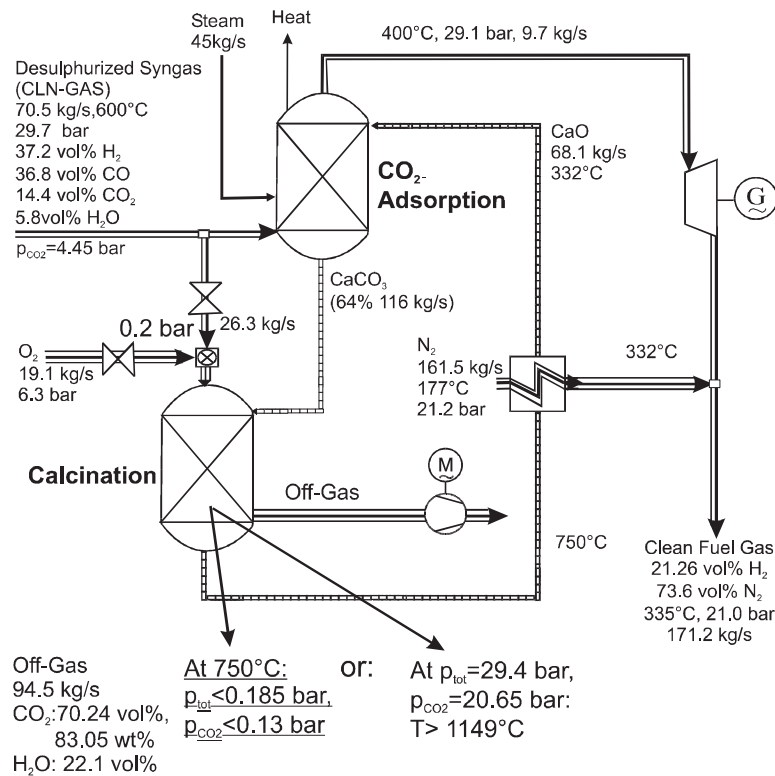


Figure 3.56: Flow diagram of CO shift reaction and CO<sub>2</sub> adsorption using CaO, with subsequent adsorbent regeneration.

### Air-Blown Gasification

Oxygen-blown gasification often fails to fully gasify all of the coal, with the result that the residual char must be burnt separately, if a high rate of fuel utilization is to be achieved. The CO<sub>2</sub> produced in burning this residual char increases the specific CO<sub>2</sub> emissions of the power plant, unless the CO<sub>2</sub> is removed using additional measures. Since the raw gas produced is diluted with atmospheric nitrogen, it is still only possible to achieve a CO<sub>2</sub> volume fraction of approx. 21%, after CO conversion, as compared to around 33% after oxygen-blown gasification. This results in an increase of around 50% in separation work, while the exergy losses in the CO conversion process remain virtually unchanged (Figure 3.36). Additionally, larger volumes of equipment are required.

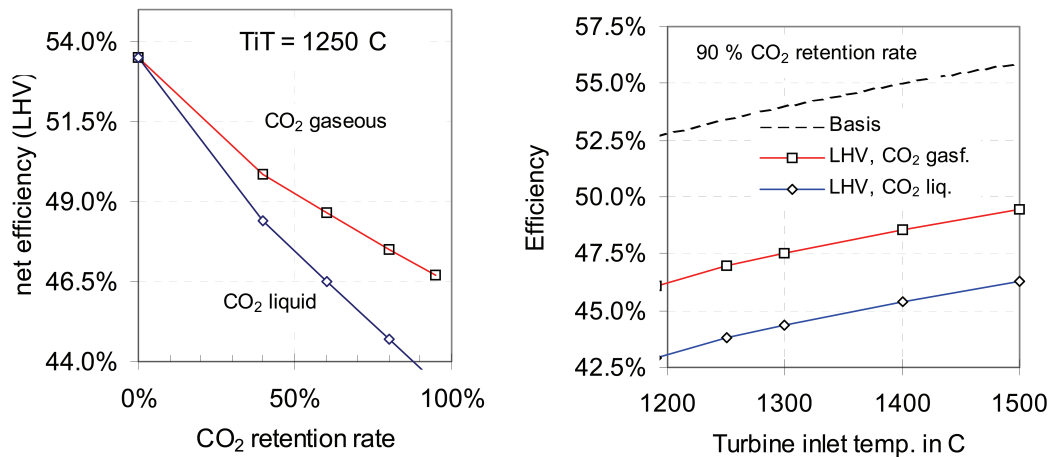


Figure 3.57: Dependence of IGCC efficiency on CO<sub>2</sub> capture ratio and gas turbine inlet temperature

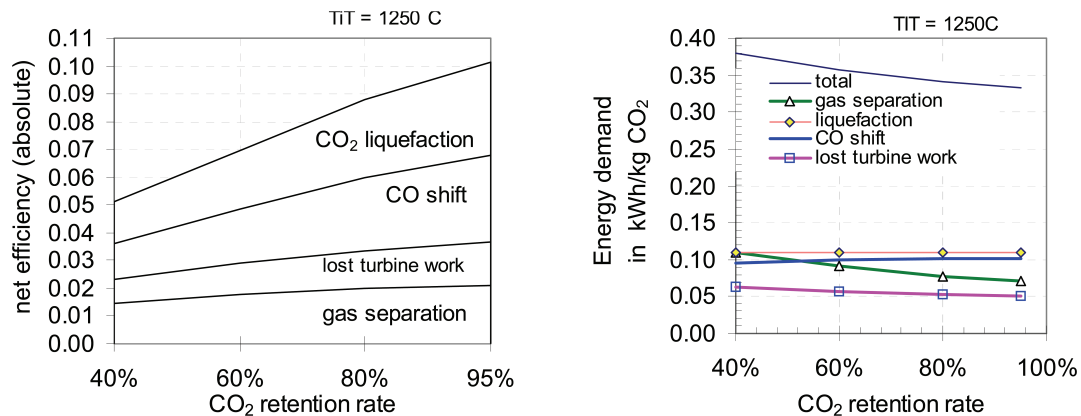


Figure 3.58: Efficiency penalty and specific energy expenditure due to the individual steps in the CO<sub>2</sub> capture process (TIT 1250C)

Carbon dioxide separation from the coal gas of an air-blown gasifier after CO conversion, with a CO<sub>2</sub> capture ratio of 90% and CO<sub>2</sub> liquefaction, incurs an efficiency penalty of around 9 percentage points (Figure 3.57, Figure 3.58, see Table 3.20 for process data). As the CO<sub>2</sub> capture ratio is increased, the contributions made by the individual steps in the CO<sub>2</sub> capture process to the efficiency penalty all become larger at the same rate, amounting to 2.4 percentage points for gas separation, 1.6 percentage points for lost gas turbine work, 2.0 percentage points for CO conversion and 3.1 percentage points for CO<sub>2</sub> liquefaction, with a CO<sub>2</sub> capture ratio of 90% (Figure 3.58).

By increasing the gas turbine inlet temperature from 1250C to 1500C (not yet feasible in practice), the efficiency achievable after retention and liquefaction of 90% of the CO<sub>2</sub> rises from 44.4% to 46.9%

(Figure 3.57). As with O<sub>2</sub>-blown gasification, the larger exergy losses, which occur at higher CO<sub>2</sub> capture ratios, are primarily caused by the exergy of the separated CO<sub>2</sub> and the exergy losses in the CO<sub>2</sub> scrubbing process (Figure 3.59).

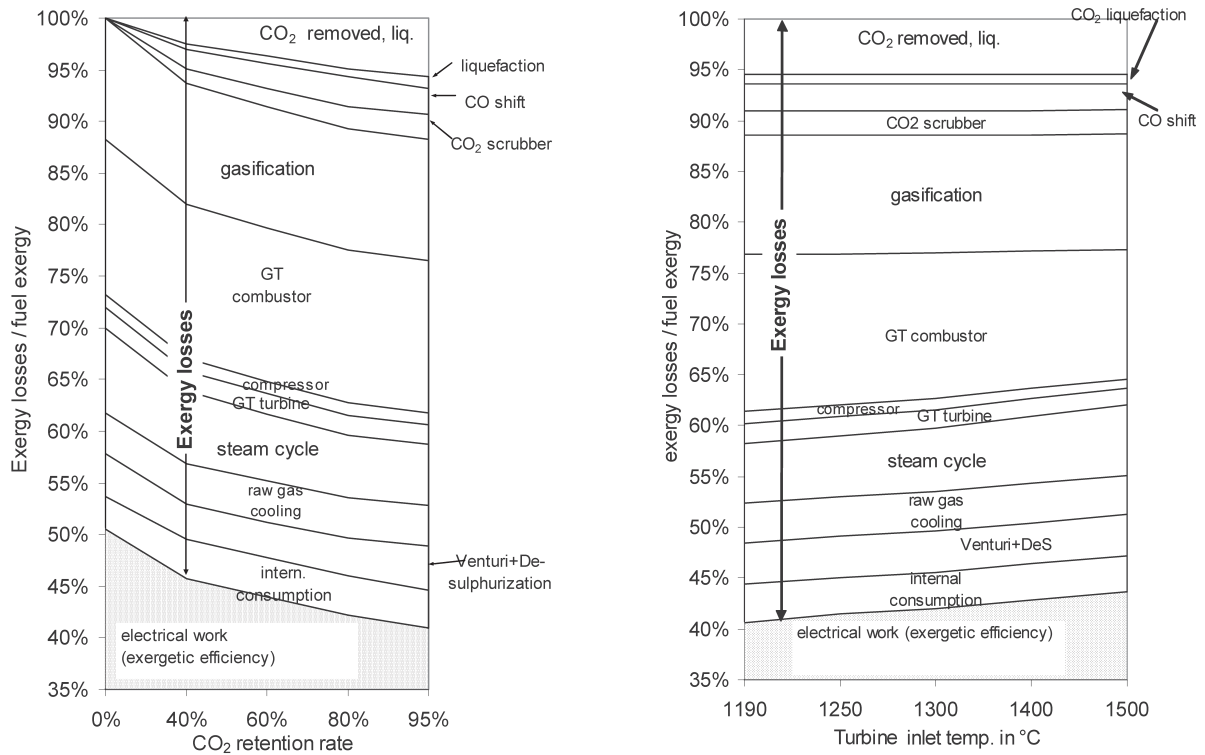


Figure 3.59: How energy conversion changes in relation to CO<sub>2</sub> capture ratio and gas turbine inlet temperature.



Table 3.20: Operating parameters and results for an IGCC power plant with air-blown gasification and CO<sub>2</sub> separation using physical scrubbing after CO shift, with variation of the CO<sub>2</sub> capture ratio

<b>Assumptions:</b>					
Gas turbine inlet temperature (ISO 2314)	1250°C				
CO <sub>2</sub> capture ratio in %	-	40	60	80	95
CO <sub>2</sub> separation factor in scrubber (synthesis gas after CO shift) in %	-	99.0			
Exergetic efficiency $\zeta$ of CO <sub>2</sub> scrubbing in %	-	30.5			
Conversion of CO in CO shift reaction in %	-	41.9	62.8	83.7	99.4
<b>Results:</b>					
<b>Output and Internal Consumption</b>	in MW (positive = delivery of electric power, negative = consumption)				
Coal energy supplied (LHV)	874.9	874.9	874.9	874.9	874.9
Gas turbine	302.15	289.37	283.53	277.69	273.31
<i>Steam from GT waste heat</i>	147.90	140.32	136.58	132.83	130.01
<i>Steam from raw gas cooling</i>	67.8	68.6	68.8	68.9	69.1
<i>Saturator heating from GT-HRSG</i>	-24.5	-23.6	-22.1	-20.6	-19.6
<i>Steam for drying coal</i>	-0.4	-0.4	-0.4	-0.4	-0.4
$\Sigma$ Steam turbine	$\Sigma$ 190.7	$\Sigma$ 184.9	$\Sigma$ 182.8	$\Sigma$ 180.8	$\Sigma$ 179.1
CO <sub>2</sub> scrubbing	0.0	-12.9	-15.6	-17.6	-18.6
Desulfurization	-3.0	-3.1	-3.2	-3.2	-3.2
Other internal consumption	-21.9	-21.9	-21.9	-21.9	-21.9
CO <sub>2</sub> compression/liquefaction at 110 bar	0.0	-12.9	-18.8	-24.7	-29.1
Net output	467.9	423.3	406.8	391.1	379.4
<b>Power plant net efficiencies</b>	in %				
LHV (CO <sub>2</sub> liquid)	53.5	48.4	46.5	44.7	43.4
LHV (CO <sub>2</sub> gaseous)	53.5	49.9	48.7	47.5	46.7
HHV (CO <sub>2</sub> liquid)	51.4	46.5	44.7	42.9	41.7
Exergy (CO <sub>2</sub> liquid)	50.5	45.7	43.9	42.2	41.0
<b>CO<sub>2</sub> emissions</b>	in kg CO <sub>2</sub> /kWh (with retention of liquid CO <sub>2</sub> )				
	0.578	0.360	0.243	0.115	0.013

### 3.5.3 Chemically Recuperated Gas Turbines (CRGT)<sup>60</sup>

Table 3.21 shows a comparison of different designs of chemically recuperated gas turbines, both with and without CO<sub>2</sub> capture. High CO<sub>2</sub> capture ratios can only be achieved by increasing the temperature of the reformer by means of additional firing (Figure 3.60). The majority of the exergy losses are caused by the cooling process, which is required prior to CO conversion and CO<sub>2</sub> scrubbing, and the condensation of water, which occurs in this process (Figure 3.61; final column of Table 3.21). In processes (d) and (e), shown in Table 3.21, the heat produced in the process of cooling the reformed gas is not used, leading to an efficiency penalty due to CO<sub>2</sub> capture of 19.5 and 17.7 percentage points, respectively. By integrating the heat, which is produced in cooling the reformed gas, into the preheating process in processes (f) (Figure 3.62) and (g) (Figure 3.63), it is possible to reduce this efficiency penalty to between 11.8 and 11.3 percentage points. With a CO<sub>2</sub> capture ratio of over 80%, efficiencies for chemically recuperated gas turbines after gaseous CO<sub>2</sub> capture range between 37.7% and 45.7%, which are better than the figures for a gas/steam turbine combined cycle with externally heated, upstream steam reforming and CO<sub>2</sub> separation.

It may be possible to further reduce exergy losses in the future by using a combination of steam reforming, CO conversion and H<sub>2</sub> retention in a membrane reactor [178], since this method allows the high

<sup>60</sup> Results of investigations into chemically-recuperated gas turbines stem from a dissertation (Koerdt [177]) written under my supervision during the preparation of this work.

excess of water which is required to be reduced, and also avoids the need for cooling prior to CO conversion and CO<sub>2</sub> scrubbing.

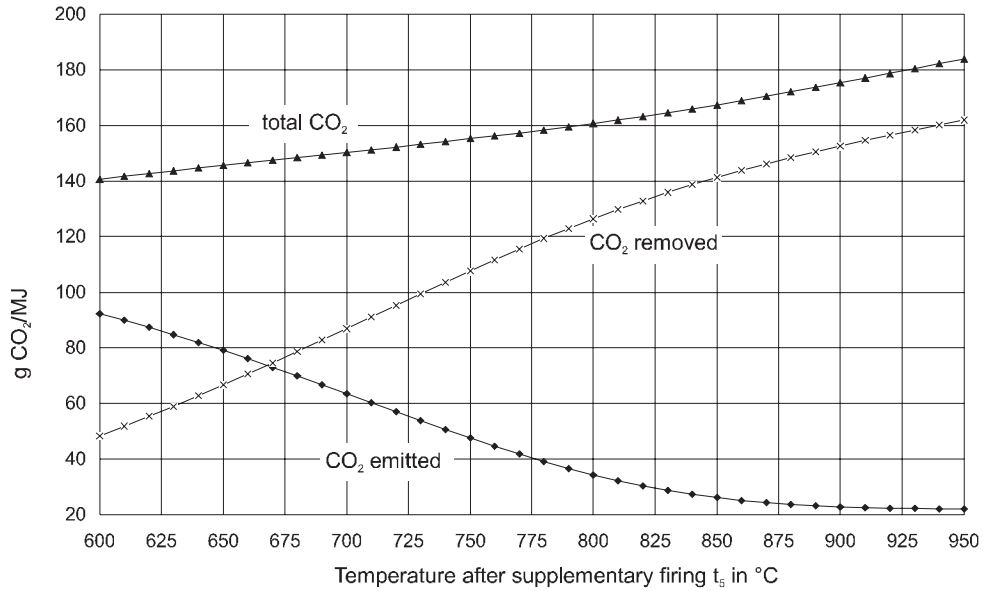


Figure 3.60: Change in the amount of separable CO<sub>2</sub> in dependence on reformer temperature after supplementary firing (constant amount of fuel to gas turbine combustion chamber, Process (d))

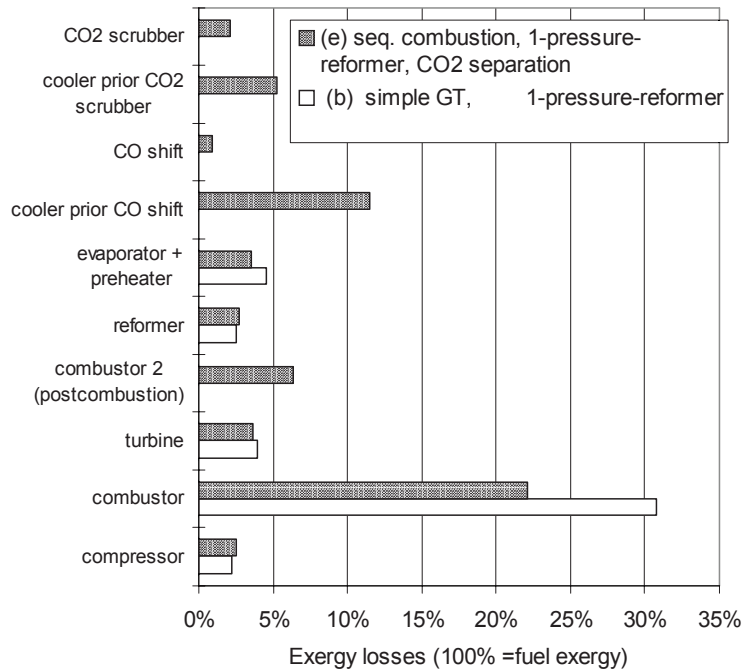


Figure 3.61: Exergy losses in a CRGT with and without CO<sub>2</sub> separation



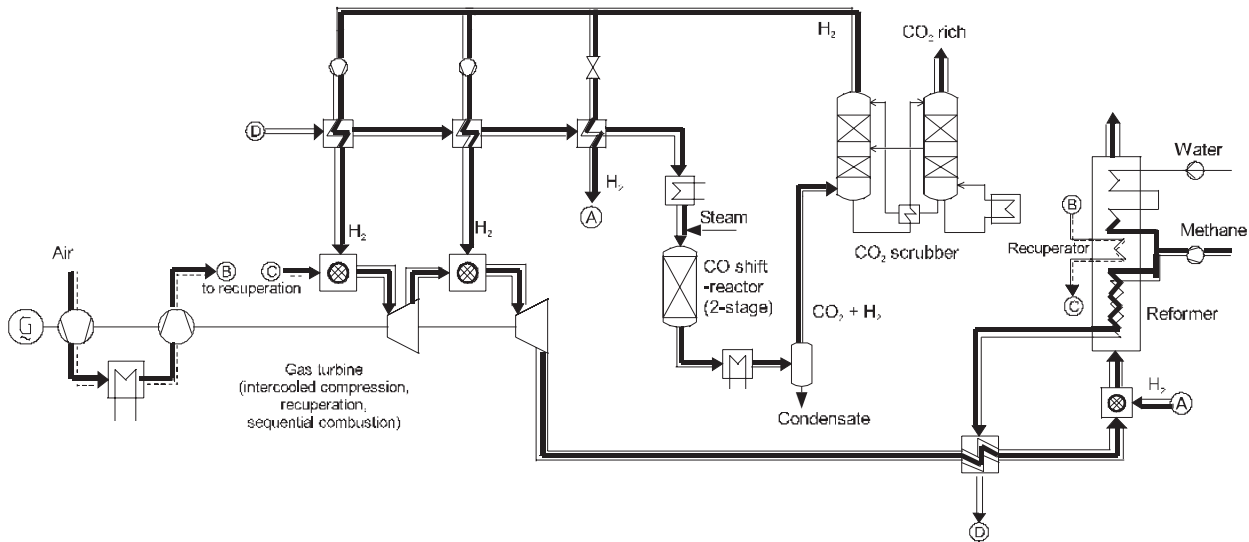


Figure 3.63: Flow diagram of a natural gas-fired CRGT power plant with recuperator, intercooled compressor, sequential combustion, single-pressure reformer, CO<sub>2</sub> separation (g)

### 3.6 Process Family II: CO<sub>2</sub>-Rich Exhaust Gas

In contrast to other methods of CO<sub>2</sub> capture, it is simple to use condensation to separate CO<sub>2</sub>, after combustion in an atmosphere of O<sub>2</sub>/CO<sub>2</sub>, from a mixture consisting primarily of CO<sub>2</sub> and H<sub>2</sub>O. The energy expended on CO<sub>2</sub> capture in this case is mostly used in the preparation of oxygen for the combustion process. This means that, in contrast to other processes, the energy expenditure due to CO<sub>2</sub> capture in this case is less dependent on the carbon content of the fuel; instead, it depends on the minimum level of oxygen required, i.e. it also depends on the hydrogen and oxygen content of the fuel. Efficiency  $KW_{O_2/CO_2}$  of the power plant cycle with CO<sub>2</sub> capture through combustion in an O<sub>2</sub>/CO<sub>2</sub> atmosphere is approximated by (see page 58):

$$PP_{O_2/CO_2} = \text{Basis} \frac{O_{\min} w_{O_2}}{m_F LHV_F} \quad (2.21)$$

where:

$O_{\min}$  minimum oxygen required,  $w_{O_2}$  specific work to generate O<sub>2</sub>,  $m_F$  mass flow of the fuel,  $LHV_F$  heating value of the fuel,  $\text{Basis}$  efficiency of the baseline power plant without CO<sub>2</sub> capture

#### 3.6.1 Oxygen Requirement and Oxygen Purity

As shown in Table 3.22, significantly more oxygen is used in burning natural gas than in burning coal. In relation to the CO<sub>2</sub> mass flow produced, O<sub>2</sub> requirements (and thus the energy requirements) are around twice as high. In relation to the fuel energy flow (LHV) used, the distinction between natural gas and coal is somewhat tempered. In the case of coal gasification, more than a third of the oxygen required is already introduced at the gasifier stage.

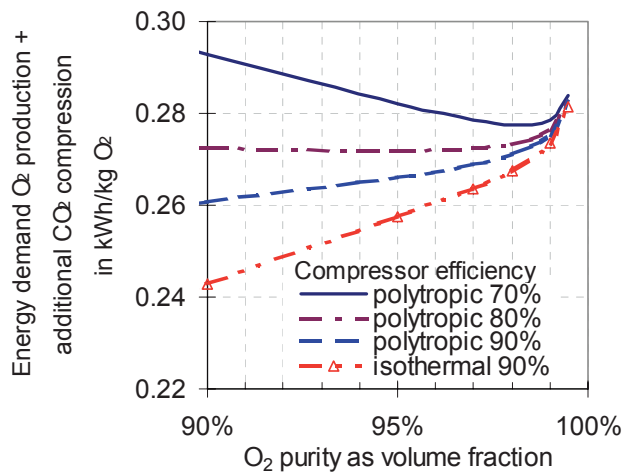
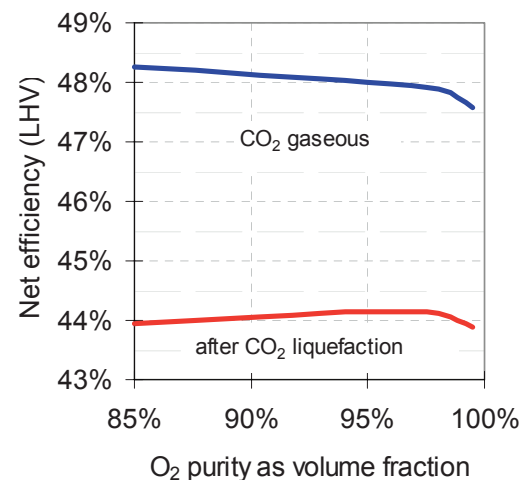
Table 3.22: CO<sub>2</sub> emissions, oxygen requirements and energy expenditure on oxygen generation, depending on fuel used

Fuel	Specific CO <sub>2</sub> emissions		Oxygen required for combustion			Energy required to generate O <sub>2</sub> (at 0.27kWh / kg O <sub>2</sub> )	
	kg CO <sub>2</sub> /kg F (maf)	kg CO <sub>2</sub> /MJ F (LHV, maf)	kg O <sub>2</sub> / kg CO <sub>2</sub>	kg O <sub>2</sub> / kg F (maf)	kg O <sub>2</sub> / MJ F (LHV, maf)	related to CO <sub>2</sub> in kWh/kg CO <sub>2</sub>	related to pri- mary energy in % of the fuel energy (LHV)
100% C	3.7	0.108	0.726	2.67	0.79	0.196	7.64
Hard coal	2.9 - 3.4	0.09 - 0.1	0.75 - 0.92	2.4 - 3.0**	0.076 - 0.11	0.21 - 0.25	7.3 - 7.6
Lignite	2.3 - 2.6	0.09 - 0.1	0.75 - 0.85	1.3 - 1.9	0.03 - 0.04	0.21 - 0.25	7.4 - 7.5
Natural gas	2.1 - 2.9	0.05 - 0.06	1.46 - 1.54	3.1 - 4.4	0.08 - 0.095	0.39 - 0.41	7.8 - 9.0

F = fuel

\*\* gasification alone: 1.0-1.3 kg O<sub>2</sub>/ MJ F

Achieving a high level of oxygen purity requires more energy to be expended in the air separation process, but simultaneously reduces the compression work in the CO<sub>2</sub> liquefaction phase, since there is less inert gas involved in the compression process. If the energy required to generate O<sub>2</sub>, and the contribution towards energy expenditure for CO<sub>2</sub> liquefaction attributable to the inert gases, are both counted together, then the total expenditure of energy rises as O<sub>2</sub> purity increases, if compressor efficiency is greater than 80% (Figure 3.64). Yet calculations carried out for the IGCC power plant as a whole, with combustion in an O<sub>2</sub>/CO<sub>2</sub> atmosphere, show that, although higher efficiency is indeed achieved at lower levels of purity in cases where gaseous CO<sub>2</sub> is retained, optimum efficiency, taking into account the increased compressor work for separated CO<sub>2</sub> more heavily mixed with inert gases, is obtained at an O<sub>2</sub> volume fraction of between 95% and 97% (Figure 3.65).

Figure 3.64: Calculated expenditure of energy on oxygen generation and compressor work for inert gas compression in the CO<sub>2</sub> product, in dependence on oxygen purity<sup>62</sup>Figure 3.65: Recalculation of how the efficiency of an IGCC power plant with combustion in an O<sub>2</sub>/CO<sub>2</sub> atmosphere is dependent on O<sub>2</sub> purity<sup>61,62</sup>.<sup>61</sup> Energy expended on O<sub>2</sub> generation according to (3.15), single-stage compression.<sup>62</sup> TIT 1250°C

### 3.6.2 Analysis of the Oxygen Supply

In order to achieve full combustion with a residual oxygen volume fraction of 2% in a coal gas-fired gas turbine (TIT 1190°C), an O<sub>2</sub> volume fraction of 11.9% is required in the recirculated flue gas, prior to the combustion chamber. The volume fraction of residual oxygen rises to 2.75% after water condensation through cooling prior to recirculation (Figure 3.66).

If the oxygen is supplied in the form of high-purity oxygen from an air separation unit, a large amount of energy will be required for the gas separation process. Only around 12% of the energy used (generally in the form of compressor work) is maintained as exergy of the oxygen (Figure 3.67). Exergy losses

$\Delta \dot{E}_{V,mix} = T_U \Delta \dot{S}_{V,mix}$  incurred in mixing the oxygen with the recirculated flue gas in the combustion chamber are even larger than the exergy of the oxygen generated. Using an O<sub>2</sub>-selective, reversible gas separation method, the difference in O<sub>2</sub> concentration would make it possible to increase the oxygen content of the recirculated flue gas almost to the point where the partial pressure of oxygen in the ambient air is achieved (Figure 3.68). A method of this type would not require any additional expenditure of energy, and would more than halve the exergy losses in the mix of the O<sub>2</sub> and recirculated flue gas (Figure 3.69).

The lower exergy losses in the mix also mean that the mix component of the exergy of the flue gas, as opposed to that of the environment, is used for O<sub>2</sub> supply. The exergy flows of the recirculated flue gas and of the gas mixture enriched with oxygen (after O<sub>2</sub> delivery) remain just as large as in cases involving the addition of high-purity oxygen.

These considerations show that, in an ideal case, when generating a flue gas consisting of CO<sub>2</sub> and H<sub>2</sub>O, no additional energy is required to supply the oxygen, assuming that the differences in oxygen partial pressure can be utilized by means of a selective transport process, without having to take the roundabout route of generating a highly concentrated stream of oxygen (and accepting the expenditure of energy this involves) and subsequently mixing this with the recirculated flue gas (with the resulting losses through mixing).

One possible way of making use of the difference in O<sub>2</sub> partial pressure between the combustion products and the ambient air in the oxygen delivery process could lie in the oxidation of metals in the ambient air and the reduction of the oxide in the combustion chamber at high temperatures, in line with the proposals, described above, from Jody et al. [120] using barium, and from Ishida [121] using nickel (Figure 2.18). Processes of this type are currently being investigated in studies and research experiments.

These comments on oxygen supply apply equally to coal-fired and natural gas-fired processes, since the only decisive parameter is the residual oxygen content after combustion. The oxygen required for gasification would still have to be covered by means of air separation.

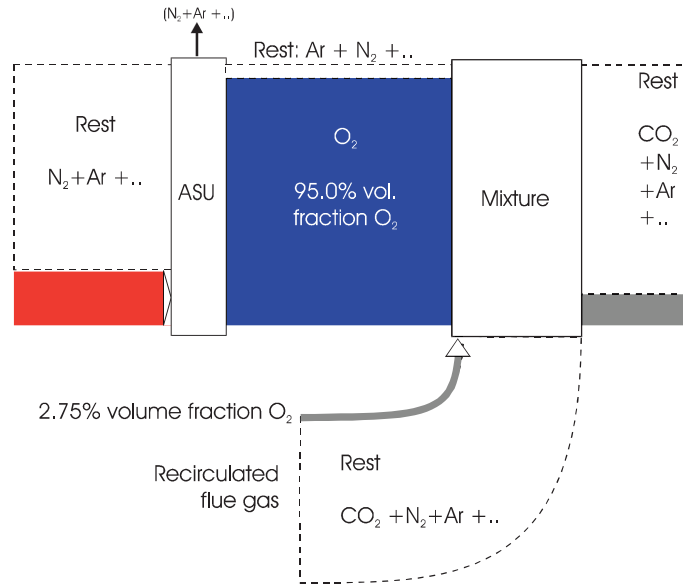


Figure 3.66: Development of O<sub>2</sub> volume fractions where oxygen supply is effected through the generation of pure oxygen using an air separation unit (ASU), all gas streams at 1 bar.

Assumption: fuel gas = coal gas, TIT = 1190°C, concentrations in the gas turbine cycle calculated for the example case.

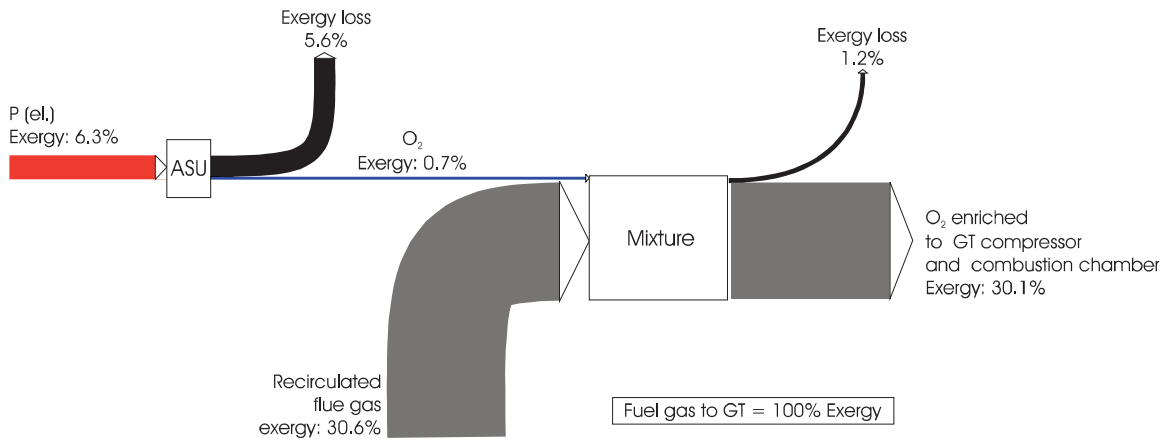


Figure 3.67: Exergy flow diagram for the case where high-purity oxygen is supplied via an air separation unit (ASU), all gas streams at 25°C, 1 bar. Assumption: energy required for oxygen generation = 0.27 kWh/kg O<sub>2</sub>,

fuel gas = coal gas, TIT = 1190°C, concentrations and exergy flows calculated for the example case.

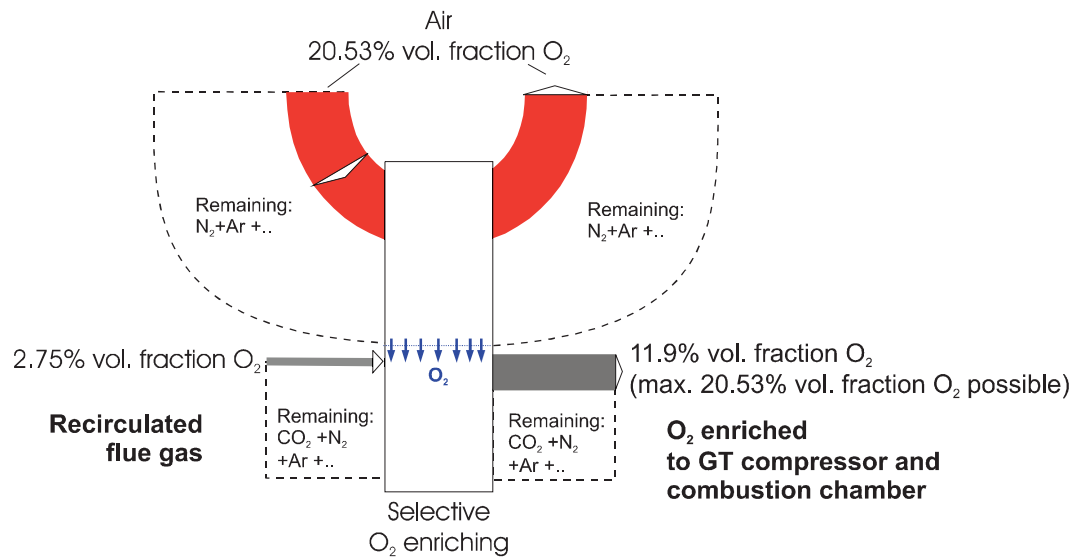


Figure 3.68: Development of O<sub>2</sub> volume fractions in the case of oxygen supply effected through selective mass transfer. Assumption: fuel gas = coal gas, TIT = 1190°C, concentrations in the gas turbine cycle calculated for the example case.

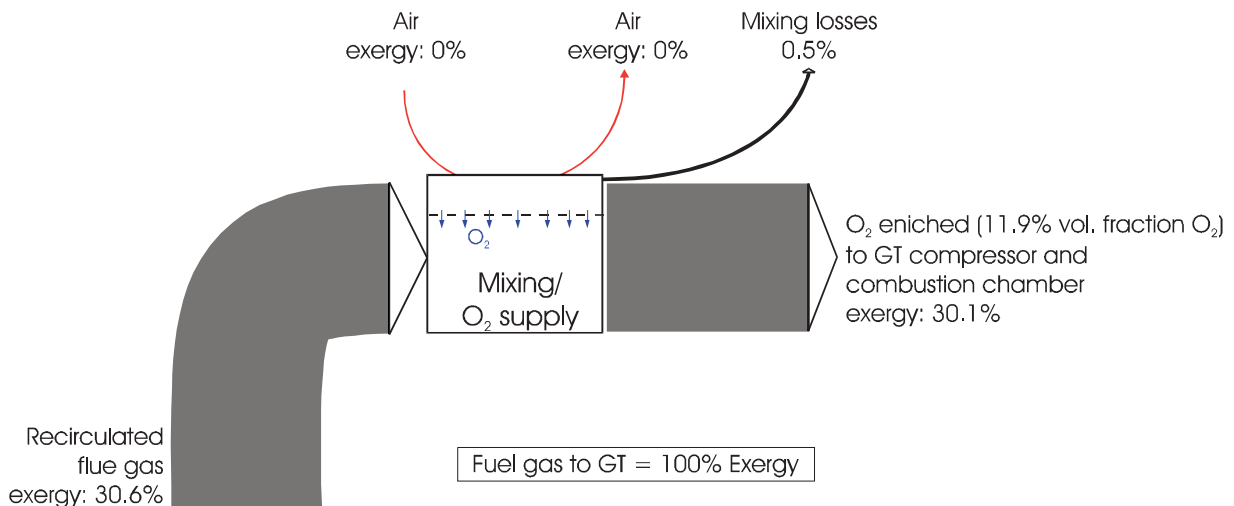


Figure 3.69: Exergy flow diagram for the case where oxygen is supplied through selective mass transfer, all gas streams at 25°C, 1 bar. Assumption: energy required for oxygen generation = 0.27 kWh/kg O<sub>2</sub>, fuel gas = coal gas, TIT = 1190°C, concentrations and exergy flows calculated for the example case.

### 3.6.3 Operation at Increased Pressure

In process cycles such as the Gohstjejn, Sulzer or 'quasi-combined'/'MATIANT' cycle (see pp 38 ff, 127 ff), the working fluid passes through the liquid phase region after condensation, which means that CO<sub>2</sub> liquefaction is already contained within these processes. In some other CO<sub>2</sub> cycles, in which the lower operating point lies above the critical point (e.g. Feher, Schabert cycle), CO<sub>2</sub> is liquefied simply by cooling it to the ambient temperature. It is also possible to perform direct liquefaction of the CO<sub>2</sub> through cooling at the cold end in a simple combustion cycle (steam power plant) or Joule cycle, if the overall level of pressure is increased.



Although operation at a higher pressure cuts down on the compression work required to compress dry, gaseous CO<sub>2</sub> to the point of liquefaction, more work must be done to increase the pressure of the O<sub>2</sub> for combustion (and potentially also for gasification).

If a comparison is made between isothermal compression work  $W_{Comp,CO_2}$  :

$$W_{Comp,CO_2} = \frac{1}{\eta_{Comp}} mRT \ln \left( \frac{p_2}{p_1} \right) \quad (3.31)$$

to compress the required oxygen, and the energy required to compress the CO<sub>2</sub> produced in the combustion of one mole of carbon, it emerges that the compressor work for one mole of O<sub>2</sub> is only slightly larger than that for one mole of CO<sub>2</sub> (the product of general gas constant  $R$  and mass  $m$  equals  $0,2598 \cdot 32 = 8,315$  for O<sub>2</sub>, which is slightly larger than the figure of  $0,1889 \cdot 44 = 8,313$  for CO<sub>2</sub>). This difference becomes more conspicuous in the case of non-isothermal compression. In terms of fuels where oxygen requirements are greater than for combustion purely of the carbon component, an increase in the working pressure therefore results in the greater energy requirements for oxygen compression outweighing the work saved in the CO<sub>2</sub> liquefaction process.

For fuels with a high water content (e.g. all hydrocarbons), it is therefore more favorable to operate the combustion chamber at the lowest possible pressure. In certain circumstances, a slight advantage may be gained by increasing the pressure in the combustion chamber when using a type of coal, which has a high oxygen component.

In the case of CO<sub>2</sub> cycles, which situate the lower operating pressure close to the critical point, the efficiency advantage posed by the more favorable cycles may outweigh the greater work done on oxygen compression, particularly if the compressor/turbine pressure ratio is lower than in other processes, meaning that only a slight increase in combustion chamber pressure is required.

### 3.6.4 Joule Cycle (Standard Gas Turbine) and Joule/Rankine Cycle (Gas/Steam Turbine Combined Cycle)

Comparing the specific useful work ( $W_t$ ) and efficiency ( $\eta$ ) of gas turbines in solo operation and gas/steam turbine combined cycles, which use air as a gas turbine working fluid, with the values of processes, in which CO<sub>2</sub> is used as a working fluid, it can be seen that the  $W_t$ - $\eta$  lines of both working fluids lie one on top of the other (if an ideal gas with constant heat capacity is assumed). If the energy required for O<sub>2</sub> generation is omitted, they differ only in the setting of the pressure ratios. If temperature-dependent heat capacity is incorporated in the calculations, the position of the graphs in relation to each other changes slightly (Figure 3.70). This leads to the conclusion that approximately the same efficiencies and useful work may be achieved using either air or CO<sub>2</sub> as a working fluid, on condition that the compressor pressure ratio for processes using CO<sub>2</sub> as a working fluid is set high enough. The reason for this is that the isentropic exponent of CO<sub>2</sub> is lower than that of air.

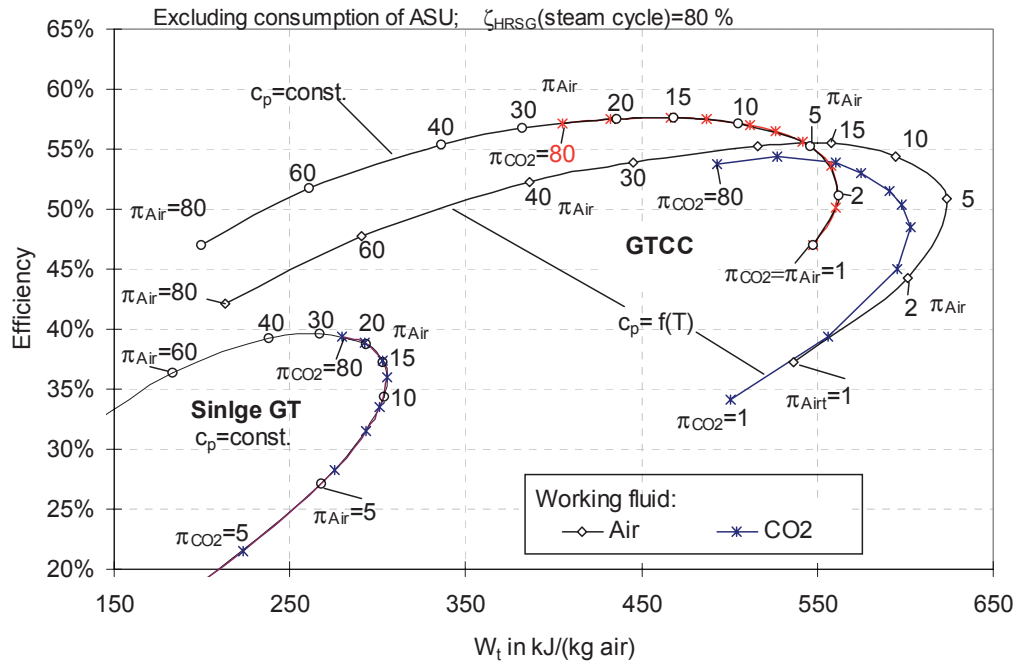


Figure 3.70: Specific useful work and overall efficiency (excluding energy requirements for  $O_2$  generation) of a gas turbine (solo operation) and combined cycle with combustion with air and with  $CO_2/O_2$ , in dependence on the compressor pressure ratio. The capacity of the heat recovery steam cycle is taken into consideration in the form of the exergetic efficiency of exergy utilization in the heat recovery steam cycle (p 66); calculation for ideal gas and constant/ temperature-dependent heat capacity; efficiencies: compressor  $\eta_{isentropic} = 92\%$ , turbine  $\eta_{isentropic} = 86\%$ .

Literature sources cite the following figures to achieve maximum work and maximum efficiency, respectively, of the  $CO_2$  gas turbine: pressure ratios of 55 and 395, respectively, [110], at a turbine inlet temperature of  $1150^\circ C$ , and pressure ratios of 15 and 140, respectively, [112] at a turbine inlet temperature of  $1200^\circ C$ . If the energy requirements for  $O_2$  generation are included, this reduces the efficiency of the  $CO_2$  gas turbine by around 10 percentage points, compared to that of a gas turbine operated using air.

### 3.6.5 Other Cycles with $CO_2$ as Working Fluid

In order to evaluate cycles using  $CO_2$ -rich flue gas as a working fluid, the quasi-combined cycle, [147] according to Figure 3.71 (as well as the variant with reheating known as the 'MATIANT' cycle [118]), and the Gohstjejn cycle were compared with the gas/steam turbine combined cycle (Joule/Rankine cycle) using  $CO_2$  as a working fluid. In the first two cycles, the working fluid is compressed after condensation and expanded in the supercritical region. In the quasi-combined or 'MATIANT' cycle, the highest process temperature comes in the combustion chamber prior to the low-pressure turbine. Before the high-pressure turbine, liquid working fluid is vaporized and superheated with hot feed gas from the low-pressure turbine using a recuperator. Without the high-pressure turbine, or with a pressure ratio of 1 for the high-pressure turbine, the quasi-combined cycle becomes the Gohstjejn cycle with single-stage expansion.



temperature of 1190°C and single-stage or three-stage working fluid compression. The achievable efficiencies in these two cases are 45.1% and 47.1%, respectively.

To calculate the process in dependence on pressure ratio, the lower process pressure is set at a constant 4 bar (corresponding to suggestions put forward by Iantovski et al. [147]) and the water content prior to compression is reduced to a value, which results from cooling to 20°C (Figure 3.72). Figure 3.74 shows the partial pressure ratios, which have been optimized for maximum efficiency, in dependence on overall pressure ratio. For overall pressure ratios below approx. 35 for single-stage compression, or below approx. 42 for three-stage compression, the high-pressure turbine is omitted, in order to avoid exit temperatures above 600°C at the low-pressure turbine. This satisfies the conditions of the Gohstjejn cycle. As shown in Figure 3.75, advantages in efficiency over the Gohstjejn cycle can only be obtained using the quasi-combined cycle if intercooled compression is used; specific work is invariably higher. Figure 3.73 shows how efficiency is influenced by the condenser temperature.

Compared to the gas/steam turbine combined cycle using CO<sub>2</sub> as a gas turbine working fluid, a gas turbine in which compression proceeds close to the critical point (e.g. Gohstjejn cycle, 'MATIANT' cycle) can obtain a roughly equally high efficiency and comparable specific work at lower pressure ratios (Figure 3.75). The advantage of the quasi-combined cycle is that CO<sub>2</sub> liquefaction is already integrated.

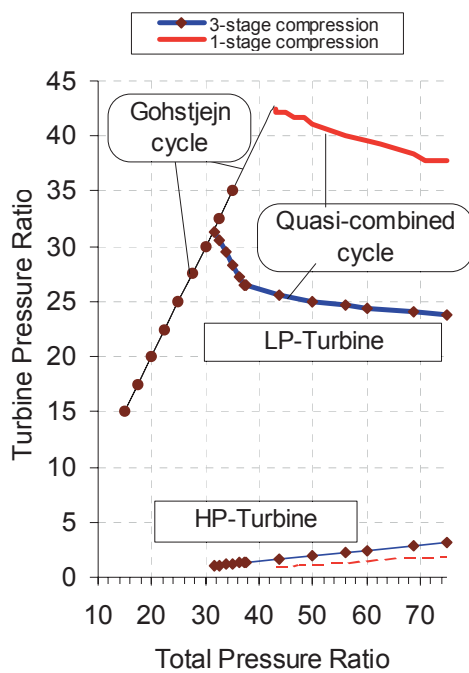


Figure 3.74: Pressure ratios in the Gohstjejn cycle and the quasi-combined cycle<sup>63</sup>

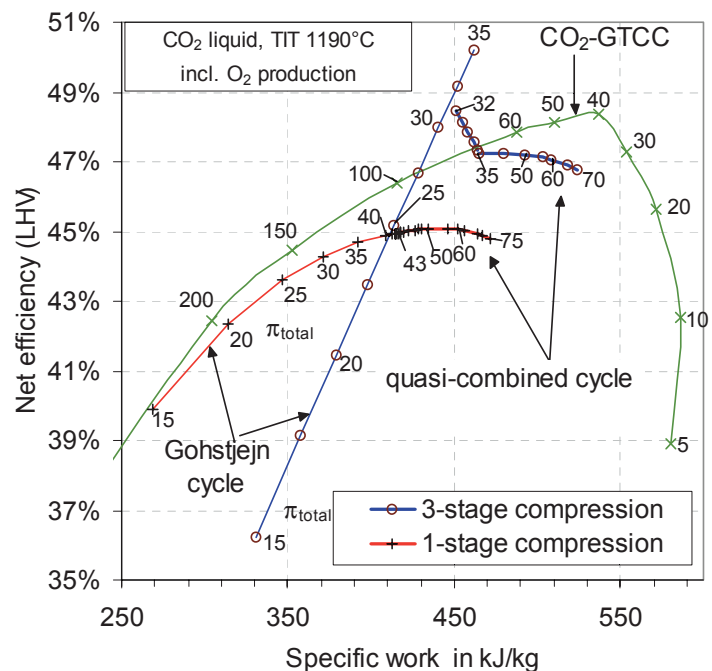


Figure 3.75: Comparison of efficiency and specific work of cycles using CO<sub>2</sub> as a working fluid, in dependence on pressure ratio (turbine inlet temperature (ISO 2314): 1190°C)<sup>63</sup>.

The efficiency potentials of the various processes, which use CO<sub>2</sub> as a gas turbine working fluid, lie too close to each other to identify any decisive process advantages based on this factor (Figure 3.75).

<sup>63</sup> Efficiency and specific work including O<sub>2</sub> generation; O<sub>2</sub> compression and pump work. Partial pressure ratios are calculated to achieve maximum efficiency. For process data, see Table 3.23; gas turbine inlet temperature 1190°C; lowest pressure 4 bar; minimum temperature 20°C.

Table 3.23: Comparison of the quasi-combined cycle with internal combustion, according to Iantovski et al. [147], with the cycle featuring sequential combustion known as the "MATIANT" cycle [118], and with my own calculations

	Quasi-combined cycle [147]		'MATIANT' cycle [118]		Own calculations (ASPENplus) (quasi-combined cycle)			
TIT (ISO) in °C	1300		1300/ IH 1300		1300		1190	
Max. temp. in the recuperator in °C	600		600		600			
HP turbine inlet* pressure in bar	240		300		240			
temp. in °C	600		600		600			
MP turbine inlet** pressure in bar	60		40 / IH 9.5		60		60	
temp. in °C	1300		1300 / IH 1300		1300		1190	
Min. pressure (H <sub>2</sub> O condensation) in bar	4		1		4			
Condenser temp. in °C	20		29		20			
Components (isentropic efficiency)	Efficiency in %	No. of stages	Efficiency in %	No. of stages	Efficiency in %	No. of stages	No. of stages	
Gas turbine (HP turbine)	85	1	75	2	90	1		
Steam turbine (MP turbine)	80	1	75	1	90	1		
CO <sub>2</sub> compressor	80	3	75	3	85	3	3	
CO <sub>2</sub> pump	60	1	75	1	73	1		
O <sub>2</sub> compressor	(pump)	1	75		85	2		
Fuel (volume fractions)	100% CH <sub>4</sub>		84% CH <sub>4</sub> , 16% CO <sub>2</sub>		100% CH <sub>4</sub>			
O <sub>2</sub> purity: vol. fraction of O <sub>2</sub> in %	98		99.5		98			
Energy expended on O <sub>2</sub> generation in kWh/kg O <sub>2</sub>	0.2		0.37		0.27			
at pressure in bar	60		40		1			
ASU energy required, in relation to fuel energy (LHV) in %	7.0		not spec.		7.9			
O <sub>2</sub> compression, in relation to fuel energy (LHV) in %	3.1		not spec.		3.8			
Specific output (related to fuel utilization in LHV, positive for production, negative for consumption)								
LP turbine in %	65.7		not spec.		62.4		61.9 62.4	
HP turbine in %	14.5		not spec.		20.1		19.5 20.1	
compressor in %	-13.2		not spec.		-18.4		-19.8 -22.3	
pumps in %	-1.4		not spec.		-2.9		-2.9 -3.5	
ASU in %	-7.0		not spec.		-7.9		-7.9 -7.9	
O <sub>2</sub> compressor in %	-3.1		not spec.		-3.7		-3.7 -3.7	
CH <sub>4</sub> compressor in %	-1.2		not spec.					
Power plant efficiency (LHV) in %	54.3		41.1		49.6		47.1 45.1	

\* = pressure at point where CO<sub>2</sub> is sluiced out

\*\* = combustion chamber pressure

### 3.6.6 Parameter Studies for IGCC Power Plants with CO<sub>2</sub> Recycling

The remaining calculations are performed on the assumption of a combined cycle with a CO<sub>2</sub> gas turbine (Joule cycle) and a subsequent steam Rankine cycle.

The development of efficiency and specific work shown in Figure 3.76 makes it clear how, in contrast to IGCC power plants using air as a gas turbine working fluid, the maximum efficiency of an IGCC power plant using CO<sub>2</sub> as a gas turbine working fluid no longer lies in the proximity of the compressor pressure ratio for maximum specific gas turbine work, but instead lies far above this.

The compressor pressure ratios, optimized for overall efficiency, in an IGCC power plant with CO<sub>2</sub> capture, after combustion in an O<sub>2</sub>/CO<sub>2</sub> atmosphere, are more than twice as high as those of the corresponding baseline IGCC power plant without CO<sub>2</sub> capture (cf. Table 3.18).

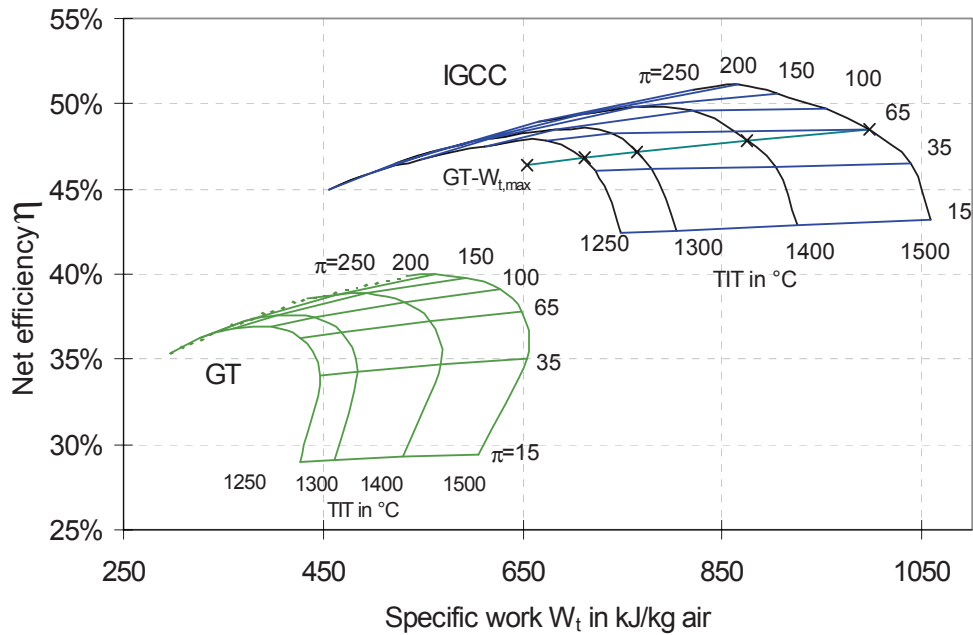


Figure 3.76: Useful work/efficiency diagram ( $\eta$ - $w_i$ ) of a gas turbine using  $\text{CO}_2$  as a working fluid (excluding ASU energy requirements), and of an IGCC power plant with combustion in an  $\text{O}_2/\text{CO}_2$  atmosphere (including ASU energy requirements), in relation to compressor pressure ratio  $\pi$  and gas turbine inlet temperature (TIT) according to ISO 2314, Joule/Rankine combined cycle.

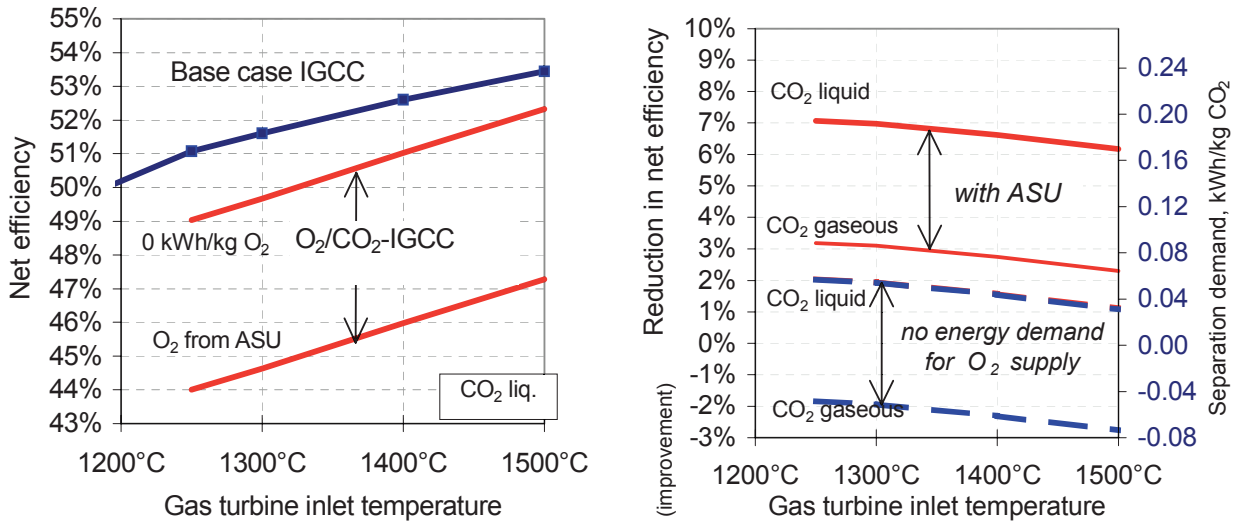


Figure 3.77: Efficiency penalty and efficiencies of an IGCC plant with combustion in an  $\text{O}_2/\text{CO}_2$  atmosphere, in dependence on gas turbine inlet temperature

Figure 3.77 shows a comparison of the achievable efficiencies, including  $\text{CO}_2$  liquefaction, as well as the efficiency penalty. As well as investigating the effect of raising the gas turbine inlet temperature, the possibility is also examined in these calculations of implementing a selective oxygen supply, without any further energy requirements (p 32 ff), for the combustion stage in the gas turbine (not for the oxygen required by the gasifier) (Figure 3.77). In this scenario, the efficiency including  $\text{CO}_2$  capture, but excluding  $\text{CO}_2$  liquefaction, is even higher than that of the baseline IGCC power plant.

As shown above, in Figure 3.70, this improvement over the baseline IGCC plant cannot be accounted for by improvements in the gas/steam turbine combined cycle, but instead is the result of improved exergy utilization in the gasifier island<sup>64</sup>, due to the higher gasification pressure, and an advantageous process arrangement which omits the addition of N<sub>2</sub>. In the baseline IGCC power plant, N<sub>2</sub> from the air separation process is compressed to the fuel gas pressure and then mixed into the fuel gas for the purpose of NO<sub>x</sub> reduction. In an IGCC plant with an O<sub>2</sub>/CO<sub>2</sub> gas turbine, dilution of the fuel gas with N<sub>2</sub> is not required and is therefore omitted. This, in turn, avoids the losses incurred through additional N<sub>2</sub> compression. Furthermore, an increase in gasification pressure improves the exergetic efficiency of the gasifier island, since, in the gasification process, a small gas volume (O<sub>2</sub>, steam) is used to produce a larger volume of fuel gas, which can deliver more expansion work at a higher pressure. Figure 3.78 shows the significant difference in the compressor pressure ratio of the gas turbine between the IGCC plant with combustion in an O<sub>2</sub>/CO<sub>2</sub> atmosphere, and the baseline IGCC. It also presents a comparison of the exergetic efficiencies of the gasifier island.

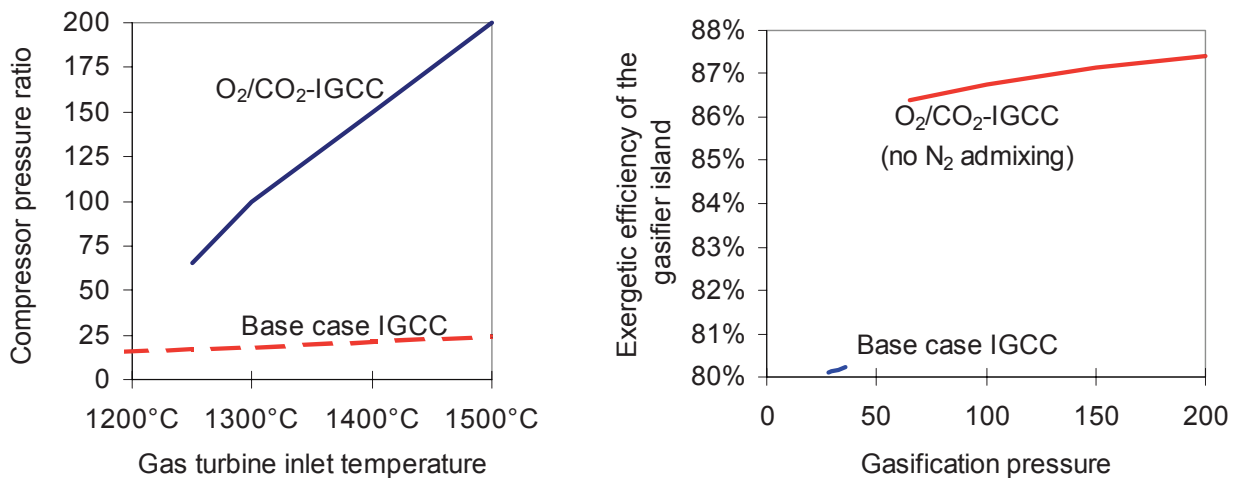


Figure 3.78: Raising the pressure ratios of the gas turbine compressor (and therefore also the gasification pressure) to achieve maximum IGCC efficiency as gas turbine inlet temperature rises, and the resulting increase of the exergetic efficiency of the gasifier island<sup>64</sup>, for an IGCC power plant with a gas turbine using air (baseline IGCC) and CO<sub>2</sub> (O<sub>2</sub>/CO<sub>2</sub> IGCC) as a working fluid.

The largest exergy losses due to CO<sub>2</sub> capture are caused by the exergy of the separated CO<sub>2</sub>, O<sub>2</sub> generation and CO<sub>2</sub> liquefaction. Exergy losses in the gasification stage and the combustion chamber, on the other hand, are lower than in the baseline IGCC. The extent to which CO<sub>2</sub> capture contributes to the efficiency penalty is determined by three sub-processes (Figure 3.79, Figure 3.80), whereby the last of these improves the efficiency:

- Generation of high-purity oxygen using an air separation unit (an efficiency penalty of approx. 4 to 4.5 percentage points),
- CO<sub>2</sub> liquefaction (efficiency penalty of approx. 4 percentage points), and
- Improvement to the exergetic efficiency of the gasifier island (efficiency improvement of between 1.8 and 2.8 percentage points, depending on the pressure).

However, the values calculated here only apply subject to the proviso that the same compressor and turbine efficiencies can be achieved as in the baseline case, even at the high pressures which are required in the CO<sub>2</sub> gas turbine. In a real case, the advantages of the increased gasification pressure will be some-

<sup>64</sup> The gasifier island comprises: the gasification, gas cooling, gas cleaning, reheating and humidification. The exergetic efficiency includes the exergy of all the imported and exported material flows (coal, O<sub>2</sub>, steam, water, fuel gas).

what tempered by lower component efficiencies. Furthermore, there is some uncertainty as to the process data to be used, e.g. in terms of required fuel gas humidification.

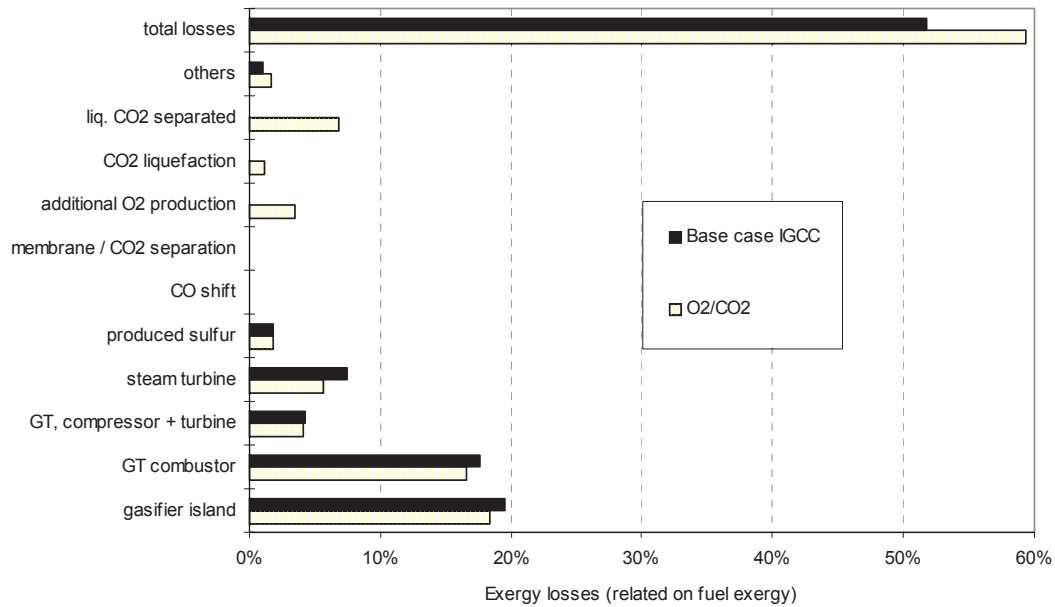


Figure 3.79: Comparison of the exergy losses of the baseline IGCC plant and an IGCC plant with combustion in an O<sub>2</sub>/CO<sub>2</sub> atmosphere

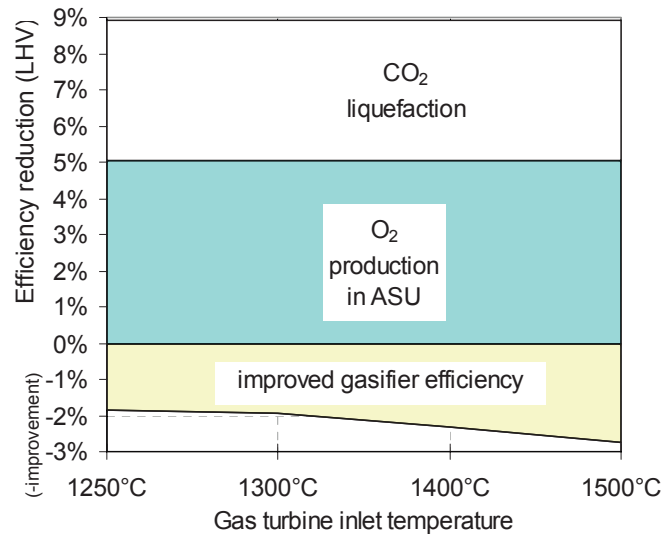


Figure 3.80: Proportions of the efficiency penalty due to CO<sub>2</sub> capture attributable to O<sub>2</sub> generation and CO<sub>2</sub> liquefaction, together with the increase in efficiency improvement as gas turbine inlet temperature is raised



Table 3.24: Operating parameters and results for IGCC power plants with an O<sub>2</sub>/CO<sub>2</sub> gas turbine with varying gas turbine inlet temperatures

<b>Assumptions</b>				
Gasification temperature	1302°C			
Gasification pressure in bar	76	111	161	261
<b>Gas turbine inlet temperature (ISO 2314)</b>	<b>1250</b>	<b>1300</b>	<b>1400</b>	<b>1500</b>
Compressor pressure ratio of gas turbine	65	100	150	200
CO <sub>2</sub> capture ratio	100%			
O <sub>2</sub> purity	95% Volume fraction			
Energy requirements for air separation	0.25 kWh/kg O <sub>2</sub>			
<b>Results:</b>				
<b>Output and Internal Consumption</b> in MW (positive = delivery of electric power, negative = consumption )				
Coal energy supplied (LHV)	874.9			
CO <sub>2</sub> gas turbine	313.72	330.16	347.34	360.46
<i>Steam from GT waste heat</i>	<i>170.18</i>	<i>159.72</i>	<i>154.64</i>	<i>152.89</i>
<i>Steam from raw gas cooling</i>	<i>39.1</i>	<i>40.5</i>	<i>42.0</i>	<i>43.3</i>
<i>Low temperature raw gas cooling</i>	<i>-8.3</i>	<i>-9.0</i>	<i>-9.7</i>	<i>-10.2</i>
<i>Steam for drying coal</i>	<i>-0.5</i>	<i>-0.5</i>	<i>-0.5</i>	<i>-0.5</i>
<i>Feedwater for gasification</i>	<i>-1.8</i>	<i>-1.9</i>	<i>-2.0</i>	<i>-2.2</i>
Σ Steam turbine output	Σ 198.8	Σ 188.8	Σ 184.4	Σ 183.4
O <sub>2</sub> +N <sub>2</sub> compression for gasification	-31.47	-32.78	-34.10	-35.07
O <sub>2</sub> generation for gas turbine	-44.00	-44.06	-44.13	-44.20
Desulfurization	-1.44	-1.07	-0.71	-0.44
Other internal consumption	-16.66	-16.66	-16.66	-16.66
CO <sub>2</sub> compression/liquefaction at 110 bar	-33.9	-34.0	-33.9	-33.9
Net output	385.0	390.4	402.3	413.5
<b>Power plant net efficiencies</b> in %				
LHV (CO <sub>2</sub> liquid)	44.0	44.6	46.0	47.3
LHV (CO <sub>2</sub> gaseous)	47.9	48.5	49.9	51.1
HHV, (CO <sub>2</sub> liquid)	42.3	42.9	44.2	45.4
Exergy (CO <sub>2</sub> liquid)	41.6	42.2	43.5	44.7
CO <sub>2</sub> emissions in kg CO <sub>2</sub> /kWh	≈ 0			

### 3.6.7 Processes with Coal Gasification and H<sub>2</sub>/CO Separation

Figures 3.81 to 3.85 and Table 3.26 contain the results of calculations, performed by the author of this study, for an IGCC power plant with an H<sub>2</sub>/CO separation membrane, in accordance with Figure 2.19, with a membrane selectivity of 60 for H<sub>2</sub> to CO and a gas turbine inlet temperature of 1190°C.

The more H<sub>2</sub> permeating through the membrane, the greater the energy supplied to the air-operated gas turbine. Since CO<sub>2</sub> also permeates through at the same time as H<sub>2</sub>, larger permeating mass flows of H<sub>2</sub> mean that less CO<sub>2</sub> is captured (Figure 3.81). An efficiency of 43.3% including CO<sub>2</sub> liquefaction (efficiency penalty of 7.9 percentage points) was calculated with a CO<sub>2</sub> capture ratio of 87.7% (Figure 3.82).

Compared to the baseline IGCC power plant, the greatest exergy losses in this case are caused by the exergy of the separated CO<sub>2</sub> and the generation of O<sub>2</sub> for burning the retentate (Figure 3.83). In addition to the energy requirements for O<sub>2</sub> generation and CO<sub>2</sub> liquefaction, efficiency is also reduced in this case due to pressure losses in the membrane (Figure 3.84). A further efficiency penalty occurs due to a unfavorable process pressure for one of the two gas turbine processes.

Based on the assumptions used in this case, the IGCC power plant with H<sub>2</sub>/CO separation achieves a higher efficiency than an IGCC power plant with CO conversion and H<sub>2</sub> separation using a membrane, but a lower efficiency than that obtained in the case of CO conversion and CO<sub>2</sub> scrubbing (Figure 3.85).

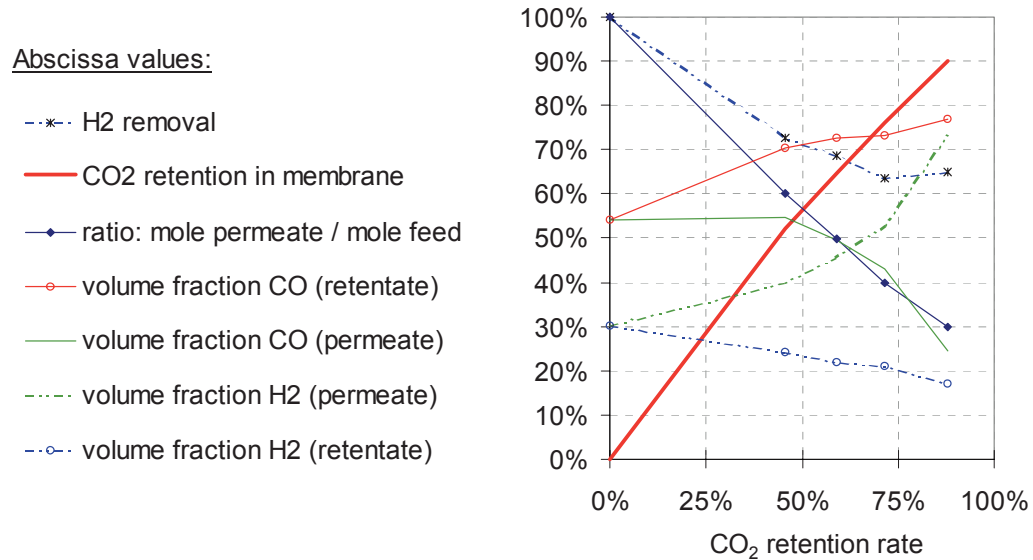


Figure 3.81: Separation characteristics of the H<sub>2</sub>/CO membrane in dependence on CO<sub>2</sub> capture ratio

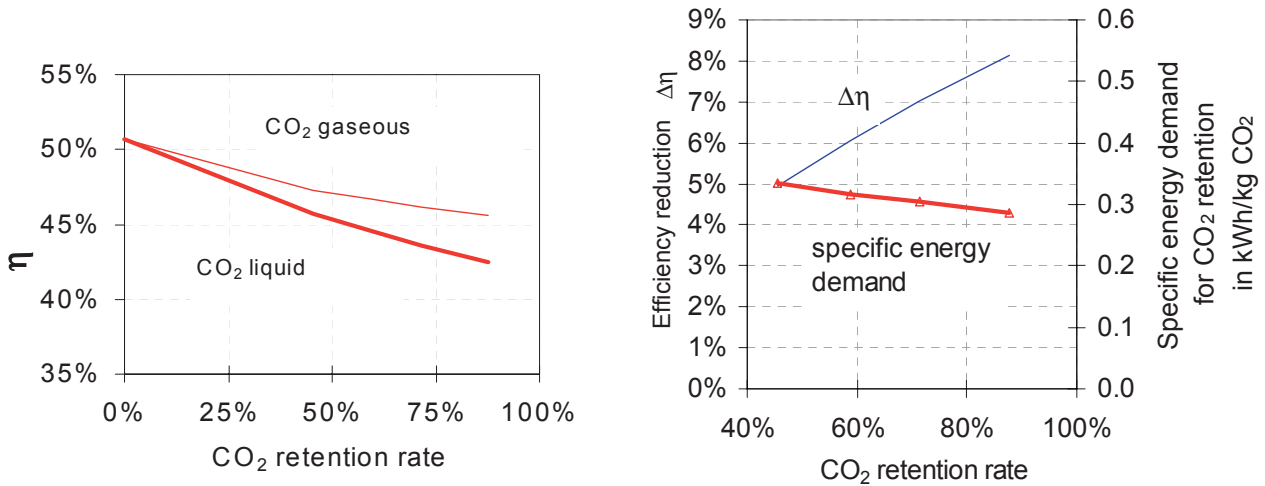


Figure 3.82: IGCC net efficiency, efficiency penalty and specific energy requirements for CO<sub>2</sub> capture in the IGCC plant with H<sub>2</sub>/CO separation according to Figure 2.19

Table 3.25: Relative permeability of the individual gas components for H<sub>2</sub>/CO separation with Knudsen diffusion according to Equation 2.4

O <sub>2</sub>	0.016
H <sub>2</sub> O	0.021
CO <sub>2</sub>	0.013
N <sub>2</sub>	0.017
Ar	0.014
SO <sub>2</sub>	0.011
H <sub>2</sub>	1
CO	0.017
CH <sub>4</sub>	0.022
H <sub>2</sub> S	0.015
COS	0.011

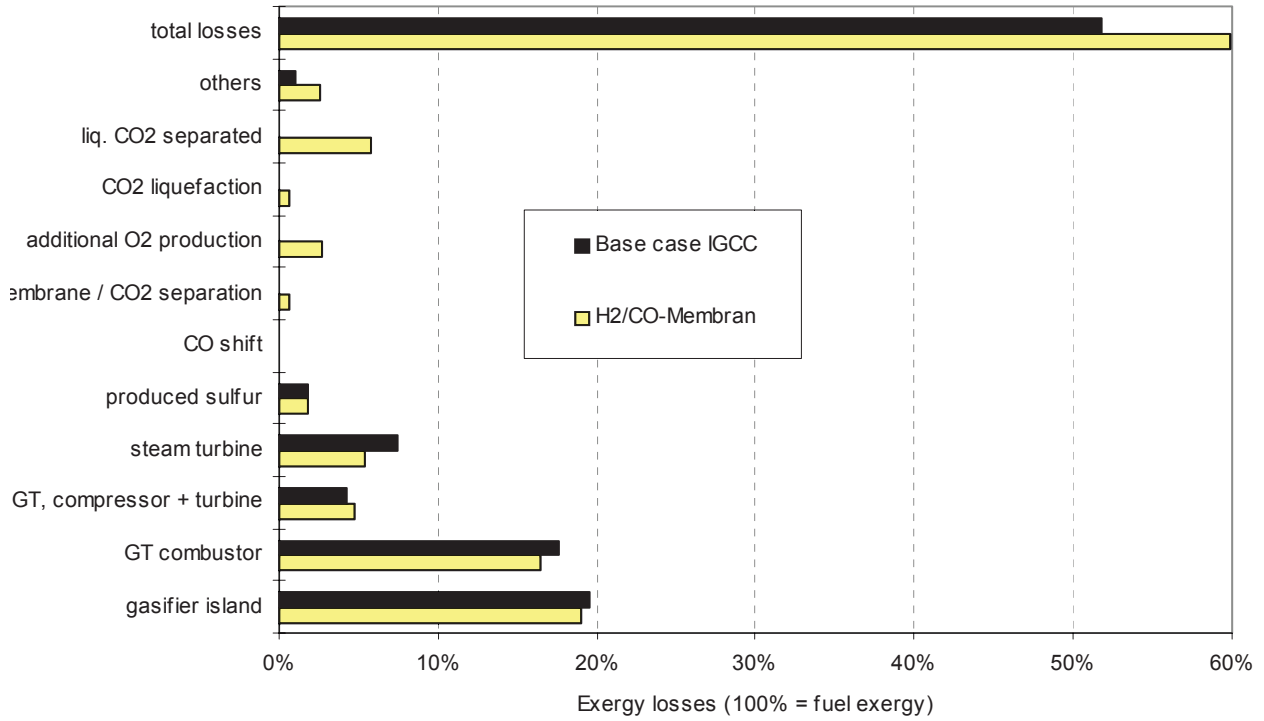


Figure 3.83: Exergy losses of the baseline IGCC power plant and of the IGCC plant with H<sub>2</sub>/CO separation with a CO<sub>2</sub> capture ratio of 87.7%

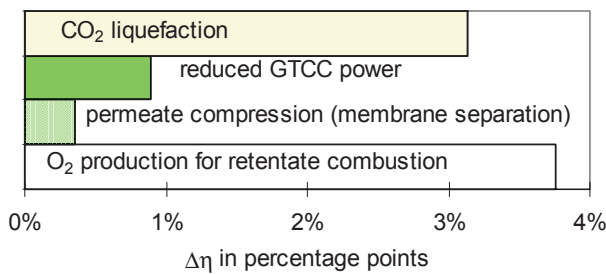


Figure 3.84: How individual process steps contribute towards the efficiency penalty

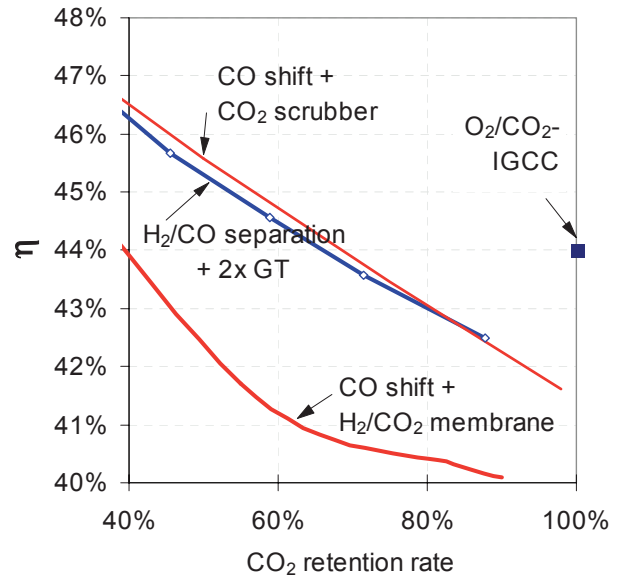


Figure 3.85: IGCC net efficiency in an IGCC power plant with H<sub>2</sub>/CO<sub>2</sub> separation or CO<sub>2</sub> scrubbing after CO conversion, an IGCC power plant with H<sub>2</sub>/CO separation, and an IGCC power plant with combustion in an O<sub>2</sub>/CO<sub>2</sub> atmosphere (TIT 1250°C)

Table 3.26: Operating parameters and results of the calculations of H<sub>2</sub>/CO separation in the membrane in an IGCC.

	min. CO <sub>2</sub> capture	max. CO <sub>2</sub> capture
Ratio of molar flow rates from permeate to feed	<b>60%</b>	<b>30%</b>
Pressure ratio permeate/feed	<b>0.44</b>	<b>0.33</b>
Selectivity H <sub>2</sub> /CO	60	60
Relative Permeability - see Table 3.25		
<b>Results:</b>		
CO <sub>2</sub> capture ratio (incl. CO, CH <sub>4</sub> , COS)	45.6%	87.7%
CO <sub>2</sub> separation factor of the membrane (retentate without CO, CH <sub>4</sub> , COS)	52.3%	90.1%
H <sub>2</sub> permeation	72.6%	65.0%
Composition of the retentate, proportions by weight		
CO <sub>2</sub>	0.8%	0.7%
H <sub>2</sub>	2.2%	1.5%
CO	90.1%	91.1%
CH <sub>4</sub>	0.2%	0.3%
kg/s	24.6	46.9
Composition of the permeate, proportions by weight		
CO <sub>2</sub>	0.6%	0.5%
H <sub>2</sub>	4.6%	16.5%
CO	88.4%	77.4%
CH <sub>4</sub>	0.3%	0.3%
kg/s	29.9	7.6
Output and Internal Consumption in MW (positive = delivery of electric power, negative = consumption)		
Coal energy delivered (LHV)	874.9	874.9
Gas turbine 1 (working fluid: air)	179.0	90.4
Gas turbine 2 (working fluid: CO <sub>2</sub> ), incl. retentate compression	108.2	191.7
<i>Steam from GT waste heat (GT 1)</i>		
	102.3	44.5
<i>Steam from GT waste heat (GT 2)</i>		
	67.4	120.0
<i>Steam from raw gas cooling</i>		
	30.7	34.2
<i>Low temperature raw gas cooling</i>		
	-10.0	-5.0
<i>Steam for drying coal</i>		
	-0.5	-0.5
<i>Feedwater for gasification</i>		
	-1.5	-1.5
Σ Steam turbine	Σ 188.4	Σ 191.7
O <sub>2</sub> +N <sub>2</sub> compression for gasification	-19.7	-19.7
ASU for gas turbine 2 (addition of O <sub>2</sub> at 1 bar prior to compressor)	-17.4	-30.6
Permeate compression	-4.4	-3.1
Desulfurization	-2.4	-2.4
Other internal consumption	-16.7	-16.7
CO <sub>2</sub> compression/liquefaction at 110 bar	-14.2	-27.4
Net output	400.7	374.0
Power plant net efficiencies in %		
LHV (CO <sub>2</sub> liquid)	45.8	42.7
LHV (CO <sub>2</sub> gaseous)	47.4	45.9
HHV (CO <sub>2</sub> liquid)	44.0	41.1
Exergy (CO <sub>2</sub> liquid)	43.3	40.4
CO <sub>2</sub> emissions in kg CO <sub>2</sub> /kWh (with retention of liquid CO <sub>2</sub> )	0.379	0.091

### 3.7 Process Family III: CO<sub>2</sub> Separation from Flue Gases

If figures are available for specific work  $w_{CO_2}$  required for CO<sub>2</sub> separation, or the equivalent electrical energy of the heat required<sup>65</sup>, Equation 2.20 may be used to approximately calculate efficiency  $\eta_1$  of the process with CO<sub>2</sub> separation from separated mass flow of CO<sub>2</sub>  $\dot{m}_{CO_2}$ , fuel energy input  $\dot{m}_F LHV_F$  and overall efficiency of the basic process without CO<sub>2</sub> separation  $\eta_0$ .

Table 3.27 shows the ranges of energy requirements of various CO<sub>2</sub> separation processes, where heat consumption is expressed in terms of reduced steam cycle performance. For chemical scrubbing, the exergetic efficiency, in relation to the reversible separation work, lies between approx. 9% and 21%. This gives an efficiency penalty attributable to CO<sub>2</sub> scrubbing of between 6 and 16 percentage points, and an equivalent electrical energy requirement<sup>66</sup> of the scrubbing process of between approx. 0.23 and 0.75 kWh per kg of separated CO<sub>2</sub> (this range also incorporates the various flue gas compositions -- Figure 3.86).

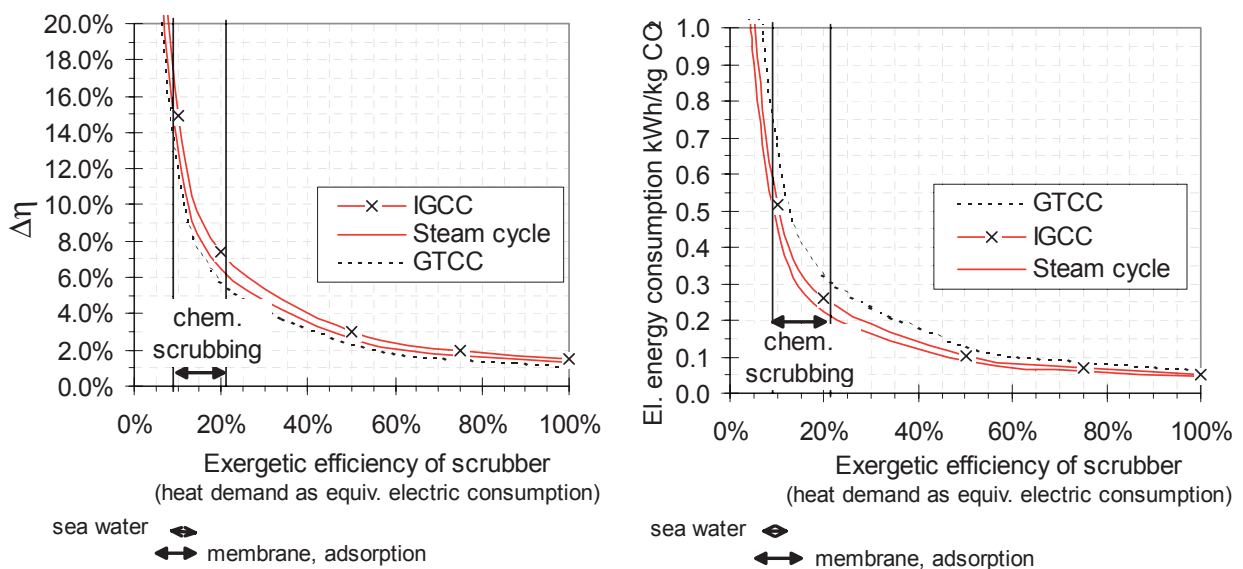


Figure 3.86: Calculation of the power plant efficiency penalty due to CO<sub>2</sub> separation from the flue gas, and the equivalent electrical energy requirements<sup>66</sup>, in hard coal-fired and natural gas-fired processes, in dependence on the exergetic efficiency of the CO<sub>2</sub> separation process (see Table 3.10 for the gas compositions used in the calculations). Ranges are drawn in, as examples, for the exergetic efficiency of chemical scrubbing, scrubbing with seawater, membrane processes and adsorption processes.

<sup>65</sup> If the heat requirement is calculated as the reduced performance of the steam turbine due to steam extraction. For more details, see Appendix, Section 6.6.

<sup>66</sup> Sum of electrical energy requirement and reduction in steam turbine output due to the heat requirement.

Table 3.27: Range of equivalent electrical energy requirements<sup>66</sup> for various CO<sub>2</sub> separation processes (flue gases with higher CO<sub>2</sub> content represent the lower end of the range of energy values given in each case)

CO <sub>2</sub> Separation Method	Absorbent / Comments	Equivalent electrical energy requirement <sup>66</sup> in kWh/kg CO <sub>2</sub>
Chemical absorption	aqueous amine, hot potassium carbonate, (Table 6.7)	0.28- 0.8
Physical absorption with seawater	absorbent: water (without regeneration, see Section 3.4, Figure 3.15)	0.38 - 1.16
Distillation		0.6 - 1
Freezing	theoretical values [74]	0.35 - 0.38
Membrane	selectivity approx. 25-40 (own calculation)	0.4 -1.5
Adsorption	(own calculation)	0.4 - 1.3

### 3.8 Process Family IV: Carbon Separation

Processes involving the separation of carbon (Process Family IV) are not analyzed in any greater depth within the context of this study, since this process does not involve CO<sub>2</sub> capture in power plants, and utilization of the fuel is incomplete.

### 3.9 Process Family V: CO<sub>2</sub> Capture with Fuel Cells

If CO<sub>2</sub> capture causes the composition of the fuel gas in the fuel cell to change, this will also have an influence on fuel conversion in the fuel cell, and on the efficiency of the fuel cell itself. However, this influence on the efficiency of the fuel cell is not evaluated in this study. Only a rough estimation is given of the expenditure required, in principle, for CO<sub>2</sub> capture.

In the case of CO<sub>2</sub> separation prior to the fuel cell from a synthesis gas after CO conversion (after coal gasification or natural gas reforming), the efficiency penalty in processes with coal gasification (as described for Process Family I) lies between 4 and 6 percentage points, plus approx. 5 percentage points for CO<sub>2</sub> liquefaction. In the case of CO<sub>2</sub> capture after natural gas reforming and CO conversion, the efficiency of a power plant using fuel cells (corresponding to the values from Process Family I) decreases by around 10 to 14 percentage points, and a further 2 to 3 percentage points are lost due to CO<sub>2</sub> liquefaction.

CO<sub>2</sub> capture performed using the method of CO conversion in the anode exhaust gas and H<sub>2</sub>/CO<sub>2</sub> separation makes the best use of the internal gas separation process (O<sub>2</sub> separation in SOFC, MCFC, and H<sub>2</sub> separation in PEMFC, PAFC). An efficiency penalty of less than 2 percentage points can be achieved in this way.

If the anode exhaust gas is subsequently burnt, and the cathode intake air is mixed in, then CO<sub>2</sub> separation from the cathode exhaust gas will produce efficiency penalties corresponding to the expenditures of Process Family III.

### 3.10 Minimum Energy Requirements of CO<sub>2</sub> Capture

Depending on the method used, the minimum energy requirement for CO<sub>2</sub> capture is defined, in the different Process Families, by reversible gas separation (separation of CO<sub>2</sub>, H<sub>2</sub> or O<sub>2</sub>) and ideal CO conversion, or ideal reforming, respectively. Ideal CO conversion, or reforming, is conceivable using a reactor with an endless number of stages, in which steam is added on a constant basis and heat is either released or, in the case of reforming, added (Section 3.5.1, Figure 3.34, Figure 3.35). In this way, a minimal excess of water and optimum heat utilization are guaranteed.

With retention of 90% of the CO<sub>2</sub> from the flue gas of a coal-fired steam power plant, CO<sub>2</sub> flue gas scrubbing using an aqueous MEA solution with a mass fraction of 20% obtains an exergetic efficiency of 14% and an efficiency penalty of approx. 9 percentage points. With reversible CO<sub>2</sub> separation, the efficiency penalty according to Figure 3.86 would be around 1.5 percentage points.

Working on the assumption of reversible gas separation, instead of a physical scrubbing process with an exergetic efficiency of 30.5%, efficiency increases by approx. 2.2 percentage points, as shown in Figure 3.39. This reduces the efficiency penalty from 5.6 to 3.4 percentage points.

Assuming an ideal reactor with an endless number of stages, as against a two-stage reactor, the exergetic efficiency of gas conversion via a CO shift reaction improves from approx. 92.3% (Figure 3.36) to 97.3% (Figure 3.34). According to Figure 3.40, the corresponding 61% reduction in exergy losses in the CO shift reaction would cause the efficiency penalty to drop by around 2.3 percentage points, i.e. increasing plant efficiency by this amount. For an IGCC power plant with reversible CO<sub>2</sub> separation after ideal CO conversion, CO<sub>2</sub> capture would cause efficiency to drop only by around 1.1 percentage points, if CO<sub>2</sub> were separated in gaseous state.

For processes involving combustion in an atmosphere of O<sub>2</sub>/CO<sub>2</sub>, the efficiency penalty can be directly attributed to the energy consumed in generating O<sub>2</sub>. If the energy consumption of an air separation unit (about 0.27 kWh per kg O<sub>2</sub>) is replaced by that of reversible separation of O<sub>2</sub> from air<sup>67</sup> (0.0336 kWh per kg O<sub>2</sub>) (Table 3.13), an efficiency penalty of just 0.5 percentage points is obtained, as against 4 percentage points with a technically feasible air separation unit. If it should become possible to supply O<sub>2</sub> through selective mass transfer of O<sub>2</sub>, this would allow the energy required for O<sub>2</sub> supply to be reduced to a negligible value (theoretically to a minimum of zero).

Comparison with ideal process steps clearly shows that, for CO<sub>2</sub> separation (the gas separation process alone), less energy is required to be expended at higher CO<sub>2</sub> concentrations, than at lower CO<sub>2</sub> concentrations. Theoretically, however, the expenditure of energy to separate O<sub>2</sub> from air for combustion in an atmosphere of O<sub>2</sub>/CO<sub>2</sub> is even lower than any type of CO<sub>2</sub> capture from flue gases or from synthesis gases.

---

<sup>67</sup> i.e. separation from air of the O<sub>2</sub> component alone, and not separation into all components, as in the case of minimum work for air separation.

## 4 ECONOMIC COMPARISON OF POWER PLANT CYCLES WITH CO<sub>2</sub> CAPTURE

This section contains a description of the additional investment and electricity generating costs of CO<sub>2</sub> capture and CO<sub>2</sub> liquefaction for the different process variants, together with a comparison of the resulting CO<sub>2</sub> avoidance costs (Equation 1.4). The section starts with an evaluation of the results of thermodynamic calculations and cost data from published examples of power plant cycles with CO<sub>2</sub> capture. This is then used as a basis for estimating cost trends in dependence on the efficiencies of the baseline power plants.

### 4.1 Procedure

Additional investment  $\Delta K_{CO_2}$  for CO<sub>2</sub> separation is composed of increased investment  $\Delta K_{Basis, CO_2, gaseous}$  for the baseline power plant due to reduced efficiency, and additional investment  $K_{equipment, CO_2 separation}$  in the equipment required for CO<sub>2</sub> separation and CO<sub>2</sub> liquefaction ( $\Delta K_{CO_2 liquefaction}$ ):

$$\Delta K_{CO_2, gaseous} = \Delta K_{Basis, CO_2, gaseous} + K_{equipment, CO_2 separation} \quad (4.1)$$

$$\Delta K_{CO_2, liquid} = \Delta K_{Basis, CO_2, liquid} + K_{equipment, CO_2 separation} + \Delta K_{CO_2 liquefaction} \quad (4.2)$$

At a constant rate of fuel consumption, specific investment  $K_{Basis}$  increases in proportion to the reduction in output by  $\Delta K_{Basis, CO_2, i}$  in relation to the net output of the baseline power plant :

$$\Delta K_{Basis, CO_2, i} = K_{Basis} \cdot \left( \left( \frac{\eta_{Basis}}{\eta_{CO_2, i}} \right)^{\bar{n}} - 1 \right) \quad (4.3)$$

*(i = gaseous, liquid).*

Assuming that the net power output is to be maintained, the lower net efficiency of the power plant means that the size of the baseline power plant must be increased. Where degression exponents  $\bar{n}$  are smaller than 1, the specific fixed-cost component caused by the efficiency penalty becomes smaller.

Investment in the equipment required for CO<sub>2</sub> separation is calculated from the specific investments  $\bar{K}_i$  in individual items of equipment  $i$  used for CO<sub>2</sub> separation, in dependence on the mass flow of the separated CO<sub>2</sub>  $\dot{m}_{CO_2, separated}$  and of the oxygen, which is additionally required for combustion  $\dot{m}_{O_2, additional}$  :

$$K_{equipment, CO_2 separation} = \sum_i \bar{K}_i \cdot \dot{m}_{CO_2, separated} + \bar{K}_{LZA} \cdot \dot{m}_{O_2, additional} \quad (4.4)$$

Specific investment  $\Delta K_{CO_2 liquefaction}$  for CO<sub>2</sub> liquefaction includes not only investment  $K_{equipment, CO_2 liquefaction}$  in the equipment required for liquefaction, but also, due to the additional efficiency penalty, increase  $\Delta K_{equipment, CO_2 separation}$  of the specific investment in the equipment used for CO<sub>2</sub> capture, as set against the separation of gaseous CO<sub>2</sub>:



$$\begin{aligned} \Delta K_{CO_2 \text{ liquefaction}} &= K_{equipment, CO_2 \text{ liquefaction}} + \Delta K_{equipment, CO_2 \text{ separation}} \\ &= K_{equipment, CO_2 \text{ liquefaction}} + K_{equipment, CO_2 \text{ separation}} \cdot \left( \left( \frac{\eta_{CO_2, \text{gaseous}}}{\eta_{CO_2, \text{liquid}}} \right)^{\bar{n}} - 1 \right) \end{aligned} \quad (4.5)$$

The electricity generating costs were calculated using the annuity method under the conditions described in Table 4.2 (Appendix, Section 6.7, [180]). The cost digression exponents  $\bar{n}$  used are given in Table 4.1. Figure 4.1 shows the proportions of the investment and electricity generating costs represented by the individual process steps in CO<sub>2</sub> capture, based on the example case of an IGCC with CO conversion and CO<sub>2</sub> scrubbing, according to the results of the thermodynamic calculations from Section 3.5, Table 3.16.

The CO<sub>2</sub> emissions reduction costs are heavily dependent on which baseline power plant is chosen as the reference case. In this example, the baseline case selected is always the same type of power plant. An alternative way to proceed would be to always relate the CO<sub>2</sub> emissions reduction costs to a steam power plant, for example.

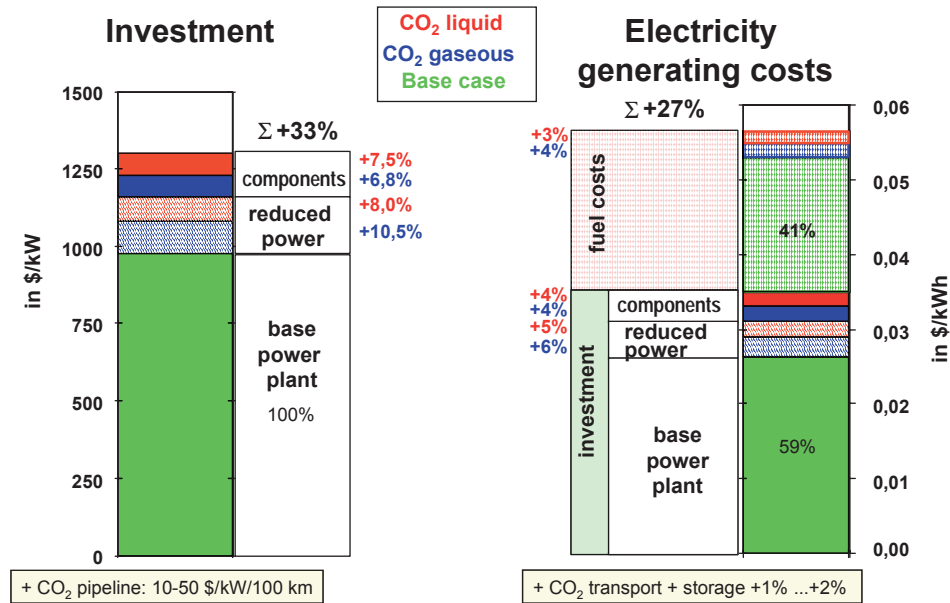


Figure 4.1: How investment and electricity generating costs are divided up for an IGCC with CO conversion and CO<sub>2</sub> scrubbing with a turbine inlet temperature of 1250°C, according to the results taken from Table 3.16 and the costing details given in Table 4.2 and Table 4.5.

Table 4.1: Cost degression exponents  $\bar{n}$  for investment according to Boeddicker [110]

Power Plant / Components	Cost Degression Exponent	Related to Output of
Gas turbine	0.57616	Gas turbine
GTCC power plant (gas/steam turbine combined cycle power plant)	0.8061	GTCC plant
IGCC	0.71221	IGCC plant
Pressurized Pulverized Coal-Fired Combined Cycle	1.09459	Whole plant
Coal-fired steam power plant (Benson boiler)	0.75	Whole plant
Steam turbine	0.76428	Steam cycle
Heat Recovery Steam Generator	0.78255	Steam cycle

Table 4.2: Factors which influence the calculation of electricity generating costs according to the annuity method (for calculation equations, see Appendix, Section 6.7, [180])

Influencing Factors		Unit	
Ta	Utilization factor	(h/a)	7000
nB	Construction period	(a)	3
fE	Client's own contribution as % of plant costs	(%)	5.0%
fZB	Interest rate during construction period (discount rate)	(%/a)	8.0%
fV	Insurance rate over period of operation	(%/a)	2.5%
fe	Increase in fuel prices	(%/a)	1.5%
kb	Fuel costs in base year	(US\$/t)	51
LHV	Heating value of the coal	(MJ/kg)	30
nP	Duration of planning period prior to start of construction	(a)	1
nL	Period of depreciation	(a)	25
fI	General price escalation (inflation)	(%/a)	3.5%
fS	Tax rate during period of construction	(%/a)	0.2%
fW	Standardized rate of maintenance and repair costs + staff costs	(%/a)	2.5%
fZ	Interest rate during period of operation	(%/a)	8.0%
Fuel costs [12]			
coal	1.52 US\$/GJ (44.58 US\$/t coal equivalent, spot market, import price, sulfur <1%, north-west Europe)		
natural gas	2.24 US\$/GJ (65.49 US\$/t coal equivalent, spot market, import price, EU)		

## 4.2 Review of Literature

To allow comparison of the data cited in literature sources at a standardized level of technology, calculations were performed of the additional investment costs, electricity generating costs and CO<sub>2</sub> avoidance costs, on the basis of the results of the thermodynamic analyses of data from the literature pertaining to levels of investment for component groups such as CO conversion, CO<sub>2</sub> scrubbing and air separation units. The costs of component groups are presented in Table 4.3. For all the examples, it is assumed that the same power output should be obtained with and without CO<sub>2</sub> capture, i.e. that the basic component of the power plant with CO<sub>2</sub> capture must be increased by a degree large enough to compensate for the efficiency penalty caused by CO<sub>2</sub> separation and liquefaction. In some cases, missing data on separated CO<sub>2</sub> mass flow was calculated from assumptions concerning the fuel. The deviation of the specific levels of investment calculated in this manner is approximately  $\pm 30\%$  compared with the

data from the literature. In some cases, the cost data contained in the literature itself for the same type of power plant differs by more than 50%.

The specific investment calculated for power plants with CO<sub>2</sub> capture was used to calculate the electricity generating costs for the first year of operation, using the factors given in Table 4.2. The electricity generating costs and the data on specific CO<sub>2</sub> emissions were then used to determine CO<sub>2</sub> avoidance costs, according to Equation 1.44, for CO<sub>2</sub> emissions reduction as compared to the baseline power plant without CO<sub>2</sub> capture. The results obtained from a review of the literature are presented in Figures 4.3 to 4.7. The figures clearly illustrate the wide range over which the costs are spread, due to uncertainties at the current level of technology in the field of CO<sub>2</sub> capture.

Although calculations for MHD combined cycle power plants are to be found in the literature, MHD plants do not fall within the current state of the technology, nor have they been constructed as demonstration facilities. Equally, combined cycle power plants using SOFC or MCFC fuel cells should also be seen as a future option.

In the majority of cases, the additional specific investment (Figure 4.3, Figure 4.4) is primarily caused by the equipment required for CO<sub>2</sub> capture, followed by the additional specific investment resulting from the reduction in efficiency of the baseline power plant. In the majority of cases, these are then followed, in almost equal proportions, by the additional investment in equipment required for CO<sub>2</sub> liquefaction, and for the efficiency penalty due to CO<sub>2</sub> liquefaction.

The rise in electricity generating costs and CO<sub>2</sub> avoidance costs is caused not only by the additional investment (equipment required, and larger baseline power plant) but also, quite substantially, by higher specific fuel consumption. In virtually all cases where electricity generating costs (Figure 4.5, Figure 4.6) and CO<sub>2</sub> avoidance costs (Figure 4.7) increase, the proportion attributable to CO<sub>2</sub> capture is larger than that attributable to CO<sub>2</sub> liquefaction.

The additional investment required, and the increase in electricity generating costs and CO<sub>2</sub> avoidance costs (related to the same type of baseline power plant), are all at their lowest in an IGCC power plant with CO<sub>2</sub> separation after CO conversion. In a comparison of the electricity generating costs, the steam power plant with CO<sub>2</sub> scrubbing from the flue gases is slightly ahead of the rest of the field, although the efficiencies are lower (Figure 4.2, Figure 4.5, Figure 4.6). According to data from the literature, the investment required for the steam power plant is also significantly lower than for the IGCC power plant (Figure 4.3). Finally, with regard to cycles with CO<sub>2</sub> capture using high-temperature fuel cells, the additional levels of investment and CO<sub>2</sub> avoidance costs may indeed be low (based on a comparable power plant, which also uses fuel cells), but the high specific investment required for the baseline power plant nevertheless means that the electricity generating costs are substantially higher than in any of the other variants.

Table 4.3: Specific investment required for the individual components of CO<sub>2</sub> separation, according to a review of the literature. See Table 4.5 for the author's own calculations. (Calculations are based on the specific investment related to the mass flow of CO<sub>2</sub> or O<sub>2</sub>, respectively. The specific investment related to electrical power plant net output merely serves as a reference value illustrating the additional investment in the power plant.)

Process Family I CO <sub>2</sub> Separation From Synthesis Gas After CO Shift			
CO Conversion			
Raw gas CO shift conversion	Clean gas CO shift conversion + Rectisol	Membrane reactor (CO shift conversion + H <sub>2</sub> membrane)	Reforming + CO shift conversion
<i>44-184 US\$/kW</i>	<i>230 US\$/kW</i>	<i>74 US\$/kW</i>	<i>170 US\$/kW</i>
170 – 680 US\$/(t CO <sub>2</sub> /s)	1190 US\$/(t CO <sub>2</sub> /s)	462 US\$/(t CO <sub>2</sub> /s)	1815 US\$/(t CO <sub>2</sub> /s)
CO <sub>2</sub> Separation (synthesis gas under pressure)			
Selexol	DEMEA	MDEA	Polymer membrane (CO/H <sub>2</sub> )
<i>70 – 80 US\$/kW</i>	<i>310 US\$/kW</i>	<i>96 US\$/kW</i>	<i>28 US\$/kW</i>
250 – 360 US\$/(t CO <sub>2</sub> /s)	1130 US\$/(t CO <sub>2</sub> /s)	1590 US\$/(t CO <sub>2</sub> /s)	125 US\$/(t CO <sub>2</sub> /s)
Process Family II CO <sub>2</sub> Concentration in the Waste Gas (flue gas recirculation, O <sub>2</sub> supply)			
Air Separation Unit (O <sub>2</sub> production)	Steam Power Plant: modifications to the boiler	Exhaust gas cooler, flue gas recirculation	
<i>≈60 US\$/kW</i>	<i>≈125 US\$/kW</i>	<i>≈40 US\$/kW</i>	
700 – 2100 US\$/(t O <sub>2</sub> /s)	500 US\$/(CO <sub>2</sub> /s)	300 US\$/(t CO <sub>2</sub> /s)	
Process Family III CO <sub>2</sub> separation from the flue gas (CO <sub>2</sub> scrubbing, chem. absorption with MEA)			
Coal-fired steam power plant (SPP)	Natural gas-fired gas/steam turbine combined cycle power plant		
<i>140 – 460 US\$/kW</i>	<i>250 US\$/kW</i>		
570 1250 US\$/(t CO <sub>2</sub> /s)	2300 US\$/(t CO <sub>2</sub> /s)		
CO <sub>2</sub> Liquefaction, Transport, Sequestration			
CO <sub>2</sub> liquefaction	Pipeline	Sequestration	
<i>30 – 480 US\$/kW</i>	<i>120 – 610 US\$/kW</i>	<i>190 – 215 US\$/kW</i>	
215 – 1930 US\$/(t CO <sub>2</sub> /s)	570 – 2550 US\$/(t CO <sub>2</sub> /s)	570 – 680 US\$/(t CO <sub>2</sub> /s)	

Table 4.4: Description of cases shown in Figures 4.3 to 4.7

No. in Figure	Original Source	Type of Power Plant	CO <sub>2</sub> Separation/Capture
<b>COAL-FIRED CYCLES</b>			
Process Family I: CO <sub>2</sub> separation from synthesis gas after CO shift			
(1)	Condorelli et al. (EPRI)[86]	IGCC, quenching with water	phys. absorption
(2)	Shell [81]	IGCC	chemical absorption
(3)	Pruschek et al. [20]	IGCC	physical absorption
(4)	Hendriks [16]	IGCC	physical absorption
(5)	Daun [87]	IGCC	physical absorption
(6)	Koetzier et al. [17]	IGCC	physical absorption
(7)	Jansen et al. [92, 93]	IGCC	membrane
(8)	Alderliesten et al. [94]	IGCC	membrane reactor
Process Family II: CO <sub>2</sub> concentration in the exhaust gas			
(9)	Hendriks [16]	IGCC	H <sub>2</sub> /CO membrane, GT with air + O <sub>2</sub> /CO <sub>2</sub> GT
(10)	Boeddicker [110]	IGCC	combustion in an atmosphere of O <sub>2</sub> /CO <sub>2</sub>
(11)	v. Steenderen [133]	IGCC	combustion in an atmosphere of O <sub>2</sub> /CO <sub>2</sub>
(12)	v. Steenderen [133]	IGCC	combustion in an atmosphere of O <sub>2</sub> /CO <sub>2</sub>
(13)	McMullan et al. [123]	IGCC hybrid	combustion in an atmosphere of O <sub>2</sub> /CO <sub>2</sub>
(14)	McMullan et al. [123]	SPP	combustion in an atmosphere of O <sub>2</sub> /CO <sub>2</sub>
(15)	IEA GHG [18]	SPP	combustion in an atmosphere of O <sub>2</sub> /CO <sub>2</sub>
(16)	Herzog et al. [124]	SPP	combustion in an atmosphere of O <sub>2</sub> /CO <sub>2</sub>
(17)	Allam et al. [125]	SPP	combustion in an atmosphere of O <sub>2</sub> /CO <sub>2</sub>
(18)	McMullan et al. [123]	MHD	combustion in an atmosphere of O <sub>2</sub> /CO <sub>2</sub>
Process Family III: CO <sub>2</sub> separation from the flue gas			
(19)	McMullan et al. [123]	MHD	chem. absorption with MEA
(20)	McMullan et al. [123]	IGCC hybrid	chem. absorption with MEA
(21)	Hendriks [16]	SPP, MEA	chem. absorption with MEA
(22)	McMullan et al. [123]	SPP, MEA	chem. absorption with MEA
(23)	Smelser et al. [154]	SPP, MEA	chem. absorption with MEA
Process Family V: CO <sub>2</sub> capture with fuel cells			
(24)	McMullan et al. [32]	IGCC/MCFC	before anode (reforming + CO shift conversion + scrubbing)
(25)	McMullan et al. [32]	IGCC/SOFC	CO <sub>2</sub> separation from anode exhaust gas after CO shift conversion
<b>NATURAL GAS-FIRED CYCLES</b>			
Process Family I: CO <sub>2</sub> separation from synthesis gas after CO shift			
(26)	Hille [100]	GTCC (combined cycle) power plant	externally-heated reforming, CO conversion, chem. absorption
(27)	Koerdt [177]	CRGT power plant	recuperatively-heated reforming, CO conversion, chem. absorption
Process Family II: CO <sub>2</sub> concentration in the exhaust gas			
(28)	de Ruyck et al. [145, 146]	REVAP (similar to HAT)	combustion in an atmosphere of O <sub>2</sub> /CO <sub>2</sub>
(29)	Bolland [144]	GTCC power plant (gas/steam turbine combined cycle power plant)	combustion in an atmosphere of O <sub>2</sub> /CO <sub>2</sub>
Process Family III: CO <sub>2</sub> separation from the flue gas			
(30)	Bolland [144]	GTCC power plant	chem. absorption with MEA

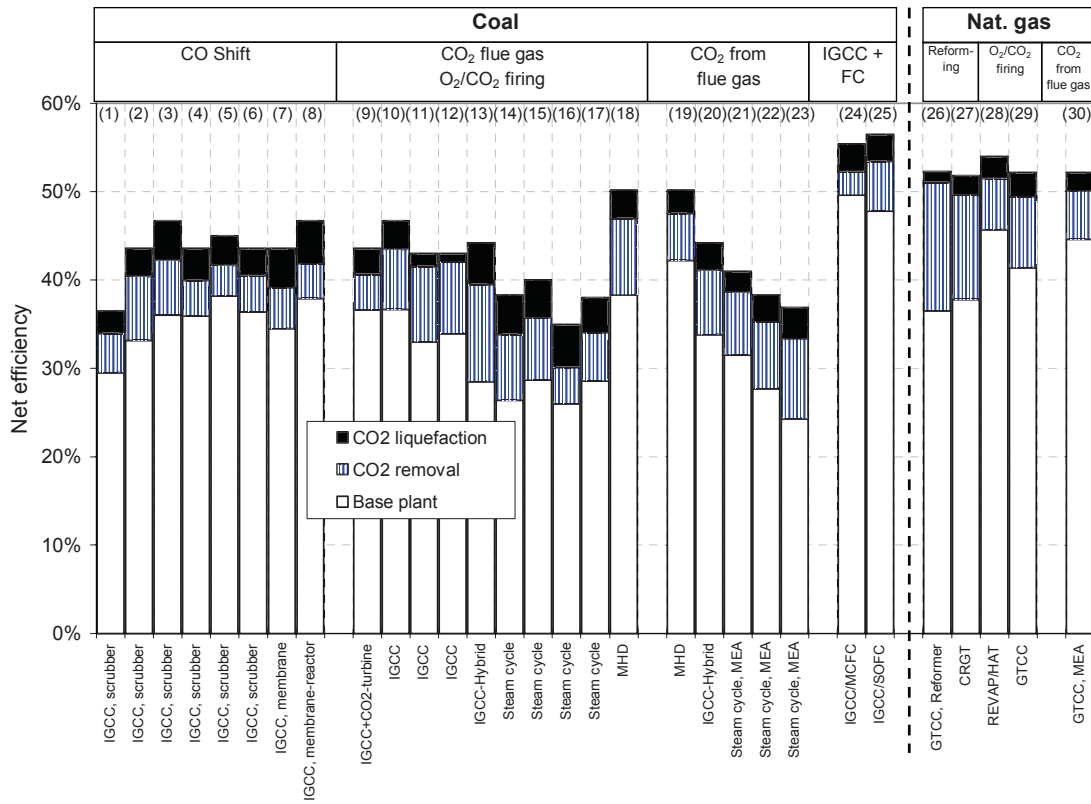


Figure 4.2: Efficiencies of power plants with CO<sub>2</sub> capture and CO<sub>2</sub> liquefaction (review of the literature, Table 4.4)

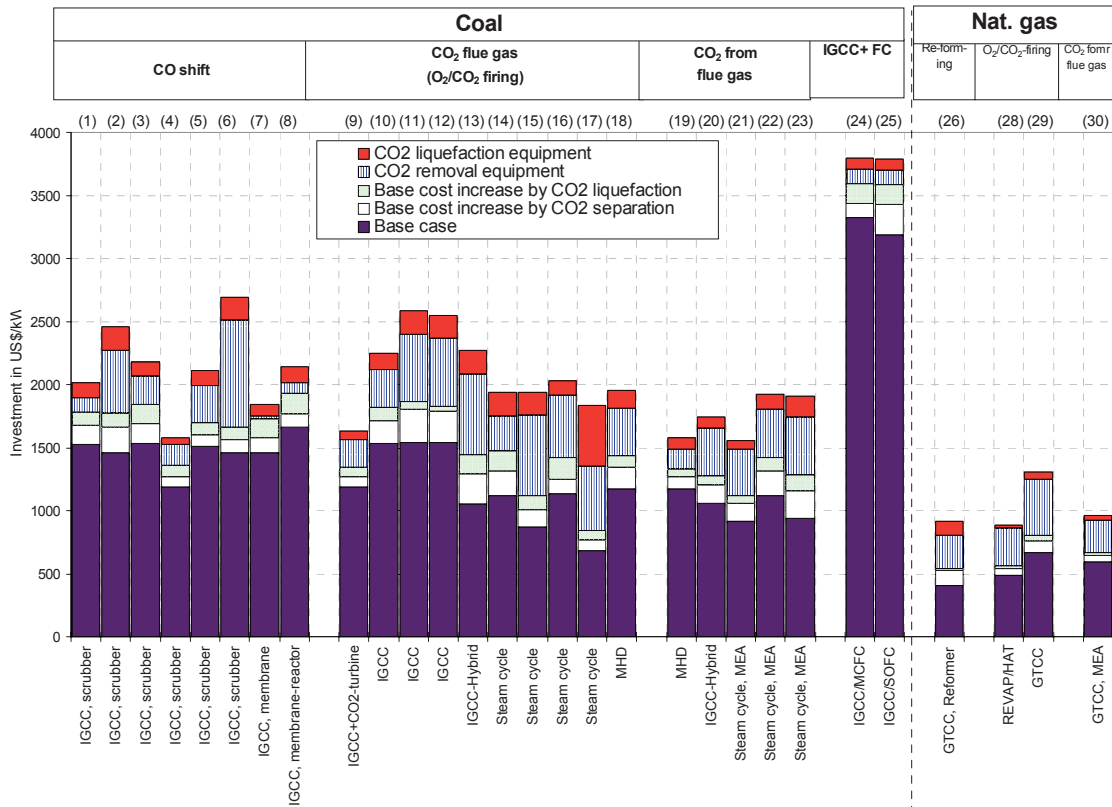


Figure 4.3: Investment required for power plants with CO<sub>2</sub> capture and CO<sub>2</sub> liquefaction (review of the literature, Table 4.4).

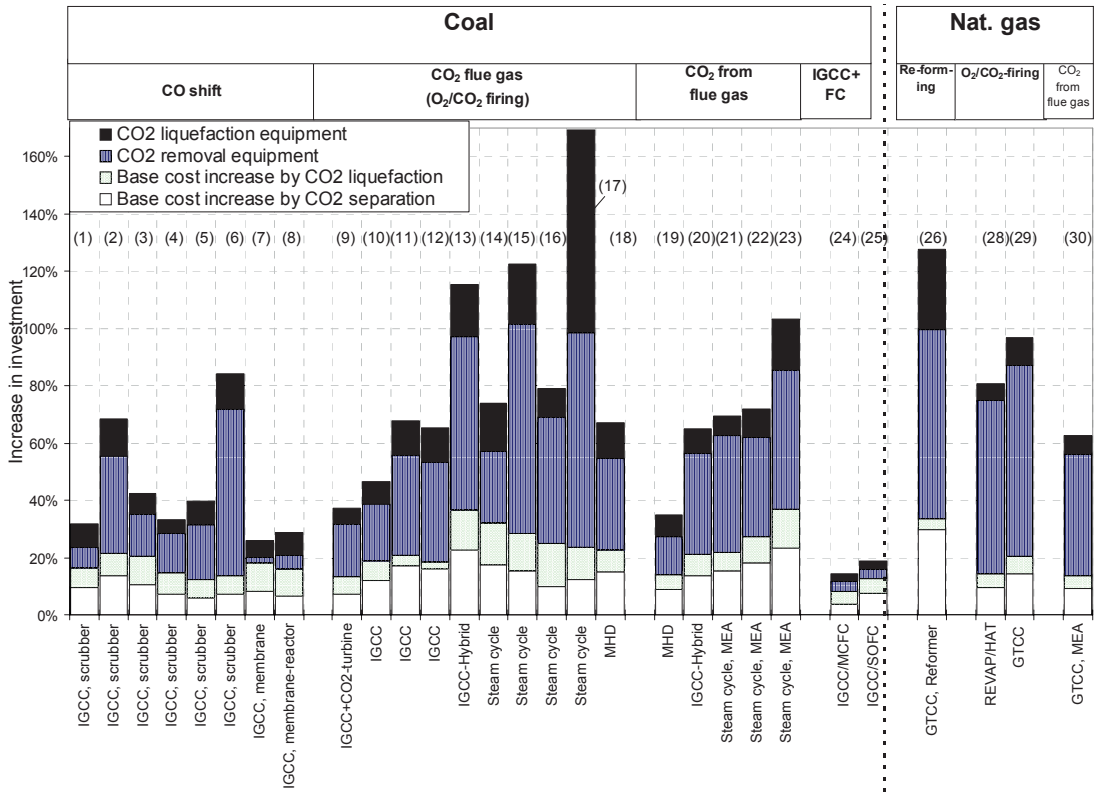


Figure 4.4: Proportions of the specific additional investment represented by CO<sub>2</sub> capture and CO<sub>2</sub> liquefaction (review of the literature, Table 4.4).

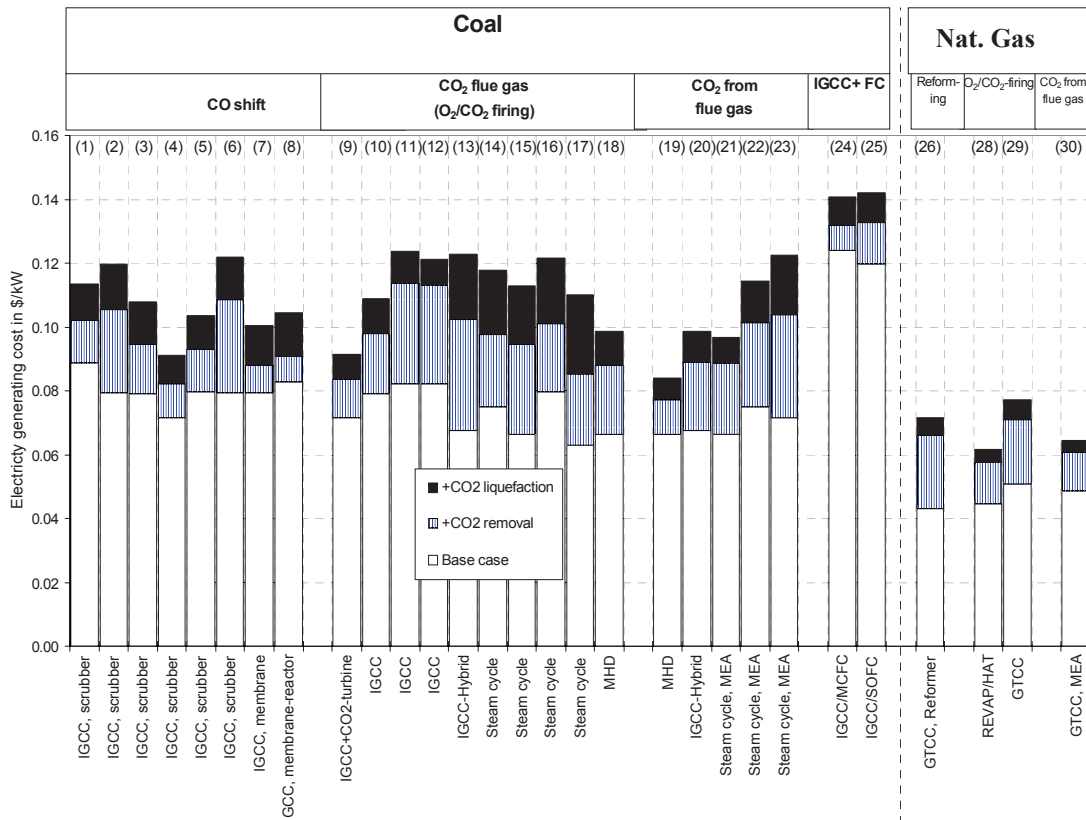


Figure 4.5: Calculated electricity generating costs (review of the literature, Table 4.4)

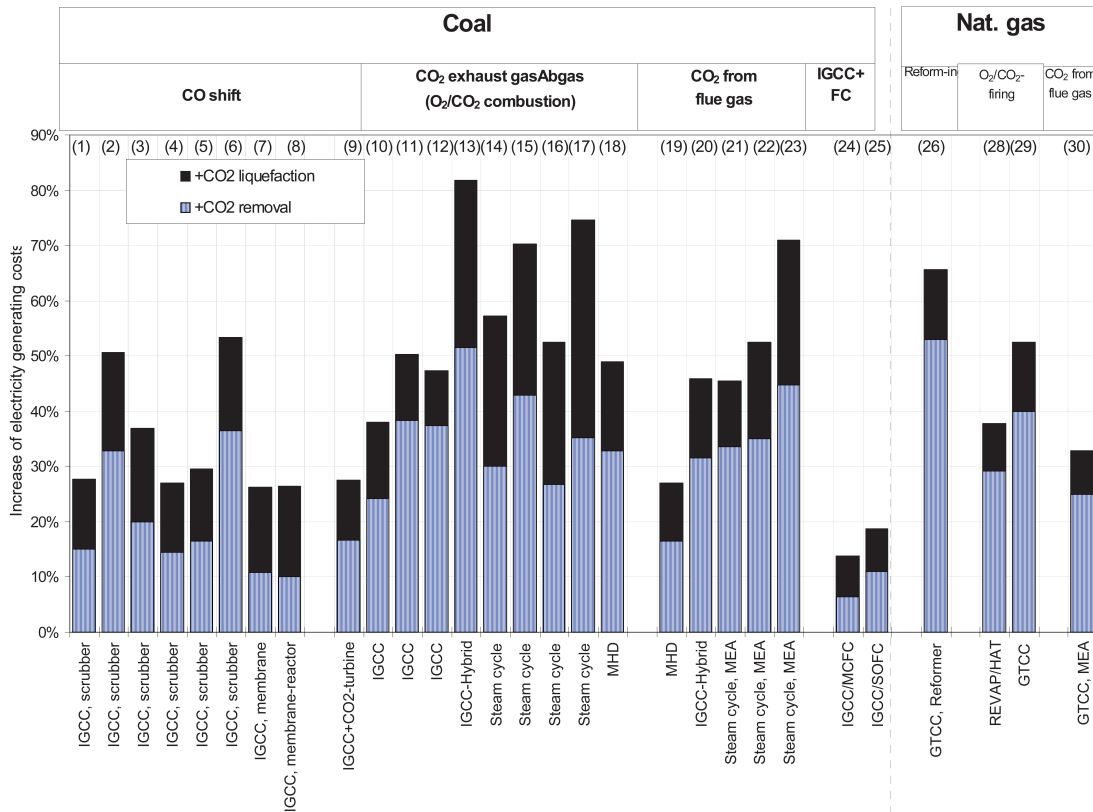


Figure 4.6: Calculated increase in electricity generating costs due to CO<sub>2</sub> capture and CO<sub>2</sub> liquefaction (review of the literature, Table 4.4)

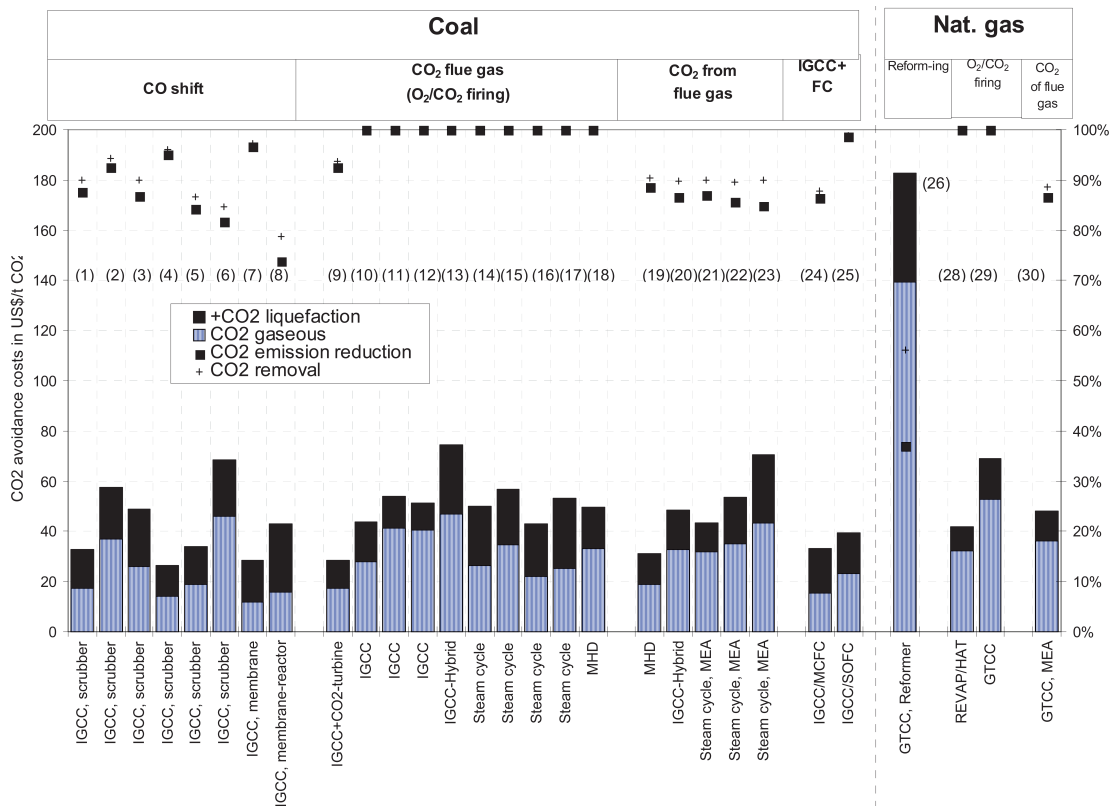


Figure 4.7: CO<sub>2</sub> avoidance costs, base line is the reference power plant of the same type in each case (recalculation using information from the literature on investment and thermodynamic data, Table 4.4)



### 4.3 Development Potential

In the last section, the performance data and overall investment figures presented in the literature sources were used to recalculate the components of the additional investment (in part from assumed partial costs) and to calculate the electricity generating costs and CO<sub>2</sub> avoidance costs under uniform conditions (Table 4.2). The same cost conditions will be used in this section to calculate the cost trend in CO<sub>2</sub> capture from an IGCC power plant, with efficiency improvement of the baseline power plant, according to the results of Section 3, and according to the specific investment described in Table 4.5.

If, in the future, gas turbine inlet temperatures can be raised to around 1500°C, then an IGCC efficiency (without CO<sub>2</sub> capture) of 54% seems achievable (Figure 4.8, results of Section 3). This, in turn, will improve the efficiency of IGCC power plants with CO<sub>2</sub> separation. According to the results of Section 3, the efficiency of an IGCC using a membrane separation method of CO<sub>2</sub> capture is lower than that of variants which use CO conversion and physical scrubbing or combustion in an O<sub>2</sub>/CO<sub>2</sub> atmosphere. For the costing of CO<sub>2</sub> capture in an IGCC power plant, only the IGCC process variants with CO conversion and physical scrubbing, and the IGCC with combustion in an O<sub>2</sub>/CO<sub>2</sub> atmosphere, are compared. For an IGCC power plant featuring combustion in an O<sub>2</sub>/CO<sub>2</sub> atmosphere, a band of values is given, ranging from the current technology of generating O<sub>2</sub> by means of air separation, to an ideal process of O<sub>2</sub> supply without any additional energy requirements (see Section 3.6.2).

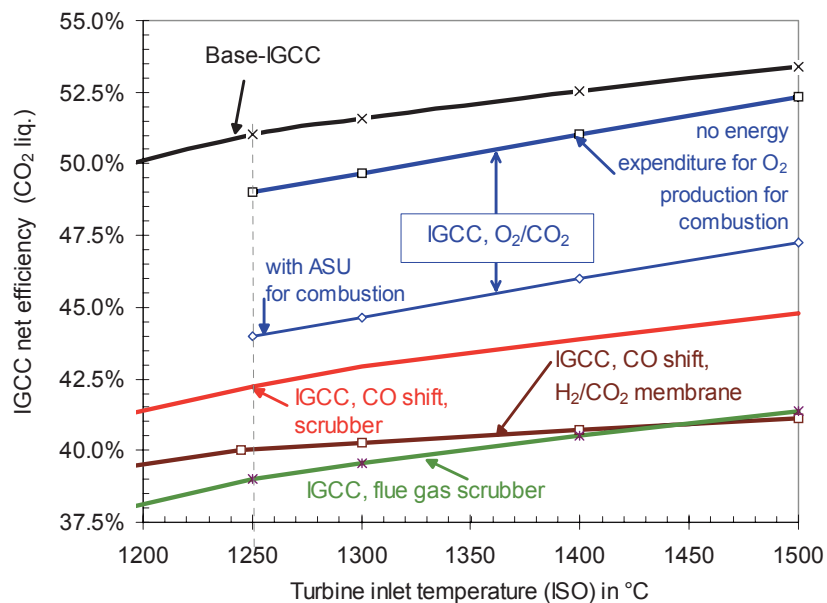


Figure 4.8: Graph showing how IGCC efficiency (with and without CO<sub>2</sub> capture) develops as gas turbine inlet temperature increases (results from Section 3).

Under the assumptions made in this case, specific investment for an IGCC power plant with CO<sub>2</sub> capture after combustion in an O<sub>2</sub>/CO<sub>2</sub> atmosphere, and with an air separation unit, is slightly higher than that of the IGCC with CO conversion and physical scrubbing (Figure 4.9). For an IGCC power plant with CO<sub>2</sub> capture after combustion in an O<sub>2</sub>/CO<sub>2</sub> atmosphere, with a selective oxygen supply which does not require additional energy, it is assumed that the additional investment related to the O<sub>2</sub> mass flow is equivalent to that of an air separation unit. The higher level of efficiency means that the specific investment for this IGCC power plant drops to approximately the value for the IGCC power plant with CO<sub>2</sub> capture by means of CO conversion and physical scrubbing. As the efficiency

of the baseline IGCC power plant increases, a decrease can be seen in the efficiency penalty due to CO<sub>2</sub> capture as a proportion of the gross power output of the power plant. Consequently, the specific investment required for the IGCC power plant with CO<sub>2</sub> capture also decreases slightly (Figure 4.9). Additionally, as the efficiency of the baseline IGCC power plant improves, there is also a drop in electricity generating costs (Figure 4.10) and CO<sub>2</sub> avoidance costs (Figure 4.11).

At current levels of technology of CO<sub>2</sub> capture from IGCC power plants, the variant with CO conversion and physical scrubbing is more economical than the variant with air separation and combustion in an O<sub>2</sub>/CO<sub>2</sub> atmosphere. Moreover, the CO<sub>2</sub> gas turbine for this latter variant is not yet commercially available, since the technology has not yet been developed.

If it should become possible to implement O<sub>2</sub> supply without any additional energy requirements, and if a CO<sub>2</sub> gas turbine should become available, the only remaining energy requirements would be for CO<sub>2</sub> liquefaction; the IGCC power plant with combustion in an O<sub>2</sub>/CO<sub>2</sub> atmosphere would then achieve the lowest costs of CO<sub>2</sub> capture in fossil fuel-fired power plants, based on the assumptions described, even if the additional investment were similar to that of the alternative air separation unit.

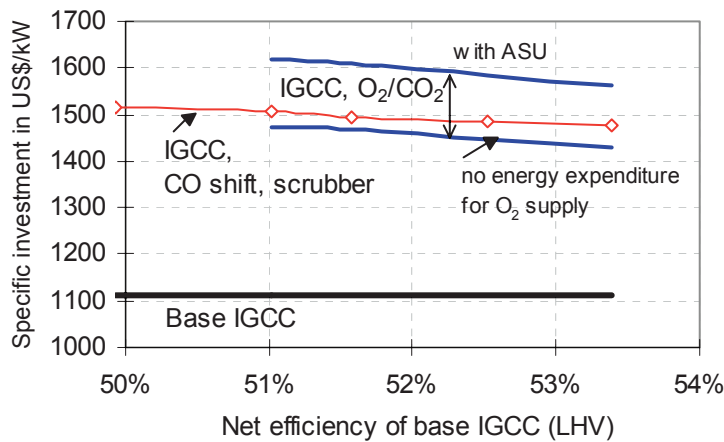


Figure 4.9: Specific investment for an IGCC power plant with CO conversion and CO<sub>2</sub> scrubbing, and an IGCC power plant with combustion in an O<sub>2</sub>/CO<sub>2</sub> atmosphere, in dependence on the efficiency of the baseline IGCC power plant without CO<sub>2</sub> capture

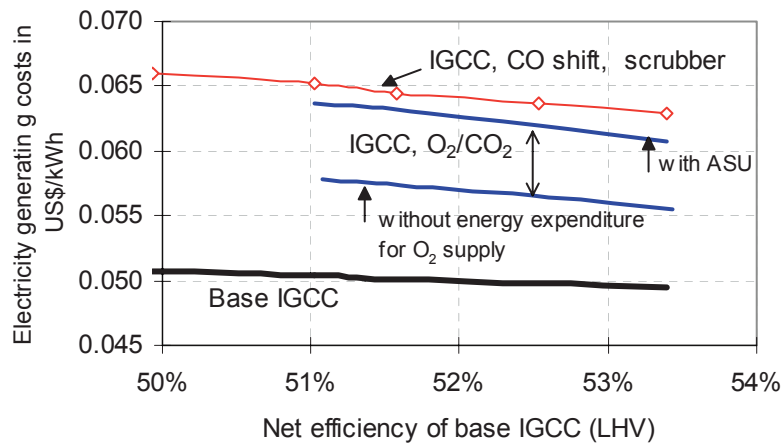


Figure 4.10: Electricity generating costs in an IGCC power plant with CO conversion and CO<sub>2</sub> scrubbing, and an IGCC power plant with combustion in an O<sub>2</sub>/CO<sub>2</sub> atmosphere, in dependence on the efficiency of the baseline IGCC power plant without CO<sub>2</sub> capture

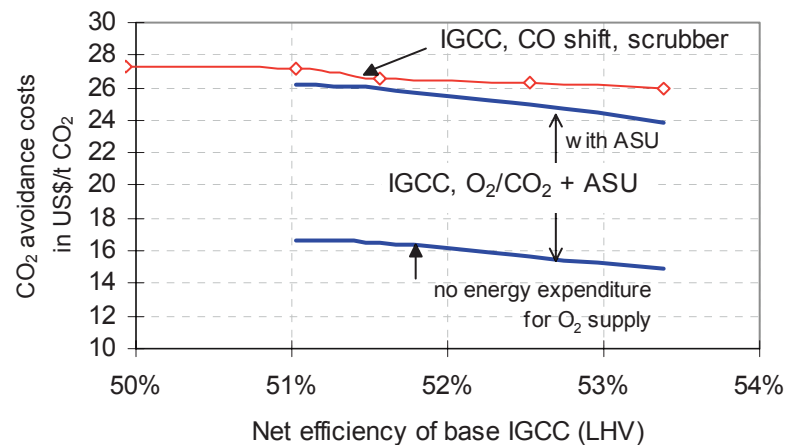


Figure 4.11: CO<sub>2</sub> avoidance costs in an IGCC power plant with CO conversion and CO<sub>2</sub> scrubbing, and an IGCC power plant with combustion in an O<sub>2</sub>/CO<sub>2</sub> atmosphere, in dependence on the efficiency of the baseline IGCC power plant without CO<sub>2</sub> capture

Table 4.5: Assumed specific level of investment for baseline power plants and components of CO<sub>2</sub> capture

Power plants without CO <sub>2</sub> separation:	
Steam power plant (hard coal)	1050 US\$/kW
IGCC power plant	1110 US\$/kW
Gas/steam turbine combined cycle power plant	510 US\$/kW
Components of CO <sub>2</sub> capture:	
CO conversion	170000 US\$/(kg CO <sub>2</sub> /s)
CO <sub>2</sub> scrubbing - Selexol	280000 US\$/(kg CO <sub>2</sub> /s)
CO <sub>2</sub> scrubbing - MEA	1400000 US\$/(kg CO <sub>2</sub> /s)
Air Separation Unit (ASU) or selective O <sub>2</sub> supply (without additional energy requirements)	1700000 US\$/(kg O <sub>2</sub> /s)
Other, e.g. CO <sub>2</sub> recycling, piping	110000 US\$/(kg CO <sub>2</sub> /s)
CO <sub>2</sub> compression, liquefaction	500000 US\$/(kg CO <sub>2</sub> /s)

#### 4.4 Comparison with Alternative Measures

The CO<sub>2</sub> avoidance costs due to CO<sub>2</sub> capture in power plants have been calculated as lying between 20 and 45 US\$ /t CO<sub>2</sub>. These figures do not include the cost of CO<sub>2</sub> transport and disposal. The transport cost, of between 6 and 8 US\$ /t CO<sub>2</sub> for a pipeline length of 1000 km, and the cost of disposal, amounting to between 1 and 6 US\$ /t CO<sub>2</sub>, must therefore be added to the figures for CO<sub>2</sub> avoidance costs (see Table 2.3). Thus, CO<sub>2</sub> avoidance costs for CO<sub>2</sub> capture in power plants and CO<sub>2</sub> disposal lie between 29 and 59 US\$ /t CO<sub>2</sub>.

Through measures such as switching to CO<sub>2</sub>-lean fuels, cogeneration efficiency improvement, and increased building of nuclear power plants, CO<sub>2</sub> emissions reductions of between approximately 8% and 14.5% can be achieved (Appendix, Table 6.20). Depending on the method used, CO<sub>2</sub> capture in power plants can result in CO<sub>2</sub> emissions from power plants being reduced by anywhere between 80% and virtually 100%. Since power plants are only one of the factors contributing to global CO<sub>2</sub> emissions (currently around 20%), the contribution towards the global reduction of CO<sub>2</sub> emissions is correspondingly lower, even if CO<sub>2</sub> capture is performed in all power plants.

CO<sub>2</sub> capture in power plants is only likely to be implemented at the point where a reduction in CO<sub>2</sub> emissions can no longer be achieved more economically using other means. According to information provided by the IW (*Institut der deutschen Wirtschaft* = Institute for Business Research), CO<sub>2</sub> avoidance costs in Germany are likely to be as follows, depending on the reduction targets [181]:

- Reducing CO<sub>2</sub> emissions in Germany by 10% would incur a reduction cost per ton of CO<sub>2</sub> of around 22 US\$.
- Reducing CO<sub>2</sub> emissions by 25% would push the cost of this reduction up to 348 US\$ per ton of CO<sub>2</sub> avoided.

For CO<sub>2</sub> emissions reduction targets of around 10%, it would therefore also be sensible to ascertain the costs of other measures for CO<sub>2</sub> emissions reduction. It is hard to estimate the cost of energy savings, where these go beyond an increase in the efficiency of energy conversion systems, e.g. factors such as avoidance of energy usage. With a saving of up to 25% of primary energy, reducing CO<sub>2</sub> emissions by improving thermal insulation in housing, through retrofitting, can be essentially self-financing. Achieving a higher rate of energy savings incurs costs of up to 369 US\$ /t CO<sub>2</sub>, depending on the intensity of the measure [87]. According to Pruschek et al. [19], specific CO<sub>2</sub> avoidance costs of between 4.3 and 26 US\$ /t CO<sub>2</sub> can be calculated for efficiency-improving retrofitting measures, which need not, however, lead to an increase in electricity generating costs, assuming that the fuel savings obtained through improved efficiency compensate for the additional investment. Replacing coal-fired power plants with wind energy converters having electricity generating costs of between 0.09 and 0.17 US\$ /kWh incurs estimated CO<sub>2</sub> avoidance costs of between 82 and 204 US\$ /t CO<sub>2</sub> [182]. The use of photovoltaics, with electricity generating costs of between 0.9 and 1.1 US\$ /kWh, incurs CO<sub>2</sub> avoidance costs of between 850 and 1200 US\$ /t CO<sub>2</sub>. In the context of negotiations on future reductions in CO<sub>2</sub> emissions, discussion has also focused on the trading of CO<sub>2</sub> emissions rights certificates at prices of between around 3 and 30 US\$ per ton CO<sub>2</sub> [183]. Other measures of reducing CO<sub>2</sub> emissions would also have to compete with this approach.

If CO<sub>2</sub> emissions were required to be reduced by 25%, CO<sub>2</sub> capture in power plants could certainly represent a cost-effective measure.

## 5 SUMMARY

In order to prevent, in the long term, CO<sub>2</sub> concentration in the earth's atmosphere exceeding a proportion by volume of 500 ppm, as against the current figure of 360 ppm, projected worldwide CO<sub>2</sub> emissions would have to be cut by around 40% as early as the year 2025. If other possible ways of reducing CO<sub>2</sub> emissions (e.g. improvements in energy efficiency and a switch to low-carbon or carbon-free fuels and primary energy sources) prove to be insufficient in the future, CO<sub>2</sub> capture in power plants could serve as an additional method, which could contribute to the reduction or avoidance of these CO<sub>2</sub> emissions. This study presents a survey of the methods of CO<sub>2</sub> capture in power plants which are currently under discussion, together with an energy analysis of the individual methods and an assessment of specific CO<sub>2</sub> emissions, the efficiency penalty due to CO<sub>2</sub> capture, additional investment required, additional electricity generating costs incurred, CO<sub>2</sub> avoidance costs and technical feasibility.

For the sake of clarity, the numerous possible variations on processes for CO<sub>2</sub> capture in power plants have been divided up into five process families:

- Process Family I: CO<sub>2</sub> separation from synthesis gases after CO shift reaction (from coal gasification or steam reforming of natural gas),
- Process Family II: CO<sub>2</sub> concentration in the exhaust gas (mostly through combustion in an atmosphere of oxygen and recirculated flue gas),
- Process Family III: CO<sub>2</sub> separation from flue gases,
- Process Family IV: Carbon separation prior to combustion (not calculated in this study),
- Process Family V: CO<sub>2</sub> capture in power plants using fuel cells (not calculated in this study).

In high-efficiency power plants, less primary energy is consumed and less CO<sub>2</sub> is produced. As efficiency increases, with power output remaining the same, the CO<sub>2</sub> mass flow to be separated become smaller, which, in turn, means that the utilization of energy and equipment for CO<sub>2</sub> capture also become smaller. The calculations in this study therefore primarily focus on those power plants, which currently have the greatest efficiency potential, namely the natural gas-fired gas/steam turbine combined cycle power plant (GTCC power plant) and the GTCC power plant with integrated coal gasification (IGCC). Fuel cell power plants with higher efficiencies, and a theoretically low expenditure of energy required for CO<sub>2</sub> capture, are a future option, offering a potential for CO<sub>2</sub> capture which is sketched out only briefly in this study.

Using as a basis the numerous published investigations of CO<sub>2</sub> capture in power plants, the particular characteristics of the various combinations of different types of power plant and gas separation method are considered, and criteria for assessing the different processes are elaborated. Comprehensive review of the literature shows that the cited efficiencies of power plants with CO<sub>2</sub> capture are spread over a wide range, as are the efficiency penalties due to CO<sub>2</sub> capture; as a result, it is difficult to ascertain the differences between the various methods of CO<sub>2</sub> capture and between the different types of power plant. The majority of the published studies of CO<sub>2</sub> capture in power plants also fail to provide a detailed analysis of the energetics.

When comparing the energy expended on CO<sub>2</sub> capture, and the efficiency penalties and additional costs incurred in this process, various points must be observed, such as standard boundary conditions, e.g. the inclusion of CO<sub>2</sub> liquefaction.

According to the results of the literature review and to calculations carried out by the author of this study (Figure 5.1), the capture and liquefaction of between 85% and 95%, or virtually 100% (Process Family II), of the CO<sub>2</sub> produced through fuel burning results in an efficiency penalty of between approx. 7 and 11 percentage points for IGCC power plants according to Process Family I or coal-fired power plants according to Process Family II. In the case of CO<sub>2</sub> separation from flue gases in coal-fired cycles, the efficiency penalty lies between approx. 11 and 14 percentage points. Even in the most advantageous case, removal of the carbon from the fuel (Process Family IV) results in an efficiency penalty of 18 percentage points. Efficiency penalties of between 6 and 9 percentage points are given for CO<sub>2</sub> capture in power plants using fuel cells (Process Family V) with integrated coal gasification.

More energy is used, per separated CO<sub>2</sub> mass, for CO<sub>2</sub> capture in natural gas-fired power plants than in coal-fired cycles. However, the lower proportion of carbon in natural gas means that the efficiency penalty is smaller. The efficiency of a gas/steam turbine combined cycle power plant is reduced by approx. 9 percentage points by CO<sub>2</sub> scrubbing after reforming (which is heated through partial combustion of natural gas), CO conversion and subsequent CO<sub>2</sub> liquefaction. With combustion in an atmosphere of O<sub>2</sub> and recirculated CO<sub>2</sub>, the efficiency penalty lies between 8 and 11 percentage points, and for CO<sub>2</sub> separation from flue gases through scrubbing, the efficiency penalty lies between approx. 7 and 13 percentage points. In natural gas-fired fuel cell power plants, too, CO<sub>2</sub> separation from the cathode exhaust gas following combustion of the anode exhaust gas also seems to be the most advantageous method.

If CO<sub>2</sub> avoidance costs and technical feasibility are included, the following methods prove to be advantageous: for coal-fired cycles, the concept of separating CO<sub>2</sub> from synthesis gases after CO conversion in an IGCC power plant (Process Family I) and, for natural gas-fired power plants, the concept of separating CO<sub>2</sub> from the flue gases (Process Family III) of gas/steam turbine combined cycle power plants. In the case of coal-fired power plants with CO<sub>2</sub> separation according to Process Family II, the CO<sub>2</sub> avoidance costs are only marginally higher. Nevertheless, a gas turbine cycle optimized for CO<sub>2</sub> as a working fluid, together with the necessary components for this process, would first have to be developed.

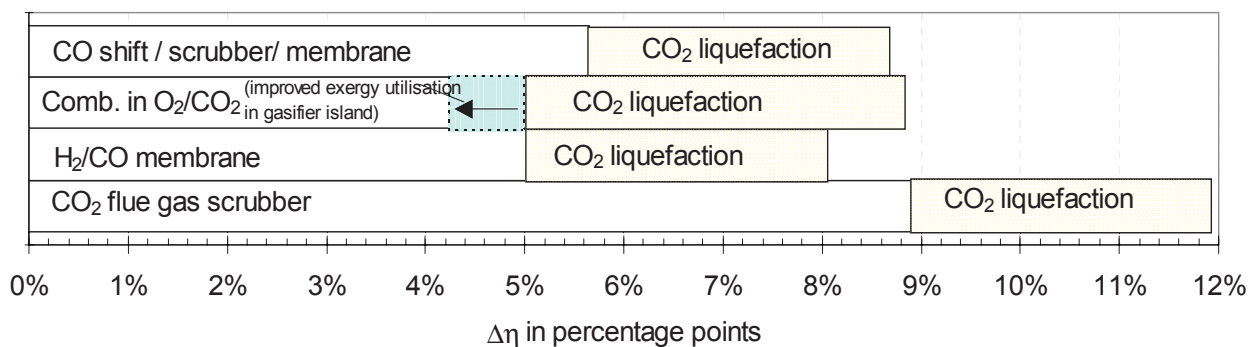


Figure 5.1: Comparison of the efficiency penalty due to CO<sub>2</sub> capture in an IGCC power plant with CO conversion, with combustion in an O<sub>2</sub>/CO<sub>2</sub> atmosphere with O<sub>2</sub> generation by means of air separation, with combustion of the CO component in an O<sub>2</sub>/CO<sub>2</sub> atmosphere after H<sub>2</sub>/CO separation and CO<sub>2</sub> separation from the flue gas (without CO<sub>2</sub> liquefaction)

The minimum energy required for gas separation is determined by the reversible separation work. With the aid of reversible separation work, it can be shown that, the higher the concentration of the gas component to be separated, the lower the energy expended on gas separation. To calculate the

exergetic efficiency of real gas separation processes, in terms of the ratio of reversible separation work to the actual expenditure of energy in a real gas separation process, information on energy requirements was taken from the literature, and from research carried out by the author of this study. For this purpose, calculation models were developed for physical and chemical scrubbing, adsorption, low-temperature processes and membranes. According to these calculations, physical adsorption processes and membrane separation processes achieve the highest exergetic efficiency for  $H_2/CO_2$  separation in synthesis gases, at between 20% and 31%; for  $CO_2$  separation from flue gases, the highest exergetic efficiency, of up to approx. 21%, is achieved by chemical scrubbing. Further calculations show the contributions of the individual process steps towards the efficiency penalty due to  $CO_2$  capture (Figure 5.2).

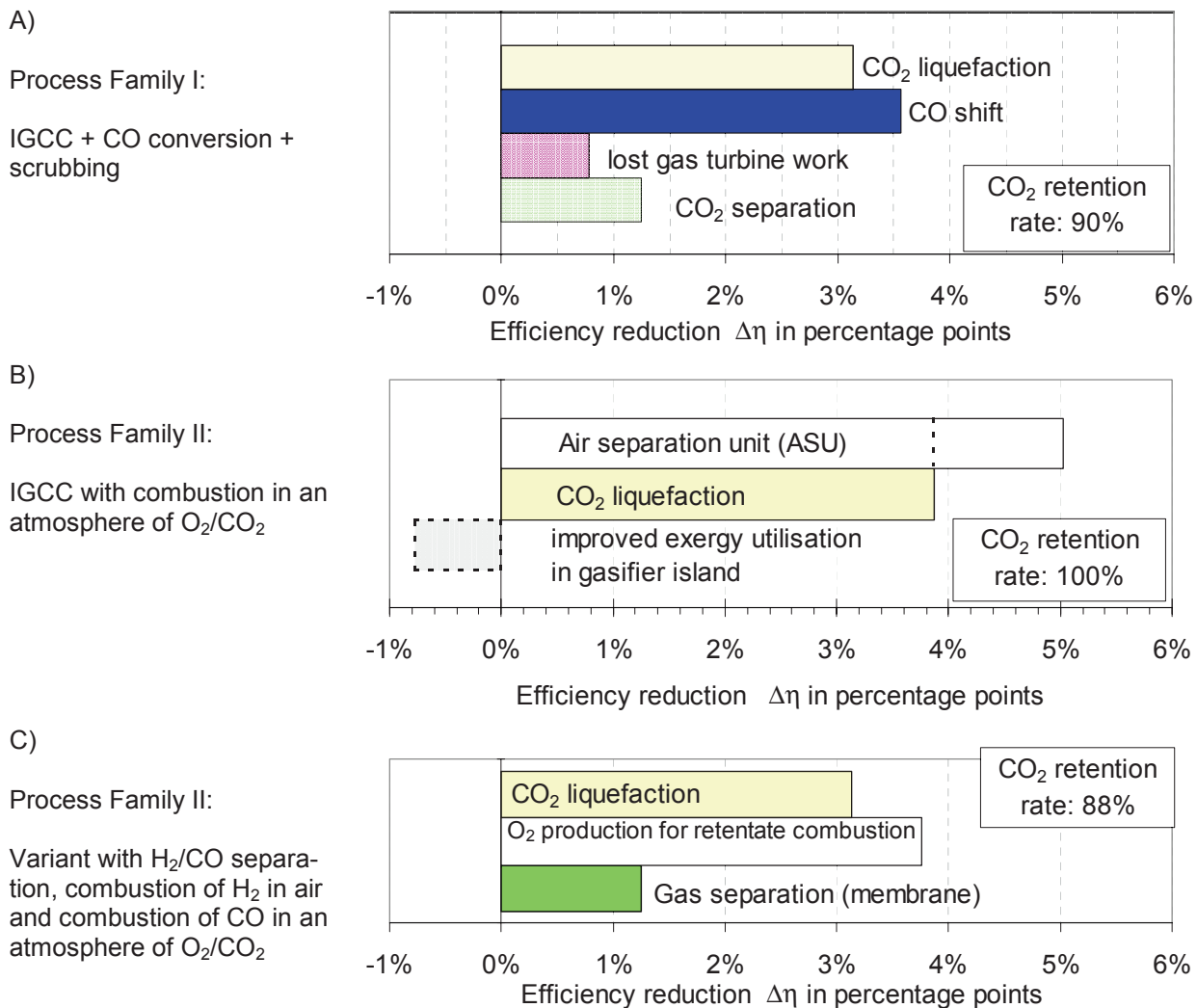


Figure 5.2: Comparison of the contributions of individual process steps to the efficiency penalty due to  $CO_2$  capture in (A) an IGCC power plant with CO conversion, (B) an IGCC power plant with combustion in an  $O_2/CO_2$  atmosphere and (C) an IGCC power plant with  $H_2/CO$  separation, combustion of  $H_2$  in air and CO in an  $O_2/CO_2$  atmosphere

CO<sub>2</sub> liquefaction makes a contribution of between 3 and 4 percentage points to the reduction in the net efficiency of a power plant. In Process Family I, the contribution of fuel conversion through CO conversion towards the reduction in power plant efficiency is around 3.6 percentage points, for gas separation approx. 1.2 percentage points, and for the non-realized expansion work of the separated CO<sub>2</sub> approx. 0.8 percentage points.

In Process Family II, the largest component of the efficiency penalty (5 percentage points) is caused by the expenditure of energy for O<sub>2</sub> generation. Calculations for Process Family II with various cycles using CO<sub>2</sub> as a working fluid (Gohstjejn cycle, quasi-combined cycle, gas/steam turbine combined cycle power plant) do not show any significant differences in levels of efficiency, as long as the optimum pressure ratios, with regard to efficiency, are set in each case (which is always higher than in cycles using air as a working fluid). For the example of gas/steam turbine combined cycle power plants which use air or CO<sub>2</sub> as a working fluid, it was demonstrated that the only difference with ideal gases lies in a shift of the pressure ratio. In IGCC power plants with combustion in an O<sub>2</sub>/CO<sub>2</sub> atmosphere (Process Family II), an increase in gasifier pressure can, however, result in better exergy utilization in the gas generation process.

The additional exergy losses due to CO<sub>2</sub> capture mainly comprise the lost exergy of the separated CO<sub>2</sub> itself (Figure 5.3). The CO<sub>2</sub> liquefaction and gas separation stages also make smaller contributions to these losses.

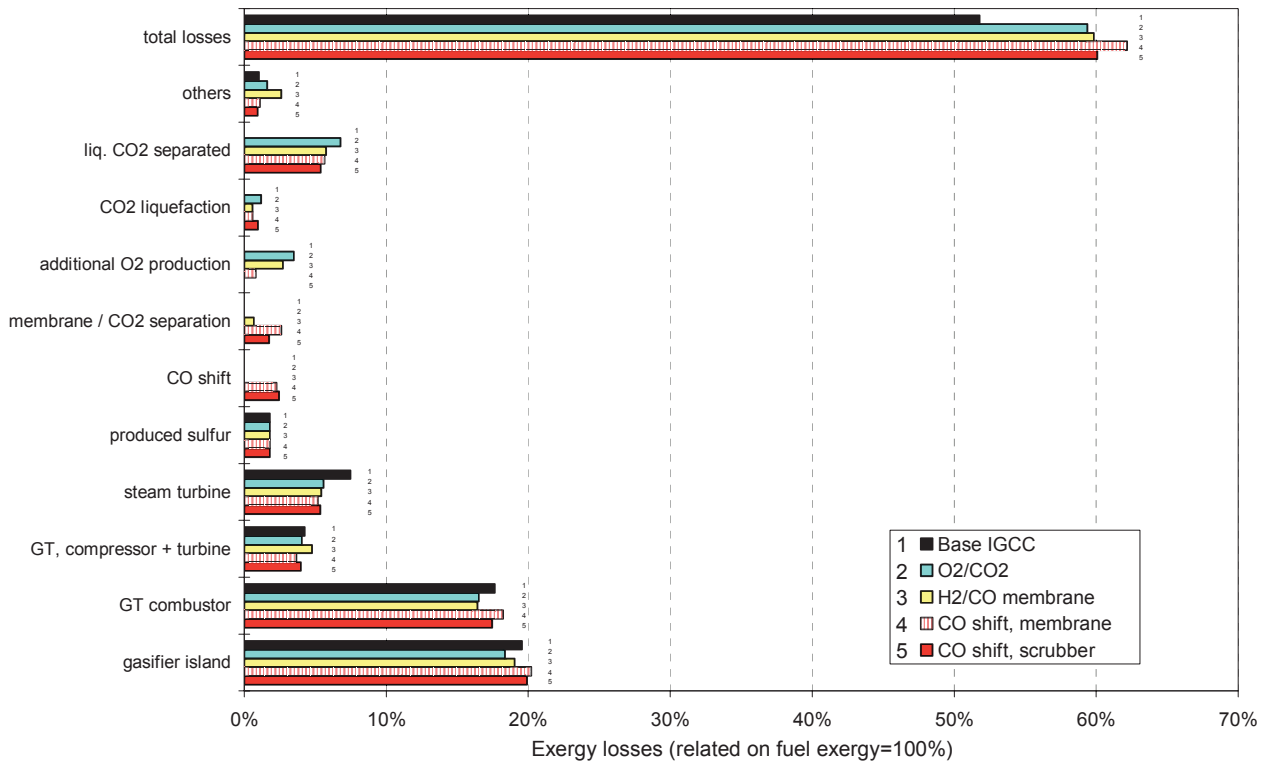


Figure 5.3: Exergy losses in the baseline IGCC power plant and in the IGCC variants with CO<sub>2</sub> capture through CO<sub>2</sub> separation after CO conversion, combustion in an O<sub>2</sub>/CO<sub>2</sub> atmosphere or combustion of the CO component in an O<sub>2</sub>/CO<sub>2</sub> atmosphere after H<sub>2</sub>/CO separation

CO<sub>2</sub> capture with reversible process steps represents the ideal case of CO<sub>2</sub> capture in power plants, and can also reveal the longer-term efficiency potential. The efficiency penalty is determined through precise process calculations and the comparison of the individual contributions of ideal process steps. The most favorable variant in this case, in terms of energy expenditure, would here be found in the



case of combustion in an O<sub>2</sub>/CO<sub>2</sub> atmosphere, with an efficiency penalty of just 0.5 percentage points, if the oxygen could be provided through reversible gas separation, followed by an IGCC power plant with CO conversion and CO<sub>2</sub> scrubbing (1.1 percentage points). The variant having the highest reversible separation work for CO<sub>2</sub> capture in coal-fired cycles is CO<sub>2</sub> separation from the flue gas (1.5 percentage points).

Regarding the processes described under Process Family II, it would theoretically be possible, in an ideal case, to provide O<sub>2</sub> for the combustion process without any additional expenditure of energy, if it were possible to implement a selective mass transfer of the O<sub>2</sub> from the ambient air into recirculated flue gas, in which the O<sub>2</sub> partial pressure lay close to zero, instead of generating a technically pure O<sub>2</sub> stream. This would make it possible to capture gaseous CO<sub>2</sub>, in an ideal case, without any additional expenditure of energy or efficiency penalty.

CO<sub>2</sub> emissions can also be reduced using other means, such as switching to CO<sub>2</sub>-lean or CO<sub>2</sub>-free primary energy sources, increasing efficiency, implementing efficient energy conservation measures, or avoiding energy use. Some of these measures -- particularly, at the present time, switching the primary energy carrier from coal to natural gas -- are more economical than CO<sub>2</sub> capture, with CO<sub>2</sub> avoidance costs of between 20 and 45 US\$ /t CO<sub>2</sub>, including CO<sub>2</sub> liquefaction, to which must be added the costs of CO<sub>2</sub> transport and CO<sub>2</sub> disposal, amounting to between around 7 and 14 US\$ /t CO<sub>2</sub> (based on a 1000 km pipeline length). This means that, working on the basis of global CO<sub>2</sub> emissions reduction targets of over 10%, CO<sub>2</sub> capture in electricity generation can only be judged to be of economic interest once the potential for a reduction in CO<sub>2</sub> emissions, which is posed by the more economical measures, has already been fully exploited. Until that point is reached, CO<sub>2</sub> capture will only be used in special cases in a relatively small number of power plants, e.g. to enhance oil and gas production (EOR), to enable CO<sub>2</sub> fertilization in greenhouses, for cost-related political reasons as a consequence of tax on CO<sub>2</sub> emissions, as in the case of Norwegian oil production, or to cover industrial demand for CO<sub>2</sub>.

CO<sub>2</sub> capture in power plant should therefore be viewed as a future option, which could come into practical use on a large-scale in 20 to 30 years time, and which could then be used to significantly reduce CO<sub>2</sub> emissions, serving as an interim solution on the path towards carbon-free power supply.

## 6 APPENDIX

### 6.1 Supplementary Information on the Climate Issue

As far back as the last century, scientists such as Fourier (in 1827) and Arrhenius (in 1896) referred to the natural greenhouse effect of the earth's atmosphere, without which the average temperature of the earth's surface would, according to current calculations, be around 33 K lower (average temperature is presently approx. 15°C). The most important natural greenhouse gas is water vapor, followed by CO<sub>2</sub> and ozone.

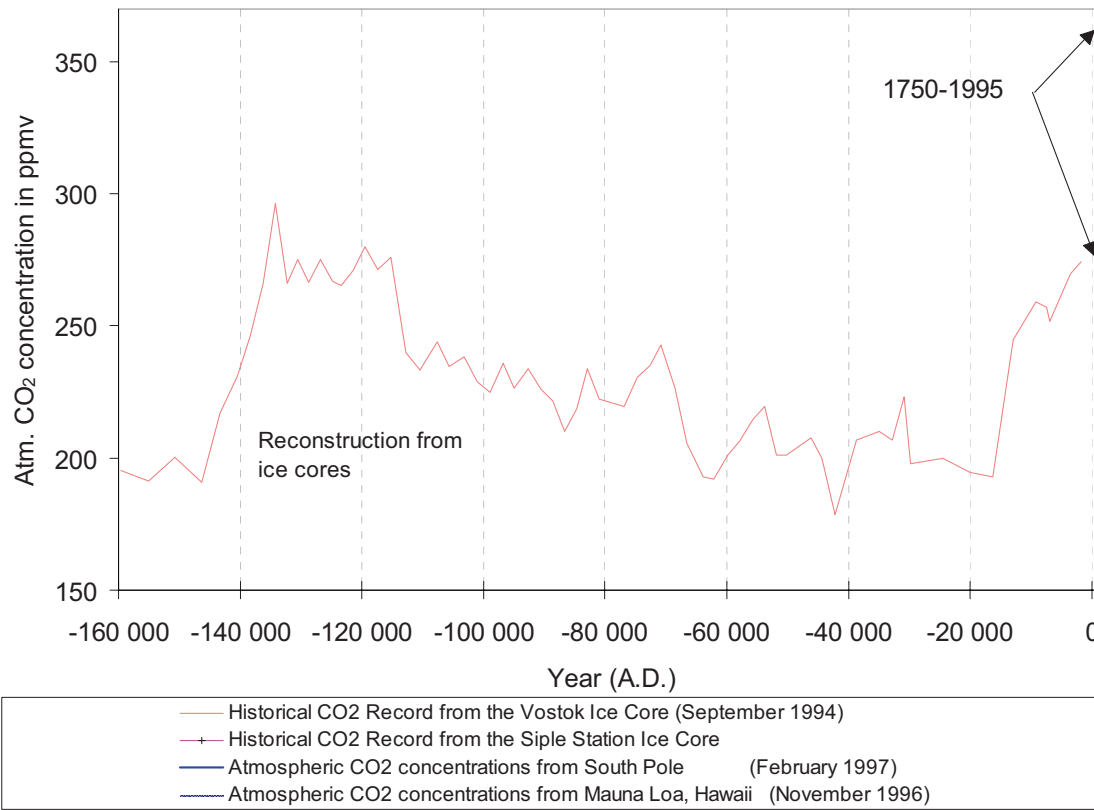


Figure 6.1: Development of CO<sub>2</sub> concentration in the earth's atmosphere from 160,000 B.C. to 1995 [184, 185, 186, 187]

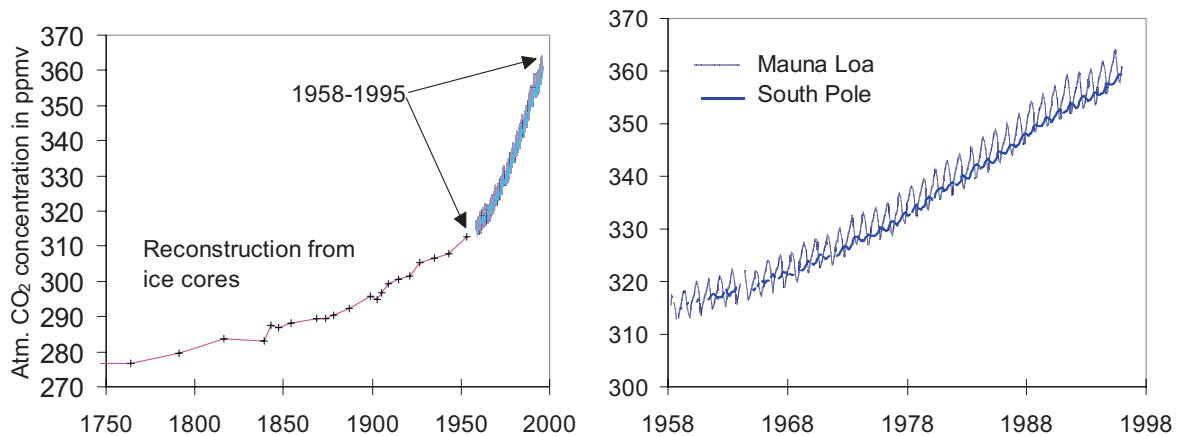


Figure 6.2: Excerpts from Figure 6.1: 1750 to 1995 and 1958 to 1995

Findings presented by the "Intergovernmental Panel on Climate Change" (IPCC) suggest there is a "discernible" human influence on world climate [10]. Indeed, average global temperature has already risen by between 0.3 and 0.6 K since the 19th century, and has contributed, to a large extent, to the rise of between 10 and 25 cm in sea level over the last 100 years. The possible warming of the earth's atmosphere is primarily caused by anthropogenic emissions of CO<sub>2</sub>, CH<sub>4</sub> and some other gases (Figure 1.1). In terms of individual molecules, other greenhouse gases cause a far more significant greenhouse effect than CO<sub>2</sub>, even taking into account the lifespan of these gases, which is generally far shorter. In relation to molecular weight and impact over a time horizon of 100 years, the greenhouse potential of the gases CO<sub>2</sub>, CH<sub>4</sub>, N<sub>2</sub>O, R11, R12, R22, R113, R114, R115, CH<sub>3</sub>CCl<sub>3</sub>, CCl<sub>4</sub> is expressed in the following ratios: 1:11:270:3400:7100:1600:4500:7000:7000:100:1300. However, seen from an absolute perspective, CO<sub>2</sub> is the main cause of the anthropogenic greenhouse effect, due to its concentration in the earth's atmosphere, and is the second most pronounced cause (after water vapor) of the natural greenhouse effect.

Based on an "average" scenario ("IS92a"), IPCC calculations estimate that the volume fraction of CO<sub>2</sub> in the atmosphere will increase from the current figure of 360 ppm to a figure of 750 ppm by the year 2100, and that annual CO<sub>2</sub> emissions will climb from the current figure of 24 Gt CO<sub>2</sub> to approx. 73 Gt CO<sub>2</sub> (approx. 44 Gt CO<sub>2</sub> in 2025, and 55 Gt CO<sub>2</sub> in 2050). Average global temperature is expected to increase by between 1.5 and 3.5 K by 2100 [10]. The IPCC concludes that annual CO<sub>2</sub> emissions will have to be limited to around 26 Gt CO<sub>2</sub> if the CO<sub>2</sub> volume fraction is to be stabilized at 500 ppm [13].

CO<sub>2</sub> emissions worldwide have more than tripled since 1950 (Figure 6.3). Even in the short period between 1990 and 1996, CO<sub>2</sub> emissions increased by 6.4% from 22.4 Gt CO<sub>2</sub> to 23.9 Gt CO<sub>2</sub> [11] and primary energy demand increased by 7.3% from 94 • 10<sup>6</sup> TWh to 101 • 10<sup>6</sup> TWh [12]. In order to counter the threat of a global increase in temperature, a decision was made at the UN conference on climate change in Kyoto in December 1997 to achieve an initial, average reduction of 5.2% in greenhouse gases by the period 2008-2012. However, predictions suggest that CO<sub>2</sub> emissions will lie between 23 and 24 Gt CO<sub>2</sub> in the year 2000, and between 28 and 31 Gt CO<sub>2</sub> in the year 2010 [188]. Energy conservation efforts have already been taken into account in calculating the lower of these figures. This growth will primarily be caused by the increased demand for primary energy in countries outside the OECD and in Eastern Europe.

In 1992, 13% of the primary energy, or 12220 TWh, was used in the form of end-use electrical energy [188]. Assuming an average efficiency of between 25% and 35%, this means that electricity supply makes up a proportion of between 38% and 53% of primary energy consumption. Of this, 39% comes from coal-fired power plants [188]. With fossil energy fuels representing 64% [188] of this electricity supply, the proportion of CO<sub>2</sub> emissions from power plants is estimated to be around 30%, and that of coal-fired power plants around 20% [189]. Total coal consumption as a proportion of primary energy consumption lies at 29% (3.4 Gt coal equivalent) and contributes 38.5% (1992) of total CO<sub>2</sub> emissions (Figure 1.2). The proportion represented by coal of primary energy consumption, which, taken as a whole, is rising, has been steadily decreasing since 1950, as liquid and gaseous fossil fuels have gained ground [15].

If a CO<sub>2</sub> volume fraction limit of 500 ppm were to be enforced over the long term, this would require that no more than 26 Gt CO<sub>2</sub> be emitted (see above), according to IPCC figures. Based on anticipated CO<sub>2</sub> production of between 28 and 31 Gt in the year 2010, and 44 Gt in 2025, this would necessitate CO<sub>2</sub> removal of between 7% and 16% in 2010, and 41% in 2025. With CO<sub>2</sub> production expected to increase to 55 Gt in 2015, and 73 Gt in 2100, it would become necessary to separate and sequester 53% and 64%, respectively, of the CO<sub>2</sub>. Since CO<sub>2</sub> separation from some sources of emissions is barely

feasible and cannot, in many cases, be financed by less developed countries, significantly higher CO<sub>2</sub> separation and emissions reduction would have to be achieved in industrialized countries, particularly in the power plant arena.

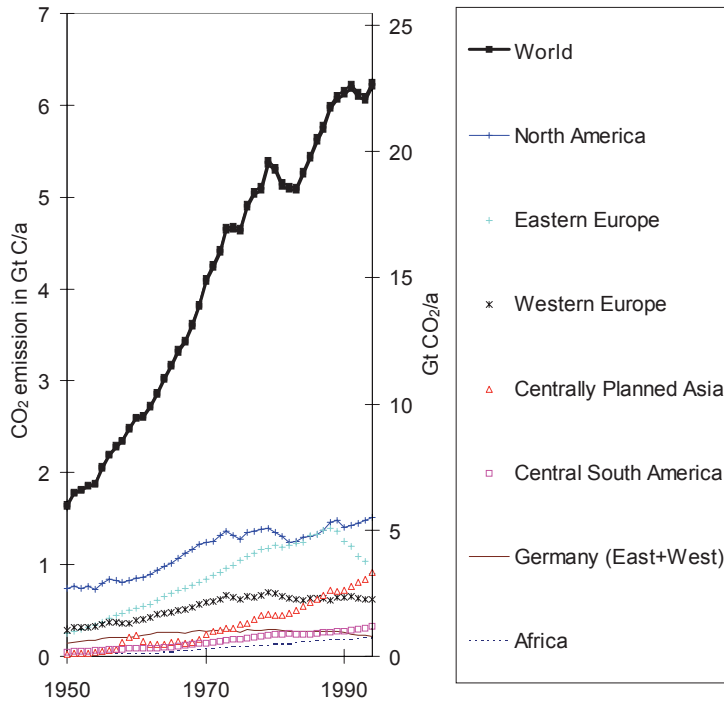


Figure 6.3: CO<sub>2</sub> emissions from the burning of fossil fuels and the production of cement (global and distributed by region) [15]

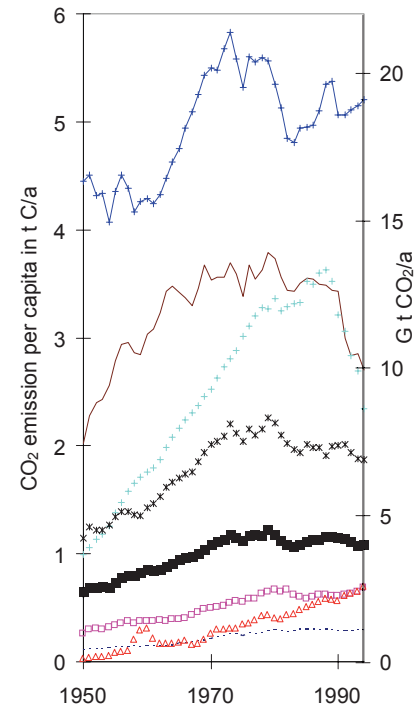


Figure 6.4: How CO<sub>2</sub> emissions per capita have developed in the various parts of the world since 1950 [15].

## 6.2 Possible Approaches Towards Reducing CO<sub>2</sub> Emissions in the Energy Supply Sector

Anthropogenic CO<sub>2</sub> emissions may be assigned to the fields of tapping and mining of deposits, and also of consumption. In the field of energy conversion and consumption, there are a variety of possible ways of reducing CO<sub>2</sub> emissions:

- Reduced end-use energy consumption
- Improved utilization of energy
- Switching from carbon-rich fossil fuels (coal) to carbon-lean fossil fuels (natural gas)
- Increased use of renewable energies
- Increased use of nuclear power plants
- CO<sub>2</sub> capture in power plants, which are fired with fossil fuels, and CO<sub>2</sub> sequestration.

### Reducing End-Use Energy Consumption

End-use energy consumption depends heavily on the industrial structure, patterns of consumption and climate of a specific region. Figure 6.4 and 6.5 clearly show the differences in CO<sub>2</sub> emissions connected to energy consumption in specific regions of the world. The figures also show how emissions in Germany (taken as a whole) and Eastern Europe have dropped, due to the collapse of inefficient industries when the centrally planned economy came to an end. Reducing end-use energy consumption will require changes to be made to the structure of industry and to peoples' lifestyles [190].

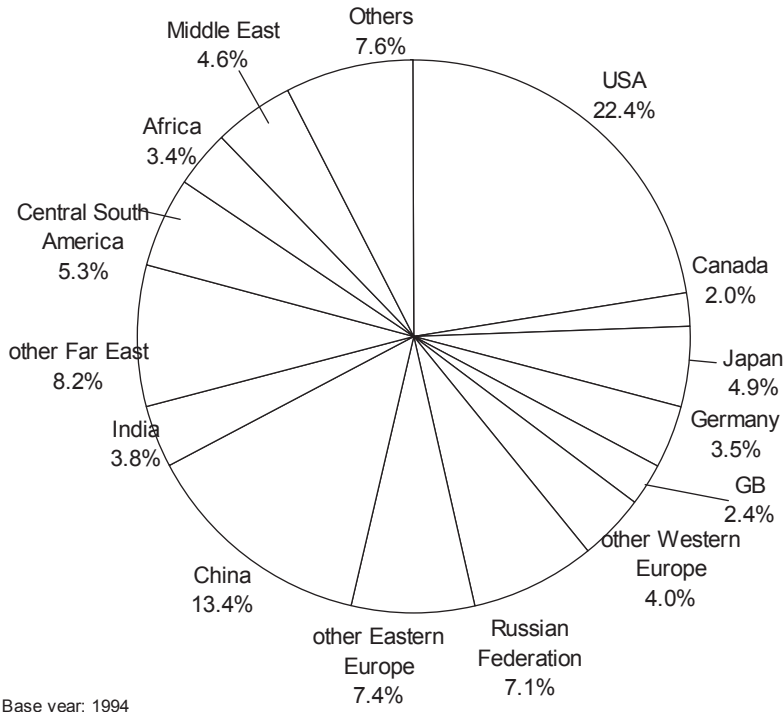


Figure 6.5: Global 1994 CO<sub>2</sub> emissions broken down by country

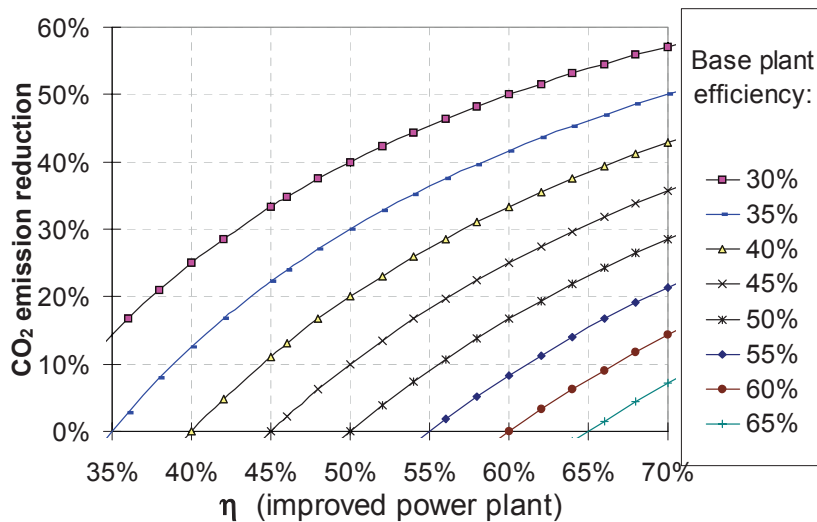


Figure 6.6: CO<sub>2</sub> emissions reduction by means of an improved power plant, as set against various benchmark power plants

### Improved Utilization of Energy

By improving efficiencies, CO<sub>2</sub> emissions can be reduced within the context of the possibilities for technical improvement. For example, by replacing a power plant, which has an efficiency of 35% (LHV),

with a new power plant, which has an efficiency of 45%, and which uses the same fuel, CO<sub>2</sub> emissions can be reduced by 22% (Figure 6.6). According to Pruscsek et al. [207], average efficiencies in Germany in 1990 were:

- 32.0% for all electricity-generating installations of the public power supply system,
- 30.0% for the lignite-fired power plants in the public power supply system,
- 34.3% for the hard coal-fired power plants in the public power supply system,
- 90.0% for heat generation in heating furnaces in the industrial sector.

With the current state of the technology, the following efficiencies can be achieved for newly-constructed plants:

- >43% for lignite-fired power plants<sup>68</sup>,
- >47% for hard coal-fired power plants<sup>68</sup>,
- >58% for natural gas-fired combined cycle power plants.

By replacing all of the old plants with this more up-to-date technology, using the same fuel, the following reductions in CO<sub>2</sub> emissions could be achieved:

- ≈ 30% in lignite-fired power plants,
- ≈ 27% in hard coal-fired power plants.

With primary energy consumption remaining the same, and taking 1990 (1997) figures for the proportion of electricity generation represented by lignite-fired power plants of 29.4% (25%) and hard coal-fired power plants of 27.8% (26%) [208], the improvements to both types of coal-fired power plants would achieve a reduction in CO<sub>2</sub> emissions in Germany of 16.3% (14.5%).

According to Pruscsek et al. [207], if the separate generation of electrical power and heat were to be replaced with industrial cogeneration, the potential CO<sub>2</sub> savings in the industrial sector alone would come to between 1.4% and 7.8% by the year 2020, related to CO<sub>2</sub> emissions in 1990.

### **Switching from Carbon-Rich Fossil Fuels (Coal) to Low-Carbon Fossil Fuels (Natural Gas)**

In terms of energy content, natural gas has the lowest specific CO<sub>2</sub> emissions of the fossil energy fuels, followed by crude oil, hard coal and lignite (Table 6.1).

By replacing coal in power plants with natural gas, on a worldwide basis, with 41% less CO<sub>2</sub> emissions per fuel energy, CO<sub>2</sub> emissions could be reduced by approx. 8%. The savings potential of this measure could actually be even higher, since higher efficiencies can be obtained with natural gas-fired combined cycle power plants than with coal-fired power plants.

---

<sup>68</sup> Steam power plants

Table 6.1: CO<sub>2</sub> emissions from fossil fuels

Fuel	Heating Value LHV in MJ/kg	kg CO <sub>2</sub> /GJ (LHV)	kg CO <sub>2</sub> /MWh (LHV)	t CO <sub>2</sub> /t coal equivalent	Relative CO <sub>2</sub> emissions
coke	29.3	107	385	3.13	119%
hard coal(anthracite)	31.0	98	354	2.87	110%
hard coal (bituminous coal)	31.0	90	323	2.62	100%
lignite	16.7	109	392	3.18	121%
crude oil	41.9	80	289	2.35	90%
natural gas	50.0	53	191	1.55	59%

### Increased Use of Renewable Energies

Operating power plants using renewable energies such as hydroelectric power, biomass, wind power, geothermal energy or solar power results in virtually zero CO<sub>2</sub> emissions<sup>69</sup>. However, some CO<sub>2</sub> emissions are caused by the consumption of fossil energy fuels to produce the plants and/or the biomass. Measured against electricity production, the overall reduction in CO<sub>2</sub> emissions can be extremely high. It is, however, important to take into account the yield factor<sup>70</sup>, which is a significant issue in the case of photovoltaic plants, for example.

There are several factors which continue to limit the potential for expansion of renewable energies: high costs (e.g. in the case of solar power, wind power), irregular availability (e.g. in the case of solar power, wind power), low energy density (solar power), and issues involving the availability of land or competition with other agricultural products (biomass). An increase in the use of wind power and solar power would have to be accompanied by appropriate storage systems, or by fossil fuel-fired power plants working on a standby basis.

In the case of hydroelectric power plants, it should also be noted that, when areas previously covered with vegetation are flooded, climate-affecting CH<sub>4</sub> and CO<sub>2</sub> emissions are produced as the original vegetation dies off.

### Increased Use of Nuclear Power Plants

Taking into consideration the whole chain of electricity generation in nuclear power plants, including fuel acquisition and disposal, the figures show energy-specific CO<sub>2</sub> emissions amounting to between a tenth and a hundredth of the CO<sub>2</sub> emissions from fossil fuel-fired power plants. This wide spread is the result of various factors including the type of fossil fuel-fired power plant used for the comparison, the quality of the uranium ore and of the uranium enrichment process, and the way in which the radioactive waste is treated [191]. By increasing the number of additional power plants to be built, global CO<sub>2</sub> emissions from the power supply sector could be reduced by 7% of their current value [209].

### CO<sub>2</sub> Capture in Power Plants Fired with Fossil Fuels, and CO<sub>2</sub> Sequestration

As explained in this study, CO<sub>2</sub> capture in power plants is certainly possible in principle, though it does require high additional input of energy and equipment, which ultimately results in lower efficiencies, greater fuel utilization, and higher plant costs and electricity generating costs (Figure 6.7). Long-term

<sup>69</sup> Biomass can be taken to be neutral in terms of CO<sub>2</sub> emissions, since the carbon emitted when it is burnt has already been extracted from the atmosphere through photosynthesis.

<sup>70</sup> Yield factor: quotient of the electrical energy output and the accumulated energy used in manufacturing the plant

sequestration of the separated CO<sub>2</sub> is also feasible, e.g. in dissolved state in the deep ocean, or in geological aquifers.

Since the number of power plants is relatively small, in comparison to other sources of CO<sub>2</sub> emissions, and the CO<sub>2</sub> mass stream emitted in each case is very large, it is possible to capture a relatively large percentage of the CO<sub>2</sub> emissions using relatively few CO<sub>2</sub> separation installations.

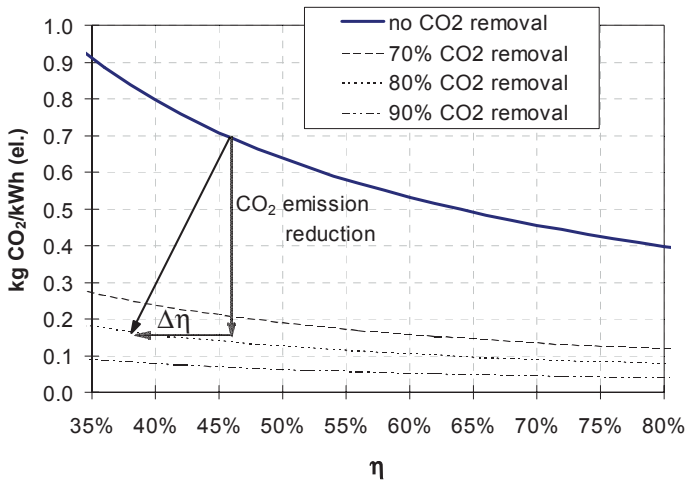
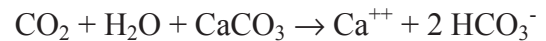


Figure 6.7: Specific CO<sub>2</sub> emissions in power plants with CO<sub>2</sub> separation

### 6.3 The Natural, Geochemical Carbon Cycle and Global Carbon Reservoirs

In the natural carbon cycle, the ocean marks the end of a chain of processes, which begins with CO<sub>2</sub> emissions (e.g. emissions from volcanic eruptions or anthropogenic activities) and which ends with CO<sub>2</sub> being fixed in sediments and, eventually, deposited on the ocean floor. This cycle involves various reactions, including examples such as [60]:

A) Weathering of carbonate rock:



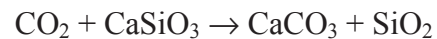
B) Weathering of silicate rocks:



C) Carbonate precipitation in the ocean:



D) Silicate weathering plus carbonate precipitation (B+C):



E) Metamorphic or magmatic decomposition of carbonates:  $\text{CaCO}_3 + \text{SiO}_2 \rightarrow \text{CaSiO}_3 + \text{CO}_2$ .

Over time, similar reactions also bind a portion of the CO<sub>2</sub> in the form of rock in cases where CO<sub>2</sub> is injected into geological deposits, which potentially increases the long-term storage capacity [49]. However, the natural process of sedimentation is an extremely slow-acting process, which would require between 10000 and 300000 years to absorb the entire quantity of atmospheric CO<sub>2</sub>, without even taking into account new emissions [60]. More rapid absorption of large quantities of CO<sub>2</sub> can be achieved by dissolving CO<sub>2</sub> in seawater.

The current CO<sub>2</sub> volume fraction of the atmosphere of around 360 ppm should be viewed in the context of the Earth's development. From an initial point where the original atmosphere of the Earth consisted mainly of CO<sub>2</sub>, geochemical and biological processes (see Muschelkalk) subsequently reduced the CO<sub>2</sub> content to its current value over the course of millions of years. The major part of all the carbon currently present on the Earth is bound up in the form of rock [192]. The oceans and seas also contain large quantities of CO<sub>2</sub> in the form of dissolved gas, carbonates, carbohydrates and carbonic acids. A further portion is bound up in fossil fuel deposits and in the biosphere.



Table 6.2: Comparison of CO<sub>2</sub> reservoirs and emissions

	Gt C/year	Gt CO <sub>2</sub> /year
<b>Global emissions from fossil fuels (1996)</b>		
all fossil fuels	~ 6.5	~ 23.7
coal	~ 3.2	~ 11.7
<b>Emissions from a hard coal-fired power plant:</b>		
700 MW (el.), η = 45%, 7000 h/a, Pittsburgh Nr. 8	0.00095	0.0035
<b>Natural reservoirs, sequestration sites and exchange processes (carbon and CO<sub>2</sub>)</b>		
Earth's atmosphere (with 348 ppm CO <sub>2</sub> volume fraction)	718	2631
Earth's crust (calcium carbonate/ limestone CaCO <sub>3</sub> , magnesium carbonate/ dolomite CaCO <sub>3</sub> /MgCO <sub>3</sub> , among other substances) [79]	1.5 · 10 <sup>16</sup>	5.5 · 10 <sup>16</sup>
Oceans and seas (dissolved gas, carbonates, hydrogen carbonate and carbonic acids) [79]	38182	140000
Biosphere [138]	600	2200
Proven, minable deposits of fossil fuels [193] (including deposits which it is not economically viable to extract)	272 >1090	1000 >4000
Carbon conversion through photosynthesis [138]	110-120	400
Exhaled by all of mankind [138]	0.46	1.7

## 6.4 CO<sub>2</sub> Pipeline Transport

For a velocity of between 2 and 3 m/s, the pressure loss in a CO<sub>2</sub> pipeline may be estimated using the equation [194]:

$$\Delta p = \rho \lambda \frac{Lu^2}{2d}$$

$$\lambda \approx 0.093 \frac{1}{(d \cdot 1000)^{0.249}} \quad (\text{Pipe friction coefficient with a roughness of } 0.5\text{mm})$$

$$u = \text{Flow rate} \left[ \frac{\text{m}}{\text{s}} \right] \quad d = \text{Pipeline diameter} \quad [\text{m}]$$

$$L = \text{Pipeline length} \quad [\text{m}] \quad \rho = \text{Density} \approx 877 \frac{\text{kg}}{\text{m}^3} (\text{CO}_2, 110\text{bar}, 25^\circ\text{C}).$$

$$\eta = \text{Viscosity} \approx 773 \cdot 10^{-7} \text{N} \frac{\text{s}}{\text{m}^2} (110\text{bar}, 25^\circ\text{C})$$

The largest available diameters, which can be used for CO<sub>2</sub> pipelines, are 1600 mm for land-based pipelines and 1500 mm for ocean pipelines [64]. Table 6.5 shows the results of pressure drop calculations and estimated figures for capacity. Assuming a pipeline diameter of 1600 mm, and a CO<sub>2</sub> flow spread evenly over the whole year, somewhere between 8 and 14 pipelines would be required to transport the CO<sub>2</sub> emissions of all the fossil-fuels power plants in Germany. Between 220 and 370 of these pipelines would be needed to deal with the energy-related CO<sub>2</sub> emissions of the whole world.

Emissions tests in the USA have demonstrated that, in the event of pipeline breakage, CO<sub>2</sub> is discharged too slowly to allow dangerously high concentrations of CO<sub>2</sub> to build up around the pipeline or to lead to extremely low temperatures in the pipeline [195].

Table 6.3: Pipeline costs per meter (±40%) [64]

Diameter	0.4 m	0.75 m	1 m	1.6 m
\$ per meter	450-950	800-1800	1100-2500	200-6600

Table 6.4: Example CO<sub>2</sub> pipelines used to transport CO<sub>2</sub> for Enhanced Oil recovery (EOR)

Project	Pipeline Length	Pipe Diameter	Pressure, Temperature	Gas Composition	Source
Sheep Mountain Colorado → Texas USA	676 km	0.5m / 0.6 m	Initial pressure 117-131 bar Minimum (at height of 2515 m): 82.7 bar	97% mol CO <sub>2</sub> 1.7% mol CH <sub>4</sub> 0.6% mol N <sub>2</sub> 0.7% mol C <sub>2</sub> H <sub>6</sub>	[196]
Cortez Colorado → Texas USA	807 km	0.3-0.6 m	96.5- 186 bar	95% mol CO <sub>2</sub> Limit: 5 % mol CH <sub>4</sub> max. 4 % mol N <sub>2</sub> max. 0.7% mol H <sub>2</sub> S max.	[197]
Central Basin West Texas USA	278 km	0.65 m	117-152 bar -4°C to +43°C	98.5% mol CO <sub>2</sub> 1.3% mol N <sub>2</sub> 0.7% mol Cl	[198]
Budafa Hungary	33 km	0.15m / 0.3m	140 bar 45°C	81 % mol CO <sub>2</sub> 15.5% mol CH <sub>4</sub> 1.9% mol N <sub>2</sub> 0.3% mol H <sub>2</sub> S	[65]

Table 6.5: Pressure drop per 100 km and respective power plant size for CO<sub>2</sub> pipelines with an inlet pressure of 110 bar. Power plant size is based on Pittsburgh Nr. 8 coal, 90% CO<sub>2</sub> separation and a net power plant efficiency of 37%. The costs shown are based on information from Table 6.3.

Pipeline Ø	Velocity in m/s	CO <sub>2</sub> mass flow (98% CO <sub>2</sub> ) in Gt CO <sub>2</sub> /a	Capacity for coal-fired power plant in MW	Pressure drop per 100 km in bar	Pipeline costs in 10 <sup>6</sup> US\$/100km	Specific costs in 10 <sup>6</sup> [US\$/kg CO <sub>2</sub> /s] /100 km
0.30	1.2	0.0023	342	47.3		
	1.5	0.0029	427	73.9		
	2	0.0038	570	131.4		
0.40	1.2	0.0041	608	33.0	42.3 – 89.2	0.40 – 0.84
	1.5	0.0051	760	51.6	42.3 – 89.2	0.32 – 0.68
	2	0.0068	1013	91.7	42.3 – 89.2	0.24 – 0.50
0.50	1.2	0.0064	949	25.0		
	1.5	0.0080	1187	39.1		
	2	0.0107	1582	69.4		
0.60	1.2	0.0092	1367	19.9		
	1.5	0.0115	1709	31.1		
	2	0.0153	2279	55.3		
0.75	1.2	0.0144	2136	15.1	75.0 – 102. 1	0.20 – 0.27
	1.5	0.0180	2670	23.5	75.0 – 102. 1	0.16 – 0.22
	2	0.0240	3560	41.8	75.0 – 102. 1	0.12 – 0.16
0.80	1.2	0.0164	2430	13.9		
	1.5	0.0204	3038	21.7		
	2	0.0273	4051	38.6		
1.06	1.2	0.0287	4267	9.8	103 – 234	0.14 – 0.31
	1.5	0.0359	5334	15.3	103 – 234	0.11 – 0.25
	2	0.0479	7112	27.2	103 – 234	0.09 – 0.19
1.50	1.2	0.0575	8545	6.3		
	1.5	0.0719	10681	9.9		
	2	0.0959	14241	17.6		
1.60	1.2	0.0654	9722	5.8	188 – 619—	0.11 – 0.36
	1.5	0.0818	12152	9.1	188 – 619—	0.09 – 0.29
	2	0.1091	16203	16.2	188 – 619—	0.06 – 0.22

## 6.5 Data Tables

The data tables presented below are referred to in the preceding chapters of this study. They provide more precise details of process data.

Table 6.6: Accuracy of the notations of physical characteristics used in this paper for the heat capacity of ideal gases according to Hougen et al. [160]

Gas Component	Max. Error in %	Average Error in %
O <sub>2</sub>	1.19	0.28
H <sub>2</sub> O	0.53	0.24
CO <sub>2</sub>	0.67	0.22
N <sub>2</sub>	0.59	0.34
SO <sub>2</sub>	0.45	0.24
H <sub>2</sub>	1.01	0.26
CO	0.89	0.37
CH <sub>4</sub>	1.33	0.57
H <sub>2</sub> S	0.76	0.47
COS	0.94	0.49

Table 6.7: Common absorption techniques for CO<sub>2</sub> scrubbing [79, 95, 176]. Figures for heat in enthalpy (desorber temperature) and equivalent electrical work<sup>65</sup> ( $\cong \dots el.$ )

Method	Absorbent	Operating Conditions	Gases Absorbed	Energy Requirements	Purity Separation factor
<b>PHYSICAL ABSORBENTS</b>					
Rectisol	Methanol	Absorber: ≈-10/-70°C $p_{CO_2} > 10$ bar	H <sub>2</sub> S, COS, organic S-compounds, CO <sub>2</sub> , NH <sub>3</sub> , HCN, aromatic compounds and higher hydrocarbons	Work: 0.038 kWh/kg CO <sub>2</sub> (incl. H <sub>2</sub> S) Heat: 0.025kWh/kg CO <sub>2</sub> ( $\cong 0.01$ kWh (el.) /kg CO <sub>2</sub> ) $\cong Total (el.): 0.048 kWh/kg CO_2$	CO <sub>2</sub> separation factor ≤90% Clean gas: H <sub>2</sub> S<0.1 ppm vol. frac. CO <sub>2</sub> <5 ppm vol. frac.
Purisol	N-methyl-2-pyrrolidone (NMP)	Absorber: -20/+40°C $p_{tot} > 20$ bar $p_{CO_2} \approx 10$ bar	H <sub>2</sub> S, COS, CO <sub>2</sub> , NH <sub>3</sub> , HCN, higher hydrocarbons, COS → H <sub>2</sub> S H <sub>2</sub> S sol. matter 12 times higher than CO <sub>2</sub>	Work: 0.07 kWh/kg CO <sub>2</sub> Heat: 0.07 kg steam (20bar) per kg CO <sub>2</sub> ( $\cong 0.02$ kWh (el.) /kg CO <sub>2</sub> ) $\cong Total (el.): 0.09 kWh/kg CO_2$	CO <sub>2</sub> separation factor ≤90% Clean gas: H <sub>2</sub> S<1 ppm vol. fraction CO <sub>2</sub> ≤1000ppm vol. frac.
Selexol	Dimethylether polyethylene glycol (DMPEG)	Absorber: $p_{tot} = 20-140$ bar $p_{CO_2} = 7-30$ bar without cooling: ≈ 20°C (120°C) with cooling: ≈ 0°C	H <sub>2</sub> S, COS, organic S-compounds, CO <sub>2</sub> , NH <sub>3</sub> , HCN, aromatic compounds, higher hydrocarbons, H <sub>2</sub> S sol. matter 9 times higher than CO <sub>2</sub>	Work: 0.03-0.06 kWh/kg CO <sub>2</sub> Heat: 0.016-0.024kWh/kg CO <sub>2</sub> ( $\cong 0.03-0.05$ kWh el./kg CO <sub>2</sub> ) $\cong Total: 0.06-0.11 kWh el./kg CO_2$	Clean gas <0.5% vol. fraction CO <sub>2</sub> <1 ppm vol. fraction H <sub>2</sub> S
Sepasolv	n-oligoethylene glycol + methyl isopropyl ether	Absorber: $p_{tot} \approx 70$ bar		Work: 2.22 kWh/kg CO <sub>2</sub> Heat: 0.05 kWh/kg CO <sub>2</sub> ( $\cong 0.01$ kWh el./kg CO <sub>2</sub> ) $\cong Total: 2.3 kWh el./kg CO_2$	
Fluor Solvent	Propylene carbonate	Absorber: below ambient temp. 3.1-6.9 MPa	H <sub>2</sub> S, COS, CO <sub>2</sub> , acetylene, propane, butane, methane		

Method	Absorbent	Operating Conditions	Gases Absorbed	Energy Requirements	Purity Separation factor
<b>CHEMICAL ABSORBENTS</b>					
<i>Amine-based</i>					
MEA monoethanolamine	Mass frac. 12% aqueous sol. + additives	Absorber: $\approx 40^{\circ}\text{C}$ , 1 - 5 bar Regenerator: 95-120 $^{\circ}\text{C}$	SO <sub>2</sub> , H <sub>2</sub> S, COS, CS <sub>2</sub> , CO <sub>2</sub>	Power: 0.05-0.3 kWh/kg CO <sub>2</sub> Heat: 2.3 kWh/kg CO <sub>2</sub> ( $\approx 0.48$ kWh el./kg CO <sub>2</sub> ) $\approx$ Total: 0.53-0.78 kWh el./kg CO <sub>2</sub>	CO <sub>2</sub> separation factor <99% (80-95%)
MEA	Mass frac. 20% aqueous sol. + additives	"-	"-	Power: 0.02-0.4 kWh/kg CO <sub>2</sub> Heat: 1.0-1.7 kWh/kg CO <sub>2</sub> ( $\approx 0.21$ -0.35 kWh el./kg CO <sub>2</sub> ) $\approx$ Total: 0.23-75 kWh el./kg CO <sub>2</sub>	"-
MEA	Mass frac. 30% aqueous sol. + additives	"-	"-	Power: $\approx 0.036$ kWh/kg CO <sub>2</sub> Heat: $\approx 1.1$ kWh/kg CO <sub>2</sub> ( $\approx 0.23$ kWh el./kg CO <sub>2</sub> ) $\approx$ Total: 0.27 kWh el./kg CO <sub>2</sub>	"-
Amine Guard FS (MEA)	5 n MEA + inhibitors	Absorber 3.4-138 bar, 80-132 $^{\circ}\text{C}$	CO <sub>2</sub> , H <sub>2</sub> S (selective), COS	Power: 4-12 10 <sup>-4</sup> kWh/m <sup>3</sup> CO <sub>2</sub> +H <sub>2</sub> S Heat: 10.3- 165 kWh/m <sup>3</sup> CO <sub>2</sub> +H <sub>2</sub> S	Separation factor: H <sub>2</sub> S $\approx$ 100% CO <sub>2</sub> 20-99.9%
Econamine (DGA)	6 n diglycolamine, mass frac.: 5-90% aqueous sol.	Absorber: 80-120 $^{\circ}\text{C}$ $p_{\text{tot}}=63$ raw Regenerator: 120-140 $^{\circ}\text{C}$ , $p_{\text{tot}}=1.3$ -2 bar	H <sub>2</sub> S, COS, CS <sub>2</sub> , CO <sub>2</sub> , aromatic compounds		
DEA and SNEA-DEA	2 n diethanolamine or 3n diethanolamine, mass frac. 20-30% aqueous sol.	Absorber: 18-55 $^{\circ}\text{C}$ $p_{\text{tot}}=5$ -75 bar $p_{\text{CO}_2}=0.5$ -26 bar	H <sub>2</sub> S, COS, CS <sub>2</sub> , CO <sub>2</sub>		
Flexsorb	Amine + hot potassium carbonate	Absorber: $p_{\text{tot}} \approx 60$ bar (flue gases)		Power: 0.43 kWh/kg CO <sub>2</sub>	
<i>Inorganic chemical absorbents</i>					
Benfield* (variants)	Potassium carbonate & catalysts (borate/ arsenic trioxide)	Absorber: 70-120 $^{\circ}\text{C}$ $p_{\text{tot}} = 3$ -140 bar $p_{\text{CO}_2} = 0.6$ -30 Regenerator: temp. as in abs. $p \approx 1.2$ bar	SO <sub>2</sub> , H <sub>2</sub> S, HCN, COS, CO <sub>2</sub>	Power: 0.2-0.7 kWh/kg CO <sub>2</sub> Heat: 1-2 kWh/kg CO <sub>2</sub> ( $\approx 0.21$ -0.42 kWh el./kg CO <sub>2</sub> ) $\approx$ Total: 0.41-1.1 kWh el./kg CO <sub>2</sub>	
Vacuum carbonate*	Sodium carbonate + catalysts	Absorber: 20-40 $^{\circ}\text{C}$ $p_{\text{tot}} = 1$ -3 bar CO <sub>2</sub> < 5% vol. fraction	SO <sub>2</sub> , H <sub>2</sub> S, HCN, CO <sub>2</sub>		
<b>PHYSICAL-CHEMICAL ABSORBENTS</b>					
Activated MDEA	2 n methyl-diethanolamine mass fraction: 40-50% aqueous sol.	Absorber: 40-90 $^{\circ}\text{C}$ $p_{\text{tot}} < 120$ bar, 1-stage abs.: $p_{\text{CO}_2}$ 0.5-5 bar 2-stage abs.: $p_{\text{CO}_2}$ 2-15 bar Regenerator: 0.5 - 1.9 bar	CO <sub>2</sub> , H <sub>2</sub> S, COS	Power: 0.023-0.027 kWh/kg CO <sub>2</sub> Heat: 0.202kWh/kg CO <sub>2</sub> ( $\approx 0.04$ kWh el./kg CO <sub>2</sub> ) $\approx$ Total: 0.063-0.067 kWh el./kg CO <sub>2</sub>	Clean gas: <20 ppm vol. frac. CO <sub>2</sub> Product: > 99.8% vol. frac. CO <sub>2</sub> CO <sub>2</sub> separation factor > 99%
Adip (DIPA & MDEA)	aqueous sol. alkanolamine 2-4n diisopropylamine 2 n methyl-diethanolamine	absorber 25-75 $^{\circ}\text{C}$ $p_{\text{tot}} < 130$ bar (wide range)	H <sub>2</sub> S (selective), COS, CO <sub>2</sub>	Wide range LP steam: 0.4-2.8 kg/kg acid gas ( $\approx 0.07$ -0.48 kWh el./ kg acid gas)	Clean gas: < 10 ppm vol. frac. H <sub>2</sub> S < 5 ppm vol. frac. COS

Method	Absorbent	Operating Conditions	Gases Absorbed	Energy Requirements	Purity Separation factor
Sulfinol-D Sulfinol-M	Mixture of DIPA or MDEA, H <sub>2</sub> O + tetrahydrothiophene dioxide	Absorber: ≈ 40°C p <sub>tot</sub> = 45-70 bar	H <sub>2</sub> S, COS, Methyl Mercaptan, hydrocarbons, aromatic compounds, CO <sub>2</sub>		Clean gas: H <sub>2</sub> S <1 ppm vol. frac.
Amisol	Mixture of methanol + MEA, DEA, diisopropyl amine (DIPAM) / diethylamine	Absorber: 35-80°C >1MPa	H <sub>2</sub> S, COS, organic sulfur, HCN, NH <sub>3</sub> , CO <sub>2</sub> , aromatic compounds, higher hydrocarbons		Clean gas: CO <sub>2</sub> : 5-100 ppm vol. frac.
Optisol	aqueous amine + physical absorbent	Absorber: 20-30°C, 17-55 bar			Clean gas: H <sub>2</sub> S < 4.2% vol. fraction CO <sub>2</sub> 0.1-12% vol. fraction

\* alkaline components may lead to problems with corrosion in downstream gas turbines

Table 6.8: Data from the literature on CO<sub>2</sub> adsorption plants

Plant Type	Raw Gas	Adsorption	Desorption	Separation Factor	Product Purity	Energy Requirements (in kWh/kg CO <sub>2</sub> )	Source
PSA	flue gas 28-34% CO <sub>2</sub>	1 bar	0.05-0.9 bar	>60%		0.16-0.18	[199]
PSA	reformed natural gas	13-21 bar	<1 bar	>89%	>99%		[200]
PSA	low CO <sub>2</sub> concentration			high		0.4	[201]
PTSA Ca-Fe + zeolite	flue gases 10% CO <sub>2</sub> 11.5% CO <sub>2</sub>	1 bar		90%	≤ 99%	0.7 0.55	[202]
TSA zeolites	synthesis gas	/ 25°C	0.0012 bar / 200°C	60-90%			[203]
Thermal regeneration (Rektisorb / Hypersorb) activated coke	coke oven waste gas	continuous fluidized bed process					[79]
Thermal regeneration MgO + CaO	flue gas / synthesis gas	high temperatures	high temperature			Power generation in the power plant reduced by around 1/3	[96]

Table 6.9: Selectivity of commercial membranes [204, 205, 206]

Manufacturer/ Brand Name	GKSS	DELAIR	Ube Type C	Ube Type B-H	UBE Type A	SEPAREX	PERMEA	GKSS	Dow
Material	polydi- methyl- siloxane	poly- phenyle- neoxide	polyimide	polyimide	polyimide	acetyl cellulose	polysulfone/ silicone rubber	polyther- imide	polyole- fine
Working temp.	30°C	30°C	60°C	60°C	60°C	30°C	30°C	30°C	
Selectivity (permeability of Gas 1 / permeability of Gas 2)									
O <sub>2</sub> /N <sub>2</sub>		5	6.1	5.0	5.0	5.5	6	9	4
CO <sub>2</sub> /N <sub>2</sub>	11.4	20	33.3	18.3	17.0	30	30	29	
CO <sub>2</sub> /CH <sub>4</sub>				27.5	25.5				
H <sub>2</sub> /CO				55.6	91.7				
H <sub>2</sub> /CO <sub>2</sub>	5		2.8	4.5	10.8				
H <sub>2</sub> /N <sub>2</sub>	190		94.4	83.3	183.3	67	72	190	
CO <sub>2</sub> /O <sub>2</sub>	5.2	4.1	5.5	3.7	3.4	5	6	3	
H <sub>2</sub> /CO				55.6	91.7	30-50	60	100	

Table 6.10: Input values and results for a simplified estimation of the energy requirements of CO<sub>2</sub> separation with methanol at -30°C (similar to Rectisol process)

Reference values			
CO <sub>2</sub> separation factor (in %)	90	Feed gas	Volume fraction in %
Pressure loss in solvent circulation (in bar)	5	H <sub>2</sub> O	28.4
Efficiency of refrigerating unit		CO <sub>2</sub>	29.4
$\eta_{RU} = \eta_{RU,rev} \cdot \epsilon$ (in %)	35		
Pinch cold recovery (in K)	15	N <sub>2</sub>	0.6
Absorption:		Ar	0.6
$T_{abs}$ (in °C)	-30.0	H <sub>2</sub>	38.3
$P_{abs,tot}$ (in bar)	20.0	CO	2.5
Desorption:		CH <sub>4</sub>	0.05
$T_{desorption}$ (in bar)	-5	H <sub>2</sub> S	0.17
$P_{CO_2,desorption}$ (in bar)	1.2		
Results			
Absorption		Refrigerating work	
Charge (in kg CO <sub>2</sub> /kg methanol)	0.049	Refrigerating unit efficiency $\eta_{RU}$ (in %)	35
Desorption		Carnot factor $\eta_c$ (in %)	22.6
Charge (in kg CO <sub>2</sub> /kg methanol)	0.015	max. coefficient of perf. $\epsilon_{rev} = Q/P = 1/\eta_c$	4.42
Absorbent balance		actual coefficient of perf. $\epsilon_{RU} = \epsilon_{rev} \eta_{RU}$	1.55
Absorbent circulation (in kg methanol/kg CO <sub>2</sub> , separated)	29.3	Feed gas cooling work (in kJ/kg CO <sub>2</sub> separated) ( $= \frac{c_p \Delta T}{x_{CO_2} r_{CO_2} \epsilon_{Cc}}$ )	80.6
Average density of methanol (in kg/m <sup>3</sup> )	835	Feed gas cooling work (kWh/kg CO <sub>2</sub> separated)	0.022
Pump work = $v \Delta p / \eta_{pump}$ (in kJ/kg CO <sub>2</sub> )	119.2		
Expansion, recovery (in kJ/kg CO <sub>2</sub> )	-33.0	Total energy required	
Pump work + recovery (in kJ/kg CO <sub>2</sub> )	86.3	(in kJ/kg CO <sub>2</sub> )	166.9
Pump work + recovery (in kWh/kg CO <sub>2</sub> )	0.024	(in kWh/kg CO <sub>2</sub> )	0.046

Table 6.11: Input values and results for CO<sub>2</sub> absorption using water as an absorbent

Gas	Coal gas after CO shift conversion	Flue gas	Flue gas	Flue gas
Power plant	IGCC power plant	Steam power plant (coal)	IGCC power plant	GTCC power plant
CO <sub>2</sub> capture ratio (in %)	90	90	90	90
Pressure loss in solvent circulation $\Delta p$ (in bar)	5	5	5	5
Absorption				
$P_1$ (gas inlet) (in bar)	1.013	1.013	1.013	1.013
$T_{abs}$ (in °C)	20.0	20.0	20.0	20.0
$P_{abs,tot}$ (in bar)	20.0	20.0	20.0	20.0
$p_{CO_2}$ (in bar)	5.9	2.2	1.5	0.6
Absorption				
Charge (in kg CO <sub>2</sub> /kg water)	0.010	0.004	0.002	0.001
Absorbent balance				
Solvent circulation (in kg water/kg CO <sub>2,separated</sub> )	99.8	264.7	402.4	937.5
Pump work (in kJ/kg CO <sub>2</sub> )	341.5	905.9	1377.1	3208.1
Water expansion, recovery (in kJ/kg CO <sub>2</sub> )	-132.8	-352.3	-535.5	-1247.6
Water: pump work - recovery (in kJ/kg CO <sub>2</sub> )	208.7	553.6	841.6	1960.5
(in kWh/kg CO <sub>2</sub> )	0.058	0.154	0.234	0.545
Gas compression (in kJ/kg Gas)	612.8	432.6	449.6	453.6
Gas expansion (recovery) (in kJ/kg Gas)	-400.1	-160.1	-164.3	-159.1
Gas compression - recovery (in kJ/kg CO <sub>2</sub> )	765.5	1972.8	2931.2	6702.1
Gas compression - recovery (in kWh/kg CO <sub>2</sub> )	0.2	0.5	0.8	1.9
Pump and compressor work (water+gas) (in kJ/kg CO <sub>2</sub> )	974.1	2526.4	3772.8	8662.6
(in kWh/kg CO <sub>2</sub> )	0.271	0.702	1.048	2.406
Feed gas	Volume fraction in %	Volume fraction in %	Volume fraction in %	Volume fraction in %
O <sub>2</sub>		6.1	12.2	13.9
H <sub>2</sub> O	28.4	6.2	13.8	6.4
CO <sub>2</sub>	29.4	11.2	7.4	3.2
N <sub>2</sub>	0.6	75.3	65.6	75.6
Ar	0.6	1.0	1.0	0.9
H <sub>2</sub>	38.3			
CO	2.5			
CH <sub>4</sub>	0.05			
H <sub>2</sub> S	0.17			

Table 6.12: Input values and results in calculating the energy requirements of various chemical CO<sub>2</sub> scrubbing processes (see Table 6.13 for details of physical characteristics)

Absorbent	MEA	MEA	MEA	DEA	TEA	MDEA	Hot potassium carbonate K <sub>2</sub> CO <sub>3</sub>	DIPA	DGA
Absorbent concentration (Mass fraction in %)	12	20	30	30	50	50	40	40	40
H <sub>2</sub> O in CO <sub>2</sub> product									
Volume fraction in %	44.8	44.8	44.8	44.8	44.8	44.8	44.8	44.8	44.8
Mass fraction in %	24.9	24.9	24.9	24.9	24.9	24.9	24.9	24.9	24.9
Temperature of CO <sub>2</sub> product (in °C)	92.2	92.2	92.2	92.2	92.2	92.2	92.2	92.2	92.2
Desorption pressure (in bar)	1.7	1.7	1.7	1.7	1.7	1.7	1.7	1.7	1.7
Temp. of desorption (in °C)	115.2	115.2	115.2	115.2	115.2	115.2	115.2	115.2	115.2
Pinch heat exchanger lean/rich solution (in K)	23	23	23	23	23	23	23	23	23
Regeneration rate	0.5	0.5	0.5	0.5	0.5	0.5	0.5	0.5	0.5
Heating (assuming heat capacity of solution as water)									
Difference in enthalpy Δh (in kJ/kg H <sub>2</sub> O)	96.7	96.7	96.7	96.7	96.7	96.7	96.7	96.7	96.7
Solvent circulation									
(in kg/s MEA/ kg/s CO <sub>2</sub> )	5.0	5.0	5.0	5.0	4.0	4.0	5.0	5.0	5.0
(in kg/s H <sub>2</sub> O / kg/s CO <sub>2</sub> )	41.7	25.0	16.7	16.7	8.0	8.0	12.5	12.5	12.5
Heating (in kJ/kg CO <sub>2</sub> )	4607	2996	2191	2191	1257	1257	1788	1788	1788
Vaporization of water (amount determined by proportion of water in CO <sub>2</sub> product)									
enthalpy of vaporization h <sub>r</sub> (in kJ/kg CO <sub>2</sub> )	551.6	551.6	551.6	551.6	551.6	551.6	551.6	551.6	551.6
Vaporization of absorbent									
kg vaporized absorbent/kg CO <sub>2</sub> (target)	0.03	0.03	0.03	0.01	0.01	0.01	0.01	0.01	0.01
Enthalpy of vaporization h <sub>r,sol</sub> (in kJ/kg CO <sub>2</sub> )	123.9	123.9	123.9	33.5	21.4	22	0	0	0
Reaction enthalpy (In kJ/kg CO <sub>2</sub> )	1636	1636	1636	1477	1409	1209	603	1674	1976
in relation to total energy consumption (in %)	19	25	29	28	35	32	16	33	37
Total energy expended on regeneration									
kJ/kg CO <sub>2</sub>	6919	5308	4503	4253	3238	3039	2943	4013	4315
kWh/kg CO <sub>2</sub>	1.92	1.47	1.25	1.18	0.90	0.84	0.82	1.11	1.20
Total energy required (regeneration as proportion of total energy expenditure = 80%)									
kJ/kg CO <sub>2</sub>	8648	6635	5628	5316	4048	3799	3678	5017	5394
kWh/kg CO <sub>2</sub>	2.40	1.84	1.56	1.48	1.12	1.06	1.02	1.39	1.50
Equivalent electrical power (exergy efficiency of heat utilization = 19 %)									
Comparative elec. consump. (in kWh/kg CO <sub>2</sub> )	0.48	0.37	0.31	0.31	0.24	0.23	0.22	0.29	0.32
Pump work (additional assessment)									
Absorber pressure (in bar)	1.02	1.02	1.02	1.02	1.02	1.02	1.02	1.02	1.02
Pressure loss in solvent circulation (in bar)	3	3	3	3	3	3	3	3	3
Pump work (in kJ/kg CO <sub>2</sub> )	36.5	23.7	17.4	17.4	10.0	10.0	14.2	14.2	14.2
CO <sub>2</sub> mass fraction in feed gas in %	10	10	10	10	10	10	10	10	10
Pressure loss in absorber (in bar)	0.05	0.05	0.05	0.05	0.05	0.05	0.05	0.05	0.05
Absorber-compressor work (in kJ/kg CO <sub>2</sub> )	42.2	42.2	42.2	42.2	42.2	42.2	42.2	42.2	42.2
With stripper (with recovery of the expansion work)									
Expansion (in kJ/kg CO <sub>2</sub> )	0	0	0	0	0	0	0	0	0
Pump work, total (in kJ/kg CO <sub>2</sub> )	78.7	65.9	59.5	59.5	52.1	52.1	56.3	56.3	56.3
Pump work, total (in kWh/kg CO <sub>2</sub> )	0.022	0.018	0.017	0.017	0.014	0.014	0.016	0.016	0.016



Table 6.13: Characteristics of chemical absorbents used in removing CO<sub>2</sub> [168]

Absorbent	Concentration (M)	Max. concentration	CO <sub>2</sub> charging (approx.)	Reaction enthalpy with CO <sub>2</sub> (enthalpy of solution)		Enthalpy of vaporization of the absorbent	Reaction rate
				kJ/mol CO <sub>2</sub>	kJ/kg CO <sub>2</sub>		
	M=mol absorbent/ mol H <sub>2</sub> O	kg MEA /kg H <sub>2</sub> O in %	kg CO <sub>2</sub> /kg MEA			kJ/kg	mol/L.s
MEA	5	30	0.4	72	1635.9	826	7600
DEA	3.5	36	0.4	65	1476.9	670	1500
TEA	3.35	50	0.5	62	1408.8	535	16.8
MDEA	4.28	50	0.5	53.2	1208.8	550	9.2
DIPA			0.4*		1673.6		400
DGA			0.4*		1975.8		
Hot potassium carbonate K <sub>2</sub> CO <sub>3</sub>			0.4*		603.1		

\*notional value

Table 6.14: Input values and results for calculating the energy requirements of CO<sub>2</sub> separation by means of condensation/sublimation of CO<sub>2</sub> from the flue gas of a gas/steam turbine combined cycle power plant

Flue gas of gas/steam turbine combined cycle power plant						
	Condensation			Freezing		
T in °C	0	-20	-56.45	-56.75	-100	-130
p <sub>0</sub> in bar	1.05	1.05	1.05	1.05	1.05	1.05
p <sub>tot</sub> in bar	9706	5460	1455	1430	39	0.86
p <sub>sat,subl</sub> in bar	34.85	19.70	5.21	5.12	0.14	0.0031
CO <sub>2</sub> capture ratio in %	90.0	89.9	90.0	90.0	90.0	90.0
Carnot coefficient of performance in %	9.2	17.8	37.6	37.8	72.2	108.3
ζ refrigerating unit (RU) in %	35	35	35	35	35	35
RU performance figure	3.8	2.0	0.9	0.9	0.5	0.3
Pinch in K	40	40	40	40	40	40
Refrigeration power in kJ/kg CO <sub>2</sub>	231.5	448.2	941.1	945.8	1795.3	2678.3
Refrigerating work in kWh/kg CO <sub>2</sub>	0.06	0.12	0.26	0.26	0.50	0.74
T after compression in °C	2798	2440	1753	1746	573	10.5
Compressor work in kJ/kg Gas	3509	3014	2084	2074	599	-15
Compressor work in kJ/kg CO <sub>2</sub>	74947	64413	44496	44274	12802	-320
T after expansion in °C	418.0	368.1	272.3	271.2	109.4	28.9
Expansion work in kJ/kg Gas	-3085	-2646	-1821	-1812	-511	19
Expansion work in kJ/kg CO <sub>2</sub>	-62478	-53613	-36869	-36682	-10350	385
Total compr. work in kJ/kg CO <sub>2</sub>	12470	10801	7628	7592	2452	65
Total compr. work in kWh/kg CO <sub>2</sub>	3.46	3.00	2.12	2.11	0.68	0.02
Total energy required in kWh/kg CO <sub>2</sub>	3.53	3.12	2.38	2.37	1.18	0.76

Table 6.15: Input values and results for calculating the energy requirements of CO<sub>2</sub> separation by means of condensation/sublimation of CO<sub>2</sub> from the flue gas of an IGCC power plant

Flue gas of IGCC power plant						
	Condensation			Freezing		
T in °C	0	-20	-56.6	-56.8	-100	-120
p <sub>0</sub> in bar	1.05	1.05	1.05	1.05	1.05	1.05
p <sub>tot</sub> in bar	3741	2114	556	555	14.85	1.4
p <sub>sat,subl</sub> in bar	34.8	19.7	5.2	5.1	0.14	0.013
CO <sub>2</sub> capture ratio in %	90.0	90.0	90.0	90.1	90.0	90.0
Carnot coefficient of performance in %	9.2	17.8	37.7	37.8	72.2	94.7
ζ refrigerating unit in %	35	35	35	35	35	35
RU performance figure	3.8	2.0	0.9	0.9	0.5	0.4
Pinch in K	40	40	40	40	40	40
Refrigeration power in kJ/kg CO <sub>2</sub>	99.2	191.8	403.0	403.8	765.3	998.4
Refrigerating work in kWh/kg CO <sub>2</sub>	0.03	0.05	0.11	0.11	0.21	0.28
T after compression in °C	2053	1788	1273	1272	366	53
Compressor work in kJ/kg Gas	2613	2237	1528	1526.3	378.4	29.3
Compressor work in kJ/kg CO <sub>2</sub>	23303	19953	13622	13596	3376	261
T after expansion in °C	318.7	281.2	208.6	208.4	81.0	30.5
Expansion work in kJ/kg Gas	-2289	-1956	-1328	-1327	-318	-23
Expansion work in kJ/kg CO <sub>2</sub>	-17871	-15271	-10365	-10345	-2486.7	-183.0
Total compressor work in kJ/kg CO <sub>2</sub>	5432	4682	3257	3251	889	79
Total compr. work in kWh/kg CO <sub>2</sub>	1.51	1.30	0.90	0.90	0.25	0.02
Total energy required in kWh/kg CO <sub>2</sub>	1.54	1.35	1.02	1.02	0.46	0.30

Table 6.16: Input values and results for calculating the energy requirements of CO<sub>2</sub> separation by means of condensation/sublimation of CO<sub>2</sub> from the flue gas of a coal-fired steam power plant

Flue gas SPP						
	Condensation			Freezing		
T in °C	0	-20	-56.6	-56.8	-100	-120
p <sub>0</sub> in bar	1.05	1.05	1.05	1.05	1.05	1.05
p <sub>tot</sub> in bar	2600	1466	386	390	10.4	0.97
p <sub>sat,subl</sub> in bar	34.8	19.7	5.2	5.1	0.139	0.013
CO <sub>2</sub> separation factor in %	90.0	89.9	89.9	90.2	90.0	90.0
Carnot coefficient of performance in %	9.2	17.8	37.7	37.8	72.2	94.7
ζ refrigerating unit (RU) in %	35	35	35	35	35	35
RU performance figure	3.8	2.0	0.9	0.90	0.5	0.4
Pinch in K	40	40	40	40	40	40
Refrigeration power in kJ/kg CO <sub>2</sub>	68.5	132.4	277.9	278.0	526.6	687.4
Refrigerating work in kWh/kg CO <sub>2</sub>	0.02	0.04	0.08	0.08	0.15	0.19
T after compression in °C	1879	1641	1151	1155	308	19
Compressor work in kJ/kg Gas	2273	1953	1312	1316	299	-6
Compression in kJ/kg CO <sub>2</sub>	14579	12531	8413	8418	1918	-37
T after expansion in C	294	263	192	192	73	26.5
Expansion work in kJ/kg Gas	-1989	-1703	-1138	-1141	-250	7
Expansion in kJ/kg CO <sub>2</sub>	-10544	-9032	-6033	-6037	-1327	39
Total compressor work in kJ/kg CO <sub>2</sub>	4034	3499	2380	2381	591	1.7
Compressor work in kWh/kg CO <sub>2</sub>	1.12	0.97	0.66	0.66	0.16	0.00
Total power required in kWh/kg CO <sub>2</sub>	1.14	1.01	0.74	0.74	0.310	0.19

Table 6.17: Input values and results for calculating the energy requirements of CO<sub>2</sub> separation by means of condensation/sublimation of CO<sub>2</sub> from the synthesis gas of an IGCC power plant after CO shift conversion

Synthesis Gas					
	Condensation			Freezing	
T in °C	0	-20	-56.57	-56.75	-75
p <sub>0</sub> in bar	25	25	25	25	25
p <sub>tot</sub> in bar	591.8	335.6	87.9	88.22	22.67
p <sub>sat,subl</sub> in bar	34.8	19.7	5.2	5.1	1.3
CO <sub>2</sub> capture ratio in %	90.0	90.0	90.0	90.1	89.9
Carnot coefficient of performance in %	9.2	17.8	37.7	37.8	50.5
ζ of refrigerating unit (RU) in %	35	35	35	35	35
RU performance figure	382.4	196.9	92.9	92.6	69.4
Pinch in K	40	40	40	40	40
Refrigeration power in kJ/kg CO <sub>2</sub>	22.1	42.4	88.2	88.3	117.0
Refrigerating work in kWh/kg CO <sub>2</sub>	0.01	0.01	0.02	0.02	0.03
T after compression in °C	409.6	322.4	149.9	150.3	18.4
Compression work in kJ/kg Gas	682.7	519.6	210.8	211.4	-10.9
Compression work in kJ/kg CO <sub>2</sub>	880.9	670.2	271.9		56.3
T after compression in °C	88.8	75.7	48.2		30.3
Expansion work in kJ/kg Gas	-577	-436	-173		-35
Expansion work in kJ/kg CO <sub>2</sub>	-103	-78.0	-30.9		-6.2
Total compr. work in kJ/kg CO <sub>2</sub>	777.7	592.3	241.0		50.1
Total compressor work in kWh/kg CO <sub>2</sub>	0.22	0.16	0.07		0.01
Total power required in kWh/kg CO <sub>2</sub>	0.22	0.18	0.09		0.04

Table 6.18: Expenditures and potential recovery of energy for CO conversion / CO<sub>2</sub> adsorption with CaO / CaCO<sub>3</sub> (without CO<sub>2</sub> liquefaction).

Adsorbent: CaO		H <sub>2</sub> O : CO (mol/mol): 2.1 : 1	
Adsorption: 600-400°C / 29.7 bar		Desorption: 750°C / pCO <sub>2</sub> <0.086 bar	
Expenditure / Exergy Losses			
	Enthalpy in MW	Electrical Energy in MW	Efficiency Penalty in Percentage Points
MP steam for CO conversion in MW	69.4	21 *	-2.4
Raw gas for CaO regeneration (750°C)	253	132.0 **	-14.9
O <sub>2</sub> generation (0.23 kWh/kg O <sub>2</sub> , 1bar)		15.8	-1.8
<u>Total losses</u>		172.4	-19.5
Heat recovery			
Adsorption enthalpy (400°C)	231	64.7 ***	+7.3
CO <sub>2</sub> waste gas (750°C)	52	15.6 *	+1.8
Effect of N <sub>2</sub> preheating on GT	26	6.5 ****	+0.7
Fuel gas expansion		2.73	+0.3
<u>Total recovery</u>		89.5	+10.1
CO <sub>2</sub> compression from 0.16 bar to 1 bar: (η <sub>is</sub> =0.9, 2 stages, intercooling at 30°C)		31.2	-3.5
<u>Total power loss</u>		110.6	-12.5
Energy input (coal)	885.14		

\* Conversion of enthalpy to electrical energy where:  $\eta \approx 0.3$

\*\* Conversion of enthalpy to electrical energy where:  $\eta = \eta_{IGCC} / \eta_{(\text{clean gas to coal})} \approx 0.4 / 0.766 = 52.2\%$

\*\*\* Conversion of enthalpy to electrical energy where:  $\eta \approx 0.28$

\*\*\*\* Conversion of enthalpy to electrical energy where:  $\eta \approx 0.25$

Table 6.19: Results of calculations for the 'quasi-combined' cycle with TITs of 1300°C and 1190°C at condenser temperatures of 18/20/23°C (single-stage GT, three-stage intercooled compression).

TIT in °C	1300	1300	1300	1190	1190	1190
Condenser temperature in °C	18	20	23	18	20	23
CO <sub>2</sub> condensation pressure in bar	67.45	69.7	73.12	67.45	69.7	73.12
T-recuperator/CO <sub>2</sub> in °C	769	771	774	669	672	674
Power output (positive = delivery of electric power, negative = consumption )						
GT in kW	31282	31213	31213	31178	30982	30905
ST in kW	10069	10070	10097	9855	9817	9812
O <sub>2</sub> compression in kW	-1883	-1883	-1883	-1883	-1883	-1883
CO <sub>2</sub> compression in kW	-9110	-9195	-9195	-9862	-9909	-9767
pump in kW	-1415	-1453	-1557	-1539	-1573	-1681
ASU in kW	-3957	-3957	-3957	-3957	-3957	-3957
net output in kW	24986	24795	24719	23791	23476	23429
Efficiencies in %						
η (LHV)	50.0	49.6	49.4	47.6	46.9	46.8
η (HHV)	45.0	44.7	44.5	42.9	42.3	42.2
Composition of separated CO <sub>2</sub> stream						
Mass fractions of CO <sub>2</sub> in %	96.5	96.5	96.5	96.5	96.5	96.5
Mass fractions of Ar in %	2.7	2.7	2.7	2.7	2.7	2.7
kg CO <sub>2</sub> /s	2.735	2.735	2.735	2.735	2.735	2.735
CH <sub>4</sub> input in kg/s	1					
LHV (CH <sub>4</sub> )	50010					
HHV (CH <sub>4</sub> )	55495					
O <sub>2</sub> mass flow in kg/s	4.071					
Energy expended in O <sub>2</sub> production in kWh/kg O <sub>2</sub>	0.27kWh/kg (at 1 bar, O <sub>2</sub> purity: 98% Volume fraction O <sub>2</sub> )					

Table 6.20: Potential for reducing CO<sub>2</sub> emissions

Measure	Potential for reducing CO <sub>2</sub> emissions	Notes
Worldwide use of natural gas instead of coal as a power plant fuel	8% (global)	Assuming that power plant efficiency remains the same
Replacing all existing power plants in Germany with new higher-efficiency models (43% for lignite power plants, 47% for hard coal power plants, 58% for natural gas power plants)	30% in relation solely to lignite power plants 27% in relation solely to hard coal power plants  14.5% in Germany (total emissions)	1) Average efficiencies [207]: 32.0% for all the electricity generating plants of the public power supply system 30.0% for the lignite power plants of the public power supply system 34.3% for the hard coal power plants of the public power supply system 2) Share of electricity generation (1997) [208]: 25% for lignite power plants, 26% for hard coal power plants
Replacing the separate generation of electrical energy and heat with power and heat cogeneration ( <i>German</i> : KWK)	1.4% to 7.8% in Germany (total emissions)	Literature source: Pruscsek et al. [207]
Increased construction of nuclear power plants on a global level	7% (only power supply sector, global)	Literature source: van de Vate [209]

## 6.6 Electrical Equivalence Factor of Heat Utilization (Extraction Steam)

Chemically-acting solvents (chemical absorption) are regenerated through an increase in temperature. Normally, steam is used to heat the regenerator. This steam is extracted from the low-pressure section of the steam turbine and fed back into the steam cycle as condensate. Extracting the steam leads to a reduction in the output of the steam turbine cycle.

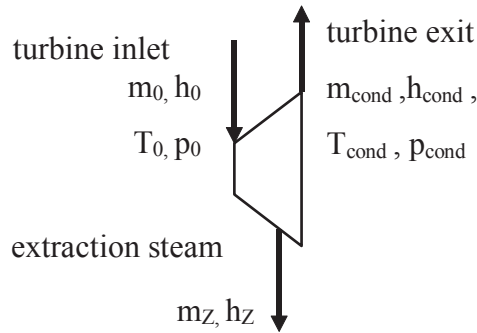


Figure 6.8: Steam extraction

The reduced output of the steam turbines  $\Delta P_T$  (mechanical equivalent of the steam) is calculated from heat consumption  $\dot{Q}$  through multiplication with a conversion factor (equivalence factor  $\alpha_{0,Q}$ ):

$$\Delta P_T = \alpha_{0,Q} \cdot \dot{Q}_{use} \quad (6.1)$$

Heat flow  $\dot{Q}_{use}$ , used in the heat consumer, is the difference  $\Delta H_{D,use}$  between the enthalpy flow of the steam prior to heat utilization and the condensed, warm water after heat utilization.

$\dot{Q}_{use}$  corresponds approximately to enthalpy  $H(p_Z, T_Z)$  of the extraction steam:

$$\dot{Q}_{use} = \Delta H_{D,use} = \dot{m}_Z h(p_Z, T_Z) \quad (6.2)$$

The ratios at the steam turbine are shown in Figure 6.8. Equivalence factor  $\alpha_{0,Q}$  of the heat utilization is the ratio of the modified turbine output  $\Delta P_T$  to the heat used  $\dot{Q}_{use}$ :

$$\alpha_{0,Q} = \frac{\Delta P_T}{\dot{Q}_{use}} = \frac{\Delta P_T}{\dot{m}_Z h(p_Z, T_Z)} \quad (6.3)$$

With the modified turbine output (mechanical equivalent of the steam):

$$\Delta P_T = \dot{m}_Z |w_t| = \dot{m}_Z [h(p_Z, T_Z) - h''(p_{cond}, x_{cond})] \quad (6.4)$$

equivalence factor  $\alpha_{0,Q}$  is calculated:

$$\alpha_{0,Q} = \frac{\Delta P_T}{\dot{Q}_{use}} = \frac{\Delta P_T}{\dot{m}_Z h(p_Z, T_Z)} = \frac{h(p_Z, T_Z) - h''(p_{cond}, x_{cond})}{h(p_Z, T_Z)} \quad (6.5)$$

The enthalpy of the condensate flowing back from the heat consumer could be used to preheat the feed water. This would enable a higher equivalence factor to be achieved. The enthalpy of fuel saved through preheating corresponds to enthalpy  $\dot{m}_z h'(p_z)$  of the condensate from the heat consumer minus enthalpy  $\dot{m}_z h'(p_{Kond})$  of the condensate after the steam turbine:

$$\Delta \dot{H}_B = \dot{m}_z (h'(p_z) - h'(p_{cond})) \quad (6.6),$$

To perform a more precise calculation of the change in power output through using the hot return flow condensate from the heat consumer for regenerative preheating in the steam turbine cycle with the same utilization of fuel, it would be necessary to take into consideration the exact process arrangement of the steam cycle with the number of preheatings, and the states and mass flow rates of the vapor. To enable a generalized statement to be given, the simplified assumption is made that efficiency  $\eta_{D,el}$  of the steam cycle is known. This enables the calculation of equivalence factor  $\alpha_{v,Q}$  of heat utilization with preheating:

$$\begin{aligned} \alpha_{v,Q} &= \frac{\Delta P_T + \eta_{D,el} \dot{m}_z (h'(p_z) - h'(p_{cond}))}{\dot{m}_z h(p_z, T_z)} \\ &= \frac{h(p_z, T_z) - h''(p_{cond}, x_{cond}) + \eta_{D,el} (h'(p_z) - h'(p_{cond}))}{h(p_z, T_z)} \end{aligned} \quad (6.7).$$

If technical limitations mean that the steam can only be expanded by the turbine to a residual humidity of around 85%, for some live steam states this will mean having to increase the condenser pressure. High wet steam pressure at the turbine inlet means that maximum humidity has already been achieved at a high pressure, which produces a higher turbine exit temperature. This also reduces the equivalence factor.

Figure 6.9 (using the enthalpy of the hot condensate from the heat consumer for preheating purposes) and Figure 6.10 (using the enthalpy of the hot condensate) show the equivalence factor for the three cases, in which the difference in enthalpy usable in the turbine:

- occurs through expansion to 0.04 bar (29°C), whereby residual humidity is dependent on the inlet state of the steam (Figure 6.11),
- is the difference between the enthalpy of the extraction steam and the enthalpy at a fixed condenser state of 0.04 bar and wet steam of 85%, or
- occurs through expansion to wet steam of 85%, and to the associated condenser pressure in dependence on the inlet state of the steam (Figure 6.12).

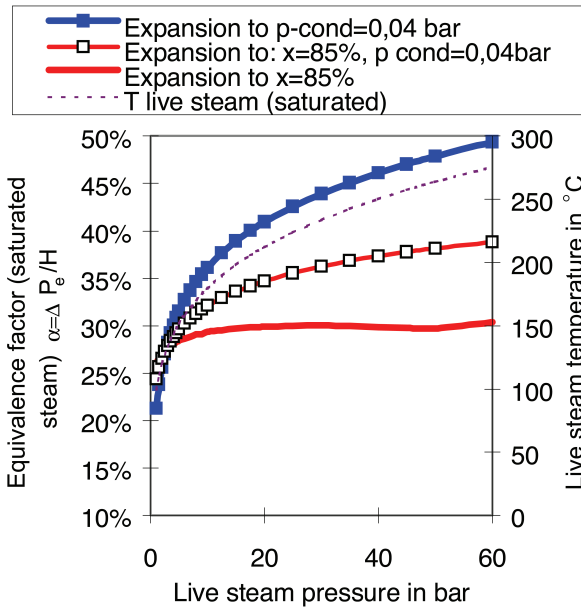


Figure 6.9: Equivalence factor using the hot condensate from the heat consumer for preheating.

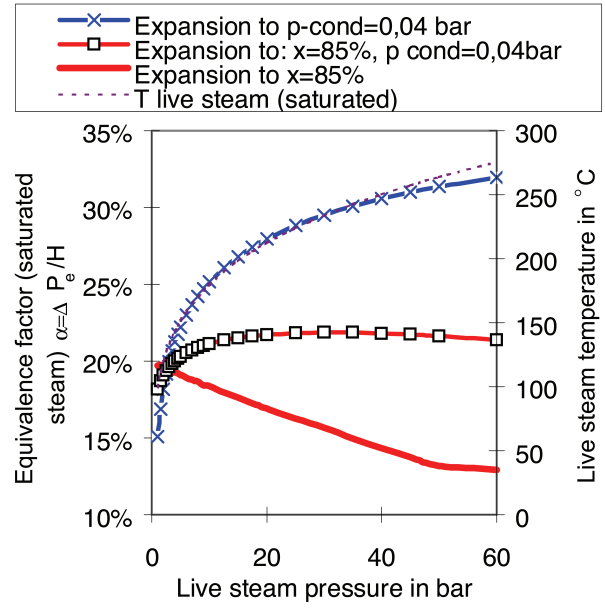


Figure 6.10: Equivalence factor without use of the hot condensate from the heat consumer

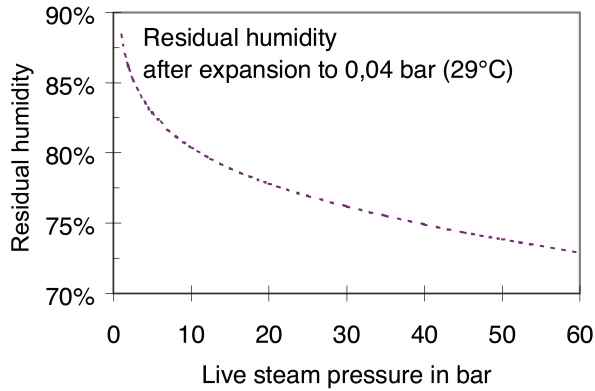


Figure 6.11: Equivalence factor using the hot condensate from the heat consumer for preheating.

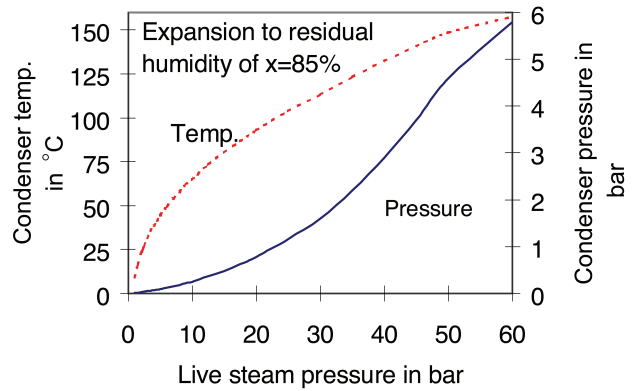


Figure 6.12: Equivalence factor without use of the hot condensate from the heat consumer

## 6.7 Calculation of Electricity Generating Costs

In calculating the electricity generating costs, it is assumed that the investment during the period of construction is made in equal annual installments, at the mid-point of each year. Table 4.2 on page 143 summarizes the values of the factors which influence the calculation.

The method of calculating the electricity generating costs is described in more detail by Pruscsek et al. [180].

$$k_{el} = \frac{I}{T_a} \cdot \alpha \cdot \beta \cdot \gamma + \frac{k_b}{\eta} \cdot \delta \cdot \varepsilon \quad (6.8)$$

where:

$$\alpha = \left(1 + \frac{f_E}{100}\right) \cdot \left(1 + \frac{f_I}{100}\right)^{n_P}$$

$$\beta = \frac{1}{n_B} \left( \sum_{x=1}^{n_B} \left(1 + \frac{f_I}{100}\right)^{(x-0.5)} \cdot \left(1 + \frac{f_{ZB}}{100}\right)^{(n_B - (x-0.5))} \right)$$

$$\gamma = \frac{q^{n_L} \cdot (q-1)}{q^{n_L} - 1} + \frac{f_S}{100} + \frac{f_V}{100} + \frac{f_W}{100} \quad \text{in } 1/a$$

$$\delta = \frac{3.6}{1000} \cdot e^{(n_P + n_B)} \quad \text{in GJ/kWh}$$

$$\varepsilon = \frac{\left(q^{n_L} - \left(1 + \frac{f_I}{100}\right)^{n_L}\right)}{q^{n_L} \cdot \left(q - \left(1 + \frac{f_I}{100}\right)\right)} \cdot \frac{q^{n_L} \cdot (q-1)}{(q^{n_L} - 1)}$$

$$q = 1 + \frac{f_Z}{100}$$

$$e = 1 + \frac{f_I}{100} + \frac{f_e}{100}$$

Table 6.21: Influencing factors in the calculation of electricity generating costs

$k_{el}$	standardized electricity generating costs in US\$/kWh	$I$	specific plant costs in base year in US\$/kW
$T_a$	annual utilization factor in h/a	$k_B$	fuel costs in base year in US\$/GJ
$\eta$	net efficiency of power plant	$n_P$	duration of planning period prior to start of construction in years
$n_B$	construction period in years	$n_L$	period of depreciation, operating life in years
$f_E$	client's own contribution as % of plant costs	$f_I$	general price escalation (inflation) in %/a
$f_{ZB}$	imputed rate of interest during construction period (discount rate) in %/a	$f_S$	standardized tax rate during period of construction in %/a
$f_V$	standardized rate of insurance over period of operation in %/a	$f_W$	standardized rate of maintenance and repair costs + staff costs in %/a
$f_Z$	imputed rate of interest during period of operation in %/a	$f_e$	increase in fuel prices in %/a



## 7 LITERATURE

- [1] Keith, D.W.; E.A. Parson (2000): A Breakthrough in Climate Change Policy. Scientific American Feb. 2000.
- [2] Strömberg, L. (2001): „Discussion on the Potential and Cost of Different CO<sub>2</sub> Emission Control Options in Europe.“ VGB power Tech, 10/2001, S. 92-97
- [3] Berner, R.A.; A.C. Lasaga (1989): "Simulation des geochemischen Kohlenstoffkreislaufs." Spektrum der Wissenschaft, Mai 1989, 54-61
- [4] Griffin A., Bill J., Marion N., Nskala N.: Controlling Power Plant CO<sub>2</sub> Emissions: A Long Range View. Power-Gen Europe, Brüssel, 2001
- [5] Winkler Ph.: Evolution of Combustion Technology to Support National Energy Needs. January 15, 2002, www.airproducts.com
- [6] Asen, K.; K. Wilhelmsen(2003): „CO<sub>2</sub> Capture in Power Plants Using Mixed Conduction Membranes (MCM).“ PowerGen Europe 2003.
- [7] Lackner K. S., Ziock H-J.: „The US Zero Emission Coal Alliance Technology,“ VGB PowerTech 12/2001, S. 57 bis 61, Essen 2001, <http://www.vgb.org>.
- [8] Köhler, D.; Krammer, Th.; Schwärzer, M. (2003): "Der Zero Emission Coal Process." BWK 3-2003, pp. 63-66.
- [9] Arrhenius, S. (1896): "On the Influence of Carbonic Acid in the Air upon the Temperature of the Ground". Philosophical Magazine and Journal of Science, Fifth Series, April 1896, London, Edinburgh and Dublin.
- [10] Houghton, J. T.; Meira Filho, L. G.; Callander, B. A.; Harris, N.; Kattenberg, A.; Maskell, K., (Eds) (1996): "Climate Change. The science of climate change". Cambridge University Press. 1996
- [11] WEC (1997): World Energy Council Journal, London, Juli 1997
- [12] BP (1998): "BP Statistical Review of World Energy 1998", British Petroleum Company p.l.c.
- [13] (ed.) Lakeman, J.A. (1995): "Climate Change 1995, The Science of Climate Change". Intergovernmental Panel on Climate Change, Cambridge University Press, 1996
- [14] Schönwiese, Chr. D. (1997): "Sichere Vorhersagen?", Interview in der Süddeutschen Zeitung vom 07.08.1997, Blickpunkt Wissenschaft.
- [15] Marland, G.; T. Boden (1997): "Regional Annual CO<sub>2</sub> Emission Estimates from Fossil-Fuel Burning, Cement Production, and Gas Flaring: 1950-94." (Oak Ridge National Laboratory), Februar 1997.
- [16] Hendriks, C.A. (1994): "Carbon Dioxide Removal from Coal-Fired Power Plants". Kluwer Academic Publishers, Dordrecht, 1994.
- [17] Koetzier, H.; van Rijen S.P.N.; Bresser, H. (1992): "Calculations on Some Complete Systems for Electricity Production with CO<sub>2</sub> Recovery, Transport and Storage". KEMA, Arnhem, The Netherlands, Juni 1992 (in Holländisch).
- [18] IEA GHG (1993): "Carbon Dioxide Capture from Power Stations". IEA Greenhouse Gas R&D Programme, Cheltenham, UK.
- [19] Pruschek, R.; Oeljeklaus, G.; Göttlicher, G.; Kloster, R. (1997): "Gas-Dampfkraftwerke mit hohen Wirkungsgraden", VDI-GET Tagung: Fortschrittliche Energiewandlung und -anwendung. Bochum, 1997.
- [20] Pruschek, R., Oeljeklaus, G.; Boeddicker, D.; Brand, V.; Folke, C.; Göttlicher, G.; Kloster, R.; Haupt, G.; Zimmermann, G.; Moricet, M.; Tränkenschuh, H.-Chr.; Schwarzott, W.; Jansen, D.; Ribberink, J. S.; Iwanski, Z. (1997): Contract JOU2-CT92-0185: "Coal-fired multicycle power generation systems for CO<sub>2</sub> control in IGCC-systems for minimum noxious gas emissions, CO<sub>2</sub> control and CO<sub>2</sub> disposal". In: "Joule II - Clean Coal Technology Programme 1992-95, Volume III: Combined Cycle Project, Final

- Reports*". Europäische Kommission, Directorate-General XII - Science, Research and Development, 1997, EUR 17524 EN, ISBN 92-828-0007-5.
- [21] Pruschek, R.; D. Jansen; B. C. Williams (1998): "*Advanced cycle technologies, Improvement of IGCCs starting from the state of the art (Puertollano)*". Second Conference: "Coal and Biomass: High-Tech Fuels for the Future, Clean Coal Technologies for Solid Fuels" (JOULE-THERMIE, 1996-1998), 11./12. November 1998, Brüssel.
- [22] Pruschek, R.; G. Oeljeklaus; V. Brand; G. Göttlicher; R. Kloster. (1995): "*COMBINED CYCLES, Including Technologies such as IGCC, PFBC, on which there Exist Considerable RD & D Efforts*". Für: Institute for Prospective Technological Studies. Sevilla, Juli 1995
- [23] van Heek, K. H. (1995): "*Erzeugung und Konditionierung von Gasen für den Einsatz in Brennstoffzellen*". VDI-Berichte Nr. 1174, 1995, pp. 97-115.
- [24] Riensche, E. (1995): "*Verfahrenstechnik der Hochtemperaturbrennstoffzelle*". VDI-Berichte Nr. 1174, 1995, p. 63-78.
- [25] IEA GHG (1998): "*Fuel Cells with Carbon Dioxide Removal*". IEA Greenhouse Gas R&D Programme, Cheltenham, UK. Report Number PH2/13, 1998.
- [26] Kjær, S. (1993): "*Die zukünftigen 400 MW-ELSAM-Blöcke in Aalborg und Skærbæk*" VGB Kraftwerkstechnik 73 (1993), 11, pp. 933-940.
- [27] Eichholtz, A.; Hourfar, D.; Kübler, D. (1994): "*Der 700-MW-Steinkohleblock der VEBA Kraftwerke Ruhr AG in Gelsenkirchen-Heßler*". VGB Kraftwerkstechnik 74 (1994), Nr. 1, pp. 25-29.
- [28] Kjaer, S. (1996): "*The Advanced Pulverized Coal-Fired Power Plants - Status and Future*". POWER-GEN EUROPE '96.
- [29] Hald, J.; B. Nath (1998): "*New High Temperature Steels for Steam power Plants*". POWER-GEN EUROPE '98, Milano, Juni 1998.
- [30] Thomsen, F.; C. M. Hansen; S. Kjær (1998): "*Danish Experiences from new USC Plants at Skærbækværket and Nordjyllandsværket*". POWER-GEN EUROPE '98, Milano, Juni 1998.
- [31] Campbell, P. E.; McMullan, J. T.; Williams, B. C. (1995): "*Fuel Cells in "Clean" Coal Power Generation*". Proceedings of the 3<sup>rd</sup> International Symposium on Coal Combustion, Science and Technology. Beijing, China, Sept. 18-21, 1995, 633-642. Science Press, Beijing, 1995.
- [32] McMullan, J.T.; Williams, B.C; Campbell, P.E; McIlveen-Wright, D.R.; Brennan, S.; McCahey, S. (1996): "*Fuel Cell Optimisation Studies*". JOULE II Programme. Final Report, Contract JOUL2-CT93-0278. 1996.
- [33] Marchetti, C. (1977): "*On Geoengineering and the CO<sub>2</sub> Problem*". Climatic Change 1 (1977), pp. 59-68, D. Reidel Publishing Company, Dordrecht-NL.
- [34] Horn, F.L.; Steinberg, M. (1982): "*An Improved Carbon Dioxide Power Plant*". Energy Progress Vol.2 No.3, Sep. 1982.
- [35] Horn, F.L.; Steinberg, M. (1982): "*Control of Carbon Dioxide Emissions from a Power Plant (and Use in Enhanced Oil Recovery)*". Fuel Vol. 61, Mai 1982.
- [36] Steinberg, M.; Cheng, H. C.; Horn, F. (1984): "*A Systems Study for the Removal, Recovery and Disposal of CO<sub>2</sub> from Fossil Fuel Power Plants in the US*". DOE /CH/000 16-2, Dez. 1984.
- [37] Steinberg, M.; Grohse, E.W. (1991): "*A feasibility study for the coprocessing of fossil fuels with biomass by the Hydrocarb process*". Research report US EPA-600/7-91-007 (NTIS DE91-011971), 1991.
- [38] Steinberg, M.; Dong, Y.; Borgwardt, R.H. (1993): "*The Coprocessing of Fossil and Biomass for CO<sub>2</sub> Emission Reduction in the Transportation Sector*". Energy Convers. Mgmt. Vol.33 No.5-8, Pergamon Press, Oxford, 1992, pp.1015-1023.

- [39] Sander, M.T.; Mariz, C. L.; (1992): "*The Fluor Daniel ECONAMINE FG Process: Past Experience and Present Day Focus*". Energy Convers. Mgmt. Vol.33 No.5-8, Pergamon Press, Oxford, 1992, pp.341-348.
- [40] Barchas, R.; Davis, R. (1992): "*The Kerr-McGee/ABB Lummus Crest Technology for the Recovery of CO<sub>2</sub> from Stack Gases*". Energy Convers. Mgmt. Vol.33 No.5-8, Pergamon Press, Oxford, 1992, pp.333-340.
- [41] Collins, S. (1992): "*Cogen plant cycles large CFB boilers, recovers CO<sub>2</sub>*". Power, pp.47-52, Apr. 1992.
- [42] Rushing, S.A.; (1993): "*Cogeneration projects can profit from CO<sub>2</sub> recovery*". Power Engineering, pp.33-34, Mai 1993.
- [43] Suda, T.; Fujii, M.; Yoshida, K.; Iijima, M.; Seto, T.; Mitsuoka, S. (1992): "*Development of flue gas carbon dioxide recovery technology*". Energy Convers. Mgmt. Vol.33 No.5-8, Pergamon Press, Oxford, 1992, pp.317-324.
- [44] IEA GHG (1996): "*Pioneering CO<sub>2</sub> Reduction*". Greenhouse Issues, Number 27, Nov. 1996. IEA Greenhouse Gas R&D Programme, Cheltenham. ISSN 0967 2710.
- [45] IEA GHG (1996): "*CO<sub>2</sub> Capture and Storage in the Natuna LNG Project*". Greenhouse Issues, Number 22, Jan. 1996. IEA Greenhouse Gas R&D Programme, Cheltenham. ISSN 0967 2710.
- [46] Seifritz, W. (1993): "*The Terrestrial Storage of CO<sub>2</sub>-Dry-Ice*". IEA Carbon Dioxide Disposal Symposium, Oxford, Energy Conv. Mgmt. Vol. 34, No. 9-11, Pergamon Press, Oxford, March 1993, pp. 1121-1141.
- [47] Marchetti, C. (1979): "*Constructive Solutions to the CO<sub>2</sub> Problem*". In: W. Bach, J. Pankrath, W. Kellogg (Eds.): "*Man's Impact on Climate*", Elsevier, New York 1979.
- [48] Baes, C.F.; Beall, S. E.; Lee, D.W. (1980): "*The Collection, Disposal and Storage of Carbon Dioxide*". In: Bach, W.; Pankrath J.; Williams, J. (Eds.): "*Interactions of Energy and Climate*", pp. 495-519, D. Reidel Publishing Company 1980.
- [49] Gunter, W.D.; E.H. Perkins; T.J. McCann (1993): "*Aquifer Disposal of CO<sub>2</sub> rich gases: reaction design for added capacity*". Energy Convers. Mgmt. 34, 941-948.
- [50] Segen, G. R.; K. H. Cole (1993). Energy Convers. Mgmt. 1993, 34, pp.857-864.
- [51] Nakashiki, N.; Oshumi, T.; Shitashima, K. (1991): "*Sequestering of CO<sub>2</sub> in a Deep- Ocean*". Central Research Institute of Electric Power Industry, Japan, 1991.
- [52] Stevens, S. C., D. Spector; P. Riemer (1998): "*Enhanced Coalbed Methane Recovery Using CO<sub>2</sub> Injection: Worldwide Resource and CO<sub>2</sub> Sequestration Potential*". Presentation STG-06 at 4<sup>th</sup> Int. Conf. Greenhouse Gas Control Technologies, Interlaken 1998. Energy Convers. Mgmt., 1999.
- [53] IEA GHG (1999): "*CO<sub>2</sub> Sequestration in Deep Coal Seams*". Greenhouse Issues, Number 40, Jan. 1999.
- [54] Freund, P.; W.G. Ormerod (1997): "*Progress Toward Storage of Carbon Dioxide*". Energy Convers. Mgmt. Vol. 38, Suppl., pp. S199-S204, 1997.
- [55] Haugen, H. A.; L. I. Eide (1996): "*CO<sub>2</sub> Capture and Disposal: The Realism of Large Scale Scenarios*". Energy Convers. Mgmt. Vol. 37, Nos. 6-8, pp. 1061-1066, 1996.
- [56] Bundesministerium für Wirtschaft (BMWi): "*Energiedaten 1992/1993*"
- [57] Riemer, P. W.; W.G. Ormerod (1995): "*International Perspectives and Results of Carbon Dioxide Capture Disposal and Utilisation Studies*". Energy Convers. Mgmt. Vol. 36, No. 6-9, pp.-813-818, 1995.
- [58] Mohn, F. H.; J. U. Grobbelaar; C. J. Soeder (1998): "*Can Microalgal Biotechnology be used to reduce the CO<sub>2</sub> Atmospheric Burden?*". Presentation BIO-P01 at 4<sup>th</sup> Int. Conf. Greenhouse Gas Control Technologies, Interlaken 1998. Energy Convers. Mgmt., 1999.
- [59] Jones, IS.F: (1996): "*Enhanced Carbon Dioxide Uptake by the World's Oceans*". Energy Convers. Mgmt. Vol. 37, Nos. 6-8, pp. 1049-1052, 1996.

- [60] Berner, R.A.; A.C. Lasaga (1989): "*Simulation des geochemischen Kohlenstoffkreislaufs*". Spektrum der Wissenschaft, Mai 1989, 54-61
- [61] Lackner, K. S.; D. P. Butt; Chr. H. Wendt (1997): "*Progress in binding CO<sub>2</sub> in Mineral Substrates*". Energy Convers. Mgmt. Vol. 38, Suppl., pp. S259-S264, 1997.
- [62] Kojima, T.; A. Naamine; N. Ueno; S. Uemiya (1997): "*Absorption and Fixation of Carbon Dioxide by Rock Weathering*". Energy Convers. Mgmt. Vol. 38, Suppl., pp. S461-S466, 1997.
- [63] Sparrow, F. T.; Wolsky, A.M.; Berry, G.F.; Brooks, C.; Cobb, T. B.; Lynch, E. P.; Jankowski, D. J.; Walbridge, E.W. (1988): "*Carbon Dioxide From Flue Gases For Enhanced Oil Recovery*". Argonne National Laboratory, ANL/CNSV-65, 1988
- [64] Skovholt, O. (1993): "*CO<sub>2</sub> Transportation System*". Energy Convers. Mgmt. Vol.34, No. 9-11, pp.1095-1103, Pergamon Press, Oxford, 1993.
- [65] Udvardi, G.; Gerecs, L.; Ouchi, Y.; Nagakura, F.; Thoes, E.A.; Wallace, C.B. (1990): "*CO<sub>2</sub> dehydration scheme aids Hungarian EOR project*". Oil & Gas Journal, Okt. 22, 1990, pp. 74-79.
- [66] Case, J. L.; Ryan, B. F.; Johnson, J. E. (1985): "*CO<sub>2</sub> streams pose new design considerations*". Oil & Gas Journal, Mai 6, 1985, pp. 175-179.
- [67] Hein, M. (1986): "*Pipeline design model addresses CO<sub>2</sub>'s challenging behaviour*". Oil & Gas Journal, Juni 2, 1986, pp. 71-75.
- [68] Riemer, P. W.; W. G. Ormerod (1995): "*International Perspectives and Results of Carbon Dioxide Capture Disposal and Utilisation Studies*". Energy Convers. Mgmt. Vol. 36, No. 6-9, pp.813-818, 1995.
- [69] Johnson, J. E.; Walter, F. B. (1985): "*Gas processing needs for EOR*". Hydrocarbon Processing, Oktober 1985, pp. 62-63.
- [70] Triefhoff, H.-J.; Andriessen, B. J.; Zeller, R.; (1981): "*Beschaffung großer Kohlendioxidmengen für Erdöl-Flutprojekte*". Erdöl und Kohle-Erdgas-Petrochemie / Brennstoff-Chemie, Bd.34, 10, 1981, pp.433-437.
- [71] Hendriks, C. A.; Blok, K.; Turkenburg, W. C. (1990): "*The Recovery of Carbon Dioxide from Power Plants*". In: P.A. Okken, R.J. Stuart and S. Zwerer (Eds.): "*Climate and Energy*". Kluwer Academic Publisher, Dordrecht 1990, pp.125-142.
- [72] Hwang, S.-K; Kammermeyer, K. (1975): "*Membranes in Separation*". John Wiley, New York, 1975.
- [73] van der Sluijs, J. P.; Hendriks, C. A.; Blok, K. (1992): "*Feasibility of Polymer Membranes for Carbon Dioxide Recovery from Flue Gases*". Energy Convers. Mgmt. Vol.33, No.5-8, Pergamon Press, Oxford, 1992, pp.429-436.
- [74] Kümmel, R.; Groscurth, H.-M.; Schübler, U. (1992): "*Thermoeconomic Analysis of Technical Greenhouse Warming Mitigation*". Int. J. Hydrogen Energy, Vol. 17, No. 4, April 1992, pp.293-298.
- [75] Matson, S. L.; Lonsdale, H. K. (1987): "*Liquid membranes for the production of oxygen-enriched air, III. Process design and economics*". Journal of membrane sciences, 31 (1987) pp.69-87.
- [76] Springmann, H. (1974): "*Auslegung moderner Tieftemperatur-Anlagen zur Gewinnung von Sauerstoff, Stickstoff und Edelgasen*". Chemie-Ing.-Techn. 46 (1974), No.21, pp. 881-887.
- [77] IEA GHG (1993): "*The capture of carbon dioxide from fossil fuel fired power stations*". IEAGHG/SR2. IEA Greenhouse Gas R&D Programme, Cheltenham.
- [78] Nowack, R. (1992): "*CO<sub>2</sub>-Emissionen aus Steinkohlekraftwerken*". Reihe Energietechnik, Shaker, Aachen, 1992 (Diss.).
- [79] Gerhartz, W.(ed.) (1985): "*Ullmann's Encyclopaedia of Industrial Chemistry*". VCH Verlagsgesellschaft, Weinheim, Germany, 1985. ISBN 3-527-20102-5.
- [80] Haldor-Topsoe: Informationsbroschüren zum Katalysatorprogramm, 1993.

- [81] Shell International Petroleum Maatschappij and Koninklijke/Shell Explorati en Productie Laboratorium (1990): "*Carbon dioxide disposal from coal based combined cycle power stations in depleted gas fields in the Netherlands*". Publikatiereeks Lucht nr. 91, Ministry of Housing, Physical Planning and Environment, Air Directorate, Leidschenham, NL, 1990.
- [82] BASF (1995): Lieferprogramm für Katalysatoren.
- [83] Nakayama, T. et al. (1990): "*Development of fixed-bed type hot gas clean-up technology for integrated coal gasification combined cycle power generation*", CRIEPI-EW-89015, Tokyo, Japan, Central Research Institute of Electric Power Industry, April 1990.
- [84] Gangwal, S. K. (1991): "*Hot-Gas Desulphurisation Sorbent Development for IGCC Systems*", IChemE Symposium series No. 123, Rugby, UK, 1991, pp 159 - 171.
- [85] Brand, V. (1996): "*Rückhaltung von Kohlendioxid in Kohlekraftwerken mit integrierter Kohlevergasung*". Dissertation Universität GH Essen, 1996.
- [86] Condorelli, P.; Smelser, S.C.; McCleary, G.J.; Booras, G.S.; Stuart, R.J. (1991): "*Engineering and Economic Evaluation of CO<sub>2</sub> Removal from Fossil-Fuel-Fired Power Plants. Volume 2: Coal Gasification Combined-Cycle Power Plants*". EPRI IE-7365. Vol. 2. 1991.
- [87] Daun, M (1993): "*Bewertung von Technologien zur Verringerung der Emission und zur Entsorgung von Kohlendioxid*". Dissertation Universität Dortmund D290, Verlag Shaker, Aachen 1993.
- [88] Booras, G.S.; Smelser, S.C. (1991): "*An Engineering And Economic Evaluation Of CO<sub>2</sub> Removal From Fossil-Fuel-Fired Power Plants*". Energy Vol.16 (1991), No.11/12, pp.1295-1305.
- [89] Goldthorpe, S.H.; Cross, P.J.I.; Davison, J.E. (1992): "*System Studies on CO<sub>2</sub> Abatement From Power Plants*". Energy Convers. Mgmt. Vol.33, No.5-8, Pergamon Press, Oxford, 1992, pp.459-466.
- [90] Hendriks, C.A.; Blok, K.; Turkenburg, W.C. (1991): "*Technology and Cost of Recovering and Storing Carbon Dioxide from an Integrated-Gasifier, Combined-Cycle Plant*". Energy Vol.16 (1991); No.11/12, pp.1277-1293.
- [91] Doctor, R.D., J. C. Molburg; P.R. Thimmapuram; G.F. Berry; C.D. Livengood (1994): "*Gasification Combined Cycle: Carbon Dioxide Recovery, Transport and Disposal*". Argonne National Laboratory ANL/ESD-24, 1994.
- [92] Jansen, D.; Oudhuis, A.B.J.; Van Veen, H.M. (1991): "*CO<sub>2</sub>-Verwijdering Bij KV-Steg-Installaties Ujtgerust Met Een Heet-Gasreinigingssysteem*". Netherlands Energy Research Foundation, Petten, The Netherlands, ECN-C-91-021, March 1991.
- [93] Jansen, D.; Oudhuis, A.B.J.; Van Veen, H.M. (1991): "*CO<sub>2</sub> reduction potential of future coal gasification based power generation technologies*". Energy Convers. Mgmt. Vol. 33, No. 5-8, Pergamon Press, Oxford, 1992, pp. 365-372.
- [94] Alderliesten, P. T.; Bracht, M.; Kloster, R.; Oeljeklaus, G.; Pruschek, R.; Haupt, G.; Zimmermann, G.; Xue, E.; O'Keefe, M.; Ross, J.; Koukou, M.; Papayanakos, N.; Bos, A.; Hemmes, K.; Oudhuis, A.; Pex, P. (1997): "*An attractive option for CO<sub>2</sub> control in IGCC systems: Water gas shift with Integrated Hydrogen/carbon dioxide Separation (WIHYS process), Phase I: Proof of principle*". In: "*JOULE II - Clean Coal Technology Programme 1992-95, Volume III: Combined Cycle Project, Final Reports*". Europäische Kommission, Directorate-General XII - Science, Research and Development, 1997, EUR 17524 EN, ISBN 92-828-0007-5.
- [95] Kohl, A., L.; Riesenfeld, F., C. (1985): "*Gas Purification*". Gulf Publishing Company, Houston, Texas, fourth edition 1985.
- [96] Heesink, A. B. M. (1993): "*Process for removing carbon dioxide regeneratively from gas streams*". International Patent Appl. No. PCT/NL93/00136, Juni, 1993.

- [97] Ito, S.; H. Makino (1998): "*Carbon Dioxide Separation from Coal Gas by physical Adsorption at Warm Temperature*". Presentation CAP-19 at 4<sup>th</sup> Int. Conf. Greenhouse Gas Control Technologies, Interlaken 1998. Energy Convers. Mgmt., 1999.
- [98] Bower, C.; Goldthorpe, S.; Summerfield, I.; Fynes, G. (1992): "*CO<sub>2</sub> Removal As A Fallback Option For Power Generation?*". Energy and Environment (Brentwood), 1992, v.3(3), pp.222-237.
- [99] Mori, Y.; Masutani, S.M.; Nihous, G.C.; Vega, L. A.; Kinoshita, C. M. (1993): "*Pre-combustion removal of carbon dioxide from hydrocarbon-fuelled power plants*". Fuel 1993, Vol. 72 (9), pp.1293-1299.
- [100] Hille, J.E (1992): "*Removal of CO<sub>2</sub> from Reformer Gas in a Power Plant*". KTI/Mannesmann, Zoetermeer, The Netherlands, Juni 1992.
- [101] Audus, H.; O. Kaarstad; G. Skinner (1998): "*CO<sub>2</sub> capture by pre-combustion decarbonisation of natural gas*". Presentation ENT-01 at 4<sup>th</sup> Int. Conf. Greenhouse Gas Control Technologies, Interlaken 1998. Energy Convers. Mgmt., 1999.
- [102] Bolland, O; H. Undrum (1998): "*Removal of CO<sub>2</sub> from gas turbine power plants: Evaluation of pre- and post combustion methods*". Presentation CAP-18 at 4<sup>th</sup> Int. Conf. Greenhouse Gas Control Technologies, Interlaken 1998. Energy Convers. Mgmt., 1999.
- [103] Jørgensen, S.L.; Nielsen, P.E.H.; Lehrmann, P. (1995): Catal. Today 25 (303), 1995.
- [104] Moritsuka, H. (1998): "*Hydrogen decomposed turbine systems for carbon dioxide recovery*". Presentation ENT-02 at 4<sup>th</sup> Int. Conf. Greenhouse Gas Control Technologies, Interlaken 1998. Energy Convers. Mgmt., 1999.
- [105] Weller, A. W.; Rising, B. W. et al. (1985): "*Experimental Evaluation of Firing Pulverized Coal in a CO<sub>2</sub>/O<sub>2</sub> Atmosphere*". Battelle Columbus Division for Argonne National Laboratory, ANL/CNSV-<sup>TM</sup>-168 (Oct. 1985).
- [106] Wolsky, A.M. (1986): "*A new method of CO<sub>2</sub> recovery*". 79<sup>th</sup> Annual Meeting of the Air Pollution Control Association, Minneapolis, Minnesota, Juni 22-27, 1986.
- [107] Abele, A.R.; Kindt, G.S.; Clark, W.D.; Payne, R.; Chen, S.L. (1987): "*An Experimental Program to Test the Feasibility of Obtaining normal Performance from Combustors Using Oxygen and Recycled Flue Gas Instead of Air*". Argonne National Laboratory, Argonne, Illinois, 1987, ANL/CNSV-TM--204, DE89 002383.
- [108] Roberts, P.A. (1997): "*Atmospheric Pulverised Coal Combustion, Final Report*". In: "*JOULE II - Clean Coal Technology Programme 1992-95, Volume II: Powder Coal Combustion Project, Final Reports*". Europäische Kommission, Directorate-General XII - Science, Research and Development, 1997, EUR 17524 EN, ISBN 92-828-0006-7.
- [109] Kimura, K.; Takano, S.; Kiga, T.; Miyamae, S. (1990): "*Experimental Studies on Pulverized Coal Combustion with Oxygen/Flue Gas Recycle for CO<sub>2</sub> Recovery*".
- [110] Boeddicker, D. (1997): "*Thermodynamische und energiewirtschaftliche Bewertung eines Kombikraftwerks mit integrierter Kohlevergasung und CO<sub>2</sub>-Rezyklierung*". Dissertation Universität GH Essen, 1997.
- [111] Bammert, K.; Mukherjee, S. K. (1975): "*Gasturbinenanlagen für Kernkraftwerke mit CO<sub>2</sub> als Arbeitsmittel*". VDI Fortschrittberichte Reihe 6, Nr. 40. VDI Verlag, Düsseldorf 1975.
- [112] Mathieu, Ph.; Dechamps, P.; Distelmans, M. (1994): "*Concepts and Applications of CO<sub>2</sub> Gas Turbines*". Power-Gen Europe '94, Köln, Mai 1994, Vol.6, pp. 7-28.
- [113] Angelino, G. (1968): "*Carbon Dioxide Condensation Cycle for Power Production*". Combustion 40 (Sept. 1968), No. 3, pp. 31-40 or ASME 68-GT-23 (1969).

- [114] Gasparovic, N. (1969): "*Fluide und Kreisprozesse für Wärmekraftanlagen mit großen Einheitenleistungen*". BWK 21, No.7, July 1969, pp. 347-359.
- [115] Pfost, H.; Seitz, K. (1971): "*Eigenschaften einer Anlage mit CO<sub>2</sub>-Gasturbinenprozeß bei überkritischem Basisdruck*". Brennst.-Wärme-Kraft Sept. 1971, 23 (9), pp. 400-405.
- [116] Griepentrog, H. (1989): "*Kohlekraftwerke mit CO<sub>2</sub>-armen Rauchgasen*". Rheinisch-Westfälischer Technischer Überwachungsverein e.V., Essen, 1989.
- [117] Iantovski, E.I.; Zwagolsky, K.N.; Gavrilenko, V.A. (1992): "*Computer Exergonomics Of Power Plants Without Exhaust Gases*". Energy Convers. Mgmt. Vol.33, No.5-8, Pergamon Press, Oxford, 1992, pp.405-412.
- [118] Mathieu, Ph.; E. Iantovski; R. Nihart (1998): "*The Zero Emission MATIANT cycle: technical issues of a novel technology*". 2<sup>nd</sup> International Workshop on Zero Emission Power Plants, University of Liege, Institut de Mecanique, Januar 1998.
- [119] Jericha, H.; M. Fesharaki; A. Lukasser; H. Tabesh (1998): "*Graz-Cycle - eine Innovation zur CO<sub>2</sub>-Minderung*". BWK 10/98, pp. 30-34.
- [120] Jody, B.J.; E.J. Daniels; A.M. Wolsky (1997): "*Integrating O<sub>2</sub> Production with Power Systems to Capture CO<sub>2</sub>*". Energy Convers. Mgmt. Vol.38, Suppl., pp.S135-S140.
- [121] Ishida, M.; H. Jin (1998): "*Greenhouse gas control by a novel combustion: no separation equipment and energy penalty*". Presentation ENT-13 at 4<sup>th</sup> Int. Conf. Greenhouse Gas Control Technologies, Interlaken 1998. Energy Convers. Mgmt., 1999.
- [122] Knoche, K.F.; H. Richter (1968): "*Verbesserung der Reversibilität von Verbrennungsprozessen*". Brennstoff-Wärme-Kraft 20 (1968), No. 5, Mai 1968.
- [123] McMullan, J.T.; Williams, B.C.; Campbell, P. E.; McIlveen-Wright, D.R. (1997): "*Techno-Economic Assessment Studies of Fossil Fuel and Wood Power Generation Technologies*". Contract JOUF0017, In: "*JOULE II - Clean Coal Technology Programme 1992-95, Volume III: Combined Cycle Project, Final Reports*". Europäische Kommission, Directorate-General XII - Science, Research and Development, 1997, EUR 17524 EN, ISBN 92-828-0007-5.
- [124] Herzog, H.; Golomb, D.; Zemba, S. (1991): "*Feasibility, Modelling and Economics of Sequestering Power Plant CO<sub>2</sub> Emissions In the Deep Ocean*". Environmental Progress, Vol.19, No.1, Feb. 1991
- [125] Allam, R.J.; Spilsbury, C.G. (1992): "*A Study of the Extraction of CO<sub>2</sub> from the Flue Gas of a 500 MW Pulverized Coal-Fired Boiler*". Energy Convers. Mgmt Vol.33, No. 5-8, Pergamon Press, Oxford, 1992, pp. 477-485.
- [126] Sijercic, M.; Hanjalic, K. (1994): "*Application of Computer Simulation in a Design Study of a New Concept of Pulverized Coal Gasification: Part II: Model of Coal Reactions and Discussion of Results*". Combust. Sci. and Tech., 1994, Vol.97, pp.351-375.
- [127] van Heek, K. H.; Mühlen, H.-J.; Jüntgen, H. (1987): "*Progress in the Kinetics of Coal and Char gasification*". Chem. Eng. Technol. 10 (1987), pp. 411-419.
- [128] Teggers, H.; Jüntgen, H. (1984): "*Stand der Kohlevergasung zur Erzeugung von Brenngas und Synthesegas*". Erdöl und Kohle - Erdgas - Petrochemie, 1984, Vol. 37 (4), pp.163-174.
- [129] Azuma, T.; Hegermann, R.; Hüttinger, K.J. (1991): "*Pressure Gasification of Brown Coal in Steam and Carbon Dioxide Atmospheres*". Erdöl und Kohle - Erdgas - Petrochemie, 1991, 44 (7/8), pp. 301-305.
- [130] Kühl, H.; Kashani-Motlagh, M. M.; Mühlen, H.-J.; van Heek, K.H. (1992): "*Controlled Gasification of different carbon materials and development of pore structure*". Fuel, Vol. 71, Aug. 1992, pp. 879-882.

- [131] Andries, J.; Becht, J.G.M. (1995): "*Pressurized Fluidized Bed Gasification of Coal Using Flue Gas Recirculation and Oxygen Injection*". IEA Greenhouse Gases: Mitigation Options Conference, London, Aug. 1995.
- [132] Tomita, A.; Ohtsuka, Y.; Tamai, Y. (1983): "*Low-temperature gasification of brown coals catalysed by nickel*". Fuel, 1983, Vol.62, pp.150-154.
- [133] van Steenderen, P. (1992): "*Carbon dioxide recovery from coal gas and natural gas-fired combined cycle power plants by combustion in pure oxygen and recycled carbon dioxide*". Comprimo Consulting Services, "First International Conference on Carbon Dioxide Removal", March 1992, Amsterdam, NL.
- [134] Pak, P. S.; Nakamura, K.; Suzuki, Y. (1989): "*Closed Dual Fluid Gas Turbine Power Plant without Emission of CO<sub>2</sub> into the Atmosphere*". Energy and the Environment (III), IFAC Symposia Series No. 14, Pergamon Press, 1991, pp.229-234.
- [135] Shao, Y.; Golomb, D. (1995): "*Power Plants with CO<sub>2</sub> Capture using Integrated Air Separation and Flue Gas Recycling*". IEA Greenhouse Gas R&D: Mitigation Options Conference, London, Aug. 1995.
- [136] Pechtl, P. A. (1991): "*CO<sub>2</sub>-Emissionsminderung*". Erdöl und Kohle - Erdgas - Petrochemie vereinigt mit Brennstoff-Chemie, Bd. 44 (4), 1991, pp. 159-165.
- [137] Wessel, R. (1988): "*Thermodynamische Analyse kombinierter Gas-Dampf-Kraftwerke mit integrierter Kohlevergasung*". Dissertation Essen, 1988.
- [138] Knoche, K.F.; Roth, M.; Poptodorow, H. (1990): "*Conversion of Carbon in Combustion Processes and in Nature*". VGB Conference "Power Plant Engineering 2000 - conservation of Resources and CO<sub>2</sub> Control", Essen, FRG, Feb. 1990. VGB-TB 120, pp. 178-181.
- [139] Leithner, R.; Wang, J.; Stamatelopoulus, G. (1994): "*New Concepts for Coal-Fired Combined Cycle Power Plants*". Power-Gen Europe '94, Köln, Mai 1994, Vol.6, pp. 177-196.
- [140] Davison, J.E.; Eldershaw, C. E. (1990): "*A Study of Coal-Fired MHD Power Generation for the Commission of the European Communities*". Coal Research Establishment (CRE, British Coal Corporation) Assessment Branch report no. 90/1, Cheltenham, March 1990.
- [141] Davison, J.E.; Eldershaw, C. E. (1992): "*A Flowsheet Model of a Coal-Fired MHD / Steam Combined Electricity Generating Cycle, Using the Access Computer Model- Part II: Oxygen-blown Firing with CO<sub>2</sub> Recirculation*". In: P.F. Sens (Ed.): "Coal-fired magnetohydrodynamic (MHD) electric power generation", Office for Official Publications of the European Communities, EUR13928, Luxembourg, 1992, pp. 206-227.
- [142] Hendriks, C.A.; Blok, K. (1992): "*Carbon Dioxide Recovery Using a Dual Gas Turbine IGCC Plant*". Energy Convers. Mgmt. Vol.33, No.5-8, Pergamon Press, Oxford, 1992, pp.387-396.
- [143] Syed, M. A.; Masutani, S.M.; Nihous, G.C.; Vega, L. A.; Kinoshita, C. M. (1992): "*A Comparison of Carbon Dioxide Removal Strategies Applied to Natural Gas Power Plants*". Society of Automotive Engineers, Warrendale: Proceedings of the 27th intersociety energy conversion engineering conference, Vol.5, pp. 5.349-5.352, San Diego CA, Aug. 1992.
- [144] Bolland, O.; Saether, S. (1992): "*New Concepts For Natural Gas-Fired Power Plants Which Simplify The Recovery Of Carbon Dioxide*". Energy Convers. Mgmt. Vol.33, No.5-8, Pergamon Press, Oxford, 1992, pp.467-475.
- [145] de Ruyck, J. (1992): "*Efficient CO<sub>2</sub> Capture Through A Combined Steam and CO<sub>2</sub> Gas Turbine Cycle*". Energy Convers. Mgmt. Vol.33, No.5-8, Pergamon Press, Oxford, 1992, pp.397-403.
- [146] de Ruyck, J.; Bram, S.; Allard, G.; Mathieu, Ph.; Ulizar, I.; Pilidis, P.; Haug, M.; Katzler, G.; Brüggemann, D.; Sjöström, K.; Liliedahl, L.; Sakelleropoulos, G. P.; Skodras, G.; Verelst, H.; van Mierlo, T.; van de Voorde, M.; Elseviers, W.; Maniatis, K. (1997): "*CO<sub>2</sub> Mitigation through CO<sub>2</sub> / Steam Gas Turbine Cycles and CO<sub>2</sub> / Steam Gasification*". In: "Joule II - Clean Coal Technology Programme



- 1992-95, *Volume III: Combined Cycle Project, Final Reports*". European Commission, Directorate-General XII - Science, Research and Development, 1997, EUR 17524 EN, ISBN 92-828-0007-5.
- [147] Iantovski, E.I.; Zwagolsky, K.N.; Gavrilenko, V.A. (1995): "*Stack Downward: the Concept of Zero Emission Fuel-Fired Power Plants*". IEA Greenhouse Gases: Mitigation Options Conference, London, Aug. 1995.
- [148] Blok, K.; Hendriks, C.; Turkenburg, W. (1989): "*The Role of Carbon Dioxide Removal in the Reduction of the Greenhouse Effect*". Dept. of Science, Technology and Society, University of Utrecht, NL, April 1989, W 89019.
- [149] Hansen, M.W. (1991): "*Fysiske Metoder Til Fjernelse Af CO<sub>2</sub> Fra Røggas*", Presentiert auf der Konferenz "Løsning af kuldioxidproblemet", Dansk Ingeniørforening, Kopenhagen, Dänemark, Feb. 1991.
- [150] Miller, D. B.; Soychak, T.J.; Gosar, D. M. (1986): "*Economics of Recovering CO<sub>2</sub> from Exhaust Gases*". Chemical Engineering Progress, Oct. 1986, pp. 38-46.
- [151] Rao, A., D.; Day, W., H. (1995): "*Mitigation of Greenhouse Gases from Gas Turbine Power Plants*". IEA Greenhouse Gases: Mitigation Option Conference, London, Aug. 1995.
- [152] Golomb, D. (1993): "*Ocean Disposal of CO<sub>2</sub>: Feasibility, Economics and Effects*". IEA Carbon Dioxide Disposal Symposium, Oxford, Energy Conv. Mgmt. Vol. 34, No. 9-11, Pergamon Press, Oxford, March 1993, pp. 967-976.
- [153] Stookey, D. J.; Pope, W. M. (1985): "*Application of Membranes in Separation of Carbon Dioxide from Gases*". In: "*Recovering Carbon Dioxide from Man-Made Sources*", Argonne National Laboratory Workshop, Argonne National Laboratory, ANL/CNSV-TM-166, February 1985, pp. 63-75.
- [154] Smelser, S.C.; Stock, R.M.; McCleary, G.J.; Booras, G. S.; Stuart, R.J. (1991): "*Engineering and Economic Evaluation of CO<sub>2</sub> Removal from Fossil-Fuel-Fired Power Plants. Volume 1: Pulverized Coal-Fired Power Plants*". EPRI IE-7365, Vol. 1, 1991.
- [155] Doctor, R.D., J. C. Molburg; P.R. Thimmapuram (1996): "*KRW Oxygen-Blown Gasification Combined Cycle: Carbon Dioxide Recovery, Transport and Disposal*". Argonne National Laboratory ANL/ESD-34, 1996.
- [156] Jansen, D.; Oudhuis, A.B.J.; Ribberink, J.S. (1992): "*Different Options for Integrated Coal Gasification Fuel Cell Power Generation Plants and their Potential to Reduce CO<sub>2</sub> Emissions*". Netherlands Energy Research Foundation, Petten, The Netherlands, ECN-RX-92-070, Nov. 1992.
- [157] IEA GHG (1997): "*Advanced Systems: Report on Expert Workshop*". 11<sup>th</sup>-12<sup>th</sup> Juni, 1997, Essen. IEA Greenhouse Gas R&D Programme, Cheltenham, Report Number PH12/16.
- [158] Schmidt, E.; U. Grigull (1989): "*Zustandsgrößen von Wasser und Wasserdampf in SI-Einheiten*". Springer-Verlag, Berlin, 4. Auflage, 1989.
- [159] Wagner, W. (1998): "*Properties of Water and Steam /Zustandsgrößen von Wasser und Wasserdampf*", Springer Berlin, 1998.
- [160] Hougen, Watson, Regatz: "*Chemical Process Principles, Part 2*". Wiley, New York, 1964.
- [161] Baehr, H.D.; E.F. Schmidt (1964): "*Die Berechnung der Exergie von Verbrennungsgasen unter Berücksichtigung der Dissoziation*." Brennstoff-Wärme-Kraft 16 (1964) 62-66.
- [162] Shindo, Y.; Hakuta, T.; Yoshitome, H. (1985): "*Calculation Methods for Multicomponent Gas Separation by Permeation*". Separation Science and Technology, 20 (5&6), pp. 445-459, 1985.
- [163] Angus, S.; Armstrong, B.; Renck, K. (1976): "*Carbon Dioxide - International Tables of the Fluid State (IUPAC), Vol.3*". Pergamon Press, Oxford-New York, 1976.
- [164] Steiner, A. (1976): "*Hilfsmittel, Ansätze und Beispiele zu Berechnung von Gas- und kombinierten Gas-/Dampfturbinenanlagen mit integrierten Gaserzeugern*". Dissertation ETH Zürich.

- [165] Renfro, J. J. (1979): "Colorado's Sheep Mountain CO<sub>2</sub> project moves forward". Oil & Gas Journal, Dec.17, 1979, pp. 51-56.
- [166] Landolt, Hans [Begr.]: "Eigenschaften der Materie in ihren Aggregatzuständen 2. Teil; Bandteil b: Lösungsgleichgewichte I". Springer-Verlag, Berlin, 1962. (aus: Landolt-Börnstein / Zahlenwerte und Funktionen aus Physik, Chemie, Astronomie, Geophysik und Technik / Hans Landolt u. Richard Börnstein. - 6. Aufl. / hrsg. von Arnold Eucken. Berlin [u.a.] : Springer, 1950)
- [167] Crovetto (P. Scharlin (ed.) (1996): "Carbon Dioxide in water and aqueous electrolytes solutions. IUPAC Solubility data series, Vol. 62". Oxford University Press, Oxford, 1996.)
- [168] Chakma, A. (1997): "CO<sub>2</sub> Capture Processes Opportunities for Improved Energy Efficiencies". Energy Convers. Mgmt. Vol. 38, Suppl., pp. S51-S56, 1997
- [169] Adorni, M (1997): "Energieaufwand zur CO<sub>2</sub>-Abtrennung aus Kraftwerksgasen durch Druckwechseladsorption". Diplomarbeit, Januar 1997; Betreuer: G. Göttlicher, R. Pruschek. Universität GH Essen.
- [170] Kast, W. (1988): "Adsorption aus der Gasphase". VCH 1988, 26
- [171] Kapoor, A.; J. A. Ritter; R. T. Yang(1988): "Gas Separation by Pressure Swing Adsorption for Producing Hydrogen from Coal". Final Report, 1988, US Department of Energy, Report No. DOE/MC/22060-2643, Contract No. DE-AC21-85MC22060.
- [172] Burkert, J. (1979): "Ermittlung von Gleichgewichtsdaten für die adsorptive Reinigung von Gasen bei hohen Drücken mit Molekularsieben". Dissertation Universität Karlsruhe, 1979.
- [173] Stern, S.A.; Wang, S.C. (1978): "Countercurrent and Cocurrent -Gas Separation in a Permeation Stage. Comparison of Computation Methods". Journal of Membrane Science, 4 (1978), pp. 141-149.
- [174] Bosnjakovic, F.; K. F. Knoche (1988): "Technische Thermodynamik". 7. Aufl., 1988. ISBN 3-7985-0759-7. Verlag Steinkopff, Darmstadt.
- [175] Harrison, D.,P; Han, C.; Silaban, A. (1993): "A Calcium Oxide Sorbent Process for Bulk Separation of Carbon Dioxide". Proceedings of the coal-fired power systems 1993, p.335-344.
- [176] Thambimuthu, K. V. (1993): "Gas cleaning for advanced coal-based power generation". IEA Coal Research, IEACR/53, March 1993.
- [177] Koerdt, M (1996): "Wirkungsgradberechnungen für eine chemisch rekuperierte Gasturbine mit CO<sub>2</sub>-Abtrennung". Diplomarbeit, September 1996; Betreuer: G. Göttlicher, R. Pruschek. Universität GH Essen, Technik der Energieversorgung und Energiewirtschaft (Prof. Pruschek).
- [178] Rostrup-Nielsen, J. R.; Aasberg-Petersen, K.; Højlund Nielsen, P. E. (1995): "Chemical recuperation and gas turbines". EPRI Conference on New Power Generation Technology, 25.-27. Oktober 1995, San Francisco, California
- [179] Janes, J. (1990): "Chemically Recuperated Gas Turbine". California Energy Commission, Staff report P500-90-001, Januar 1990.
- [180] Pruschek, R.; U. Renz; E. Weber (1990): "Kohlekraftwerk der Zukunft". Im Auftrag des Ministers für Wirtschaft, Mittelstand und Technologie des Landes Nordrhein-Westfalen, Düsseldorf, 1990.
- [181] Informationsdienst IWD - Online (1998): "CO<sub>2</sub>-Emissionen in Deutschland, Klima - vom Menschen beeinflussbar?". Ausgabe Nr. 6, Jg. 24, 5. Februar 1998, Institut der deutschen Wirtschaft (IW), Köln.
- [182] Borsch, P.; H. J. Wagner: "Energie und Umweltbelastung". Springer Verlag, Berlin, 2. Auflage, 1998
- [183] World Energy Council / IIASA (1998). "Global Energy Perspectives", Report 1998.
- [184] Keeling, C.D.; Whorf, T.P. (1996): "Atmospheric CO<sub>2</sub> records from sites in the SIO air sampling network." In: Boden, T.A.; Kaiser, D. P.; Sepanski, R.J.; Stoss, F.W.: "Trends '97: A Compendium of

- Data on Global Change*", pp. 18-28. ORNL/CDIAC-65. Carbon Dioxide Information Analysis Center, Oak Ridge National Laboratory, Oak Ridge, Tenn., USA. Updates im Internet veröffentlicht.
- [185] Barnola, J. M.; Raynaud, D.; Lorius, C.; Korotkevich, Y.S. (1994): "*Historical record from the Vostok ice core*". In: Boden, T.A. et al.: "*Trends '97: A Compendium of Data on Global Change*", pp. 7-10. ORNL/CDIAC-65. Carbon Dioxide Information Analysis Center, Oak Ridge National Laboratory, Oak Ridge, Tenn., USA. Updates im Internet veröffentlicht.
- [186] Neftel, A. H.; Friedli, H.; Moor, E.; Lötscher, H.; Oeschger, H.; Siegenthaler, U.; Stauffer, B. (1994): "*Historical CO<sub>2</sub> record from the Siple Station ice core*". In: Boden, T.A. et al.: "*Trends '97: A Compendium of Data on Global Change*", pp. 11-14. ORNL/CDIAC-65. Carbon Dioxide Information Analysis Center, Oak Ridge National Laboratory, Oak Ridge, Tenn., USA. Updates im Internet.
- [187] Keeling, C.D.; T.P. Whorf (Februar 1997): "*Atmospheric CO<sub>2</sub> concentrations from South Pole*". Scripps Institution of Oceanography, University of California, Daten über Internet veröffentlicht.
- [188] IEA (1996): "*World Energy Outlook - 1995*". International Energy Agency, 1996
- [189] Freund, P. (1998): "*Abatement and mitigation of carbon dioxide emissions from Power Generation*". Power Gen Europe '98.
- [190] Levi, W. (1997): "*Nachhaltige Entwicklung und Energieversorgung*". atw 42. Jhg. Heft 1
- [191] The Netherlands Ministry of Economic Affairs (1993): "*Nuclear Energy Dossier*". Den Haag, The Netherlands.
- [192] Allegre, C.J.; S.H. Schneider (1995): "*Die Entwicklung der Erde*". Spektrum der Wissenschaft. SPEZIAL: Leben und Kosmos, 1995.
- [193] O'Callaghan, P.W. (1993): "*Energy Resources, CO<sub>2</sub> Production and Energy Conservation*". Applied Energy 44 (1993) pp. 65-91.
- [194] Kowaczek, J.; Kurth, K.; Schubert, H. (1974): "*Tabellenbuch für die Gastechnik*". VEB Deutscher Verlag für die Grundstoffindustrie, Leipzig 1974.
- [195] Eagleton, H.,N. (1980): "*Transportation of carbon dioxide by pipeline*". Int. Pipeline Tech. 8<sup>th</sup> Interpipe Conf., Houston, Feb. 1980, pp. 225-242.
- [196] Price, B., C.; Gregg, F., L. (1983): "*CO<sub>2</sub> / EOR from source to resource*". Oil & Gas Journal, Aug. 22, 1983, pp. 116-122.
- [197] Barry, D. W. (1985): "*Design of Cortez CO<sub>2</sub> system detailed*". Oil & Gas Journal, July 22, 1985, pp. 96-104.
- [198] McCollough, D. E. (1986): "*The Central Basin Pipeline: A CO<sub>2</sub> Systems in West Texas*". Energy Progress, Vol.6, No.4, Dec. 1986, pp. 230-234.
- [199] Wakamura, O.; Shibamura, K.; Uenoyama, K. (1992): "*Development of PSA Plant for Manufacture of Carbon Dioxide from Combustion Waste Gas*". Nippon Steel Technical Report No. 55, October 1992, pp. 51-55.
- [200] Sircar, S.; Kratz, W.C. (1988): "*Simultaneous Production of Hydrogen and Carbon Dioxide from Steam Reformer Off-Gas by Pressure Swing Adsorption*". Separation Science and Technology, 23 (14&15), pp.2397-2415, 1988.
- [201] Richter, E.; Harder, K.; Knoblauch, K.; Jüntgen, H. (1984): "*Neue Entwicklungen zur Druckwechsel-Adsorption*". Chem. Ing. Tech. 56 (1984), Nr.9, p. 684-691.
- [202] Ishibashi, M., H. Ohta, N. Akutsu, S. Umeda, M. Tajilka, J. Izumi, A. Yasutake, T. Kabata, Y. Kageyama (1995): "*Technology for Removing Carbon Dioxide from power Plant Flue Gas by the Physical Adsorption Method*". Energy Convers. Mgmt. Vol. 37, No. 6-8, pp. 929-933.

- [203] Makino, H.; Kimoto, M. (1995): "*Activities of CO<sub>2</sub> control technology in Japanese electric industry.*" CRIEPI -Veröffentlichung.
- [204] Koros, W.J.; Fleming, G. K.; Jordan, S. M.; Kim, T. H.; Hoehn, H. H. (1988): "*Polymeric Membrane Materials for Solution-Diffusion Based Permeation Separations.*" Prog. Polm. Sci., Vol.13, pp. 339-401, 1988.
- [205] Baker, R.W., et al. (1990): "*Low Cost Hydrogen / Novel Membrane Technology for Hydrogen Separation from Synthesis Gas (Final Report)*". US Department of Energy, Office of Fossil Energy, Morgantown, West Virginia, USA, DOE/MC/22130-2983, Oct. 1990.
- [206] UBE (1990): Firmenprospekt
- [207] Pruschek, R.; G. Oeljeklaus; A. Lokurlu; H. Vogelsang (1995): "*Ermittlung und Verifizierung der Potentiale und Kosten der Treibhausgasminderung durch Kraft-Wärme-Kopplung in der Industrie.*" Universität GH Essen, Studie im Auftrag der Enquete Kommission "Schutz der Erdatmosphäre", 1994
- [208] Bundesministerium für Wirtschaft (BMWi): "*Energiedaten 1997/1998*"
- [209] Van de Vate (1993): "*Electricity generation and alleviating global climate change; the potential role of nuclear power*". Paper presented at the UNIPeDE/IEA conference on Thermal Power Generation and the Environment, Hamburg, 1.-3. September 1993



